ACTA PROTOZOOLOGICA

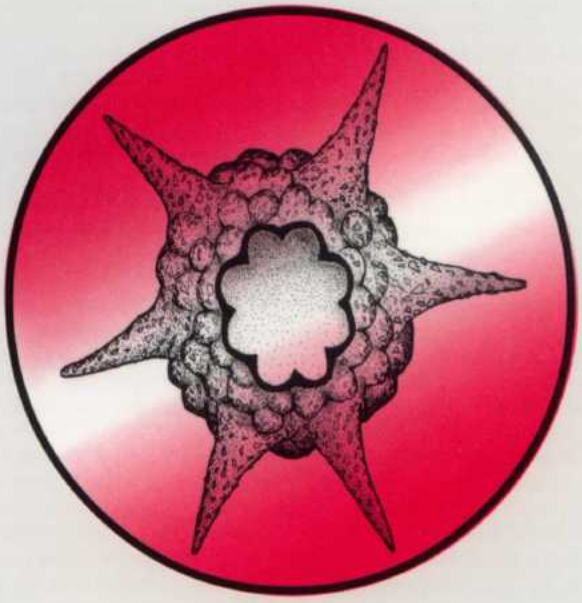

NENCKI INSTITUTE OF EXPERIMENTAL BIOLOGY
WARSAW, POLAND
2005
VOLUME 44 NUMBER 3
ISSN 0065-1583

Polish Academy of Sciences
Nencki Institute of Experimental Biology
and
Polish Society of Cell Biology

ACTA PROTOZOOLOGICA
International Journal on Protistology

ACTA PROTOZOOLOGICA appears quarterly.

The price (including Air Mail postage) of subscription to *Acta Protozoologica* at 2006 is: 200.- € by institutions and 120.- € by individual subscribers. Limited numbers of back volumes at reduced rate are available. Terms of payment: check, money order or payment to be made to the Nencki Institute of Experimental Biology account: 91 1060 0076 0000 4010 5000 1074 at BPH PBK S.A. Warszawa, Poland. For the matters regarding *Acta Protozoologica*, contact Editor, Nencki Institute of Experimental Biology, ul. Pasteura 3, 02-093 Warszawa, Poland; Fax: (4822) 822 53 42; E-mail: j.sikora@nencki.gov.pl For more information see Web page **http://www.nencki.gov.pl/ap.htm**

Front cover: Yang J., Beyens L., Shen Y. and Feng W. (2004) Redescription of *Difflugia tuberspinifera* Hu, Shen, Gu *et* Gong, 1997 (Protozoa: Rhizopoda: Arcellinida: Difflugiidae) from China. *Acta Protozool.* **43:** 281-289

This publication is supported by the State Committee for Scientific Research

Desktop processing: Justyna Osmulska, Information Technology Unit of the Nencki Institute
Printed at the MARBIS, ul. Poniatowskiego 1
05-070 Sulejówek, Poland

Acta Protozool. (2005) 44: 189 - 199

ACTA
PROTOZOOLOGICA

The Amoeboid Parabasalid Flagellate *Gigantomonas herculea* of the African Termite *Hodotermes mossambicus* Reinvestigated Using Immunological and Ultrastructural Techniques

Guy BRUGEROLLE

Biologie des Protistes, UMR 6023, CNRS and Université Blaise Pascal de Clermont-Ferrand, Aubière Cedex, France

Summary. The amoeboid form of *Gigantomonas herculea* (Dogiel 1916, Kirby 1946), a symbiotic flagellate of the grass-eating subterranean termite *Hodotermes mossambicus* from East Africa, is observed by light, immunofluorescence and transmission electron microscopy. Amoeboid cells display a hyaline margin and a central granular area containing the nucleus, the internalized flagellar apparatus, and organelles such as Golgi bodies, hydrogenosomes, and food vacuoles with bacteria or wood particles. Immunofluorescence microscopy using monoclonal antibodies raised against *Trichomonas vaginalis* cytoskeleton, such as the anti-tubulin IG10, reveals the three long anteriorly-directed flagella, and the axostyle folded into the cytoplasm. A second antibody, 4E5, decorates the conspicuous crescent-shaped structure or cresta bordered by the adhering recurrent flagellum. Transmission electron micrographs show a microfibrillar network in the cytoplasmic margin and internal bundles of microfilaments similar to those of lobose amoebae that are indicative of cytoplasmic streaming. They also confirm the internalization of the flagella. The arrangement of basal bodies and fibre appendages, and the axostyle composed of a rolled sheet of microtubules are very close to that of the devescovinids *Foaina* and *Devescovina*. The very large microfibrillar cresta supporting an enlarged recurrent flagellum resembles that of *Macrotrichomonas.* The parabasal apparatus attached to the basal bodies is small in comparison to the cell size; this is probably related to the presence of many Golgi bodies supported by a striated fibre that are spread throughout the central cytoplasm in a similar way to *Placojoenia* and *Mixotricha*.

Key words: *Gigantomonas, Hodotermes*, immunofluorescence, parabasalid, protozoa, termite, ultrastructure.

INTRODUCTION

Most of the parabasalids are endocommensal, parasitic or symbiotic flagellates represented by about 80 genera. They are classically divided into two subgroups - the simple trichomonads with few flagella, and the more complex hypermastigids with many flagella (Brugerolle and Lee 2001). All but one genus have flagella for movement and most of them have kept amoeboid abilities. Although amoeboid movement is normally associated with locomotion in protozoa (Hausmann *et al.* 2003), in parabasalids it is only used for the phagocytosis of food since parabasalids have no cytostome (Brugerolle and Lee 2001). Among the trichomonads, *Dientamoeba fragilis* of the human intestine has no flagella and is strictly amoeboid (Wenrich 1944, Camp *et al.* 1974, Windsor and Johnson 1999) and *Histomonas meleagridis*, an amoeboflagellate parasite of the liver and gut of birds that has one flagellum, is also

Address for correspondence: Guy Brugerolle, Biologie des Protistes, UMR 6023, CNRS and Université Blaise Pascal de Clermont-Ferrand, 63177 Aubière Cedex, France; Fax: 33 04 73 40 76 70; E-mail: Guy.Brugerolle@univ-bpclermont.fr

largely amoeboid (Wenrich 1943, Schuster 1968, Honigberg and Bennett 1971). There are only limited modern studies of both in the literature. There are more reports available on the parasitic flagellate of humans, *Trichomonas vaginalis*, which is able to become amoeboid when adhering to host cells or other substrates, although it retains its flagellar apparatus (Honigberg and Brugerolle 1990, Alderete *et al*. 1995, Gonzales-Robles *et al.* 1995, Brugerolle *et al.* 1996). In amoeboid cells of *T. vaginalis*, the cytoplasmic border contains a microfibrillar network where actin, α-actinin and coronin appear to be the major components (Brugerolle *et al.* 1996; Bricheux *et al.* 1998, 2000).

Termites feed on wood or plant and are an important factor in plant decomposition and soil formation (Wood 1988, Lobry de Bruyn and Conacher 1990, Black and Okwakol 1997). Termites secrete their own cellulases (Watanabe *et al.* 1998) to digest wood in association with the bacteria, yeast and protozoa living in their posterior gut (Breznak and Brune 1994, Inoue *et al.* 2000, König *et al.* 2002), which Brune (1998) described as the "smallest bioreactor in the world". Most of the protozoa species of termites phagocytose wood particles on their flagella-free cell surface and contribute to wood digestion (Mannesmann 1972, Odelson and Breznak 1985, Yoshimura 1995, König *et al*. 2002). Only lower termites of the six families Mastotermitidae, Kalotermitidae, Hodotermitidae, Termopsidae, Rhinotermitidae, and Serritermitidae are known to harbour flagellate protozoa including oxymonads and parabasalids in their posterior gut (Honigberg 1970, Yamin 1979, König *et al*. 2002, Brugerolle and Radek 2005). Higher termites, the Termitidae, do not harbour many protozoa, but nevertheless they also digest wood. Though many termite species have not been explored, most of the genera/species of flagellates have been identified by light microscopy and cell staining in the course of the last century (listed in Yamin 1979, Brugerolle and Lee 2001, Brugerolle and Patterson 2001). Important advances on cytology and phylogeny have been made in the last thirty years with the use of electron microscopy, but a lot of work remains to be completed on termite flagellates (Brugerolle and Radek 2005). Consequently, the lack of a correct morphological identification is now a major drawback to assigning a sequence to a species in the molecular phylogeny studies of these flagellates (Keeling *et al*. 1998, Ohkuma *et al*. 2000, Gerbod *et al*. 2002).

The African termite *Hodotermes mossambicus* is a subterranean species that collects grass on the ground surface to feed it underground in the nest (Nel and Hewith 1969). It lives only a few days out of its colony and culture in the laboratory requires strict ecological conditions. The first study of the intestinal protozoa of this termite was performed in the country of origin in East Africa by Dogiel (1916), who identified about six protozoa genera/species comprising the remarkable amoeboid parabasalid *Gigantomonas herculea.* This first study was completed by Kirby (1946) who updated a flagellate, an amoeboflagellate and an amoeboid form that represent the phases of development of the same organism *G. herculea*. The morphological studies of Dogiel (1916) and Kirby (1946) using haematoxylin staining demonstrated the presence of a completed flagellar apparatus in the flagellate stage, and a reduction of this flagellar apparatus culminating in its complete disappearance in the amoeboid stages. Kirby (1946) concluded by the presence of a crescent fibre or cresta under the recurrent flagellum, that *G. herculea* was a devescovinid close to *Macrotrichomonas* and other devescovinid genera he had studied extensively (Kirby 1941, 1942a, b, 1946); this taxonomic position was also supported by Grassé (1952).

Since the investigations of Dogiel (1916) and Kirby (1946), no other observations have been published on *G. herculea*. I have recently had the opportunity to study the symbiotic protozoan fauna of *Hodotermes mossambicus*, including the joeniid flagellate *Joenoides intermedia* (Brugerolle and Bordereau 2003). Instead of the conventional haematoxylin, I used monoclonal antibodies generated against several trichomonads to reveal the structures of the flagellar apparatus of *J. intermedia* by light microscopy. I have also applied a similar approach combined with transmission electron microscopy, to reinvestigate *G. herculea*, and these results are presented in this paper.

MATERIALS AND METHODS

Hodotermes mossambicus termites were collected in Kenya several years ago and maintained in a terrarium at the laboratory of the Université de Bourgogne in Dijon, France (Brugerolle and Bordereau 2003). The hindgut of a termite was opened with a pair of tweezers and the fluid content mixed into a drop of either Ringer's or PBS (buffered phosphate saline) solution. Living protozoa were observed and photographed under a phase contrast or a differential contrast microscope using a Leica DMRH microscope equipped with a Station Q-Fish Light.

For immunofluorescence, cells were immediately permeabilized in 0.25% Triton X-100 (final concentration) in Tris-maleate buffer (20 mM Tris - maleate, 10 mM EGTA, 10 mM $MgCl_2$, sodium azide 0.1%, pH 7) for 1 min, then fixed in 3.7% formaldehyde (final

concentration) in phosphate buffer for 5 min. After adjustement of cell concentration, the cells were deposited and air-dried on immunofluorescence slides previously coated with 0.1% poly-L-lysine (Sigma); slides were stored at -20°C. Before use, the slides were washed twice in PBS for 1 h, then blocked with 1% bovine serum albumin in PBS for 15 min and incubated overnight at room temperature with the undiluted of monoclonal antibodies. After three washes in PBS for 1 h, the cells were incubated with a 1/200 dilution of a secondary antibody, an anti-mouse Ig:IgG/M antibody conjugated with fluorescein isothiocyanate (FITC) (Sigma) for 2 h at 37°C. After several washes in PBS for 1 h, the slides were mounted in 1/1 PBS/glycerine containing 10 mg/ml DABCO (Sigma) as an anti-fading agent. The monoclonal antibodies (Mab) used were prepared at the laboratory by the author from mice immunized with *Trichomonas vaginalis* cytoskeletons, according to the procedure described in Brugerolle and Viscogliosi (1994). The microtubular fibres were labelled by the anti-tubulin Mab IG10, both microtubular and fibrous structures by Mab 24E3, the cresta structure by Mab 4E5 and fibrillar actin by Mab XG3 (Bricheux *et al.* 1998).

For transmission electron microscopy (TEM), the entire gut fauna was fixed in a solution of 1% glutaraldehyde (Polysciences) in 0.1 M phosphate buffer, pH 7, for 1 h at room temperature. After centrifugation and two washes in the buffer, cells were postfixed in 1% osmium tetroxide in the buffer for 1 h. After a water rinse, cells were pre-embedded in 1% agar (Difco), stained "en bloc" with saturated uranyl acetate in 70% ethanol for 1 h, completely dehydrated in an alcohol series, and embedded in Epon 812 resin (Merck). Sections were cut on a Reichert Ultracut S microtome, stained with lead citrate for 15 min, and examined under a JEOL 1200 EX electron microscope at 80 kV.

RESULTS

Light microscopy and immunofluorescence. Opening the gut in Ringer's or PBS solution revealed mostly amoeboid cells of an average diameter of 70 µm (40-100), showing a hyaline margin of cytoplasm and a central granular area (Figs 1-3). A higher magnification revealed fibrous structures which appeared to be an undulating flagellum and an axostyle curved inside the cytoplasm (Figs 3, 4).

Immunofluorescence microscopy with the anti-tubulin Mab IG10 revealed a stout trunk of the axostyle of even thickness and sharpened at the posterior end, and the axostyle capitulum wraping the nucleus at the other side (Figs 5, 6). Three long anterior flagella of about 80 µm were also stained in a few cells (Figs 6, 7). Their base is enveloped in an expansion of the axostyle capitulum. A second antibody, Mab 24E3, used alone or in association with the anti-actin Mab XG3 in a double-labelling, highlighted the axostyle and a conspicuous crescent-shaped fibre, the cresta, which are embedded and diversely folded inside the cytoplasm of the amoeboid cells (Figs 7-9). A third antibody, Mab 4E5, labelled the crescent-shaped lamellar structure or cresta originating from the flagellar bases close to the nucleus and narrowing at its posterior end (Fig. 10). Double-labelling with the anti-tubulin Mab IG10 and the anti-cresta Mab 4E5 antibodies revealed that the peripheral edge of the cresta is delineated by the undulating recurrent flagellum (Fig. 11), which detaches in some portions (Fig. 7). Dividing cells were observed to have a microtubular paradesmosis stretched between two nuclei, as identified by the anti-tubulin Mab IG10 (Fig. 12).

Transmission electron microscopy. Sections observed by TEM concerned only the amoeboid form. Amoeboid cells had a peripheral microfibrillar zone of about 5 µm width without organelles (Figs 13, 14), and a central area containing the nucleus, fibrous organelles including the flagella, the cresta and axostyle structures, and cytoplasmic organelles such as Golgi bodies, hydrogenosomes, bacteria inside vacuoles and many vesicles (Figs 13-15).

Higher magnification shows that the cytoplasm of the peripheral zone is composed of a microfibrillar network, and also has more condensed microfibrillar areas (Fig. 16). In some cells, bundles of parallel microfilaments that resemble the actin microfilaments were also observed to form a bridge between a broad pseudopodium and the cell body (Fig. 17, inset).

The central area close to the nucleus contains a set of four flagella (Figs 18-22). Their bases are arranged like those of trichomonads or devescovinids with the basal bodies (#1, #2, #3) of the three anteriorly-directed flagella arranged around the basal body of the recurrent flagellum (R). Basal body #2 bears the sigmoid fibres that line the microtubular row of the axostyle capitulum (Figs 18, 20). Basal bodies #1 and #3, situated on each side of basal body #2, were recognized by the arched lamina they bear (Fig. 20). Basal body R is at the origin of the recurrent flagellum that has a large diameter of about 1 µm (Fig. 22). Attached to basal bodies, there are two main striated parabasal fibres supporting a Golgi body (Fig. 21). There is also a thin striated fibre not associated with a Golgi body, that moves along the surface of the nucleus (Fig. 18). Two unequally-sized dense structures are appended to the basal bodies and represent the atractophores that are the centrosome equivalent in parabasalids (Figs 18, 21). In dividing cells, these dense structures give rise at their periphery to radiating spindle microtubules comprising kinetochore microtubules and the pole-to-pole microtubules of the paradesmosis (Figs 18, 19, 21).

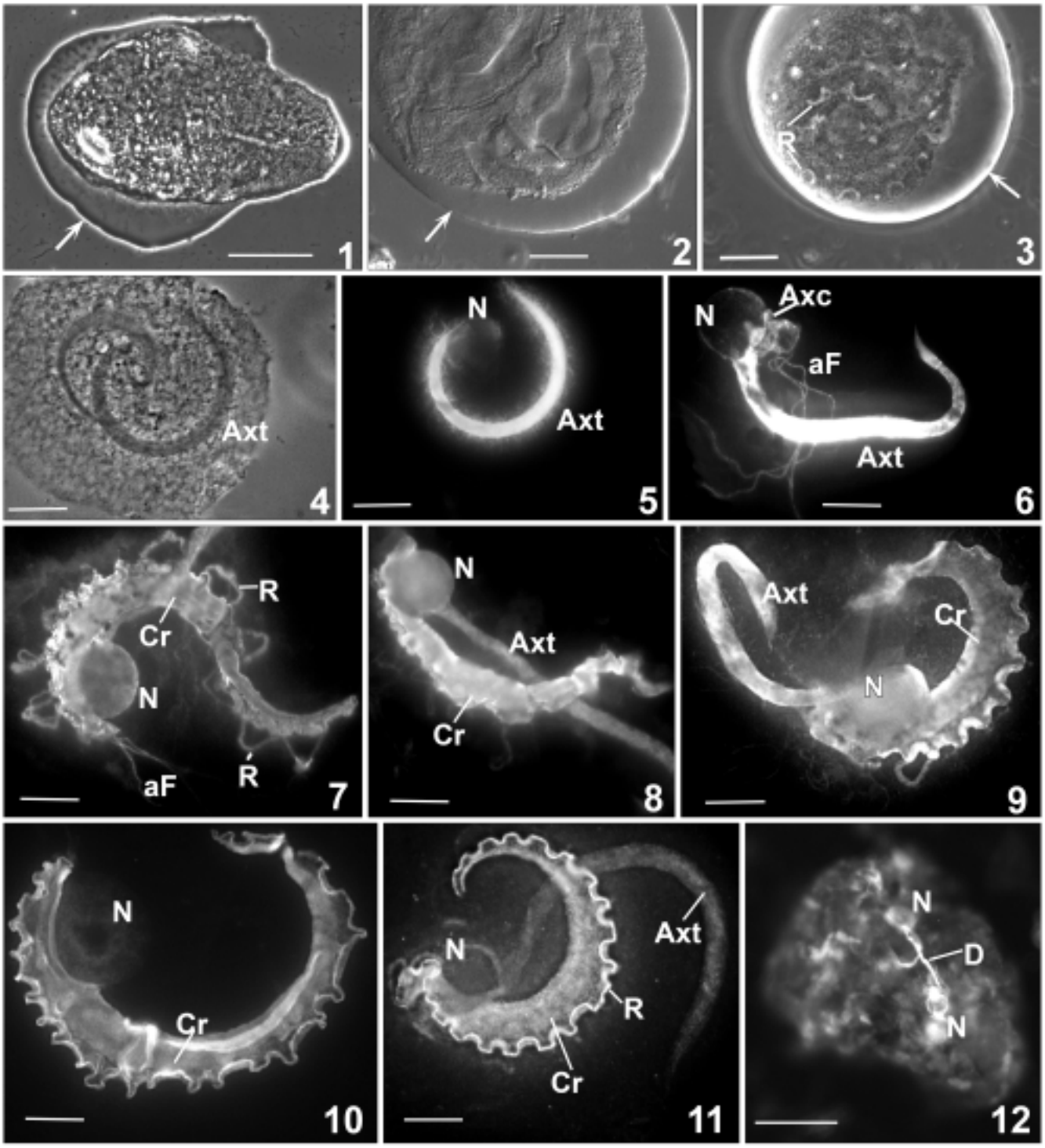

Figs 1-12. Light and immunofluorescence microscopy of the amoeboid stage of *Gigantomonas herculea*. **1** - phase contrast and; **2, 3** - differential contrast showing the hyaline margin (arrow) and the central granular area containing fibrous structures such as an undulated flagellum (R) (3); **4, 5** - permeabilized cell (4) and axostyle labelling (Axt) (5) with the anti-tubulin Mab IG10; **6** - three long anteriorely-directed flagella (aF), axostyle trunk (Axt) and axostyle capitulum (Axc) around the nucleus (N) labelled with Mab IG10; **7-9** - axostyle trunk (Axt), anterior flagella (aF), cresta (Cr) and recurrent flagellum (R) labelled with Mab 24E3, nucleus (N); **10** - cresta (Cr) revealed with Mab 4E5 and nucleus (N) at the anterior end; **11** - double-labelling of the cresta (Cr) with Mab 4E5, and axostyle (Axt), and recurrent flagellum (R) with Mab IG10; **12** - paradesmosis (D) stretched between two nuclei (N) revealed with Mab IG10 in a dividing cell. Scale bars 50 µm (1, 12), and 10 µm (2-11).

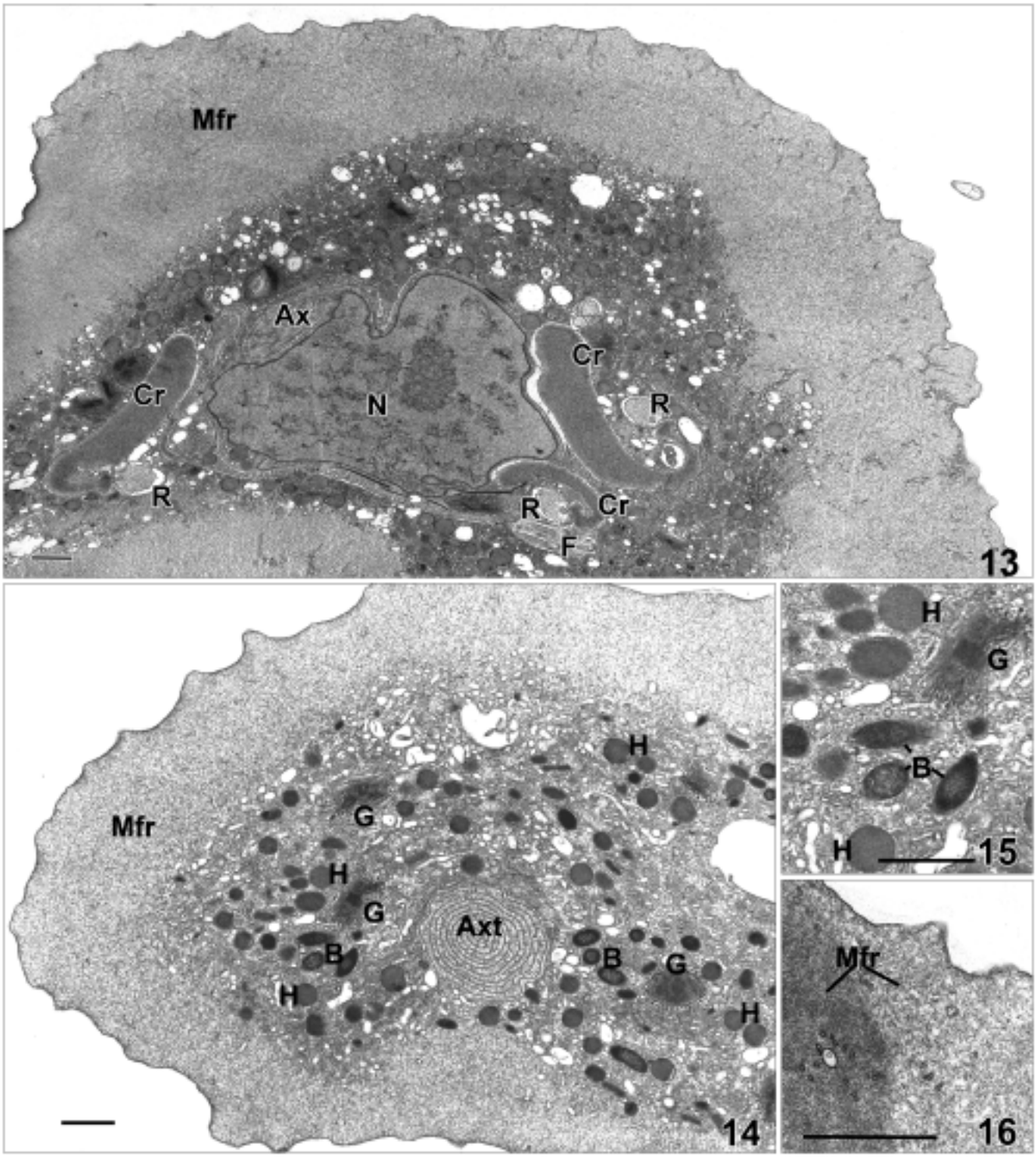

Figs 13-16. Transmission electron micrographs of the amoeboid stage of *Gigantomonas herculea*. **13** - general view, microfibrillar border (Mfr) and central area with the nucleus (N), cresta sections (Cr), recurrent flagellum (R), axostyle (Ax), anterior flagella (F); **14** - microfibrillar network (Mfr) in the border, and central area with the axostyle trunk (Ax), Golgi bodies (G), hydrogenosomes (H), bacteria (B) and vesicles; **15** - high magnification of a section of figure **14** to show a Golgi body (G), hydrogenosomes (H) and bacteria (B); **16** - peripheral microfibrillar network (Mfr) with a condensed zone of microfibrils. Scale bars 1 µm.

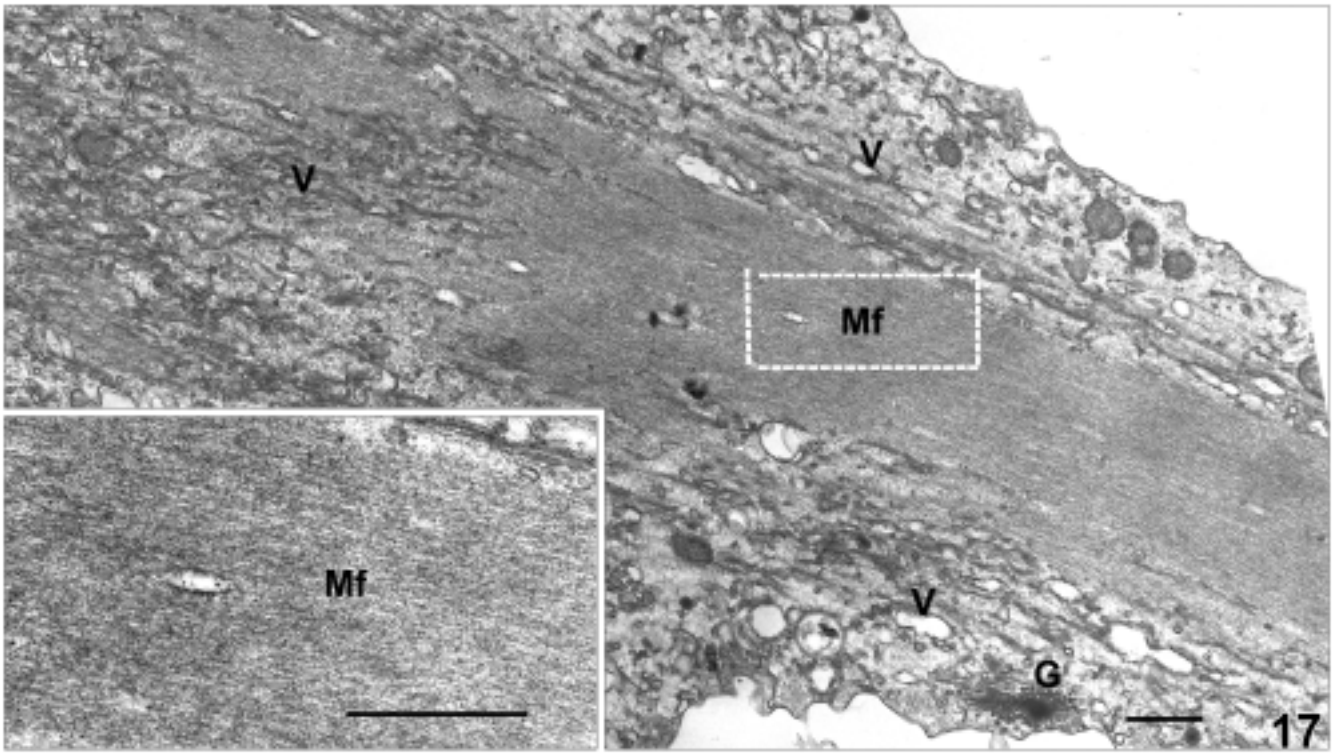

Fig. 17-inset. Transmission electron micrograph to show a bundle of microfilaments (Mf) forming a bridge between a broad pseudopodium and the cell body; many flat vesicles (V) and a Golgi body (G). Scale bar 1 µm.

The flagella are internalized or envacuolated inside the cytoplasm, the recurrent flagellum adhering to the cresta is located in a tube, and the three anteriorly-directed flagella are also envacuolated together (Fig. 23). The cresta structure is a thick microfibrillar lamina not surrounded by a membrane, and that joins the surface plasma membrane in a pad to which the recurrent flagellum adheres (Figs 24, 25). At its origin, the cresta is connected to the basal body R of the recurrent flagellum and to one parabasal fibre (Fig. 24). In the enlarged recurrent flagellum, the flagellar membrane forms a sheath containing the axoneme and loosely-packed microfibrillar material (Figs 24, 25). The junction of the recurrent flagellum adhering to the plasma membrane resembles a small desmosome with dense material associated with the two opposite membranes (Fig. 25). The axostyle trunk is composed of a rolled sheet of microtubules giving rise to a stout bundle of fibres (Figs 26-28).

Numerous Golgi bodies spread throughout the cytoplasm are supported by a thin striated parabasal fibre (Figs 14, 29). Hydrogenosomes were mixed with dense rod-shaped bacteria of the same diameter, but the latter were distinguished by a surrounding vacuolar membrane (Figs 14, 15). *G. herculea* phagocytoses large prey and also wood particles (not shown).

DISCUSSION

The present study confirms the identity and morphology of this amoeboid devescovinid. Results from immunofluorescence labelling are in strong agreement with the results of the former authors Dogiel (1916) and Kirby (1946), who used haematoxylin staining. Both techniques show the axostyle, the three long anteriorly-directed flagella, and the cord-like recurrent flagellum associated with a conspicuous cresta structure. Electron microscopy shows that the recurrent flagellum of *G. herculea* is as in other devescovinids- cord-shaped in *Foaina* or ribbon-shaped in *Devescovina* (Kirby 1941, 1942a, b; Mignot *et al.* 1969; Brugerolle 2000). The axostyle is organized as a rolled sheet of microtubules as in other devescovinids such as *Devescovina* and *Foaina*

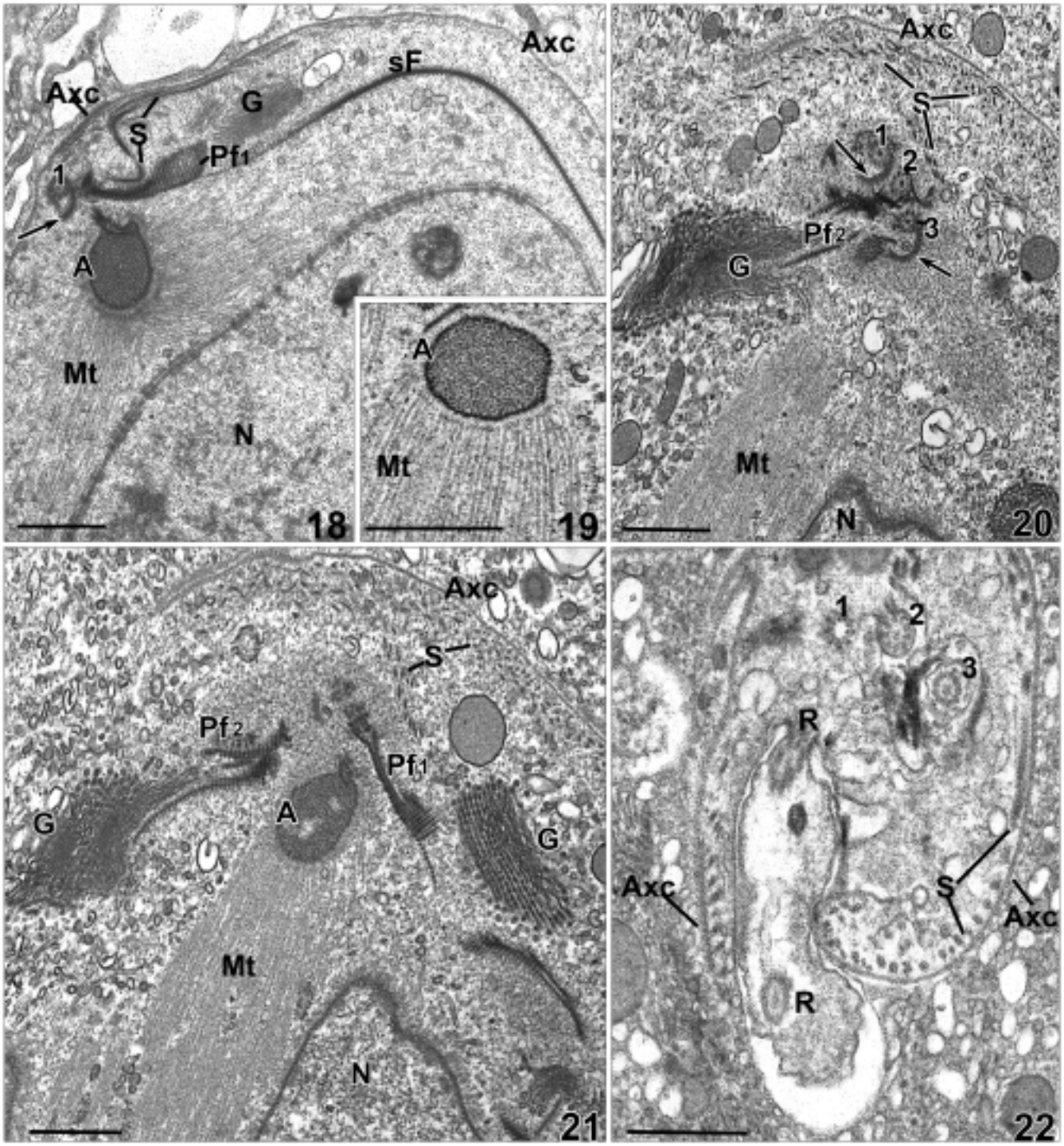

Figs 18-22. Transmission electron micrographs of the amoeboid stage of *Gigantomonas herculea*. **18-21** - basal bodies #1, #2, #3 of the anterior flagella, basal body #2 bearing the sigmoid fibres (S) that line the axostylar capitulum (Axc), basal bodies #1 and #3 bearing a hook-shaped lamina (arrows) **20**, the two parabasal fibres Pf1 and Pf2 attached to basal bodies and supporting a Golgi body (G) **21**, atractophore (A) attached to basal bodies with arising microtubules (Mt) **19**, thin striated fibre (sF) **18** close to the nucleus (N); **22** - section showing the three anteriorly-directed flagella #1, #2, #3 and the conspicuous recurrent flagellum (R) arising from the cell body and surrounded by the axostylar capitulum (Axc). Scale bars 1 µm.

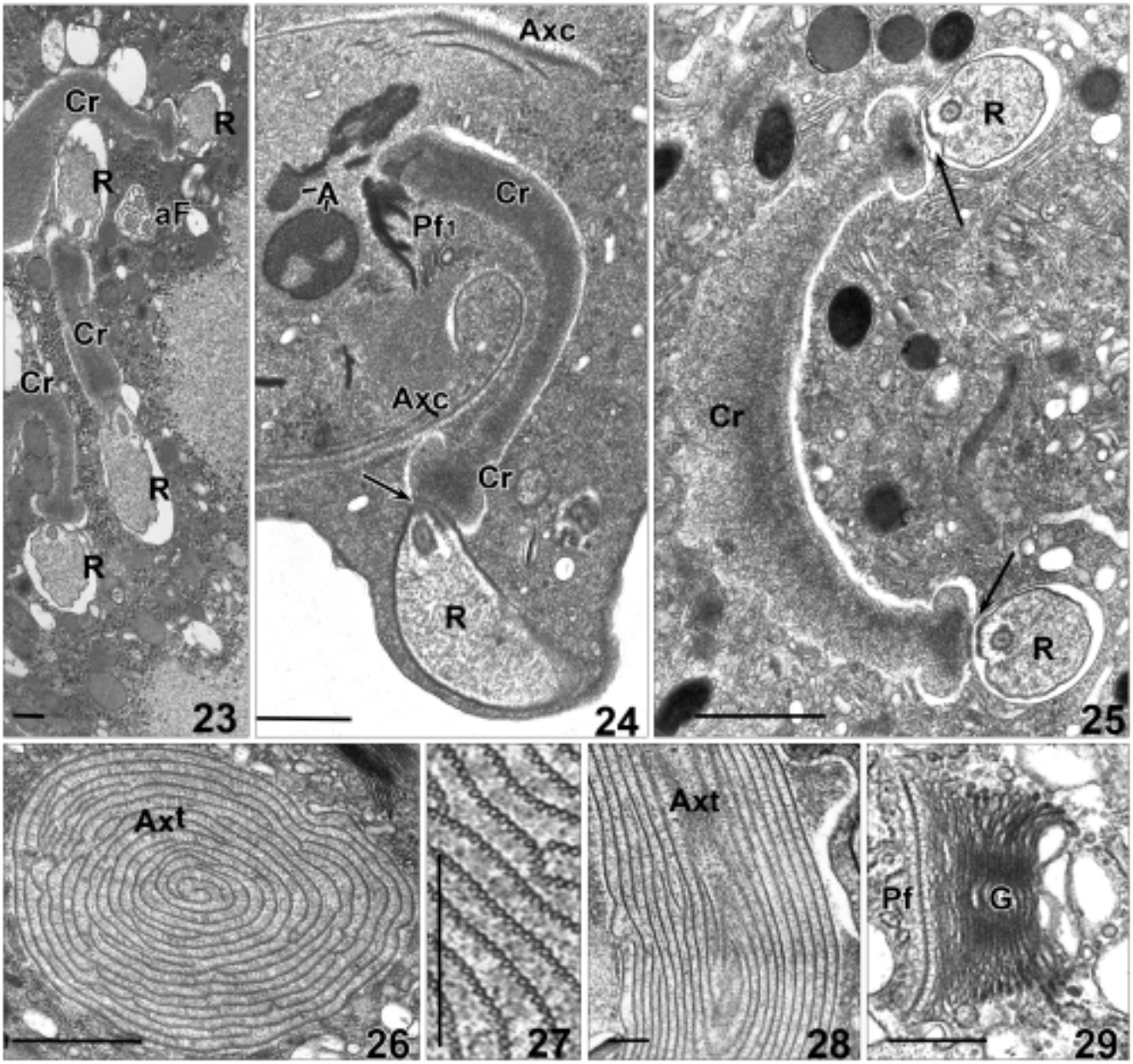

Figs 23-29. Transmission electron micrographs of the amoeboid stage of *Gigantomonas herculea*. **23 -** section showing the internalized flagella with the three anterior flagella (aF) and the enlarged recurrent flagellum (R) adhering to the cresta structure (Cr); **24, 25 -** the microfibrillar cresta structure (Cr) is linked to the parabasal fibre (Pf1) **24**, and the enlarged recurrent flagellum (R) adheres to the pad-like border of the cresta (Cr, arrows) **25**, axostylar capitulum (Axc), atractophore (A); **26, 27** - Transverse section of the axostyle trunk (Axt) showing the spiralled arrangement of the microtubular rows; **28 -** longitudinal section of the axostyle trunk (Axt) to show the organization of the microtubular rows; **29** - one of the Golgi bodies (G) supported by a striated fibre (Pf) that are spread throughout the central cytoplasm. Scale bars 1µm (23-26, 28, 29) and 0.5 µm (27).

(Brugerolle 2000) or some joeniids (Brugerolle and Patterson 2001). The close identity between the cresta structure of *Gigantomonas* and that of devescovinids is demonstrated. The cresta is the common structure to all the devescovinid genera described (Kirby 1941, 1942a, b), and its ultrastructure has been shown in *Devescovina* (Mignot *et al.* 1969), *Macrotrichomonas* (Hollande and Valentin 1969) and *Foaina* (Brugerolle 2000, Brugerolle and Radek 2005). It contains centrin protein as demonstrated by immunofluorescence labelling with the anti-centrin Mab 20H5 (Sanders and Salisbury 1994, Brugerolle *et al.* 2000). This finding is

confirmed by the labelling of the conspicuous cresta of *G. herculea* by Mab 4E5 which also labels the cresta of *Foaina grassei* from *Kalotermes flavicollis* (not shown).

The large cells of *G. herculea* have large atractophores, a centrosome equivalent (Hollande 1972), which are at the origin of spindle microtubules, and it is remarkable that Kirby (1946) observed them as "two unequal granules" at the base of the flagella in interphase cells. Similarly, Kirby (1946) also described the paradesmosis present in dividing cells after haematoxylin staining and which corresponds to my observations using light and electron microscopy. No parabasal apparatus was observed by Dogiel (1916), nor by Kirby (1946). Electron microscopy study only identifies a relatively small parabasal apparatus close to the nucleus. However numerous Golgi bodies are spread throughout the cytoplasm, and are supported by discrete striated parabasal fibres which are not obviously connected to the main fibres of the parabasal apparatus. The two main parabasal fibres subdivide into several thin fibres which might support Golgi bodies in their distal part, but their spatial distribution could not be studied further through the sections. This is reminiscent of similar observations in *Placojoenia* (Radek and Hausmann 1994) and *Mixotricha* (Brugerolle 2004).

Kirby (1946) identified three forms or stages in *G. herculea*, the motile flagellate form, the amoeboid form with a complete or reduced flagellar apparatus, and the plasmodial amoeboid form with many nuclei which was apparently not associated with a flagellar apparatus. The present study has only shown the amoeboid form that exhibits a complete internal flagellar apparatus. The motile flagellates were present but I was unable to identify a sufficient number for a study. Also, I did not find the large multinucleated plasmodial forms free of flagella described by Kirby (1946). The amoeboid form with internalized flagella was the most numerous in the termites I observed and with the procedure I used. Kirby (1946) noted that amoeboid cells placed in 0.67% salt solution transformed into flagellates after a few minutes, but I was unfortunately unable to perform such an experiment. The ability to internalize flagella is shared by the trichomonad genera *Trichomitus* and *Tritrichomonas* (Mattern *et al.* 1973, Stachan *et al.* 1984). When the cells of *Trichomitus batrachorum* or *Tritrichomonas muris* are transfered from their growth medium to the Ringer solution they transform in pseudocysts with internalized flagella. In contrast to *G. herculea*, they do not develop amoeboism and the associated microfibrillar structures.

Amoeboid cells of *G. herculea* are reminiscent of cells of other amoeboid parabasalids such as *Dientamoeba fragilis*, which has no flagella/basal bodies but has retained a parabasal apparatus and atractophore structures which polarise the paradesmosis of the dividing spindle (Camp *et al.* 1974). *G. herculea* seems different from heterolobosean amoeboflagellates such as *Naegleria* (Dingle and Fulton 1966) and *Tetramitus*, and other heteroloboseans which transform from flagellate form to amoeba form and *vice versa*. These amoeboflagellates lose their flagellar apparatus, including the basal bodies, when transforming into amoebae. In *G. herculea* only the internalization of the flagella is observed, but the large plasmodial form seems to be free of flagella under light microscopy analysis in Kirby's (1946) study.

Many parabasalids, such as *Dientamoeba*, *Histomonas*, *Gigantomonas, Trichomonas vaginalis* and also the large polymastigotes *Joenia* and *Trichonympha* (unpublished observations) exhibit amoeboism for phagocytosis to different degrees. In the better studied *Trichomonas vaginalis*, a microfibrillar network with a condensed area is associated with the adhering plasma membrane (Gonzales-Robles *et al.* 1995, Brugerolle *et al.* 1996, Bricheux *et al.* 2000), and this study shows that *G. herculea* exhibits the same structures. Remarkably, *G. herculea* is the first parabasalid in which long parallel microfilaments have been observed, and this indicates cytoplasmic streaming such as that found in the lobose amoebae *Amoeba proteus* and *Physarum* (Stockem and Klopocka 1988, Grębecki 1994, Stockem and Brix 1994). These observations should be correlated with those of Kirby (1946) who noted a "slow streaming in various directions, a limax type of locomotion in a limited degree" in the amoeboid *Gigantomonas* cells. Furthermore, he noted that these cells are able "to change shape slowly with long narrow processes and broad pseudopodia". Because *G. herculea* is symbiotic, it is difficult to cultivate and use for further studies on amoeboism. *Trichomonas vaginalis*, which is easy to cultivate and well on the way to having its genome sequenced, remains the most accurate model in parabasalids for such studies.

Incidentally, figures 4f-h of a dividing cell of *Gigantomonas herculea* were erroneously attributed to *Joenoides intermedia* in the paper Brugerolle and Bordereau (2003).

Acknowledgments. I would like to thank Dr C. Bordereau and A. Robert from the University of Dijon for culturing termites, and J.-L. Vincenot for printing photographs.

REFERENCES

Alderete J. F., Lehker M. W., Arroyo R. (1995) The mechanisms and molecules involved in cytoadherence and pathogenesis of *Trichomonas vaginalis. Parasitol. Today* **11:** 70-74

Black H. I. L., Okwakol M. J. N. (1997) Agricultural intensification, soil biodiversity and agroecosystem function in the tropics: the role of termites. *Appl. Soil Ecol.* **8:** 37-53

Breznak J. A., Brune A. (1994) Role of microorganisms in the digestion of lignocellulose by termites. *Ann. Rev. Ento.* **39:** 453-487

Bricheux G., Coffe G., Pradel N., Brugerolle G. (1998) Evidence for an uncommon α-actinin protein in *Trichomonas vaginalis*. *Mol. Biochem. Parasitol.* **95:** 241-249

Bricheux G., Coffe G., Bayle D., Brugerolle G. (2000) Characterization, cloning and immunolocalization of a coronin homologue in *Trichomonas vaginalis. Europ. J. Cell Biol.* **79:** 413-422

Brugerolle G. (2000) A microscopic investigation of the genus *Foaina*, a parabasalid protist symbiotic in termites and phylogenetic considerations. *Europ. J. Protistol.* **36:** 20-28

Brugerolle G. (2004) Devescovinid features, a remarkable surface cytoskeleton, and epibiotic bacteria in *Mixotricha paradoxa*, a parabasalid flagellate. *Protoplasma* **224:** 49-59

Brugerolle G., Bordereau C. (2003) Ultrastructure of *Joenoides intermedia* (Grassé 1952), a symbiotic parabasalid flagellate of *Hodotermes mossambicus*, and its comparison to other joeniid genera. *Europ. J. Protistol.* **39:** 1-10

Brugerolle G., Lee J. J. (2001) Phylum Parabasalia. In: An Illustrated Guide to the Protozoa, (Eds. J. J. Lee, G. F. Leedale, P. C. Bradbury). Society of Protozoologists Lawrence Kansas, 2nd ed., **II:** 1196-1250

Brugerolle G., Patterson D. J. (2001) Ultrastructure of *Joenina pulchella* Grassi, 1917 (Protista, Parabasalia), a reassessment of evolutionary trends in the parabasalids, and a new order Cristamonadida for devescovinids, calonymphids and lophomonad flagellates. *Org. Divers. Evol.* **1:** 147-160

Brugerolle G., Radek R. (2005) Symbiotic protozoa of termites. In: Intestinal Microorganisms of Termites and other Invertebrates, (Eds. H. König, A. Varma). New Series Soil Biology, Springer-Verlag, Heidelberg, (in press)

Brugerolle G., Viscogliosi E. (1994) Organization and composition of the striated roots supporting the Golgi apparatus, the so-called parabasal apparatus, in parabasalid flagellates. *Biol. Cell* **81:** 277-285

Brugerolle G., Bricheux G., Coffe G. (1996) Actin cytoskeleton demonstration in *Trichomonas vaginalis* and in other trichomonads. *Biol. Cell* **88:** 29-36

Brugerolle G., Bricheux G., Coffe G. (2000) Centrin protein and genes in *Trichomonas vaginalis* and close relatives. *J. Eukar. Microbiol.* **47:** 129-138

Brune A. (1998) Termites guts: the world's smallest bioreactors. *Trends Biotechnol.* **16:** 16-21

Camp R. R., Mattern C. F. T., Honigberg B. M. (1974) Study of *Dientamoeba fragilis* Jepps & Dobell. I. Electron microscopic observations of the binucleate stages. II. Taxonomic position and revision of the genus. *J. Protozool.* **21:** 69-82

Dingle A., Fulton C. (1966) Development of the flagellar apparatus of *Naegleria. J. Cell Biol.* **31:** 43-54

Dogiel V. A. (1916) Researches on the parasitic protozoa from the intestine of termites. Tetramitidae. *Zool. Zh.* **1:** 1-35 (Russian), 36-54 (English)

Gerbod D., Noël C., Dolan M. F., Edgcomb V. P., Kitade O., Noda S., Dufernez F., Ohkuma F., Kudo T., Capron M., Sogin M. L., Viscogliosi E. (2002) Molecular phylogeny of parabasalids inferred from small subunit rRNA sequences, with emphasis on the Devescovinidae and Calonymphidae (Trichomonadae). *Mol. Phylogenet. Evol.* **25:** 545-556

Grębecki A. (1994) Membrane and cytoskeleton flow in motile cells with emphasis on the contribution of free-living amoebae. *Int. Rev. Cytol.* **148:** 37-79

Gonzales-Robles A., Lazaro-Haller A., Espinosa-Cantellano M., Anaya-Velazquez F., Martinez-Palomo A. (1995) *Trichomonas vaginalis*: ultrastructure bases of the cytopathic effect. *J. Eukar. Microbiol.* **42:** 641-651

Grassé P.-P. (1952) Ordre des Trichomonadines. In: Traité de Zoologie, Flagellés, (Ed. P.-P. Grassé). Masson et Cie, Paris, **1:** 705-779

Hausmann K., Hülsmann N., Radek R. (2003) Protozoology, 3rd ed., Schweizerbart, Stuttgart

Hollande A. (1972) Le déroulement de la cryptomitose et les modalités de la ségrégation des chromatides dans quelques groupes de Protozoaires. *Ann. Biol.* **11:** 427-466

Hollande A., Valentin J. (1969) La cinétide et ses dépendances dans le genre *Macrotrichomonas* Grassi. Considérations générales sur la sous-famille des Macrotrichomonadinae. *Protistologica* **5:** 335-343

Honigberg B. M. (1970) Protozoa associated with termites and their role in digestion. In : Biology of Termites, (Eds. K. Krishna, F. M. Weesner), Academic Press, New York, **2:** 1-36

Honigberg B. M., Bennett C. J. (1971) Light microscopic observations on structure and division of *Histomonas meleagridis* (Smith). *J. Protozool.* **18:** 687-697

Honigberg B. M., Brugerolle G. (1990) Structure. In: Trichomonads Parasitic in Humans, (Ed. B. M. Honigberg). Springer Verlag, New York 5-35

Inoue, T., Kitade O., Yoshimura T., Yamaoka I. (2000) Symbiotic associations with protists. In: Termites: Evolution, Sociability, Symbioses, Ecology, (Eds T. Abe, D. E. Bignell, M. Higashi). Kluwer, the Netherlands 275-288

Keeling P. J., Poulsen N., McFadden G. I. (1998) Phylogenetic diversity of parabasalian symbionts from termites, including the phylogenetic position of *Pseudotrypanosoma* and *Trichonympha. J. Eukar. Microbiol.* **45:** 643-650

Kirby H. (1941) Devescovinid flagellates in termites I. The genus *Devescovina*. *Univ. Calif. Pub. Zool.* **45:** 1-92

Kirby H. (1942a) Devescovinid flagellates of termites II. The genera *Caduceia* and *Macrotrichomonas. Univ. Calif. Pub. Zool.* **45:** 93-166

Kirby H. (1942b) Devescovinid flagellates of termites III. The genera *Foaina* and *Parajoenia*. *Univ. Calif. Pub. Zool.* **45:** 167-246

Kirby H. (1946) *Gigantomonas herculea* Dogiel, a polymastigote flagellate with flagellated and amoeboid phases of development. *Univ. Calif. Publ. Zool.* **53:** 163-226

König H., Fröhlich J., Berchtold M., Wenzel M. (2002) Diversity and microhabitats of the hindgut flora of termites. *Recent Res. Devel. Microbiol.* **6:** 125-156

Lobry de Bruyn L. A., Conacher A. J. (1990) The role of termites and ants in soil modifications: a review. *Aust. J. Soil Res.* **28:** 55-93

Mannesmann R. (1972) Relationship between different wood species as a termite food source and the reproduction of termite symbionts. *Z. ang. Ent.* **72:** 116-128

Mattern C. F. T., Honigberg B. M., Daniel W. A. (1973) Fine structural changes associated with pseudocyst formation in *Trichomitus batrachorum. J. Protozool.* **20:** 222-229

Mignot J.-P., Joyon L., Kattar M. R. (1969) Sur la structure de la cinétide et les affinités systématiques de *Devescovina striata* Foa, Protozoaire flagellé. *C. R. Acad. Sci. Paris* **268:** 1738-1741

Nel J. J. C., Hewith P. H. (1969) A study of the food eaten by a field population of the harvester termite *Hodotermes mossambicus* (Hagen), and its relation to population density. *J. Entomol. Soc. Africa* **32:** 123-131

Odelson D. A., Breznak J. A. (1985) Cellulase and other polymer-hydrolyzing activities of *Trichomitopsis termopsidis*, a symbiotic protozoan from termites. *App. Env. Microbiol.* **49:** 622-626

Ohkuma M., Ohtoko K., Iida T., Tokura M., Moryia S., Usami R., Horikoshi K., Kudo T. (2000) Phylogenetic identification of hypermastigotes, *Pseudotrichonympha*, *Spirotrichonympha*, *Holomastigotes*, and parabasalian symbionts in the hindgut of termites. *J. Eukar. Microbiol.* **47:** 249-259.

Radek R., Hausmann K. (1994) *Placojoenia sinaica* n. g., n. sp., a symbiotic flagellate from the termite *Kalotermes sinaicus*. *Europ. J. Protistol.* **30:** 25-37

Sanders M. A., Salisbury J. F. (1994) Centrin plays an essential role in microtubule severing during flagellar excision in *Chlamydomonas reinhardtii*. *J. Cell Biol.* **124:** 795-805

Schuster F. L. (1968) Ultrastructure of *Histomonas meleagridis* (Smith) Tyzzer, a parasitic amoebo-flagellate. *J. Parasitol.* **54:** 725-737

Stachan R., Nicol C., Kunstyr I. (1984) Heterogeneity of *Tritrichomonas muris* pseudocysts. *Protistologica* **20:** 157-163

Stockem W., Brix K. (1994) Analysis of microfilament organization and contractile activities in *Physarum. Int. Rev. Cytol.* **149:** 145-215

Stockem W., Klopocka W. (1988) Amoeboid movement and related phenomena. *Int. Rev. Cytol.* **112:** 137-184

Watanabe H., Noda H., Tokura G., Lo N. (1998) A cellulase gene of termite origin. *Nature* **394:** 330-331

Wenrich D. H. (1943) Observations on the morphology of *Histomonas* (Protozoa, Mastigophora) from pheasants and chickens. *J. Morphol.* **72:** 279-303

Wenrich D. H. (1944) Nuclear structure and nuclear division in *Dientamoeba fragilis* (Protozoa). *J. Morphol.* **74:** 467-491

Windsor J. J., Johnson E. H. (1999) *Dientamoeba fragilis*: the unflagellated human flagellate. *Biomed. Sci.* **56:** 293-306

Wood T. G. (1988) Termites and the soil environment. *Biol. Fertil. Soils* **6:** 228-236

Yamin M. A. (1979) Flagellates of the Orders Trichomonadida Kirby, Oxymonadida Grassé, and Hypermastigida Grassi & Foà reported from lower termites (Isoptera families Mastotermitidae, Kalotermitidae, Hodotermitidae, Termopsidae, Rhinotermitidae, and Serritermitidae) and from the wood-feeting roach *Cryptocercus* (Dictyoptera: Cryptocercidae). *Sociobiology* **4:** 1-120

Yoshimura T. (1995) Contribution of the protozoan fauna to nutritional physiology of the lower termites *Coptotermes formosanus* Shiraki (Isoptera: Rhinotermitidae). *Wood Res*. **82:** 68-129

Received on 7th December, 2004; revised version on 25th February, 2005; accepted on 3rd March, 2005

Acta Protozool. (2005) 44: 201 - 215

ACTA
PROTOZOOLOGICA

The Unusual, Lepidosome-coated Resting Cyst of *Meseres corlissi* (Ciliophora: Oligotrichea): Light and Scanning Electron Microscopy, Cytochemistry

Wilhelm FOISSNER[1], Helga MÜLLER[2] and Thomas WEISSE[3]

[1]Universität Salzburg, FB Organismische Biologie, Salzburg, Austria; [2]Private Laboratory, Constance, Germany; [3]Institut für Limnologie der Österreichischen Akademie der Wissenschaften, Mondsee, Austria

Summary. *Meseres corlissi* Petz *et* Foissner, 1992 is a planktonic, spirotrich ciliate closely related to the common *Halteria grandinella*. Pure cultures were established with *Cryptomonas* sp. as a main food source. Thus, resting cyst formation and structure could be studied by light and scanning electron microscopy and cytochemical methods. The resting cyst of *M. corlissi* belongs to the kinetosome-resorbing (KR) type and has a conspicuous coat of extracellular organic scales, here termed lepidosomes, embedded in mucus mainly composed of acid mucopolysaccharides, as shown by the strong reaction with alcian blue. The lepidosomes, which likely consist of glycoproteins, are finely faceted, hollow spheres with a diameter of 2-14 µm. They are formed underneath the cortex and liberated almost concomitantly to the external surface of the cell before the cyst wall is produced. Resting cyst size is dependent on temperature, the average diameter is 46 µm (without lepidosome coat) at 20°C. The cyst wall, which contains considerable amounts of glycoproteins and a layer of chitin, is smooth, 1.5-2 µm thick, and composed, in the light microscope, of two distinct layers highly resistant to various inorganic and organic solvents. The cyst doubles the diameter during excystment and the lepidosome coat is left behind. The occurrence of lepidosomes throughout the ciliate phylum, their genesis and function, and the conspicuous morphological similarity with leafhopper's brochosomes are discussed.

Key words: brochosomes, Cicadellidae, Colpodea, encystment, Haptorida, organic scales, plankton ciliates, protozoa, Trachelophyllida.

INTRODUCTION

Many ciliates form a dormant stage, the resting cyst, when environmental conditions become adverse and/or food is depleting. The cyst is composed of a several µm thick wall protecting the cell from a wide variety of detrimental influences, such as drought, heat, and chemicals (Corliss and Esser 1974, Foissner 1987, Gutiérrez *et al.* 2001). The wall is a complex structure usually composed of three layers, that is, the ectocyst, the mesocyst, and the endocyst. Chemically, these layers consist of varying amounts of carbohydrates (often in form of chitin), proteins, and glycoproteins (Mulisch 1993, Gutiérrez *et al.* 2003, Rosati *et al.* 2004). Usually, ciliate resting cysts are spherical or ellipsoidal and several have a preformed orifice through which the excysting cell leaves the cyst. The external cyst wall morphology is highly different among the various ciliate groups and species, that is, the wall may be smooth,

Address for correspondence: Wilhelm Foissner, Universität Salzburg, FB Organismische Biologie, Hellbrunnerstrasse 34, A-5020 Salzburg, Austria; E-mail: Wilhelm.Foissner@sbg.ac.at

tuberculate, faceted, or spiny (for reviews, see Foissner 1993; Berger 1999; Foissner *et al.* 1999, 2002).

Generally, data on ciliate resting cysts are rather incomplete, most coming from only two groups, viz., the spirotrichs (e.g., *Oxytricha*, *Euplotes*, *Blepharisma*; for reviews, see Wirnsberger-Aescht *et al.* 1990, Berger 1999 and Gutiérrez *et al.* 2001) and the Colpodea (for reviews, see Foissner 1993 and Gutiérrez *et al.* 2003). Few data are available from the oligotrichine spirotrichs (for a brief review, see Müller 2000), of which *Meseres corlissi* and the common *Halteria grandinella* are representative examples.

The present study, which consists of two parts, provides the first detailed morphological investigation of the resting cyst of an oligotrichine, halteriid spirotrich, using light and electron microscopy and some cytochemical methods. Such data are urgently needed for comparative purposes and the discussion of the systematic position of halteriid spirotrichs (Foissner *et al.* 2004). In contrast to some other investigators, we perform detailed investigations not only on preserved but also on living cysts because various features, especially morphometrics and colour may greatly change or even remain unrecognized in fixed material, as is the case in various colpodids (Foissner 1993, Díaz *et al.* 2003). Further, such data enhance the interpretation of the electron microscopical findings and the identification of cysts by ecologists. Indeed, the resting cyst of *M. corlissi* is so characteristic that it can be easily identified in field collections of cysts, as performed by ecologists (Müller 2000).

Our investigations show that the resting cyst of *M. corlissi* is unique in having spherical, nicely faceted epicortical scales reminiscent of those found in trophic trachelophyllid ciliates (Nicholls and Lynn 1984, Foissner *et al.* 2002). A detailed literature search showed that epicortical structures occur in trophic and cystic ciliates from various classes. This, however, remained obscure because they have been described under a huge variety of names. Thus, we suggest to collect epicortical structures under a single term: lepidosomes.

MATERIALS, METHODS AND TERMINOLOGY

Origin of cultures and stock culture conditions. Most morphological investigations were performed on a *Meseres corlissi* population collected by Prof. Dr. Walter Till (Vienna University, Austria) in the Dominican Republic, viz., in the tanks of *Guzmania ekmanni*, a bromeliad plant found on a tree of the fog rain forest on the Pico Diego del O'Campo near the town of Santiago. The senior author identified the species according to the original description by Petz and Foissner (1992). The observations on encystment and the cytochemical investigations were performed on cysts from the type population, re-sampled in the city area of Salzburg (Austria) in November 2002.

Raw cultures of *M. corlissi* were established on Eau de Volvic (French table water) enriched with some squashed wheat grains. This raw culture was purified and adapted to an algal diet composed of *Cryptomonas* sp. strain 979-4 (Culture Collection of Algae, SAG, Göttingen, Germany). Both the ciliate and cryptophyte were maintained in modified Woods Hole medium (MWC medium, Guillard and Lorenzen 1972) at 15 ± 1°C and continuous light (100 µmol photons $m^{-2}s^{-1}$).

Induction of encystment and excystment. Cultures in the stationary growth phase were transferred to room temperature (~ 19°C) and starved which caused encystment of most cells within 48 h. Starved cells were pipetted into thin micro-aquaria made of vaseline and a cover glass on a microscope slide and observed for encystment every 30 min. Excystment could be induced by transferring a cyst containing culture from 15 to 24°C.

Temperature response experiments. *Cryptomonas* sp. was offered at saturating food levels to Dominican Republic *M. corlissi* in sterile 200 ml tissue-culture bottles. Samples were taken from experimental containers 48 h after the beginning of the experiment and fixed with Lugol's iodine (final concentration 2% vol/vol). The fraction of cysts was calculated as the number of cysts in a sample, divided by the total number of trophic plus encysted cells. Length and width of cysts were measured by inverted microscopy and image analysis (LUCIA version 4.51, Laboratory Imaging Ltd.). Details of these experiments have been reported elsewhere (Weisse 2004).

Morphological and cytological methods. Cysts were studied *in vivo*, in protargol preparations, and with the scanning electron microscope, using the methods described in Foissner (1991). *In vivo* measurements were conducted at a magnification of ×1000. The nature (organic, inorganic) and chemical composition of the lepidosomes were determined with cytochemical methods described in Adam and Czihak (1964), Tracey (1955) and Romeis (1968), on both, cysts fixed with ethanol (96%) or neutral formalin (5%). Then, the cysts were washed in distilled water, mounted on slides with albumen-glycerol, air-dried, and the albumen hardened in ethanol (100%). For the cytochemical methods, the slides were rehydrated *via* a graded ethanol series. Tests with alcian blue, Lugol's solution, and osmium acid (2%) were made also on unfixed cysts. However, results were similar to those obtained with fixed cysts. This applies also to cysts fixed either with ethanol or formalin. Thus, results are not shown separately in Table 3. Cyst wall solubility was determined with several inorganic and organic solvents mentioned in the results section.

Chitin was detected with the Van Wisselingh colour test, as described in Tracey (1955). This simple, fast method deacetylates chitin with KOH to chitosan which gives a deep, redbrown colour with iodine. Landers (1991) used the method for revealing chitin in the cyst wall of *Hyalophysa chattoni*, a parasitic ciliate on shrimps. Our experiences with cysts of *Meseres* and other ciliates and materials suggest that this test is highly reliable for both, chitin and cellulose. Thus and because it disappeared from the modern literature, we provide the full protocol, as described in Tracey (1955).

"About a milligram of the material to be tested is heated, in a small tube closed with a Bunsen valve, with potassium hydroxide solution saturated at room temperature (dissolve about 120 g KOH in 100 ml water). The contents of the tube are heated by immersing the lower portion in a glycerine bath the temperature of which is raised to 160°C over a period of 15-20 mins. It is held at this temperature for a further 15 mins and allowed to cool to room temperature. If no insoluble material is present then chitin in appreciable quantities is absent. Any insoluble material is transferred manually, or after centrifugation, to 95% alcohol and washed successively with 70%, 50%, and 30% alcohol and finally with water (solutions of glycerol may be used in place of alcohol). Few substances other than cellulose and inorganic material [either adventitious (sand) or intrinsic (barium sulphate in some fungi)] are likely to withstand this treatment. A portion of the material is placed on a slide and covered with a drop of 0.2% iodine in potassium iodide solution. The material will turn brown and this colour will be replaced by a red-violet on the addition of 1% sulphuric acid if chitosan is present. Replacement of the acid iodine solution by 75% sulphuric acid will result in the dissolution of the material. If cellulose is present it will not be coloured by the acid iodine reagent, but will turn blue and swell, instead of dissolving, on the addition of 75% sulphuric acid.

Notes. (1) Washing with progressive dilutions of alcohol has the advantage that less dissolution of the material occurs and that the yield of chitosan appears to be increased.

(2) Many attempts have been made to simplify the alkali treatment by using weaker solutions for longer periods, by evaporating to dryness in alkali, or by boiling in alkali. None gives such satisfactory results as that outlined above.

(3) Some material may have a reddish colour after the alkali treatment. If this is so it is probably as well to relay on the chitosan sulphate test.

(4) Failure to get the colour reaction is not conclusive evidence of the absence of chitin. Delicate structures such as butterfly scales may disperse completely during the normal time of heating, and the iodine colour test may be occasionally negative when the chitosan sulphate test is positive.

(5) It may be desirable to pretreat some materials. Dilute alkali will remove much organic matter thus concentrating chitin in the material to be tested. 0.2 M sodium chlorate at pH 5.0 and 75°C will decolourise the darkest fungal material besides greatly reducing the proportion of non-chitinous organic material."

The sole critical step is the time of KOH treatment. Usually, ciliate cysts dissolve completely if treated for 30 min, as given above. Thus, we used 15-20 min. Further, the complicated heating described above can be simplified by pre-heating 3 ml KOH to 160°C in a glass centrifuge tube and adding the concentrated material directly into the hot KOH solution for 15-20 min. For *Meseres*, the test was performed with the original and the modified protocol with the same result. The modification runs as follows: the cysts were concentrated by centrifugation and the pellet put in 3 ml saturated, hot (160°C), aquaous potassium hydroxide solution (KOH) for 20 min at 160°C. Small, cleaned parts of meal beetle larvae (*Tenebrio molitor*) and some cotton wool served as controls and were added to the preparation. After heating, the probe was diluted with tap water to 10 ml and centrifuged for one min at 3000 x g. The resulting pellet was washed five times in tap water, some drops of 1% sulphuric acid were added to the last wash to dissolve minute (carbonate?) crystals. Finally, a minute drop of the washed pellet was put on a slide, covered with a coverslip, and investigated at a magnification of ×1000 (oil immersion). This revealed many very hyaline, globular cyst "ghosts" which stained reddish to deep redbrown when Lugol´s solution was added from the margin of the coverslip. Controls were treated in the same way and differentiated as described above.

Terminology. Terminology is according to Corliss (1979) and Gutiérrez *et al.* (2003), while the systematic classification follows Lynn (2003) and Agatha (2004). However, we introduce "lepidosomes" (lepidotos Gr. - scaled, soma, Gr. - body) as a new term for all kinds of epicortical (extracellular), organic structures of definite shape produced intracellularly by trophic and/or cystic ciliate species. For details, see first chapter of Discussion.

RESULTS

Trophic cells

The specimens from the Dominican Republic are highly similar to those from the Austrian type population (Fig. 7), but are, both in the field sample and well-growing cultures, frequently distinctly conical and may even have a short tail (Fig. 4). However, conical cells occur also in flourishing pure cultures of the Austrian population. Broadly ellipsoidal cells, as shown in the original description (Petz and Foissner 1992), occur mainly in old and/or oxygen-depleting cultures. The specimens have a size of about 75 × 50 µm *in vivo* and are covered by circa eight equidistant rows of about 16 µm long bristles. The anterior body end is occupied by about 16 collar and 15 ventral adoral membranelles (Figs 4, 7).

Trophic and dividing specimens, including the somatic cilia and adoral membranelles, are coated by a skin-like layer of slime, especially the peristomial bottom, where the layer is thickened. This coat is invisible *in vivo*, but becomes distinct in the scanning electron microscope (Figs 4-6) and when living cells are immersed in alcian blue, especially in the oral area, where flakes of bluish material are released. Depending on the state of preservation, the slime coat appears granular (well preserved) or reticular (poorly preserved), partially exposing the smooth pellicle and the cilia in the scanning electron microscope (Fig. 6). The slime coat is also obvious in the Austrian specimens studied by Petz and Foissner (1992), who did not comment on it. The strong reaction with alcian blue indicates that the coat contains considerable amounts of acid mucopolysaccharides (Adam and Czihak 1964).

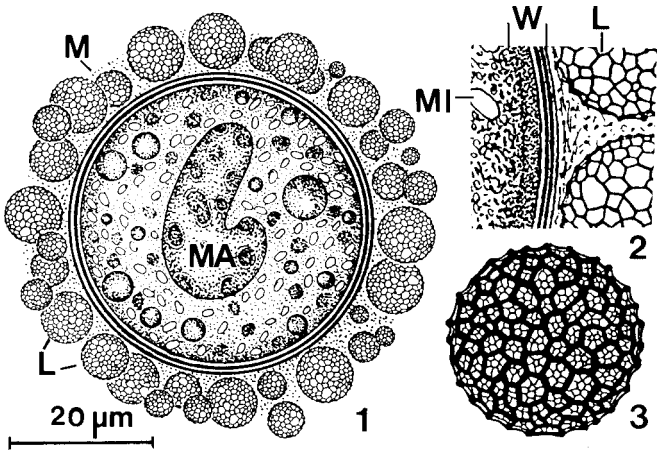

Figs 1-3. *Meseres corlissi*, resting cyst of a specimen from the Dominican Republic in the light (1, 2) and scanning electron microscope (3). **1** - Overview, diameter with lepidosome coat about 60 µm; **2** - detail from figure 1 showing, inter alia, the about 1.6 µm thick cyst wall composed of two main layers; **3** - lepidosome at high magnification, diameter 9 µm. L - lepidosomes, M - mucus, MA - macronucleus, MI - mitochondrium (?), W - cyst wall.

Encystment

Of 20 specimens isolated from a non-flooded Petri dish raw culture (Foissner 1987), 17 (85%) produced perfect resting cysts within 12 h. When specimens from the Dominican Republic were cultivated at 19°C and transferred to 4°C, encystment was accomplished within 1 h. In growth experiments, encystment was negligible at temperatures >20°C but increased dramatically if temperature was below 20°C (Table 1). The ciliate did not grow at temperatures <15°C, and food had little effect on cyst production (Weisse 2004). Note that the encystment success may decrease to a few percent in strains cultivated for several months in the laboratory, and many of the cysts may appear defect. Obviously, encystment depends on many factors whose investigation was outside the scope of the present study.

The microaquaria worked quite well, that is, many starved cells produced cysts within 12 h. However, the percentage of non-producers is often near 50%, that is, these specimens do not encyst and most die within 24 h. As the dying specimens become globular, they are frequently not easily distinguished from ordinary, encysting cells. Further, the microscopic observation with oil immersion appears to disturb more or less distinctly the encystment process. Thus, some luck and patience are needed to see and document the following details.

When encystment commences, the cell rounds up and resorbes the somatic and oral cilia and basal bodies (Figs 21, 22). This is not only shown by the transmission electron microscopical investigations (Foissner 2005), but also by observations on protargol-impregnated cysts (no micrographs are provided because they would show only very small areas due to the globular shape of the cyst). 100 well-impregnated cysts each from three different cultures and of three different ages showed the following pattern: 4 days old cysts (99 without, 1 with basal bodies), 9 days old (89/11), 30 days old (97/3). Thus, only 5% of the cysts show basal bodies and their maintenance is not age-related. Only 1 of the 15 cysts with basal body remnants maintained the complete ciliary pattern, though in rather distorted condition, while the others preserved merely small parts of the ventral adoral zone of membranelles. Similar results were obtained with silver carbonate impregnation. Thus, *M. corlissi* belongs to the kinetosome-resorbing (KR) cyst type, according to the classification of Walker and Maugel (1980).

During rounding up, the cell secretes a thin layer of fluffy mucus. Fully developed lepidosomes with faceted wall become visible underneath the cortex when the cell has rounded up (Figs 22–24); frequently, the proximal part of the somatic and oral cilia is still recognizable. Next, the lepidosomes and additional mucus are released almost concomitantly within a few minutes. We could see details of this process only once, and from this it appears that the lepidosomes are released concomitantly by an exocytotic process. We never observed additional lepidosome release in cysts with a lepidosome coat, likely because cyst wall formation commences immediately after release of the lepidosomes (Fig. 25).

Resting cysts

Morphology: Resting cysts are very similar in the Dominican Republic and the Austrian specimens (cp. Figs 15, 16, 27). However, only cysts of the former were studied in detail. The cysts are firmly attached to the bottom of the culture dishes, likely by the mucilage described below. Even strong shaking or water flushes do not detach all from the substrate. Thus, the mucus and the lepidosome coat are usually partially destroyed when cysts are collected for SEM preparations or transferred with a pipette to the microscope slide.

The resting cysts have an average diameter of 58 × 58 µm with and 47 × 45 µm without the lepidosome coat, that is, they are usually spherical, rarely slightly ellipsoi-

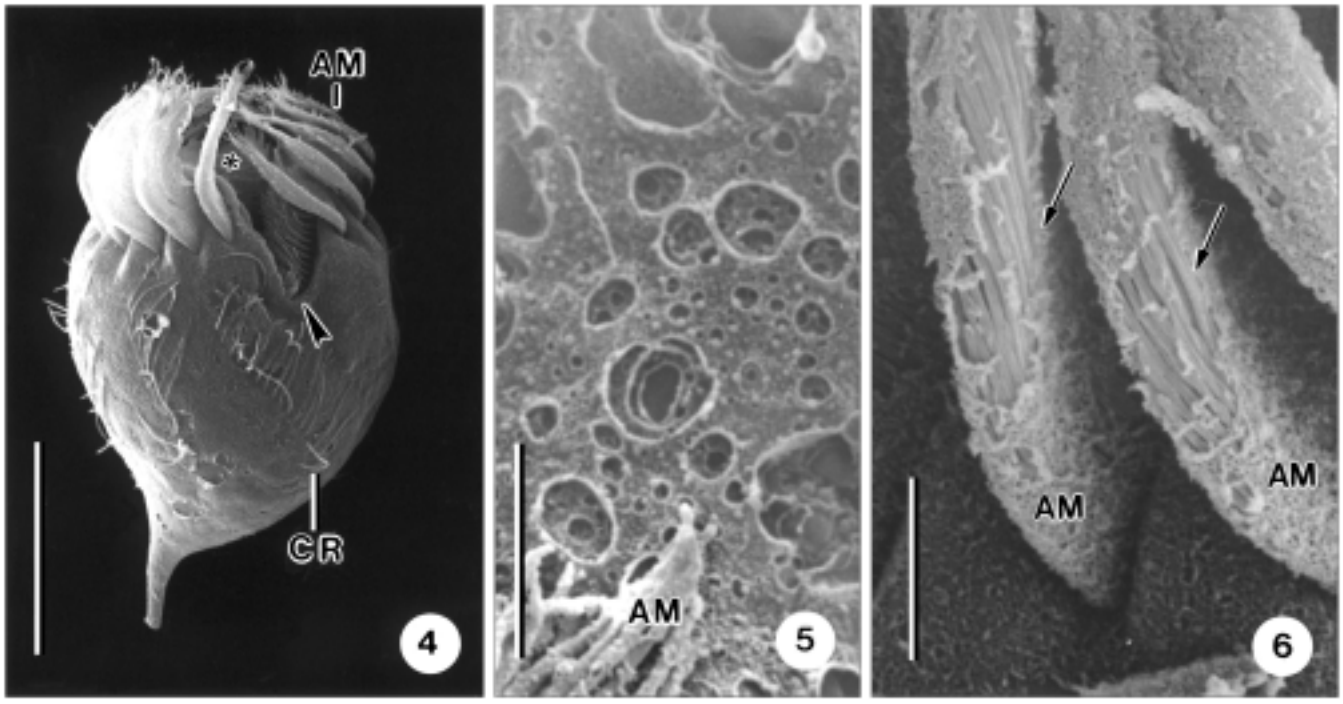

Figs 4-6. *Meseres corlissi*, trophic cells from the Dominican Republic in the scanning electron microscope. These figures show a mucilaginous layer coating the whole cell, including somatic cilia and adoral membranelles. **4** - ventral view of a tailed specimen. The mucilaginous coat is damaged left of the ciliary row (CR). The arrowhead denotes the buccal vertex. The asterisk marks the peristomial bottom, shown at higher magnification in the next figure; **5** - the peristomial bottom is covered by a thicker mucilage, whose circular structures are likely preparation artifacts; **6** - proximal portion of three adoral membranelles which are also covered with mucilage. Arrows mark regions where the coat is damaged exposing the membranellar cilia. AM - adoral membranelles, CR - somatic ciliary row. Scale bars: 30 µm (4) and 5 µm (5,6).

dal with a maximum of 47 × 40 µm (Table 2). Temperature significantly impacted length and width of resting cysts, that is, size increased from 15 to 20°C and declined rapidly at 22.5°C (Table 1). At temperatures >20°C, the few cysts that were formed during the experiments appeared defective. Sizes of live and Lugol-fixed cysts were not different at 19-20°C (cp. Tables 1, 2). The wall is colourless, while the cyst content is more or less distinctly orange due to the cryptomonad food. The cyst wall is smooth, 1.6 µm thick on average, and consists of two flexible layers, viz., an about 0.6 µm thick outer layer and an about 1 µm thick, gelatinous inner layer; the outer zone comprises several sublayers in fortunate preparations and collapses to a single layer under too heavy coverslip pressure (Figs 1, 2, 14). Wall flexibility is high because cysts can be flattened considerably by coverslip pressure without destroying the wall (Figs 14-16). Underneath the cyst's wall, likely in the cortex of the cell, are distinct, radially extending fibres providing the cyst with an axis; they impregnate with protargol and have a granular or smooth appearance *in vivo* (Figs 12, 13). The densely granulated content consists of (i) the centrally located, broadly reniform macronucleus with conspicuously bright nucleoli; (ii) some lipid droplets 1-10 µm across (stain with Sudan red and become blackish in osmic acid); (iii) many pale granules about 3 × 2 µm in size, likely mitochondria; and (iv) many 3-6 µm-sized (autophagous?) vacuoles with granular content (Figs 1, 2, 15, 27).

The cyst is covered by a conspicuous coat of lepidosomes embedded in an about 10 µm thick layer of mucus which is very hyaline and structureless *in vivo*, while composed of many fibres forming a more or less dense reticulum in the scanning electron microscope (Figs 1, 10, 11, 15, 19, 20). The mucus often forms a finely reticular coat from which only the larger lepidosomes stand out as inconspicuous hemispheres. The mucus fibres connect also individual lepidosomes and are 0.06-0.12 µm thick in the scanning electron microscope. We believe that these comparatively thick

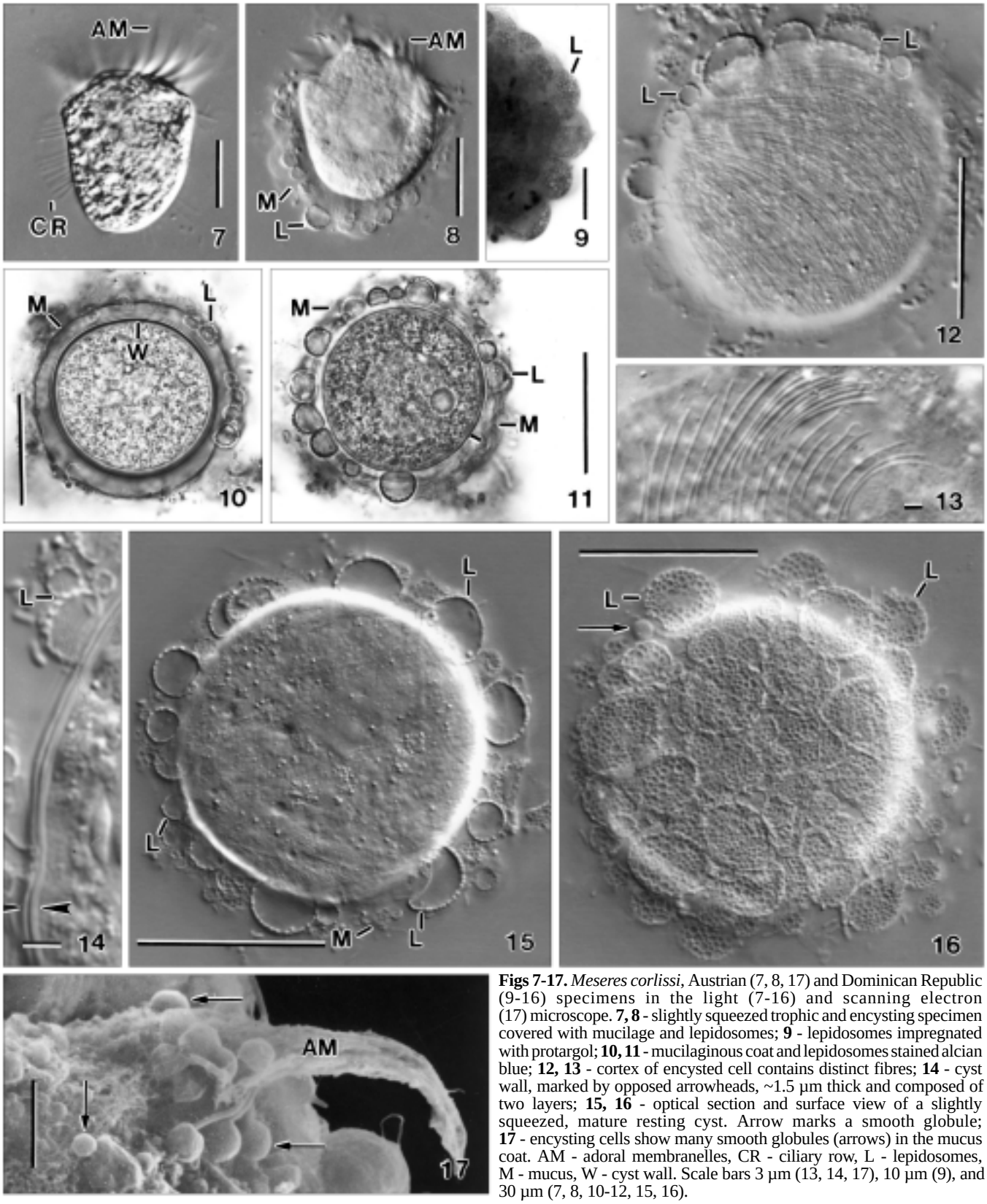

Figs 7-17. *Meseres corlissi*, Austrian (7, 8, 17) and Dominican Republic (9-16) specimens in the light (7-16) and scanning electron (17) microscope. **7, 8** - slightly squeezed trophic and encysting specimen covered with mucilage and lepidosomes; **9** - lepidosomes impregnated with protargol; **10, 11** - mucilaginous coat and lepidosomes stained alcian blue; **12, 13** - cortex of encysted cell contains distinct fibres; **14** - cyst wall, marked by opposed arrowheads, ~1.5 µm thick and composed of two layers; **15, 16** - optical section and surface view of a slightly squeezed, mature resting cyst. Arrow marks a smooth globule; **17** - encysting cells show many smooth globules (arrows) in the mucus coat. AM - adoral membranelles, CR - ciliary row, L - lepidosomes, M - mucus, W - cyst wall. Scale bars 3 µm (13, 14, 17), 10 µm (9), and 30 µm (7, 8, 10-12, 15, 16).

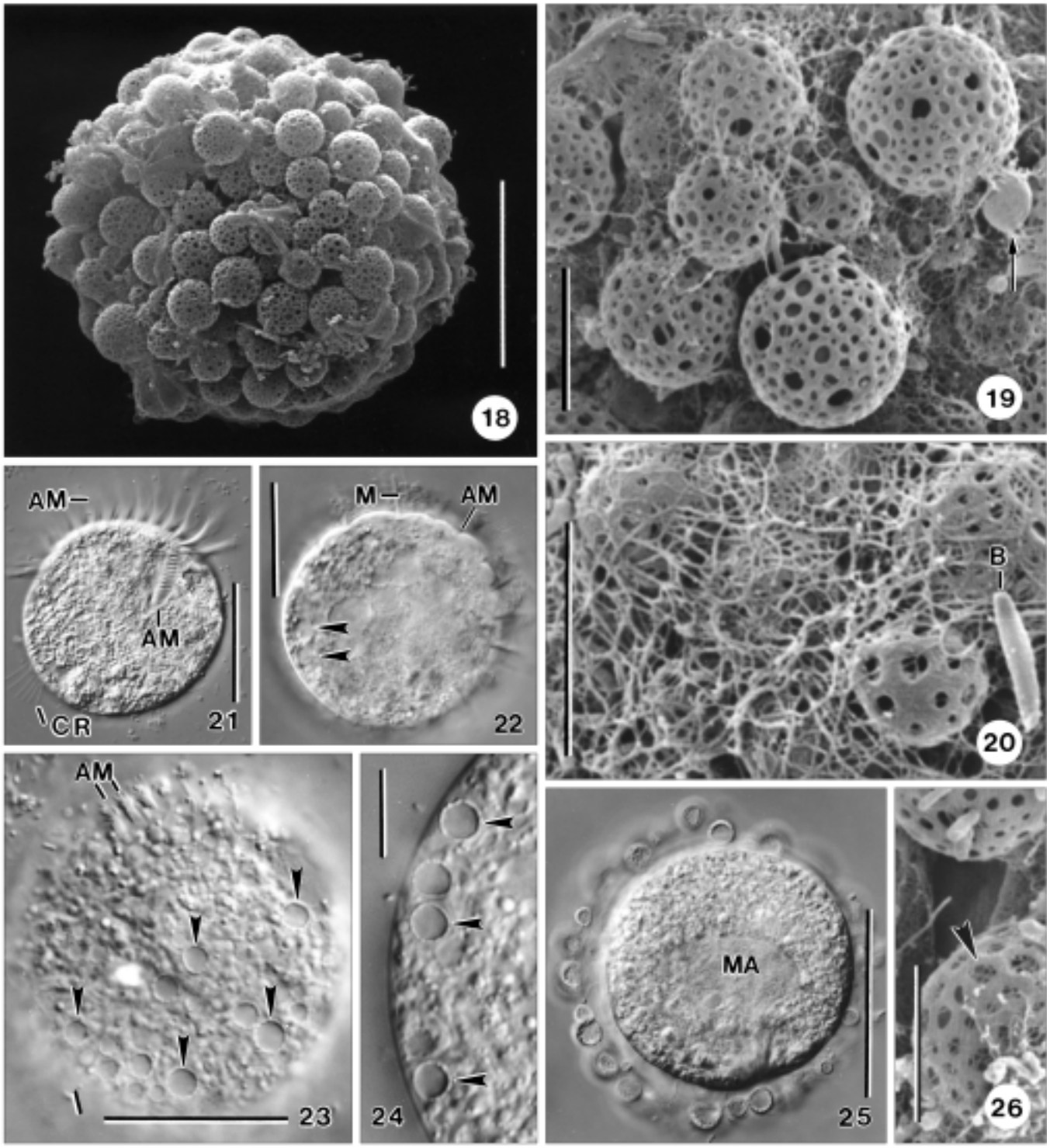

Figs 18-26. *Meseres corlissi*, encysting specimens (21-25) and mature resting cysts (18-20, 26) from the Dominican Republic (18-20, 26) and Austria (21-25) in the light (21-25) and scanning electron (18-20, 26) microscope. **18** - overview; **19, 20, 26** - the faceted lepidosomes are embedded in a fibrous mucilage and the facets may have a sieve-like substructure (26, arrowhead). The arrow marks a smooth globule (lepidosome?); **21** - encysting specimens become globular and reduce the ciliary structures; **22-24** - globular, encysting specimen with proximal portion of adoral membranelles still recognizable. The cell is coated with mucilage and contains many lepidosomes (arrowheads) underneath the cortex. The lepidosomes already have a faceted structure (24); **25** - an encysting specimen with lepidosomes just released. The cyst wall has not yet formed. AM - adoral membranelles, B - bacterial rod, CR - somatic ciliary row, MA - macronucleus. Scale bars 5 µm (19, 20, 26), 10 µm (24), 20 µm (18), and 30 µm (21-23, 25).

Table 1. Temperature effects on size (µm) and production of resting cysts of *Meseres corlissi* from the Dominican Republic.

Temperature (°C)	Length[a,b]	SD[c]	Width[a,b]	SD[c]	n[c]	% cysts[d]
15	41.1	2.9	37.7	3.5	66	83.7
17.5	44.6	4.1	41.1	4.5	150	76.9
20	46.3	4.0	43.3	4.2	114	16.0
22.5	36.9	4.8	32.8	4.9	31	0.93

[a]Without lepidosome coat. [b]All value combinations significantly different (one-way ANOVA, Tukey test; P<0.001). [c]SD - standard deviation, n - number of cysts investigated. [d]Denotes the proportion of encysted cells as percentage of all trophic and encysted cells.

Table 2. Morphometric data on resting cysts of *Meseres corlissi* from the Dominican Republic. Data based on living, two-weeks-old cysts from a pure culture. Measurements in µm. CV - coefficient of variation in %, M - median, Max - maximum, Min - minimum, n - number of cysts investigated, SD - standard deviation, $\bar{x}$ - arithmetic mean.

Characteristics	$\bar{x}$	M	SD	CV	Min	Max	n
Length (with wall)	47.3	47.0	3.3	6.9	42	55	21
Width (with wall)	45.4	45.0	4.0	8.7	40	55	21
Wall, thickness	1.6	1.5	0.4	23.4	1	2	21
Length (with wall and lepidosome coat)	59.5	58.0	4.9	8.3	50	70	21
Width (with wall and lepidosome coat)	58.2	58.0	5.2	8.9	50	68	21
Largest lepidosomes (diameter)	9.1	9.0	1.7	19.1	6	14	21
Smallest lepidosomes (diameter)	3.7	3.5	0.9	25.5	2	5	21

Table 3. Cytochemical analysis of *Meseres corlissi* resting cysts.

Materials to be revealed	Methods	Structures analysed[a]			
		lepido-somes	mucous coat	cyst wall	cyst contents
Carbohydrates (glycogen, polysaccharides)	PAS (A)	–	–	+++	+++
	PAS (B)	–	–	+++	+++
	Bauer-reaction	–	–	±	+ to +++
	Lugol solution	–	±	±	+++
Acid mucopolysaccharids	Alcian blue at several pHs and with/without $MgCl_2$	±	++ to +++	–	–
Cellulose	Chlor-zinc-iodine	–	–	–	+
Chitin	Van Wisselingh test	–	–	++ to +++	–
Proteins	Alloxan Schiff-reaction	+	+	+	+ to +++
Lipids	Oil red	–	–	–	+ to +++
	Sudan red	–	–	–	+ to +++
	Sudan black	–	–	+	+ to +++
	Osmium acid	–	–	–	++
	Acetalphosphatids	–	–	–	+++

[a]Slight (+), moderate (++), strong (+++), uncertain (±) reaction.

fibres are a preparation artifact because they could not be observed *in vivo* and the transmission electron microscope (Foissner 2005).

About 200 lepidosomes coat the cyst wall in two more or less distinct layers (Figs 1, 15, 16, 18, 27). When the cyst is squashed, the lepidosomes do not disperse, showing that they are embedded in the mucous coat described above; some can be removed by strong water flushes, for instance, by sucking the cyst through a narrow pipette several times. Most lepidosomes are perfect spheres with an about 0.5 µm thick, polygonally faceted wall; those touching the cyst wall may be hemispherically flattened. The diameter varies highly from about 2-14 µm, with an average of near 6 µm (Table 2). If exposed to strong coverslip pressure, nothing is released from the lepidosomes, perhaps except of water, and they become flattened and deformed, but never break, showing that they are very flexible (Figs 15, 16). The facets, which have a size of about 0.1-1 µm, are recognizable in even the smallest lepidosomes and cause a granular appearance of the wall in optical section; small and large facets occur without any regularity (Figs 12, 15). Frequently, the inner side of the facets is covered by a sieve-like lattice which is possibly very fragile and thus only partially preserved in the scanning electron microscopic preparations (Figs 19, 20, 26). Usually, there are some smooth spheres 0.5-2 µm across between and on the lepidosomes, especially in encysting specimens (Figs 16, 17, 19). We could not clarify, whether these are imperfect lepidosomes, mucus accumulations, or coccal bacteria.

Cytochemical investigations. The data on cyst chemistry are summarized in Table 3. They match the general knowledge that proteins, glycoproteins, and carbohydrates are the main constituents of the ciliate cyst wall (Rosati *et al.* 1984, Gutiérrez *et al.* 2003); rarely, inorganic substances play a role, viz., silicon in *Bursaria* (Bussers 1976) and calcium phosphate or calcium carbonate in a strobilidiid oligotrich (Reid 1987). The cyst content stains distinctly for carbohydrates, proteins, and lipids (Table 3).

Few chemical data are available on the mucous coat of ciliate cysts (Bussers 1976), although it is common throughout the phylum (Foissner 1993, Berger 1999, Foissner *et al.* 1999). This coat, which is usually not identical with that what is called the ectocyst (Gutiérrez *et al.* 2003), adheres the cyst to various substrates, such as plant residues and the walls of the culture dishes. Thus, it is usually partially or completely lost when the cysts are collected for investigations. Additionally, the coat is often very hyaline, as in *M. corlissi*, and thus easily overlooked. In *M. corlissi*, the mucous coat stains deeply with alcian blue under various conditions, showing that acid mucopolysaccharides are a main component (Adam and Czihak 1964, Romeis 1968, Hayat 1989); frequently, acid mucopolysaccharides occur also in the cyst wall (Delgado *et al.* 1987). The mucus is membrane-like and deeply stained around the cyst wall, gradually becoming fluffy and lightly stained distally (Fig. 11); if the stain is applied to living cysts, the coat may collapse to a deep blue, wall-like structure (Fig. 10). The coat shows also a slight stain for proteins and carbohydrates (Table 3), which thus might be minor constituents.

The lepidosomes are of organic nature because they are flexible (Fig. 27) and stain with a variety of histological dyes, such as hematoxylin and silver compounds (protargol, silver carbonate; Fig. 9). Of the cytochemical tests applied, the lepidosomes show a weak reaction for proteins. There is also a slight stain for acid mucopolysaccharids, but this is probably caused by adhering mucus from the mucous coat; however, some stain cannot be excluded because the lepidosome wall is very thin, decreasing staining intensity in general. Thus and because chitin and cellulose can be excluded, glycoproteins are likely a main component of the lepidosomes.

The cyst wall reacts with tests for carbohydrates and proteins, suggesting glycoproteins as a main constituent. This is in accordance with data from other ciliates (Gutiérrez *et al.* 2003). There is also a weak reaction for lipids using sudan black. The significance of this observation is not yet clear, but it matches data from *Didinium nasutum* (Rieder 1973) and other protists (Mulisch and Hausmann 1989). Part of the carbohydrates is chitin, as shown by the strong reaction with the Van Wisselingh colour test (Figs 33-36). The ghosts obtained after hot KOH treatment are very hyaline and structureless globules 25-45 µm across with an about 0.5 µm thick wall. Unfortunately, we could not recognise which part of the wall forms the globule and reacts with the test because all other cyst structures dissolved. The Van Wisselingh reaction for chitin was very convincing, both in the *Meseres* cysts and the control (Figs 33-35). Thus, an artifact can be excluded. Indeed, the presence of chitin is not unexpected because Bussers and Jeuniaux (1974) observed chitin in resting cysts of 14 out of 22 ciliate species investigated. Further, many ciliate loricas contain or consist of chitin (Mulisch 1993).

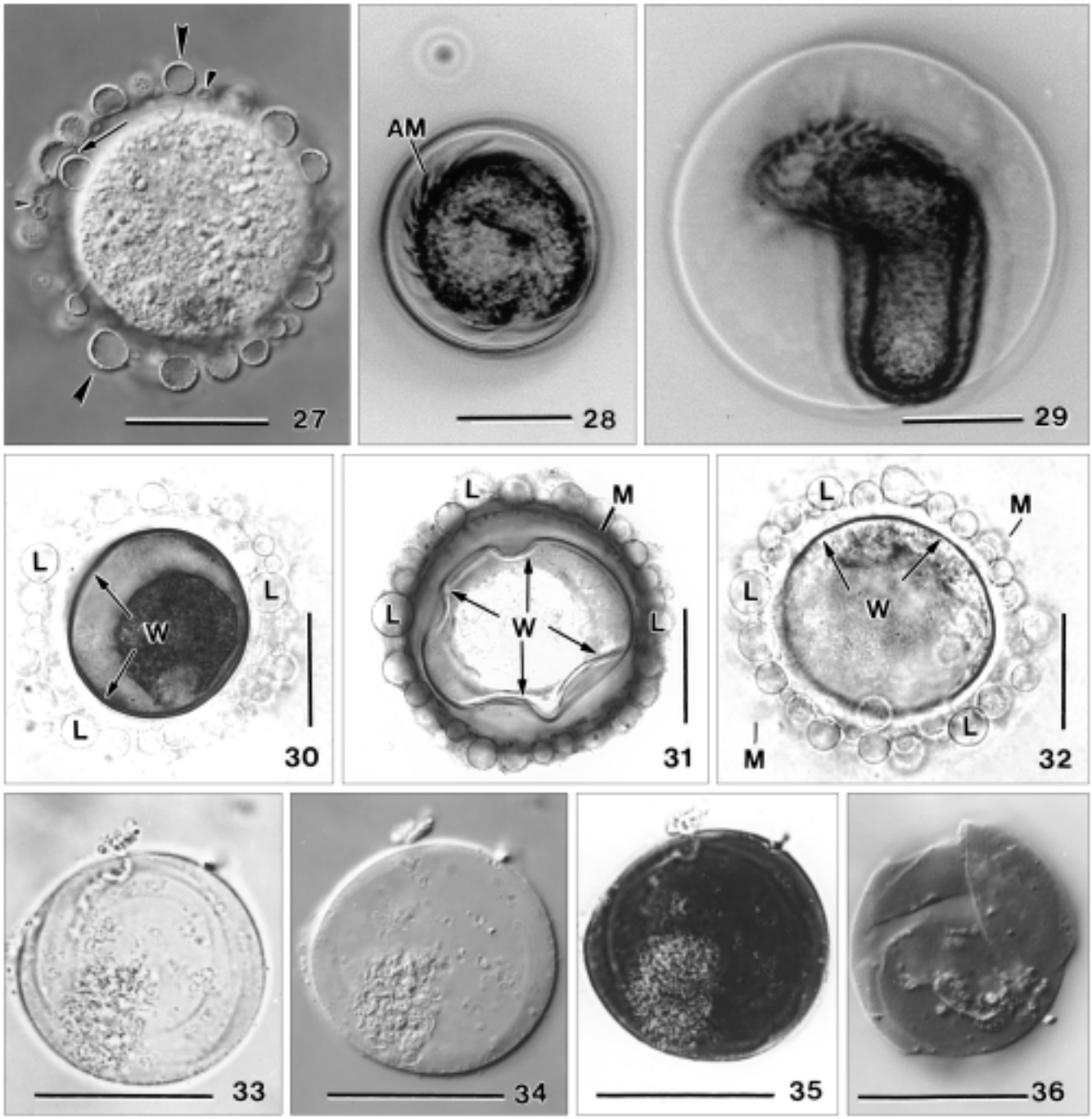

Figs 27-36. *Meseres corlissi*, Austrian (27, 30-36) and Dominican Republic (28, 29) specimens *in vivo* (27-29, contrast inversed in 28 and 29) and after various cytochemical stains (30-36). **27** - mature resting cyst, diameter 55 µm. Note the very different size of the lepidosomes (arrowheads) and their flexibility (arrow); **28** - when excystment commences, the adoral membranelles become visible and the ciliate begins to rotate; **29** - late excystment stage. The cell increases in size and the cyst swells to double size, likely due to a swelling of the cyst wall and the vigorous movements of the cell; **30** - bright field micrograph of a formalin-fixed, PAS-stained resting cyst. The cyst wall (W) and the cyst content are deeply stained, showing the presence of carbohydrates. The lepidosomes (L) and the mucous coat are unstained and thus very faint; **31** - bright field micrograph of a formalin–fixed, alcian blue-stained resting cyst. The cyst is covered by the deeply stained mucous coat (M), which becomes fluffy and faint distally. The intense staining of the coat causes that the unstained, wrinkled cyst wall (W) and the lepidosomes (L) increase in contrast (cp. Fig. 30); **32** - bright field micrograph of a formalin-fixed, alloxan-stained resting cyst. The mucous coat (M), the lepidosomes (L), the cyst wall (W), and the cyst content are slightly stained (cp. Fig. 30), showing the presence of proteins; **33**-**35** - Van Wisselingh´s chitin test. The same cyst (chitin) wall is shown after KOH treatment in bright field (33), interference contrast (34), and after iodine treatment (35), where the wall becomes deeply redbrown and thus appears black in the micrograph; **36** - same as before, but partially destroyed showing sharp-edged breaks. AM - adoral membranelles, L - lepidosomes, M - mucous coat, W - cyst wall. Scale bars 25 µm.

The cyst wall, the mucous coat, and the lepidosomes are very resistant to a variety of inorganic and organic solvents. They do not change in xylene, pyridine, propylene oxide, acetone, and alcohol. Hydrochloric acid (0.05 N) dissolves the cyst content within 10 min, while the wall, the lepidosomes, and the mucous coat appear unchanged even after 1 h of treatment; the lepidosomes are slightly swollen, but still show the faceted wall. Sodium hydroxide (2 M) dissolves the lepidosomes within 30 min, while the mucilage and the wall, which loses its bipartite structure, are still recognizable. The wall is maintained even after 1 h of treatment, while most of the mucilage disappears or disintegrates to a reticulate, very hyaline material. Concentrated sodium hypochlorite (Eau de Javelle with 12-13% active chlorine) dissolves the lepidosomes and the wall within 5-10 min, while the mucous coat is still recognizable after 1 h of treatment; thus, the cysts are still globular, although they are heavily damaged. Cold, saturated potassium hydroxide does not dissolve the cyst wall and the lepidosomes within 1 h of treatment; however, the lepidosomes often appear wrinkled, and the mucous coat is likely dissolved. Hot (160°C), saturated KOH dissolves the cysts within 20 min, except for the chitinous portion (see above).

These observations match some literature data on the cyst wall of a soil ciliate, *Colpoda cucullus*, which is also very resistant to various solvents (Corliss and Esser 1974, Foissner 1993). Further, the observations agree with data from Gutiérrez *et al.* (1984) on cyst wall lysis of a freshwater ciliate, *Laurentiella acuminata*.

Excystment

To study excystment, a cyst-containing culture from the Dominican Republic was transferred from 15°C to 24°C. On the following day, several cysts in the early stage of excystment were present. With a pasteur pipette, these were transferred to a Sedgewick-Rafter chamber and observed at a magnification of × 500 with phase contrast. Morphologically, three stages can be distinguished. First, the adoral membranelles become visible within the cyst and the ciliate commences to rotate (Fig. 28). Next, the ciliate gradually increases in size, likely through uptake of water, and the cyst roughly doubles its diameter, probably due to partial lysis of the wall, as in *Colpoda steinii* (Foissner 1993), and the vigorous movements of the ciliate (Fig. 29). Finally, the cyst wall ruptures and the ciliate escapes leaving behind the now very thin, wrinkled and shapeless cyst wall. No special emergence pore exists. The mucous coat and the lepidosomes within are lost when the ciliate commences to excyst. Basically, these processes are very similar to those described, for instance, in colpodids (Foissner 1993) and stichotrichine spirotrichs (Gutiérrez *et al.* 1981).

DISCUSSION

The term "lepidosomes"

We define lepidosomes as epicortical, organic structures of definite shape produced intracellularly by trophic and/or cystic ciliate species. Accordingly, the term excludes unstructured, mucous coats and any kind of lorica. In a more general sense, lepidosomes belong to the "scales", as defined by Preisig *et al.* (1994).

We shall show below that lepidosomes likely evolved convergently and possibly have different functions in various ciliate groups. Thus, a common term might be considered as inappropriate. On the other hand, lepidosomes have been described under a bewildering variety of names, making identification in the literature difficult (see next chapter). Thus, the term can be a useful "collector" at the present state of knowledge. Later and if necessary, it can be confined to the scales of trachelophyllid haptorids, the group which sponsored the name (*Lepidotrachelophyllum*; Nicholls and Lynn 1984). For the moment, the term should be understood as purely descriptive, like "coccoliths" for the calcified scales of the coccolithophores.

Distribution and structure of ciliate lepidosomes

Coatings composed of organic scales are widespread among trophic and cystic protists (Margulis *et al.* 1989). In ciliates, they occur rarely and under different names: Schleim, mucilage, gelatinous covering (in some trophic trachelophyllid and encheliid haptorids; Kahl 1930 and earlier authors); foam, organic scales, scale layer, external scale layer, extracellular scales (trophic trachelophyllid haptorids; Nicholls and Lynn 1984); mucilaginous layer, mucilaginous envelope, epicortical scales (trophic trachelophyllid haptorids; Foissner *et al.* 2002); external chalice-like structures (trophic *Peritromus*, Heterotrichea; Rosati *et al.* 2004); curieux éléments, écailles, fines baguettes fourchues (trophic cyrptopharyngid karyorelictids and in *Ciliofaurea*; Dragesco 1960); epipellicular scales (trophic cryptopharyngid karyorelictids; Foissner 1996); network structures (precystic and cystic *Colpoda cucullus*; Kawakami and Yagiu 1963a,b); yellow or brownish globules, brown-

ish discs, highly refractive globules, roundish discs arranged like scales and covered with tri-armed structures (various cystic Colpodea; Foissner 1993 and literature cited therein); papilla-like structures (cystic *Colpoda inflata* and *C. cucullus*; Chessa *et al.* 1994, 2002).

Obviously, lepidosomes have been reported from only few and taxonomically very distant ciliate groups, viz., the Karyorelictea, Haptorida, and Colpodea. Our report of lepidosomes in *Meseres* is the first for oligotrichs. There is evidence that lepidosomes are probably more common in general and particularly in oligotrichs, though they are absent in the common *Halteria grandinella*, a close relative of *Meseres* (Foissner, unpubl.). However, in another, new *Halteria* species from the Dominican Republic, the cyst is covered by conical scales highly resembling lepidosomes (Foissner, unpubl.). Further, cysts of several strombidiids and tintinnids have spine-like processes (for a brief review, see Müller 2000), which might also be lepidosomes. Possibly, they occur, as temporary structures, in *Strombidium oculatum* because Fauré-Fremiet (1948) observed the release of globules, which intensely stained with congo red, in encysting specimens. Likewise, *Didinium*, a relative of the trachelophyllids, secretes so-called clathrocysts, sacculate structures which are involved in mesocyst formation and disappear in the mature cyst (Holt and Chapman 1971). The foamy blisters forming the ectocyst of *Enchelydium*, another relative of the trachelophyllids, also resemble lepidosomes (see chapter below).

Among the trachelophyllid lepidosomes known (Foissner *et al.* 2002), only those of *Spetazoon australiense* Foissner, 1994 resemble the cyst lepidosomes of *M. corlissi*. However, the facets in the lepidosome wall are much coarser in *S. australiense* than in *M. corlissi*.

Few of these epicortical structures have been investigated with transmission electron microscopy. The available data show three organization types. In the first type, represented by trachelophyllids and *Meseres*, the lepidosomes are hollow structures with the wall composed of extremely fine, interwoven fibres (Nicholls and Lynn 1984, Foissner 2005). The second type is found in *Peritromus*, where the lepidosomes are made of organic material forming 60 nm-sided triangular, crystal-like elements (Rosati *et al.* 2004). The third type occurs in many colpodids, where the cysts are covered by small discs or globules composed of a strongly osmiophilic, spongiform material, in which a paracrystalline organization can be recognized (Kawakami and Yagiu 1963a, b; Chessa *et al.* 2002).

Nothing is known about the chemical composition of lepidosomes. Our attempts in *M. corlissi* were only partially successful, that is, show a weak reaction for protein (Table 3).

All these data suggest that lepidosomes evolved convergently in various ciliate groups, which is emphasized by the evidences shown in the last chapter.

Genesis of lepidosomes

Little is known about lepidosome genesis. In *M. corlissi*, the lepidosomes are produced in the cell's periphery within less than one hour. However, the exact sites of genesis are not known and need electronmicroscopical investigations; probably, they are assembled in dictyosomes, as supposed by Lynn and Nicholls (1984) in *Lepidotrachelophyllum fornicis*. In this species, the lepidosomes are generated in large endoplasmic vesicles, and some sections suggest that these vesicles are transported near to the cortex. Here, vesicle extensions may fuse with the plasmalemma and liberate the lepidosomes to the external surface of the cell (Lynn and Nicholls 1984). In *Colpoda cucullus*, the lepidosomes originate from minute, granular, membrane-bound precursors, most located in the cell´s periphery. When completed, they traverse the cell's cortex in the precystic specimens (Kawakami and Yagiu 1963a). These data suggest that lepidosome genesis may be similar in *M. corlissi*, trachelophyllids and colpodids, while *Peritromus kahli* possibly assembles the lepidosomes externally. Rosati *et al.* (2004) did not find lepidosomes or distinct lepidosome precursors in the cytoplasm of *Peritromus kahli* and thus supposed that the "material which composes the lepidosomes may be secreted through cortical invaginations present all over the dorsal surface".

Meseres cysts misidentified as cysts of *Enchelydium*, and lepidosomes of misidentified *Colpoda* species

Foissner *et al.* (2002) described the resting cyst of *Enchelydium blattereri*, a large, rapacious haptorid ciliate discovered in floodplain soil from Australia. The "forming cysts", Foissner *et al.* (2002) described and illustrated (Figs 20h and 306o in their work), are obviously mature cysts of *Meseres corlissi*, which occurred, according to the original notes and protargol slides, together with *E. blattereri* and was present also in the semipure cultures of this species. The resting cyst of *E. blattereri* is, indeed, similar to that of *M. corlissi* (Figs 20i, j in Foissner *et al.* 2002) because the ectocyst is composed of foamy blisters with walls composed of a

fibrous material perforated by minute pores. However, the blisters are not individualized structures, as the lepidosomes of *Meseres* and trachelophyllids, but are an integral component of the ectocyst, that is, cannot be removed without destroying the cyst.

Misidentifications can also explain contradicting results about the occurrence of lepidosomes in *Colpoda inflata* and *C. cucullus*. In a detailed SEM and TEM study on *C. inflata*, Martín-Gonzalez *et al.* (1992a, b, 1994) did not describe lepidosomes, while other investigations showed them by light microscopy (Foissner 1993) and scanning electron microscopy (Chessa *et al.* 1994). Unfortunately, Martín-Gonzalez *et al.* (1992a, b; 1994) described the vegetative specimens very briefly. However, the SEM micrograph in Martín-Gonzalez *et al.* (1992b) indicates that it could have been *C. maupasi* which, indeed, lacks lepidosomes (Foissner 1993). The second case concerns *C. cucullus*, where Kawakami and Yagiu (1963a, b) and Chessa *et al.* (2002) showed lepidosomes by transmission electron microscopy, while Foissner (1993) did not find any in the light microscope. However, *C. cucullus* is a complex of several rather similar species (Foissner 1993), some of which have lepidosomes (*C. lucida*, *C. flavicans*), while others have not (*C. cucullus*, *C. simulans*, *C. henneguyi*). Unfortunately, both studies lack details on the species investigated, and thus *a posteriori* identification is impossible.

Ciliate lepidosomes and leafhopper brochosomes

Leafhoppers (Insecta: Cicadellidae) and occasionally also their egg nests are covered by so-called brochosomes, whose origin and structure is highly reminiscent of the trachelophyllid lepidosomes and the cyst lepidosomes of *M. corlissi*. Brochosomes are synthesized in the Golgi vesicles of cells of the Malpighian tubules, are excreted *via* the anus, and distributed onto the integument by the legs. Size and structure of the brochosomes vary among species, but in the majority of examined leafhoppers they are hollow spheres, 0.2-0.6 µm across, with a honeycomb-like surface; they are insoluble in organic solvents and are rigid and durable in the dry form. Chemically, brochosomes consist of protein and lipid, but details are not known (Rakitov 2002).

Function of brochosomes and lepidosomes

The function of the leafhopper brochosomes is still in discussion. The available evidence suggests that they form a protective coating which (i) repels water and sticky honeydew and/or (ii) prevents fungal infection (Rakitov 2002). However, many other functions have been suggested, such as protection against microbes and desiccation, accommodation of hypothetical pheromones, and even that they are waste products (Humphrey and Dworakowska 2002, Rakitov 2002).

The function of the ciliate lepidosomes is not known. Like in leafhoppers, there is no obvious relation to the organisms' ecology and biology because trachelophyllids and *Meseres* usually occur together with many other ciliates lacking a lepidosome coat. However, the large number and complicated structure of the lepidosomes are energy demanding, suggesting an important function in the organism's life history. Some preliminary experiments with plasticine models, as advised by Padisák *et al.* (2003), showed that the lepidosome coat does not significantly change buoyancy, that is, cyst dispersal by floatation, likely because the gain of surface area is compensated by the increased diameter of the cyst (Padisák *et al.* 2003). Further, any effect of the lepidosomes on cyst buoyancy would be outweighted by the mucous coat in which they are embedded. This very fluffy substance has likely less specific mass than water and thus might indeed increase cyst buoyancy, as in several algae (Ruttner 1940). Fauré-Fremiet (1910) suggests that the lepidosomes of *Mycterothrix tuamotuensis*, a marynid colpodid, are pycnotic food vacuoles because they contain granular material. This is contradicted by data on other colpodids, in which the lepidosomes are clear and homogenous (Foissner 1993), and electron microscopic investigations showing a spongious fine structure (Kawakami and Yagiu 1963a, b, Chessa *et al.* 2002). Kawakami and Yagiu (1963a) suggest that the lepidosomes of *Colpoda cucullus* form a mucous layer attaching the cyst to various substrates. However, lepidosomes in the process of transforming to mucus are not shown. Likely, mucus secretion and lepidosome release are different processes in colpodids (Foissner 1993), as in *Meseres corlissi* (Fig. 22).

Thus, no substantiated hypothesis is available for the function of the ciliate lepidosomes. And the matter becomes even more complex when their distribution in the life cycle is considered: *Meseres* has lepidosomes only in the cystic stage, while they are restricted to the trophic stage in trachelophyllids (Foissner, unpubl.). Further, the occurrence of lepidosomes varies even within a single genus: they are present, for instance, in *Colpoda inflata* and a *C. cucullus* - like species (Foissner 1993; Chessa *et al.* 1994, 2002), while absent in *C. magna* and

C. minima (Foissner 1993, Diaz *et al.* 2003). All these data indicate that lepidosomes may have different functions in various ciliates.

Acknowledgements. Financial support was provided by the Austrian Science Foundation, FWF project P16796-B06. The senior author thanks Dr. Erna Aescht and Dr. Sabine Agatha for important literature sources. The technical assistance of Dr. B. Moser, Dr. E. Herzog and P. Stadler is gratefully acknowledged.

REFERENCES

Adam H., Czihak G. (1964) Arbeitsmethoden der makroskopischen und mikroskopischen Anatomie. Ein Laboratoriumshandbuch für Biologen, Mediziner und technische Hilfskräfte. G. Fischer, Stuttgart

Agatha S. (2004) A cladistic approach for the classification of oligotrichid ciliates (Ciliophora: Spirotricha). *Acta Protozool.* **43:** 201-217

Berger H. (1999) Monograph of the Oxytrichidae (Ciliophora, Hypotrichia). Kluwer, Dordrecht, Boston, London

Bussers J. C. (1976) Structure et composition du kyste de résistance de 4 protozoaires ciliés. *Protistologica* **12:** 87-100

Bussers J. C., Jeuniaux C. (1974) Recherche de la chitine dans les productions métaplasmatiques de quelques ciliés. *Protistologica* **10:** 43-46

Chessa M. G., Delmonte Corrado M. U., Carcupino M., Pelli P. (1994) Ultrastructural cortical aspects of cell differentiation during long-term resting encystment in *Colpoda inflata*. In: Contributions to Animal Biology, (Eds. R. Argano, C. Cirotto, E. Grassi Milano, L. Mastrolia). Halocynthia Association, Palermo, 169-172

Chessa M. G., Largana I., Trielli F., Rosati G., Politi H., Angelini C., Delmonte Corrado M. U. (2002) Changes in the ultrastructure and glycoproteins of the cyst wall of *Colpoda cucullus* during resting encystment. *Europ. J. Protistol.* **38:** 373-381

Corliss J. O. (1979) The Ciliated Protozoa. Characterization, Classification and Guide to the Literature. 2nd ed. Pergamon Press, Oxford, New York, Toronto, Sydney, Paris, Frankfurt

Corliss J. O., Esser S. C. (1974) Comments on the role of the cyst in the life cycle and survival of free-living protozoa. *Trans. Am. microsc. Soc.* **93:** 578-593

Delgado P., Calvo P., Torres A. (1987) Encystment in the hypotrichous ciliate *Paraurostyla weissei*: ultrastructure and cytochemistry. *J. Protozool.* **34:** 104-110

Díaz S., Martín-González A., Rico D., Gutiérrez J. C. (2003) Morphogenesis of the division and encystment process of the ciliated protozoan *Colpoda minima*. *J. Nat. Hist.* **37:** 2395-2412

Dragesco J. (1960) Ciliés mésopsammiques littoraux. Systématique, morphologie, écologie. *Trav. Stn. biol. Roscoff* (N.S.) **12:** 1-356

Fauré-Fremiet E. (1910) Le *Mycterothrix tuamotuensis (Trichorhynchus tuamotuensis*) Balbiani. *Arch. Protistenk.* **20:** 223-238

Fauré-Fremiet E. (1948) Le rythme de marée du *Strombidium oculatum* Gruber. *Bull. biol. Fr. Belg.* **82:** 3-23

Foissner W. (1987) Soil protozoa: fundamental problems, ecological significance, adaptations in ciliates and testaceans, bioindicators, and guide to the literature. *Progr. Protistol.* **2:** 69-212

Foissner W. (1991) Basic light and scanning electron microscopic methods for taxonomic studies of ciliated protozoa. *Europ. J. Protistol.* **27:** 313–330

Foissner W. (1993) Colpodea. *Protozoenfauna* **4/1: I-X + 798 p**

Foissner W. (1994) *Spetazoon australiense* nov. gen., nov. spec., ein neues Wimpertier (Protozoa, Ciliophora) von Australien. *Kataloge des OÖ. Landesmuseums* (N. F.) **71:** 267-278

Foissner W. (1996) The infraciliature of *Cryptopharynx setigerus* Kahl, 1928 and *Apocryptopharynx hippocampoides* nov. gen., nov. spec. (Ciliophora, Karyorelictea), with an account on evolution in loxodid ciliates. *Arch. Protistenk.* **146:** 309-327

Foissner W. (2005) The unusual, lepidosome-coated resting cyst of *Meseres corlissi* (Ciliophora: Oligotrichea): Transmission electron microscopy and phylogeny. *Acta Protozool.* **44:** 217-230

Foissner W., Berger H., Schaumburg J. (1999) Identification and ecology of limnetic plankton ciliates. *Bayer. Landesamt für Wasserwirtschaft* **3/99:** 1-793

Foissner W., Agatha S., Berger H. (2002) Soil ciliates (Protozoa, Ciliophora) from Namibia (Southwest Africa), with emphasis on two contrasting environments, the Etosha Region and the Namib Desert. *Denisia* (Linz) **5:** 1-1459

Foissner W., Moon-van der Staay S. Y., van der Staay G. W. M., Hackstein J. H. P., Krautgartner W.-D., Berger H. (2004) Reconciling classical and molecular phylogenies in the stichotrichines (Ciliophora, Spirotrichea), including new sequences from some rare species. *Europ. J. Protistol.* **40:** 265-281

Guillard R. R. L., Lorenzen C. J. (1972) Yellow-green algae with chlorophyllide c. *J. Phycol.* **8:** 10-14

Gutiérrez J. C., Torres A., Perez-Silva J. (1981) Excystment cortical morphogenesis and nuclear processes during encystment and excystment in *Laurentiella accuminata* (Hypotrichida, Oxytrichidae). *Acta Protozool.* **20:** 145-152

Gutiérrez J. C., Torres A., Perez-Silva J. (1984) Composition of the cyst wall of the hypotrichous ciliate *Laurentiella acuminata*: I. Cytochemical, cytophotometrical, enzymatic analysis. *Protistologica* **20:** 313-326

Gutiérrez J. C., Callejas S., Borniquel S., Benítez L., Martín-González A. (2001) Ciliate cryptobiosis: a microbial strategy against environmental starvation. *Int. Microbiol.* **4:** 151-157

Gutiérrez J. C., Diaz S., Ortega R, Martín-González A. (2003) Ciliate resting cyst walls: a comparative review. *Recent Res. Devel. Microbiol.* **7:** 361-379

Hayat M. A. (1989) Principles and Techniques of Electron Microscopy. Biological Applications. MacMillan Press, London

Holt P. A., Chapman G. B. (1971) The fine structure of the cyst wall of the ciliated protozoon *Didinium nasutum*. *J. Protozool.* **18:** 604-614

Humphrey E. C., Dworakowska I. (2002) The natural history of brochosomes in *Yakuza gaunga* (Hemiptera, Auchenorrhyncha, Cicadellidae, Typhlocybinae, Erythroneurini). *Denisia* (Linz) **4:** 433-454

Kahl A. (1930) Urtiere oder Protozoa I: Wimpertiere oder Ciliata (Infusoria) 1. Allgemeiner Teil und Prostomata. *Tierwelt Dtl.* **18:** 1-180

Kawakami H., Yagiu R. (1963a) An electron microscopical study of the change of fine structure in the ciliate, *Colpoda cucullus*, during its life cycle. II. From the preencystment stage to the early stage of the formation of the first layer of resting cyst membrane. *Zool. Mag.* **72:** 146-151

Kawakami H., Yagiu R. (1963b) The electron microscopical study of the change of fine structure in the ciliate, *Colpoda cucullus*, during its life cycle. III. From the stage of completion of the first layer of resting cyst membrane to the completion of the resting cyst. *Zool. Mag.* **72:** 224-229

Landers S. C. (1991) Secretion of the reproductive cyst wall by the apostome ciliate *Hyalophysa chattoni*. *Europ. J. Protistol.* **27:** 160-167

Lynn D. H. (2003) Morphology or molecules: how do we identify the major lineages of ciliates (phylum Ciliophora)? *Europ. J. Protistol.* **39:** 356-364

Lynn D. H., Nicholls K. H. (1984) Cortical microtubular structures of the ciliate *Lepidotrachelophyllum fornicis* Nicholls & Lynn, 1984 and phylogeny of the litostomate ciliates. *Can. J. Zool.* **63:** 1835-1845

Margulis L., Corliss J. O., Melkonian M., Chapman D. J. (1989) Handbook of Protoctista. Jones and Bartlett Publishers, Boston

Martín-Gonzalez A., Benitez L., Palacios G., Gutiérrez J. C. (1992a) Ultrastructural analysis of resting cysts and encystment in

Colpoda inflata 1. Normal and abnormal resting cysts. *Cytobios* **72:** 7-18
Martín-Gonzalez A., Benitez L., Gutiérrez J. C. (1992b) Ultrastructural analysis of resting cysts and encystment in *Colpoda inflata* 2. Encystment process and a review of ciliate resting cyst classification. *Cytobios* **72:** 93-106
Martín-Gonzalez A., Palacios G., Gutiérrez J. C. (1994) Cyst wall precursors of *Colpoda inflata*: a comparative ultrastructural study and a review of ciliate cyst wall precursors. *Cytobios* **77:** 215-223
Müller H. (2000) Evidence of dormancy in planktonic oligotrich ciliates. *Verh. Internat. Verein. Limnol*. **27:** 3206-3209
Mulisch M. (1993) Chitin in protistan organisms. Distribution, synthesis and deposition. *Europ. J. Protistol.* **29:** 1-18
Mulisch M., Hausmann K. (1989) Localization of chitin on ultrathin sections of cysts of two ciliated protozoa, *Blepharisma undulans* and *Pseudomicrothorax dubius*, using colloidal gold conjugated wheat germ agglutinin. *Protoplasma* **152:** 77-86
Nicholls K. H., Lynn D. H. (1984) *Lepidotrachelophyllum fornicis* n. g., n. sp., a ciliate with an external layer of organic scales (Ciliophora, Litostomatea, Haptorida). *J. Protozool.* **31:** 413-419
Padisák J., Soróczki-Pintér É., Rezner Z. (2003) Sinking properties of some phytoplankton shapes and the relation of form resistance to morphological diversity of plankton - an experimental study. *Hydrobiologia* **500:** 243-257
Petz W., Foissner W. (1992) Morphology and morphogenesis of *Strobilidium caudatum* (Fromentel), *Meseres corlissi* n. sp., *Halteria grandinella* (Müller), and *Strombidium rehwaldi* n. sp., and a proposed phylogenetic system for oligotrich ciliates (Protozoa, Ciliophora). *J. Protozool.* **39:** 159-176
Preisig H. R., Anderson O. R., Corliss J. O., Moestrup Ø., Powell M. J., Roberson R. W., Wetherbee R. (1994) Terminology and nomenclature of protist cell surface structures. *Protoplasma* **181:** 1-28
Rakitov R. A. (2002) What are brochosomes for ? An enigma of leafhoppers (Hemiptera, Cicadellidae). *Denisia* (Linz) **4:** 411-432
Reid P. C. (1987) Mass encystment of a planktonic oligotrich ciliate. *Mar. Biol.* **95:** 221-230
Rieder N. (1973) Elektronenoptische und histochemische Untersuchungen an der Cystenhülle von *Didinium nasutum* O. F. Müller (Ciliata, Holotricha). *Arch. Protistenk.* **115:** 125-131
Romeis B. (1968) Mikroskopische Technik. R. Oldenbourg Verlag, München,Wien
Rosati G., Modeo L., Melai M., Petroni G., Verni F. (2004) A multidisciplinary approach to describe protists: a morphological, ultrastructural, and molecular study on *Peritromus kahli* Villeneuve-Brachon, 1940 (Ciliophora, Heterotrichea). *J. Eukaryot. Microbiol.* **51***:* 49-59
Ruttner F. (1940) Grundriss der Limnologie. Walter de Gruyter & Co., Berlin
Tracey M. V. (1955) Chitin. *Methoden der Pflanzenanalyse* **3:** 264-274
Walker G. K., Maugel T. K. (1980) Encystment and excystment in hypotrich ciliates II. *Diophrys scutum* and remarks on comparative features. *Protistologica* **16:** 525-531
Weisse T. (2004) *Meseres corlissi*, a rare oligotrich ciliate adapted to warm water temperature and temporary habitats. *Aqu. Microb. Ecol.* **37:** 75-83
Wirnsberger-Aescht E., Foissner W., Foissner I. (1990) Natural and cultured variability of *Engelmanniella mobilis* (Ciliophora, Hypotrichida); with notes on the ultrastructure of its resting cyst. *Arch. Protistenk.* **138:** 29-49

Received on 10th January, 2005; revised version on 8th March, 2005; accepted on 22nd March, 2005

Acta Protozool. (2005) 44: 217 - 230

ACTA
PROTOZOOLOGICA

The Unusual, Lepidosome-coated Resting Cyst of *Meseres corlissi* (Ciliophora: Oligotrichea): Transmission Electron Microscopy and Phylogeny

Wilhelm FOISSNER

Universität Salzburg, FB Organismische Biologie, Salzburg, Austria

Summary. This is the first detailed study on the fine structure of the resting cyst of an oligotrichine ciliate, that is, the halteriid *Meseres corlissi* Petz and Foissner (1992), using a new, "strong" fixative composed of glutaraldehyde, osmium tetroxide, and mercuric chloride. The cyst wall consists of five distinct layers (from inside to outside): metacyst, endocyst, mesocyst, ectocyst, and the pericyst, a new term for all materials produced by the encysting cell and deposited upon the ectocyst. Structurally, the five layers of the *Meseres* cyst are similar to those of the stichotrichine (e.g., *Oxytricha*) and phacodinine (*Phacodinium*) spirotrichs, except of the thin ectocyst which is not lamellar but coarsely granular. The ectomesocyst likely corresponds to the chitin layer demonstrated by the Van Wisselingh colour test. The lepidosomes are within the fluffy, mucous pericyst whose proximal zone forms a reticulate, membrane-like structure on the ectocyst. The mucus consists of very fine filaments with a diameter of about 3 nm, while the lepidosomes are composed of fibres about 20 nm across. The encysted cell is similar to other kinetosome-resorbing ciliate cysts, except of curious inclusions possibly related to the lepidosomes. The data are compared with respect to the classification of the halteriids. While the general wall structure indicates a stichotrichine relationship, the ectocyst, the lepidosomes, and the chitin layer in the cyst wall suggest the halteriids as a distinct group more closely related to the oligotrichine than stichotrichine spirotrichs.

Key words: ciliate classification, metacyst, new fixation method, pericyst, phylogeny, stichotrichs.

INTRODUCTION

In the electron microscope, the wall of ciliate resting cysts conventionally consists of three distinct layers, that is, the endocyst, the mesocyst, and the ectocyst. Depending on the group of ciliates investigated, there might be also a metacyst and/or a pericyst, a new term for all materials produced and deposited upon the ectocyst by the encysting cell, often mucus and/or lepidosomes (Gutiérrez *et al*. 2003, Foissner *et al*. 2005). However, the light microscopical findings show a much greater diversity of cyst wall structures (Reid and John 1983, Reid 1987, Foissner 1993, Berger 1999, Foissner *et al*. 2002), suggesting that refined electron microscopical and cytochemical analyses will show many new structures, such as the lepidosomes in *Meseres* and some other ciliates (Foissner *et al*. 2005).

The unusual, lepidosome-coated resting cyst of *Meseres corlissi* was a good opportunity to contribute to the fine structure of ciliate resting cysts. Transmission electron microscopy of ciliate cysts has been neglected and most descriptions are rather meagre lacking, for instance, detailed morphometrics and a diagrammatic

Address for correspondence: Wilhelm Foissner, Universität Salzburg, FB Organismische Biologie, Hellbrunnerstrasse 34, A-5020 Salzburg, Austria; E-mail: Wilhelm.Foissner@sbg.ac.at

presentation. Thus, reliable data are available for less than 30 species (for literature, see Gutiérrez *et al*. 2003 and the present paper). Indeed, the present study is the first which describes in detail the fine structure of the resting cyst of an oligotrichous ciliate, a large group dominating the freshwater and marine ciliate plankton (Lynn *et al*. 1991, Foissner *et al*. 1999). For a general introduction to ciliate resting cysts, see Corliss and Esser (1974), Gutiérrez *et al*. (2003), and part 1 of the study (Foissner *et al*. 2005).

MATERIALS, METHODS AND TERMINOLOGY

Material. Pure cultures of *Meseres corlissi* Petz and Foissner (1992) from the Salzburg type locality were obtained as described in Weisse (2004). Cysts were collected from 3-weeks-old cultures devoid of active cells, that is, were detached from the bottom and wall of the culture dishes by strong shaking.

Methods. Ciliate resting cysts are difficult to fix due to the dense wall structures. Of several attempts made, the following protocol provided reasonable results: 10 ml glutaraldehyde (25%) + 6 ml aquaous osmium tetroxide (2%) + 10 ml saturated aquaous mercuric chloride. Mix just before use, fix for 1h, wash in 0.05 M cacodylate buffer, and transfer to Epon 812 *via* a graded ethanol series and propylene oxide. Flat-embedding in aluminium weighing pans allowed cysts to be investigated light microscopically (× 400) and to select well-preserved specimens for electron microscopy, that is, to cut off from the flat molds and mount onto the face of epoxy blocks. Ultrathin sections were cut with a diamond knife mounted on a Reichert ultracut. Sections were viewed in a Zeiss EM 910, either unstained or after staining with uranyl acetate followed by bismuth (Riva 1974) or, as usual, uranyl acetate followed by lead citrate (U/L staining). The Riva method is referred to "bismuth stain" throughout the paper. The images were digitalized and improved electronically. The results base on 17 sectioned cysts, of which 6 were investigated in detail.

Terminology. General terminology is according to Corliss (1979); systematic categories are based on the new classification by Agatha (2004); and cyst wall terminology is according to Gutiérrez *et al*. (2003). However, I introduce also a new term, viz., pericyst (*peri* Gr. - around/upon ectocyst), which comprises all materials produced and deposited upon the ectocyst by the encysting cell, for instance, mucus and/or lepidosomes in *Meseres* and cortical granules in *Engelmanniella* (Wirnsberger-Aescht *et al*. 1990).

RESULTS

Morphometry and a main artifact

Fixed cysts differ conspicuously from vital ones by an about 5 µm wide, clear zone between ectocyst and pericyst (Figs 4, 22; Table 2). Measurements suggest that this space is caused by about 15% cyst shrinkage, while the pericyst tends to become inflated (Table 1). Epon embedded, unsectioned cysts have a very similar size as those from thin sections, showing the lack of shrinkage in the post-fixational preparation steeps (Tables 1, 2).

Influence of staining and the chitin layer

Unstained sections provide sufficient contrast to be compared with conventionally (U/L) stained specimens. Both look quite similar, except of the endocyst which is more prominent in the unstained sections (cp. Figs 7, 8, 22, 23).

Bismuth staining shows two main differences (Figs 19, 20): the ectomesocyst is stronger stained than the endomesocyst (*vice versa* in U/L stains) and the ectocyst appears not dark and coarsely granular but alveolate with bright, membrane-like boundaries, likely corresponding to the minute spaces between the ectocyst flocs. There are also changes in the cytoplasm: the greyish granules (U/L staining) and the black chromatin bodies (U/L staining) appear bright.

The alkaline bismuth solution applied stains polysaccharides, including glycogen (Hayat 1989). In *Meseres*, the strongest stain is found in the ectomesocyst (Figs 19, 20), suggesting that it comprises the globular chitin layer (ghosts) demonstrated with the Van Wisselingh colour test (Foissner *et al*. 2005). This is supported in that the ectomesocyst is a rather thick layer (~ 350 nm), as is the wall of the KOH ghosts in the Van Wisselingh test. Further, only the ectomesocyst shows a fine structure resembling that of chitin (Westheide and Rieger 1996).

Lepidosomes

The cysts of *M. corlissi* are very sticky and must be detached by strong shaking from the walls of the culture dish (Foissner *et al*. 2005). This causes loss of the lepidosomes and the mucus on the side they are attached (Fig. 4). Most lepidosomes are spherical, except some of those which touch the cyst wall and become hemispherical.

The lepidosomes hardly shrink by the preparation procedures and consist of a thin, about 50 nm thick base from which the polygonal crests (facets) arise, providing the wall with a total thickness of 348 nm on average (Table 2). Both the base and the crests consist of about 20 nm thick fibres likely longer than 1 µm. The individual fibres form minute bundles which unite with other bundles becoming gradually thicker and reticulate. Although the resulting mould appears highly disordered, it produces the conspicuous crests, that is, the polygonally faceted

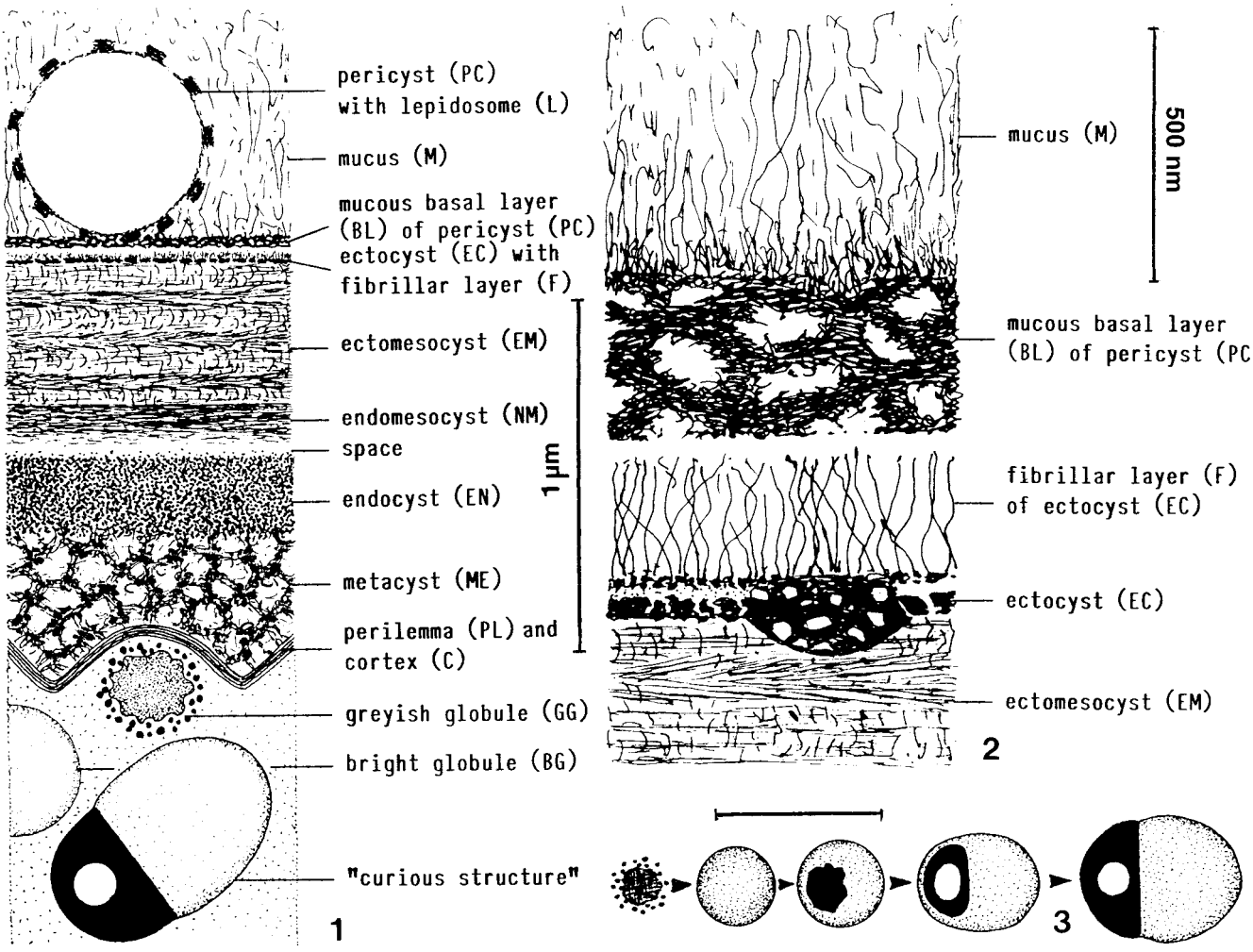

Figs 1-3. *Meseres corlissi*, semischematic figures of resting cyst structures. All based on transmission electron microscopical investigations and drawn to scale, using average values shown in Table 2, except of the lepidosome in figure 1 which is reduced in size by a factor of 10. **1** - overview with terminology and abbreviations used in this study. Scale bar 1 µm; **2** - details of pericyst and ectocyst. **3** - development of the "curious structures". Scale bars: 1µm (1, 3); 500 nm (2).

lepidosome surface (Figs 1, 4, 5, 9-14, 22; for SEM micrographs, see Foissner *et al*. 2005). Usually, the base is somewhat perforated, and thus bacteria may enter the lepidosomes (Fig. 9). In scanning preparations, the lepidosome base is frequently not preserved (Foissner *et al*. 2005).

Cyst wall

In vivo, the cyst wall is smooth, while minute ridges occur in fixed specimens (Fig. 4). These scattered ridges are shrinking artifacts, which become very conspicuous in poorly fixed (formalin, ethanol) cysts, as used for cytochemistry (Foissner *et al*. 2005). In the electron microscope, the wall consists of five distinct layers and several sublayers, while it is basically bipartite in the light microscope (Foissner *et al*. 2005). The morphometric data show that the inner, slightly thicker layer is composed of the metacyst and the endocyst (together 657 nm average, Table 2), while the slightly thinner, outer layer comprises the mesocyst and the ectocyst (together 566 nm on average and without the delicate microfibrillar layer, Table 2). The semischematic figures 1 and 2 summarize the structures seen.

Metacyst: The metacyst touches the ciliate's cortex and has an average thickness of 450 nm. It consists of fibrous material forming an alveolate mass, the thick-

Table 1. *Meseres corlissi*, morphometric data on resting cysts from life (upper line; from Foissner *et al*. 2005) and after Epon-embedding (lower line) as used for transmission electron microscopy. Measurements in µm. CV - coefficient of variation in %, M - median, Max - maximum, Min - minimum, n - number of cysts investigated, SD - standard deviation, $\bar{x}$ - arithmetic mean.

Characteristics	$\bar{x}$	M	SD	CV	Min	Max	n
Length (without pericyst)	47.3	47	3.3	6.9	42	55	21
	41.1	41	2.0	4.8	38	45	19
Width (without pericyst)	45.4	45	4.0	8.7	40	55	21
	36.8	38	4.5	12.3	28	45	19
Length (with lepidosome coat)	59.5	58	4.9	8.3	50	70	21
	65.6	68	4.3	6.6	52	70	19
Width (with lepidosome coat)	58.2	58	5.2	8.9	50	68	21
	62.0	64	5.4	8.8	48	68	19
Length (distance between basal layer of pericyst)	about as length without pericyst						
	52.5	52	4.2	8.0	43	60	19
Width (distance between basal layer of pericyst)	about as width without pericyst						
	48.8	48	3.8	7.7	40	52	19

Table 2. *Meseres corlissi*, morphometric data on resting cyst fine structures seen in the transmission electron microscope. CV - coefficient of variation in %, M - median, Max - maximum, Min - minimum, n - number of cysts (not sections, to avoid pseudoreplication) investigated, SD - standard deviation, $\bar{x}$ - arithmetic mean.

Characteristics	$\bar{x}$	M	SD	CV	Min	Max	n
Largest diameter in middle third and without pericyst (µm)	41.3	42	2.9	7.1	37	45	6
Largest diameter in middle third from pericyst base to pericyst base (µm)	52.0	50	7.0	13.4	47	66	6
Space between ectocyst and pericyst base (µm)	5.3	3	4.3	80.2	2	14	6
Cyst wall, thickness without pericyst (nm)	1240.7	1292	330.0	26.6	750	1792	10
Metacyst, thickness (nm)	455.5	450	184.1	40.4	210	733	11
Endocyst, thickness (nm)	201.5	211	51.8	25.7	120	289	11
Space between endocyst and mesocyst, thickness (nm)	63.1	62	23.5	37.2	27	100	11
Mesocyst, thickness (nm)	478.2	482	143.1	29.9	280	750	10
Ectocyst, thickness (nm)	87.7	80	35.7	40.7	44	158	11
Ectocyst flocs, size (nm)	81.3	100	48.2	59.3	20	180	12
Fibrillar layer on ectocyst, thickness (nm)	306.5	233	254.9	83.2	167	1100	12
Pericyst, thickness of basal layer (nm)	350.7	320	138.5	39.5	185	600	10
Largest lepidosome, diameter (µm)	10.3	10	1.8	17.5	8	13	9
Lepidosome base, thickness (nm)	51.5	50	24.0	46.6	27	100	8
Lepidosome wall, total thickness (nm)	348.0	316	122.2	35.1	200	555	10
Greyish globules in cytoplasm, diameter (nm)	277.6	224	122.9	44.3	200	583	12
Greyish globules in cortex ridges, diameter (nm)	235.8	216	44.2	18.7	187	300	12
Bright globules, diameter (nm)	465.3	500	140.4	30.2	233	667	12
”Curious structures”, length (nm)	979.9	933	51.8	19.1	750	1333	13
”Curious structures”, width (nm)	723.6	700	146.0	20.2	567	1000	13
Mitochondria, largest diameter (µm)	1.3	1	0.3	20.9	1	2	8

ened edges of which provide the layer with a more or less distinct granular appearance. It is distinctly stained with bismuth (Figs 1, 7, 8, 19, 20; Table 2).

Endocyst: The endocyst has an average thickness of about 200 nm and is usually attached to the metacyst (Table 2); rarely, both are separated by a thin, bright zone. The endocyst appears structureless at even a magnification of ×100 000 (Figs 1, 7, 8) and in bismuth stains (Figs 19, 20). In unstained sections, it has more contrast than the metacyst and the mesocyst, indicating that is more compact (Fig. 23).

Mesocyst: The mesocyst has an average thickness of 478 nm and is thus the thickest layer of the wall (Table 2). It is separated from the endocyst by a bright, about

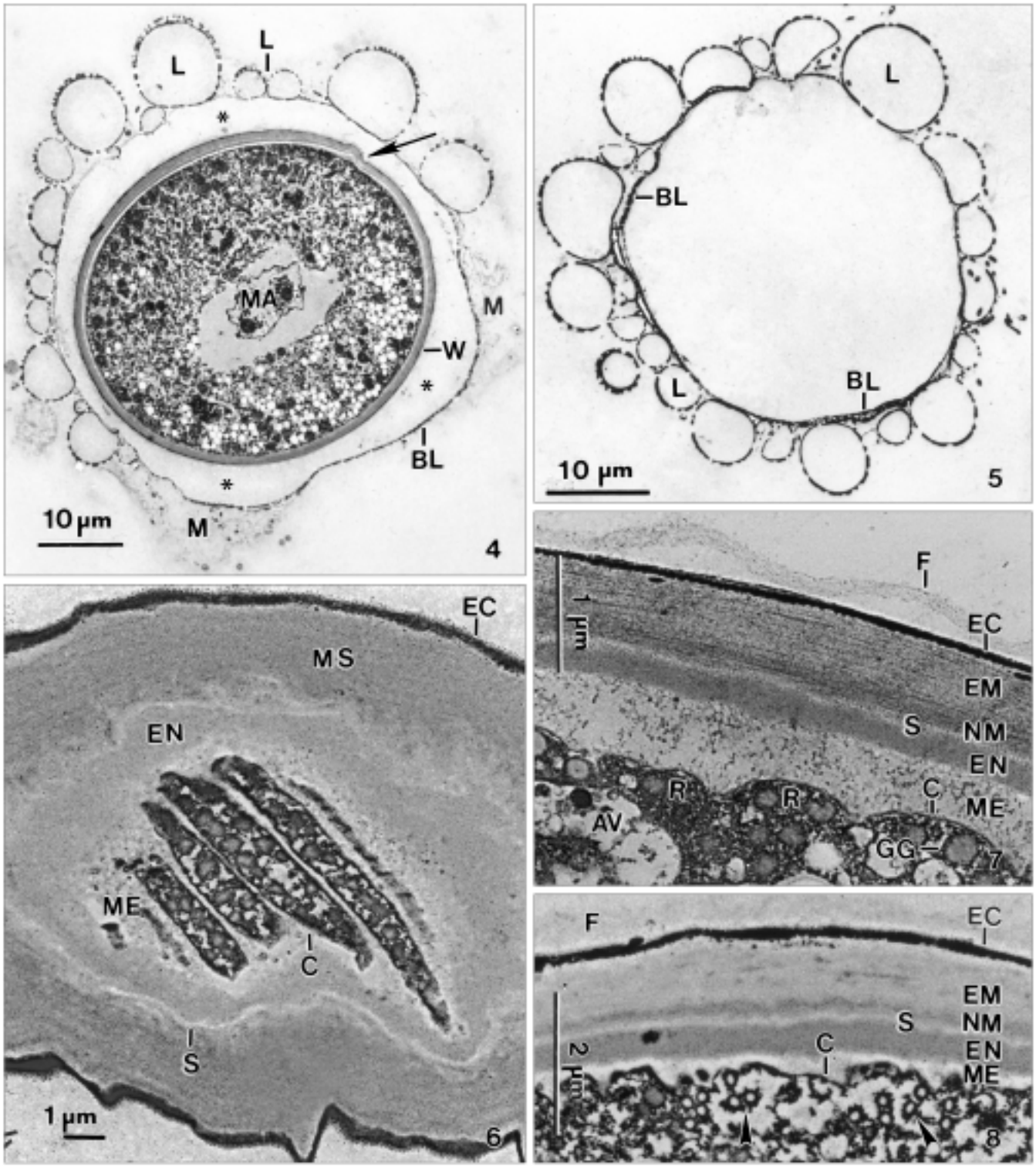

Figs 4-8. *Meseres corlissi*, transmission electron micrographs of resting cysts. **4** - overview in middle third. Two main artifacts are recognizable, viz., a shrinkage ridge (arrow) and a wide space (asterisks) between ectocyst and basal layer of pericyst. The lepidosomes were lost during collection on the side the cyst was attached to the culture dish; **5** - grazing section of the pericyst showing the lepidosomes attached to the mucous basal layer; **6** - grazing section showing cortical ridges possibly appearing as fibres in the light microscope (cp. Figure 7); **7, 8** - cyst wall details from two specimens. The cyst shown in figure 8 has maintained some adoral basal bodies (arrowheads). BL - basal layer of pericyst, C - cortex, EC - ectocyst, EM - ectomesocyst, EN - endocyst, F - microfibrillar layer, L - lepidosomes, M - mucus, MA - macronucleus, ME - metacyst, MS - mesocyst, NM - endomesocyst, R - cortical ridges, S - space, W - cyst wall.

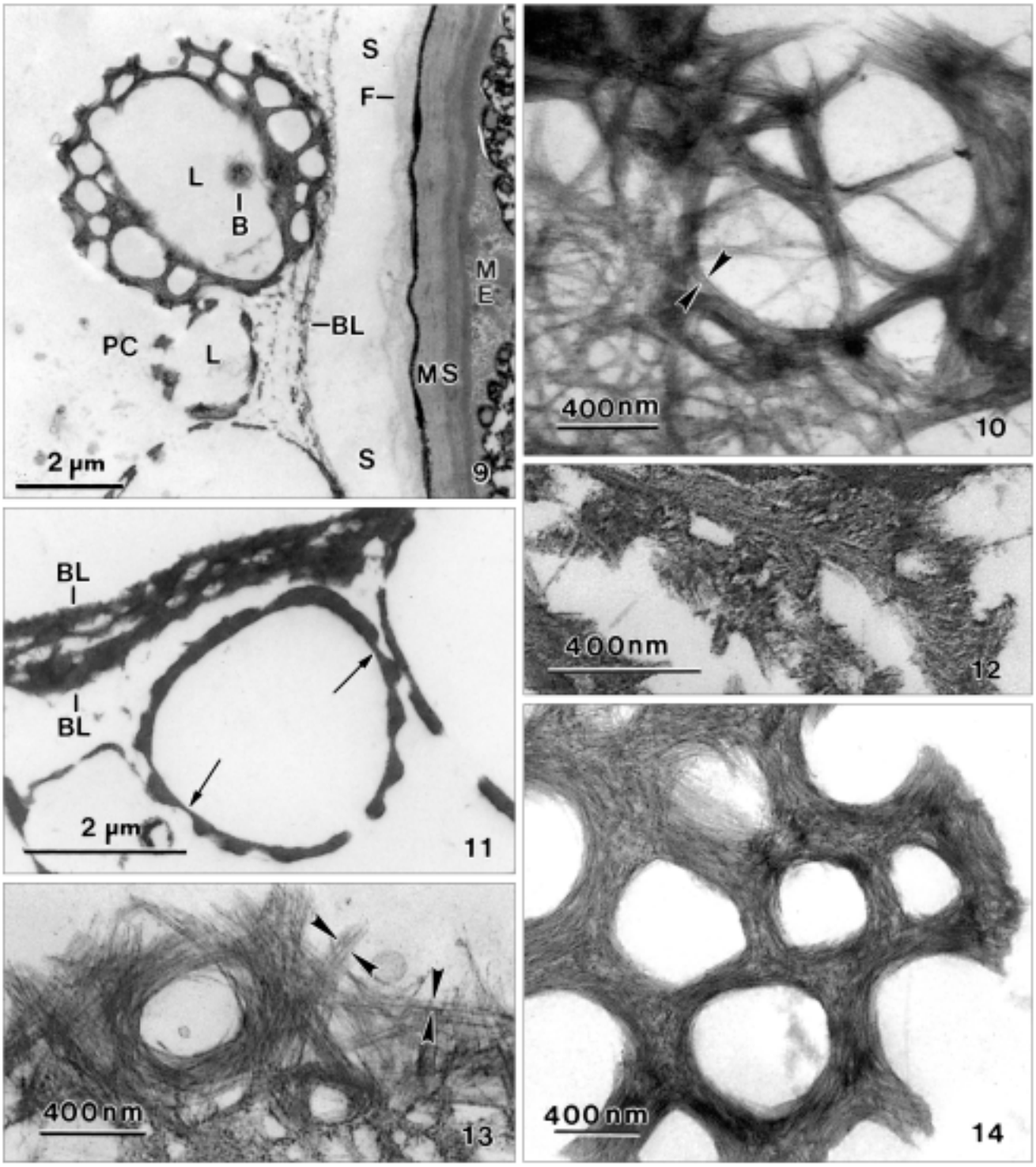

Figs 9-14. *Meseres corlissi*, transmission electron micrographs of the lepidosomes coating the resting cyst. **9-12** - overview (9) and details (10-12) of the cyst wall and the lepidosomes. Figure 9 shows the spatial relationship of the various layers of the cyst wall, beginning with the mucous, lepidosome-containing pericyst to the granular metacyst, which is thickened in the area labeled. Gracing sections of the lepidosomes (9, 10) reveal the lepidosome base (Fig. 11, arrows) composed of about 20 nm thick fibres (Fig. 10, opposed arrowheads) forming a finely reticulate sheet (10). In contrast, the basal layer of the pericyst consists of very thin (< 5 nm) fibres forming a coarsely reticulate mould (11, 12); **13, 14** - the facets of the lepidosomes (14) consist of highly interwined, about 20 nm thick fibres some marked by opposed arrowheads in figure 13. B - bacterial rod, BL - basal layer of pericyst, F - microfibrillar layer, L - lepidosomes, ME - metacyst, MS - mesocyst, PC - pericyst, S - artificial space between pericyst and ectocyst.

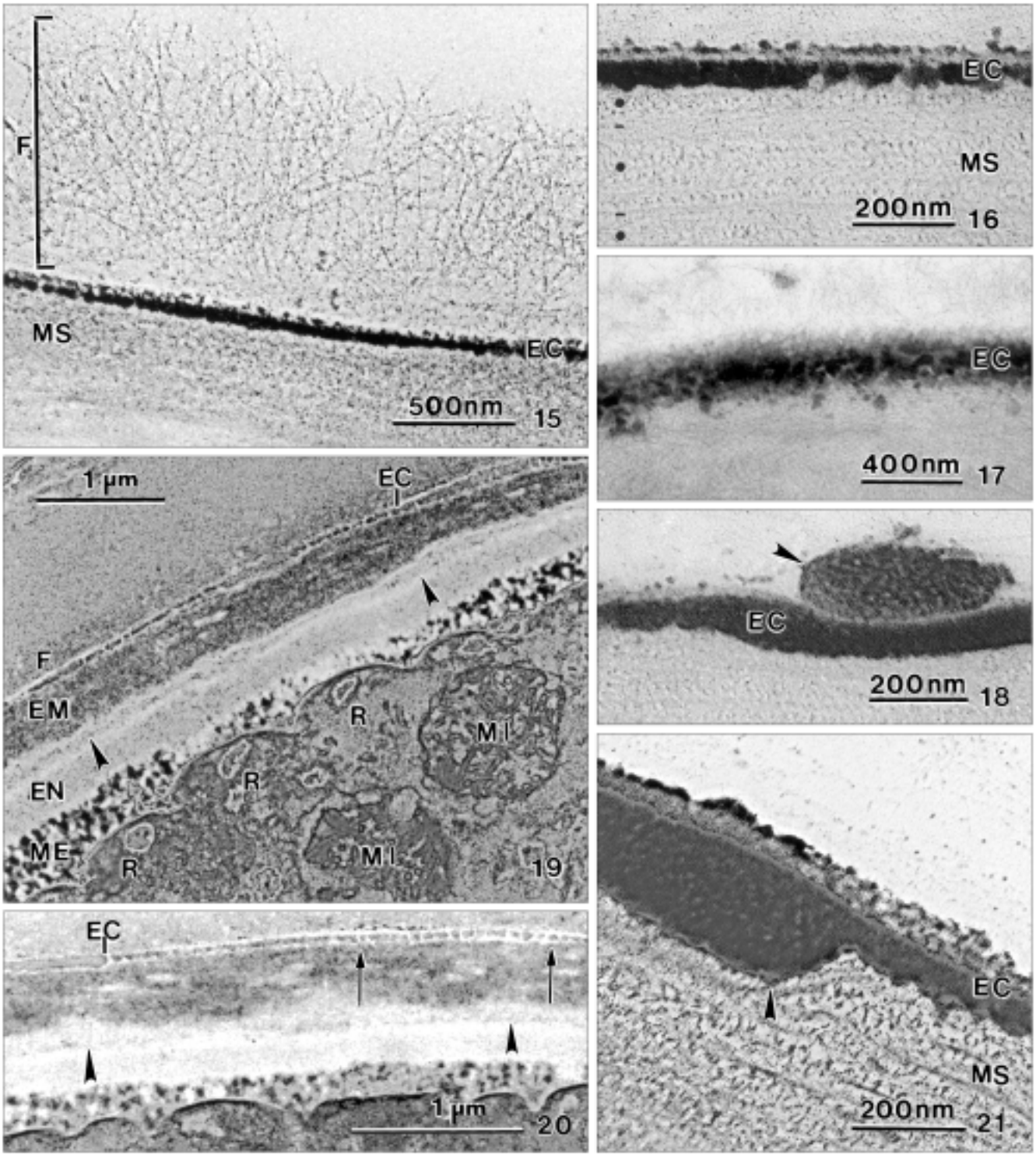

Figs 15-21. *Meseres corlissi*, transmission electron micrographs of the cyst wall after uranyl acetate/lead citrate (15-18, 21) and bismuth (19, 20) staining. **15 -** the ectocyst consists of a microfibrillar layer (F) attached to an electron-dense, granular sheet; **16, 17 -** the dark (electron-dense) portion of the ectocyst is bilayered and consists of granules and polygonal platelets. The alternating dots and lines in figure 16 mark stacks of helicoidally arranged bundles of microfibrils; **18, 21 -** the ectocyst may have reticulate plaques (arrowheads) on the outer and inner surface. Note the microfibrillar structure of the mesocyst in figure 21; **19, 20 -** bismuth stained sections reveal the ectocyst composed of small and large platelets (arrows). Note the alveolate structure of the metacyst. The endomesocyst (arrowheads) is much lighter stained than the ectomesocyst (EM) and in conventionally contrasted sections (Figs 7, 8). This suggests a different chemical composition. EC - ectocyst, EM - ectomesocyst, EN - endocyst, F - microfibrillar layer, MI - mitochondria, MS - mesocyst, R - cortical ridges.

63 nm thick zone; the separation is not sharp, but both the mesocyst and the endocyst become gradually lighter. In the best preparations, the mesocyst shows two zones, viz., an endomesocyst and an ectomesocyst (Figs 1, 4, 7, 8, 16, 19-21). The endomesocyst, which occupies the proximal fifth, stains slightly darker than the ectomesocyst and consists of very densely arranged, stratified fibres. The ectomesocyst is also composed of very fine fibres connected by countless, minute bridges. The arrangement of the fibres reminds the helicoidal pattern of cellulose and chitin microfibrills in plant and animal tissues (Westheide and Rieger 1996), that is, the layer appears to be composed of stacks of helicoidally arranged bundles of microfibrils. Thus, it is likely this layer which shows the positive reaction for chitin (see above and Foissner *et al*. 2005).

Ectocyst: The ectocyst is complex, that is, composed of an about 90 nm thick, dark (electron-dense) zone from which fine fibres emerge and extend vertically to the pericyst, forming an approximately 300 nm thick, delicate layer (Figs 1, 2, 7, 15; Table 2). Thus, the ectocyst has an average total thickness of about 400 nm. The darker zone, which is electron-dense in both unstained and U/L stained sections, is bipartite consisting of small (mainly in distal half) and up to 180 nm large (mainly in proximal half) granules and polygonal platelets (flocs) with more or less sharp edges; frequently, the zone thickens to or has attached plaque-like accumulations with a coarsely reticulate fine structure (Figs 1, 2, 6-9, 15-23).

The microfibrillar layer on the dark zone likely represents a distinct part of the ectocyst because the fibres are vertically oriented and may form a conspicuous layer, which may detach from the dark zone (Figs 7, 9, 15). Alternatively, it could be part of the pericyst's basal layer which, however, is less likely because the basal layer consists of a dense, reticulate mass of fibres (see next paragraph).

Pericyst: The pericyst consists of the lepidosomes described above and the cyst's mucous envelope, which comprises two more or less distinct zones. The about 350 nm thick basal layer is a dense, reticulate mass of very fine (~ 3 nm), bundled fibres forming a membrane-like cover on the cyst; structurally, it resembles the base of the lepidosomes. However, both are different because the fibres have a different diameter (~ 3 *vs.* 20 nm) and only the mucous layer distinctly stains with alcian blue (Foissner *et al*. 2005). Distally, the basal layer dissolves into a fluffy, microfibrillar (mucous) material extending beyond the lepidosomes and usually colonized by bacteria and small protists (Figs 1, 2, 4, 5, 9, 22, 23; Table 2).

The encysted cell

Cortex: In interphase specimens, the cortex is smooth; covered by two to five perilemma layers, each consisting of a unit membrane; and supported by a single sheet of microtubules (Fig. 25). In encysted cells, the cortex has over 200 convex ridges; two perilemma membranes; and all microtubules and ciliary structures disappeared (Figs 4, 7-9, 19, 20, 22, 25, 26). The cortical ridges, which extend between the poles of the cyst, usually contain greyish stained granules arranged one after the other and 236 nm across on average (Fig. 6, Table 2). Likely, the ridges are identical with the "fibres" seen in the light microscope (Foissner *et al*. 2005). The cortical membranes are usually poorly preserved, but some specimens and sections show five of them with a total thickness of about 20 nm (from outside to inside): two perilemma membranes, separated from each other by a 3-5 nm wide, bright zone; the cell membrane; and the outer and inner alveolar membrane (Figs 25, 26).

The entire somatic and oral infraciliature is resorbed. Of six cysts investigated in detail, one showed a small field of scattered basal bodies (Fig. 8). This is in accordance with the light microscopical data showing that 5% of the specimens have remnants of the ventral adoral membranelles (Foissner *et al*. 2005).

Cytoplasm: At low magnification, the cyst's cytoplasm is spotted by bright and dark globules (Fig. 4). The latter are 1-2 µm-sized mitochondria with a tendency to accumulate in the cell's periphery. Most of the bright inclusions, which have an average diameter of 465 nm, are precursors of, or belong to curious structures never seen in ciliate cysts and thus probably related to the lepidosomes. These curious structures, which have an average size of 980 × 724 nm, are composed of a large, lightly stained portion, which rarely contains a crystal-like particle, and a small, electron dense portion with a central, bright globule sometimes containing a filamentous reticulum (Figs 1, 3, 22, 28-33; Table 2). Likely, these strange structures develop from about 278 nm sized, greyish stained, finely granular precursors *via* a globular, bright stage 465 nm across on average; the greyish precursors are frequently wrinkled and usually surrounded by masses of ribosomes (Figs 3, 22, 31; Table 2).

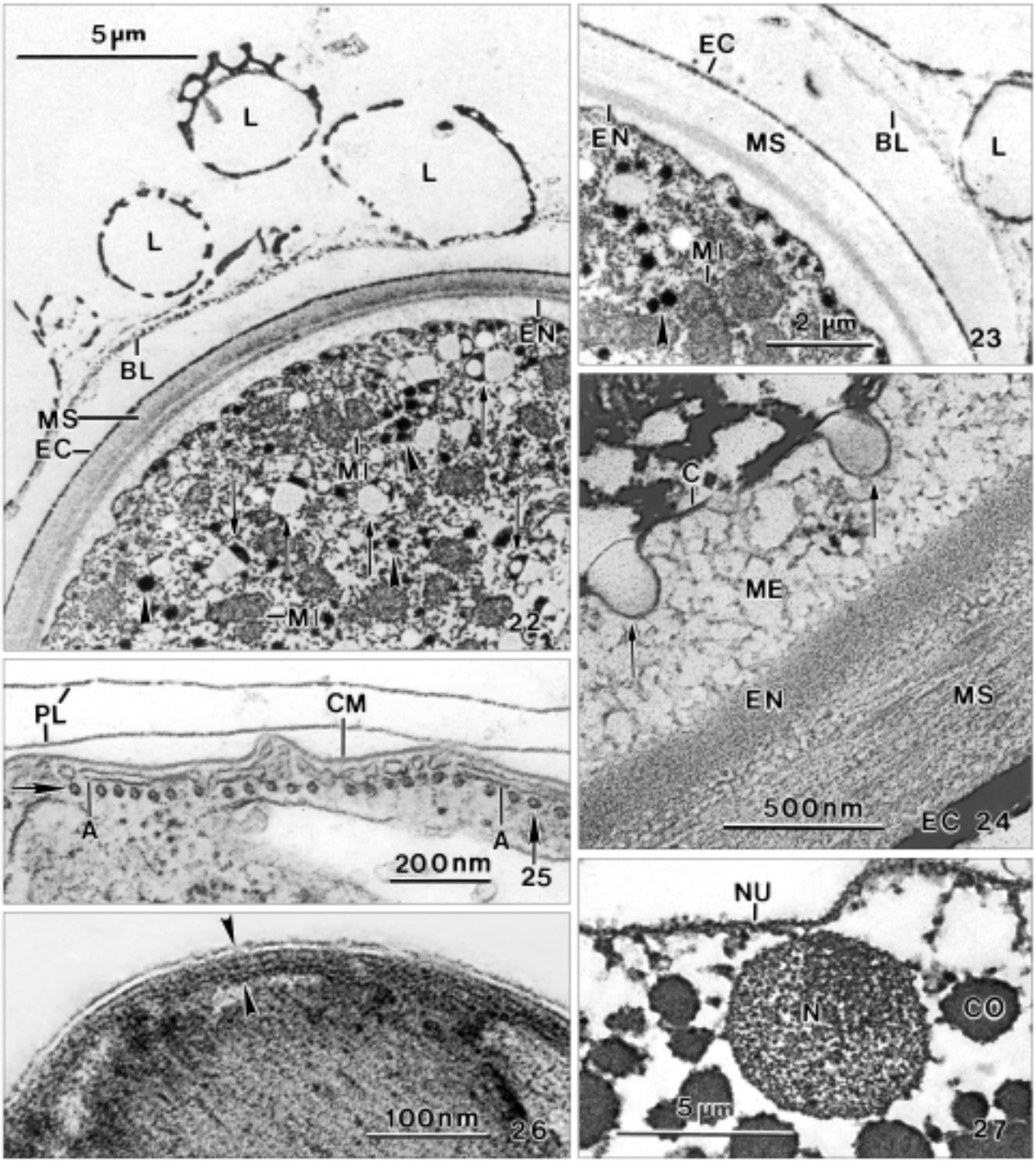

Figs 22-27. *Meseres corlissi*, transmission electron micrographs of resting cysts (22-24, 26, 27) and an active specimen (25); unstained (22, 23) and contrasted with uranyl acetate and lead citrate (24-27). **22, 23** - unstained sections show good contrast, but the microfibrillar layer of the ectocyst and the metacyst are hardly recognizable. The mesocyst and the space between mesocyst and endocyst are recognizable in some sections (22), but not in others (23). The granular layer of the ectocyst and the endocyst are electron-dense and thus well recognizable. Note the furrowed cortex and the curious structures (arrows) and their precursors (arrowheads) shown in detail on the following plate; **24** - the cortex may form spherical protuberances projecting into the alveolate metacyst. Note the finely granular endocyst; **25, 26** - both active (25) and encysted (26, arrowheads) specimens are covered by five unit membranes: two perilemma membranes, the cell membrane, and the outer and inner alveolar membrane. The microtubule sheet (25, arrows) has been resorbed in the cyst (26); **27** - part of macronucleus. A - cortical alveoli, BL - basal layer of pericyst, C - cortex, CM - cell membrane, CO - chromatin bodies, EC - ectocyst, EN - endocyst, L - lepidosomes, ME - metacyst, MI - mitochondria,; MS - mesocyst, N - nucleolus, NU - nuclear membrane, PL - perilemma membranes.

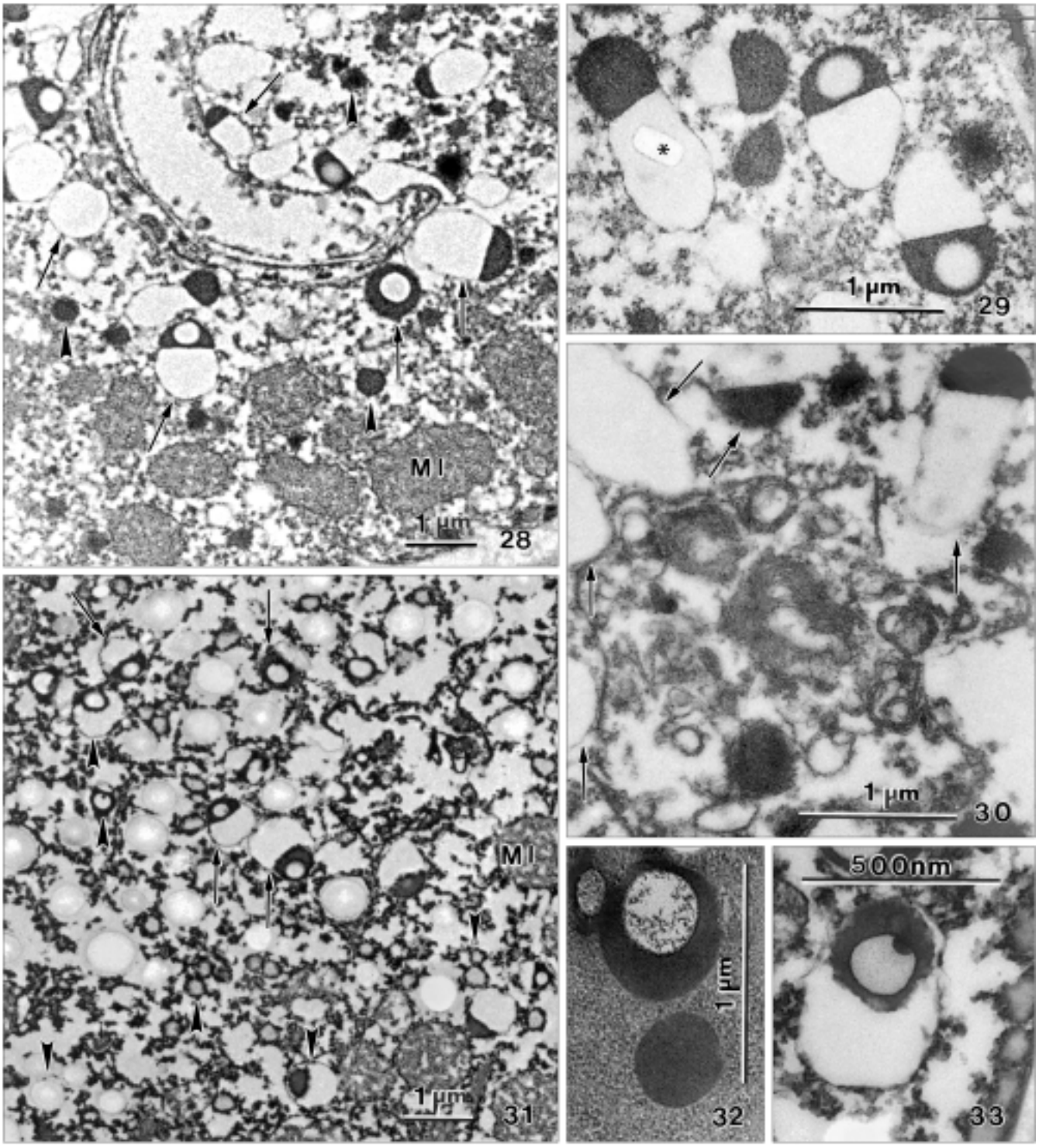

Figs 28-33. *Meseres corlissi*, transmission electron micrographs of unstained sections of the resting cyst cytoplasm. **28, 29, 31, 32** - most resting cysts are packed with curious, ellipsoidal structures (arrows) composed of two bright thirds and a dark (electron-dense) third containing a bright globule sometimes filled with flocculent material (32). There are many precursors (arrowheads) of the curious, about 1 µm long structures, which are likely related to lepidosome production. Rarely, the bright portion contains a crystal-like inclusion (29, asterisk). See figure 3 for an interpretation of the genesis of the curious structures; **30** - an autophagosome surrounded by the curious structures (arrows) shown in figures 28, 29, and 31; **33** - a late developmental stage of the curious structures. MI - mitochondria.

The histochemical data show that there are also lipid droplets and glycogen granules in the cytoplasm (Foissner *et al*. 2005). Both are difficult to identify in the mass of structures described above. There are also some autophagous vacuoles about 2-3 µm across, containing membrane-like structures and other debris (Fig. 30).

DISCUSSION

Terminology: pericyst and metacyst

Light microscopical and electron microscopical resting cyst terminology are neither consistent nor complete, making comparisons difficult and circumstantial. For example, the mesocyst is called endocyst and the endocyst is named intimocyst by Rieder (1973). The unclear terminology also influences the recognition and classification of the individual cyst wall layers, as shown for instance, by the *Colpoda cucullus*-like ciliate (for identification, see Foissner *et al*. 2005) investigated by Chessa *et al*. (2002). In my interpretation, the distal portion of the so-called ectocyst is a pericyst because it is obviously composed of flocculent mucus containing many lepidosomes, as in *Meseres* (Figs 1, 4, 5); further, this interpretation matches the light microscopical findings (Foissner 1993) which were not considered by Chessa *et al*. (2002). The proximal portion of Chessa's ectocyst is likely the ectomesocyst, while the narrow, strongly osmiophilic layer between pericyst and ectomesocyst is the ectocyst, as in stichotrichine spirotrichs and *Meseres* (Figs 1, 7, 8). Thus, this *Colpoda* has a four-layered cyst wall composed of pericyst, ectocyst, mesocyst, and endocyst. A similar re-interpretation needs the resting cyst wall of *Colpoda magna*, where Frenkel (1994) named the pericyst ectocyst and the ectocyst "granular layer". It is beyond the scope of this study to re-interprete the literature which will be often difficult considering the poor fixation and incomplete presentation of the structures.

A first attempt for a more clear cyst wall terminology was undertaken by Gutiérrez and Walker (1983), who introduced the terms "metacyst" (for the "granular layer" between ciliate cortex and endocyst), ectomesocyst, and endomesocyst (for the two layers of the mesocyst). Unfortunately, this attempt largely remained unrecognized likely because it was published as a meeting abstract only.

I not only support the terminology of Gutiérrez and Walker (1983) and Gutiérrez *et al*. (2003), but introduce "pericyst" as a new term for all materials produced and deposited upon the ectocyst by the encysting cell. Usually, this is a more or less voluminous, sticky coat of mucus sometimes containing lepidosomes, as in *Meseres* and various colpodids. The mucous coat is often very hyaline and sticky and thus easily overlooked or lost when cysts are collected; further, it is sometimes partially or completely eroded by bacteria, especially in old specimens.

Martin-Gonzalez *et al*. (1992a) do not consider the mucous coat as a real cyst layer. I disagree, not only because it is produced by the encysting cell and may contain the highly characteristic lepidosomes, but also because it has two important ecological functions: (i) it adheres the cyst to the substrate and (ii) increases buoyancy, that is, cyst dispersal by floatation because the flocculent mucus has a low specific mass very near to that of water (Ruttner 1940, Padisák *et al*. 2003).

Comparative and phylogenetic analyses

Among the halterine spirotrichs, detailed investigations on resting cyst morphology have been performed only in *M. corlissi* (Foissner *et al*. 2005 and the present study). Unfortunately, the same is true for the oligotrichine spirotrichs: only Reid (1987) published three TEM micrographs from the resting cyst of *Strombidium crassulum* (a misidentification; the light microscopic figures of the trophic cells show a strobilidiid oligotrich). Thus, the within-group comparison is very limited. However, if the two examples are representative, then halterine and oligotrichine spirotrichs have very different resting cysts. In the species studied by Reid (1987), the cyst wall is extremely massive and appears to be made of crystalline material (X-ray analysis), similar as in the colpodid *Bursaria* (Bussers 1976), possibly calcium phosphate or calcium carbonate in an organic matrix arranged in 6-11 alternating light and dark laminae. Separated from the main wall by a clear area of variable height is an outer spiny membrane 0.1-0.2 µm in thickness. The spines have solid bases and appear to be made of a similar material to the cyst wall, but details are not recognizable. Reid (1987) emphasized that TEM fixation of the cyst was notoriously difficult, and thus it cannot be excluded that further layers exist but were not preserved.

The halterine spirotrichs, such as *M. corlissi* and *Halteria grandinella*, are a hot spot in ciliate classification (for a review, see Foissner *et al*. 2004): while gene sequences suggest a close relationship with the stichotrichine spirotrichs (e.g. *Oxytricha, Stylonychia*),

morphology and ontogenesis indicate a relationship with the oligotrichine spirotrichs (e.g. *Strombidium, Tintinnidium*). Thus, Foissner *et al*. (2004) called for further morphological and molecular data to solve the puzzle. The *Meseres* study provides four new features, most of which support the classic view.

A five-layered cyst wall, as found in *M. corlissi*, is quite typical for stichotrichine spirotrichs, especially the possession of a metacyst. This seemingly supports the molecular view of a close relationship of halterine and stichotrichine spirotrichs. However, a metacyst occurs also in the euplotine (Walker and Maugel 1980) and phacodinine (Calvo *et al*. 1992) spirotrichs, suggesting that it is a plesiomorphic feature useless for phylogenetic purposes. This is emphasized by *Blepharisma*, which was considered as a typical spirotrich for a long time (Corliss 1979), but now is in a different subphylum (Lynn 2003). *Blepharisma* has a metacyst according to figures 1 and 6 in the paper of Mulisch and Hausmann (1989) and the description of Larsen and Nilsson (1995): "the endocyst of *B. lateritium* is separated from the encysted ciliate by a narrow, amorphous, low density zone". None the less, the *Blepharisma* cyst is rather different from those of stichotrichine and halterine spirotrichs because the ectocyst is composed of fine, weakly staining, fibrous material, while the endocyst is made of electron-dense plates (lamellae) embedded in an amorphous and fine-filamentous matrix (Mulisch and Hausmann 1989, Larson and Nilsson 1995). The opposite pattern occurs in stichotrichine and halterine spirotrichs (Figs 1, 4, 7, 8).

The three other features mentioned above, that is, the structure of the ectocyst, the lepidosomes, and the cyst wall composition relate *Meseres* more distinctly to the oligotrichine than to the stichotrichine spirotrichs. The ectocyst is lamellar in stichotrichine and phacodinine spirotrichs (Calvo *et al*. 1992, Gutiérrez *et al*. 2003), amorphous and weakly stained in euplotine spirotrichs (Walker and Maugel 1980), while coarsely granular and dense in *Meseres* (Figs 1, 7, 15-21). Unfortunately, no detailed data are available, except those of Reid (1987) discussed above, from the oligotrichine spirotrichs, such as *Strombidium, Strobilidium,* and *Tintinnidium.* Thus, the phylogenetic significance remains obscure, but it is obvious that the ectocyst is different in stichotrichine and halterine spirotrichs, giving some support to the hypothesis that the later form a distinct group outside of the stichotrichs (Foissner *et al*. 2004). This is emphasized by the lepidosomes (Figs 1, 4, 5), a special feature not found in cysts and trophic cells of more than 50 stichotrich species (Berger 1999, Gutiérrez *et al*. 2003, Foissner, unpubl. data from more than 30 species), while present in a new species of *Halteria* (Foissner, manuscript in preparation) and likely also in several oligotrichs *s. str*. A SEM-reinvestigation of the cyst of the freshwater *Pelagostrombidium* studied by Müller (2002) showed spines very similar to those of the new *Halteria* species mentioned above, that is, the spines are lepidosomes attached to a filamentous, membrane-like structure distal of the ectocyst (Foissner, unpubl.). The same interpretation applies to the marine species studied by Reid (1987) and discussed above. Thus, the occurrence of lepidosomes is likely a main synapomorphy of halterine and oligotrichine Oligotrichea.

Part of the *Meseres* cyst wall is made of chitin (Foissner *et al*. 2005). Chitin occurs also in the cyst wall of other ciliates, including heterotrichs (e.g. *Stentor, Blepharisma*) and euplotine and phacodinine spirotrichs (e.g. *Euplotes, Phacodinium*), while the cyst of several stichotrichine spirotrichs (*Onychodromus grandis, Oxytricha* sp., and *Urostyla trichogaster*) lacks chitin (Bussers and Jeuniaux 1974). Later, however, chitin was reported in *Oxytricha bifaria*, using a combined protease-chitinase treatment of ultrathin sections (Rosati *et al*. 1984). Thus, some chitin is likely present also in stichotrichine spirotrichs. In general, however, chitin distribution indicates that *Meseres* is more closely related to euplotine and phacodinine than stichotrichine spirotrichs (see also Mulisch 1993). Unfortunately, data are lacking from the oligotrichs *s. str*.

In estimating the phylogenetic significance of resting cyst morphology and composition, it must be taken into account that detailed data are available from less than 30 species! Certainly, this is a very incomplete sample, considering the high light microscopical diversity of ciliate resting cysts (for representative compilations, see Reid and John 1983, Reid 1987, Foissner 1993, Berger 1999, Foissner *et al.* 2002). Thus, any phylogenetic interpretation of cyst morphology and composition is a risky adventure.

None the less, cysts have been suggested to be an important tool in ciliate classification and phylogeny (Walker and Maugel 1980, Reid and John 1983, Rawlinson and Gates 1986, Martin-Gonzalez *et al*. 1992b), referring to the split of the hypotrichs in stichotrichine end euplotine spirotrichs (Lynn 2003). Mulisch (1993) additionally suggested chitin distribution as an indicator of the phylogenetic distance between euplotine (with chitin) and stichotrichine (without chitin; but see above) spirotrichs.

And Rios *et al*. (1988) speculated that the four-layered cyst wall of oxytrichid stichotrichs evolved from the three-layered wall of urostylid stichotrichs by adding the mesocyst. Much phylogenetic significance has been attributed to the infraciliature, that is, whether or not cilia, basal bodies, and cortical microtubules are preserved or resorbed in the resting cyst (Walker and Maugel 1980, Martin-Gonzalez *et al*. 1992b). Three cyst types can be distinguished with this feature: kinetosome-resorbing (KR), partial-kinetosome-resorbing (PKR), and non-kinetosome-resorbing (NKR) cysts. However, phylogenetic relationships are not (yet?) recognizable. For instance, the PKR type occurs in *Colpoda magna* (Colpodea), *Dileptus anser* (Haptoria), and *Kahliella simplex* (stichotrichine spirotrichs).

Acknowledgements. Financial support was provided by the Austrian Science Foundation, FWF project P 16796-B06. The technical assistance of Mag. Maria Pichler is greatly acknowledged. Thanks to Prof. Thomas Weisse and Mag. Elke Gächter for providing cultures of *M. corlissi*.

REFERENCES

Agatha S. (2004) A cladistic approach for the classification of oligotrichid ciliates (Ciliophora: Spirotricha). *Acta Protozool.* **43:** 201-217

Berger H. (1999) Monograph of the Oxytrichidae (Ciliophora, Hypotrichia). Kluwer, Dordrecht, Boston, London

Bussers J. C. (1976) Structure et composition du kyste de résistance de 4 protozoaires ciliés. *Protistologica* **12:** 87-100

Bussers J. C., Jeuniaux C. (1974) Recherche de la chitine dans les productions métaplasmatiques de quelques ciliés. *Protistologica* **10:** 43-46

Calvo P., Serrano S., Fernández-Galiano D., Arregui L., Campos I. (1992) Ultrastructural aspects of the mature resting cyst and encystment process in *Phacodinium metchnikoffi*. *Europ. J. Protistol.* **28:** 334

Chessa M. G., Largana I., Trielli F., Rosati G., Politi H., Angelini C., Delmonte Corrado M. U. (2002) Changes in the ultrastructure and glycoproteins of the cyst wall of *Colpoda cucullus* during resting encystment. *Europ. J. Protistol.* **38:** 373-381

Corliss J. O. (1979) The Ciliated Protozoa. Characterization, Classification and Guide to the Literature. 2 ed. Pergamon Press, Oxford, New York, Toronto, Sydney, Paris, Frankfurt

Corliss J. O., Esser S. C. (1974) Comments on the role of the cyst in the life cycle and survival of free-living protozoa. *Trans. Am. microsc. Soc.* **93:** 578-593

Foissner W. (1993): Colpodea. *Protozoenfauna* **4/1 I-X + 798 p**

Foissner W., Berger H., Schaumburg J. (1999) Identification and ecology of limnetic plankton ciliates. *Informationsberichte des Bayer. Landesamtes für Wasserwirtschaft* **3/99:** 1-793

Foissner W., Agatha S., Berger H. (2002) Soil ciliates (Protozoa, Ciliophora) from Namibia (Southwest Africa), with emphasis on two contrasting environments, the Etosha Region and the Namib Desert. *Denisia* (Linz) **5:** 1-1459

Foissner W., Moon-van der Staay S. Y., van der Staay G. W. M., Hackstein J. H. P., Krautgartner W.-D., Berger H. (2004) Reconciling classical and molecular phylogenies in the stichotrichines (Ciliophora, Spirotrichea), including new sequences from some rare species. *Europ. J. Protistol.* **40:** 265-281

Foissner W., Müller H., Weisse T. (2005) The unusual, lepidosome-coated resting cyst of *Meseres corlissi* (Ciliophora: Oligotrichea): Light and scanning electron microscopy, cytochemistry. *Acta Protozool.* **44:** 201-215

Frenkel M. A. (1994) The cyst wall formation in *Tillina magna* (Ciliophora, Colpodidae). *Arch. Protistenk.* **144:** 17-29

Gutiérrez J. C., Walker G. K. (1983) Cystology: a new area in protozoology. Proceed. 5th Europ. Conf. Ciliate Biology, Geneva (unpaged abstract)

Gutiérrez J. C., Diaz S., Ortega R, Martín-González A. (2003) Ciliate resting cyst walls: a comparative review. *Recent Res. Devel. Microbiol.* **7:** 361-379

Hayat M. A. (1989) Principles and Techniques of Electron Microscopy. Biological Applications. Mac Millan Press, London

Larsen H. F., Nilsson J. R. (1995) Fine structure of mature *Blepharisma lateritium* cysts. 2nd Europ. Congr. Protistol., Clermont-Ferrand, Progr. & Abstracts, 62

Lynn D. H. (2003) Morphology or molecules: How do we identify the major lineages of ciliates (phylum Ciliophora)? *Europ. J. Protistol.* **39:** 356-364

Lynn D. H., Montagnes D. J. S., Dale T., Gilron G. L., Strom S. L. (1991) A reassessment of the genus *Strombidinopsis* (Ciliophora, Choreotrichida) with descriptions of four new planktonic species and remarks on its taxonomy and phylogeny. *J. mar. biol. Ass. U. K.* **71:** 597-612

Martín-Gonzalez A., Benitez L., Palacios G., Gutierrez J. C. (1992a) Ultrastructural analysis of resting cysts and encystment in *Colpoda inflata* 1. Normal and abnormal resting cysts. *Cytobios* **72:** 7-18

Martín-Gonzalez A., Benitez L., Gutierrez J. C. (1992b) Ultrastructural analysis of resting cysts and encystment in *Colpoda inflata* 2. Encystment process and a review of ciliate resting cyst classification. *Cytobios* **72:** 93-106

Müller H. (2002) Laboratory study of the life cycle of a freshwater strombidiid ciliate. *Aquat Microb. Ecol.* **29:** 189-197

Mulisch M. (1993) Chitin in protistan organisms. Distribution, synthesis and deposition. *Europ. J. Protistol.* **29:** 1-18

Mulisch M., Hausmann K. (1989) Localization of chitin on ultrathin sections of cysts of two ciliated protozoa, *Blepharisma undulans* and *Pseudomicrothorax dubius*, using colloidal gold conjugated wheat germ agglutinin. *Protoplasma* **152:** 77-86

Padisák J., Soróczki-Pintér É., Rezner Z. (2003) Sinking properties of some phytoplankton shapes and the relation of form resistance to morphological diversity of plankton - an experimental study. *Hydrobiologia* **500:** 243-257

Petz W., Foissner W. (1992) Morphology and morphogenesis of *Strobilidium caudatum* (Fromentel), *Meseres corlissi* n. sp., *Halteria grandinella* (Müller), and *Strombidium rehwaldi* n. sp., and a proposed phylogenetic system for oligotrich ciliates (Protozoa, Ciliophora). *J. Protozool.* **39:** 159-176

Rawlinson N. G., Gates M. A. (1986) A morphological classification of encysting species of *Euplotes* (Ciliophora: Nassophorea: Euplotida). *Trans. Am. microsc. Soc.* **105:** 301-310

Reid P. C. (1987) Mass encystment of a planktonic oligotrich ciliate. *Mar. Biol.* **95:** 221-230

Reid P. C., John A. W. G. (1983) Resting cysts in the ciliate class Polyhymenophorea: phylogenetic implications. *J. Protozool.* **30:** 710-713

Rieder N. (1973) Elektronenoptische und histochemische Untersuchungen an der Cystenhülle von *Didinium nasutum* O. F. Müller (Ciliata, Holotricha). *Arch. Protistenk.* **115:** 125-131

Rios R. M., Pérez Silva J., Fedriani C. (1988) Cytochemical and enzymatic studies on the cyst wall of *Urostyla grandis* (Hypotrichida, Urostylidae). *Cytobios* **56:** 163-169

Riva A. (1974) A simple and rapid staining method for enhancing the contrast of tissues previously treated with uranyl acetate. *J. Microscopie* **19:** 105-108

Rosati G., Verni F., Ricci N. (1984) The cyst of *Oxytricha bifaria* (Ciliata Hypotrichida). III. Cytochemical investigation. *Protistologica* **20:** 197-204

Ruttner F. (1940) Grundriss der Limnologie. Walter de Gruyter & Co., Berlin

Walker G. K., Maugel T. K. (1980) Encystment and excystment in hypotrich ciliates II. *Diophrys scutum* and remarks on comparative features. *Protistologica* **16:** 525-531

Weisse T. (2004) *Meseres corlissi*, a rare oligotrich ciliate adapted to warm water temperature and temporary habitats. *Aqu. Microb. Ecol.* **37:** 75-83

Westheide W., Rieger R. (1996) Spezielle Zoologie. Erster Teil: Einzeller und Wirbellose Tiere. Fischer, Stuttgart, Jena, New York

Wirnsberger-Aescht E., Foissner W., Foissner I. (1990) Natural and cultured variability of *Engelmanniella mobilis* (Ciliophora, Hypotrichida); with notes on the ultrastructure of its resting cyst. *Arch. Protistenk.* **138:** 29-49

Received on 10th January, 2005; revised version on 8th March, 2005; accepted on 22nd March, 2005

Acta Protozool. (2005) 44: 231 - 236

ACTA
PROTOZOOLOGICA

The 3' Untranslated Region of mRNAs from the Ciliate *Nyctotherus ovalis*

Elodie DESTABLES[1], Nadine A. THOMAS[1], Brigitte BOXMA[2], Theo A. Van ALEN[2], Georg W. M. Van der STAAY[2], Johannes H. P. HACKSTEIN[2] and Neil R. McEWAN[1]

[1]Rowett Research Institute, Greenburn Road, Bucksburn, Aberdeen, Scotland; [2]Department of Evolutionary Microbiology, Faculty of. Science, Radboud University Nijmegen, Nijmegen, The Netherlands

Summary. The 3' untranslated regions (3'UTRs) of cDNAs from *Nyctotherus ovalis*, a ciliate from the digestive tract of cockroaches, were examined for their sequence composition. All 3' sequences studied here were characteristically short – generally having around 20 to 30 nucleotides between the stop codon and the first nucleotide of the polyA tail. The stop codon used in all sequences studied was UAA, which although one of the "universal" stop codons, is often used to encode glutamine in other ciliates such as *Tetrahymena*. The polyadenylation signal used in *N. ovalis* could not be determined from the sequence information, but it is clearly not the 'universal' AAUAAA signal. Furthermore, in messages encoding cathepsin B the 3'UTRs were of variable length, with the position where polyadenylation was initiated varying - despite a high conservation of the coding part of the message.

Key words: cathepsin, *Nyctotherus ovalis*, polyadenylation signals, stop codons.

INTRODUCTION

For any living organism, the proper control of expression of a gene is as important as the gene's informational content, i.e. the protein (or RNA) encoded by this particular gene. In its most simplistic form, a gene has an untranslated sequence located 5' of the coding sequence, and an untranslated sequence downstream of the coding sequence, representing the 3' end of the gene. The sequence 5' of the gene generally contains components such as promoters and enhancers, whereas the 3' sequence of the gene (3' UTR = Untranslated Region) is characterized by a number of motifs, which in eukaryotes, predominantly include sequences controlling the addition of a poly-A tail to the nascent mRNA chain (Zhao *et al.* 1999, Proudfoot and O'Sullivan 2002). Both the 5' UTR and 3' UTR cooperate in controlling the processing and translation of the mRNA (Proudfoot 2004).

Most mRNAs in eukaryotes possess a polyadenylate sequence, comprising anything from 30 to 200 adenylate residues at their 3' termini (Graber *et al.* 1999). This poly-A tail is added after transcription, in the course of the maturation of the mRNA, which occurs in the nucleus of the cell. First, the nascent RNA transcript is cleaved, and then the polyA sequence is added to the newly created 3' end of the message. In animals, cleavage occurs approximately 20 nucleotides downstream of a "polyadenylation signal", which, in the majority of the studies, is a hexanucleotide sequence

Address for correspondence: N. R. McEwan, Rowett Research Institute, Greenburn Road, Bucksburn, Aberdeen AB21 9SB, Scotland, U.K.; Fax. +44 1224 715349; E-mail: n.mcewan@rowett.ac.uk

(AAUAAA), which seemed to be highly conserved. Experimental studies revealed that a single substitution of any of these six nucleotides led to a significant decrease in the efficiency of both polyadenylation and RNA cleavage (Sheets *et al.* 1990, Graber *et al.* 1999).

Initially, the AAUAAA sequence (and its derivative AUUAAA - which can function at around 70% efficiency) was regarded as a universally conserved motif. More recently however, a number of studies have revealed that other eukaryotes make use of alternative polyadenylation motifs. Examples of organisms which use alternative motifs include yeast and plants, (Hyman *et al.* 1991, Rothnie 1996, Li and Hunt 1997, Graber 2003). Moreover, there can be a degree of flexibility which is not just restricted to sequence composition. For example there can be variation in the polyadenylation site based on the carbon sources used in experiments with yeast (Sparks and Dieckmann 1998) or with the cell-type (male germ cells) in mouse (MacDonald and Redondo 2002).

In general, studies analysing polyadenylation in organisms other than man, mice, *Drosophila*, *Saccharomyces cerevisiae*, *Arabidopsis thaliana*, and *Oryza sativa* are sparce. In particular, there is a remarkable lack of information about polyadenylation in protists, which represent a much greater biodiversity and divergence that animals, fungi and plants altogether. With respect to ciliates, which represent a particularly species-rich and very diverse taxon (Corliss 2004), only a few papers have been published dealing with the analysis of polyadenylation of a few genes (Williams and Herrick 1991, Liu and Gorovsky 1993, Ghosh *et al.* 1994, McEwan *et al.* 2000), and these papers deal with sequence analysis for proposed polyadenylation rather than providing experimental evidence. In the rumen ciliate *Entodinium caudatum* (McEwan *et al.* 2000), it was concluded that the "universal" AAUAAA signal was absent, although a similar sequence, AUAAA was often present in the region where the polyadenylation signal would normally be found. Similarly, the "universal" signal was not found in cDNAs from *Euplotes* (Ghosh *et al.* 1994), where the motif (A/U)UAAAA was proposed as a possible alternative polyadenylation signal. Limited sequence information led to the suggestion that *Oxytricha fallax* (Williams and Herrick 1991), uses three motifs-TAAAC, TGAAC and AGAAC, which might be described by the consensus sequence (tRAAC). In *Tetrahymena thermophila*, the motifs $TGTGT(N)_{1-8}TAA(N)_{0-11}AAGTATT$ have been described in four histone mRNAs (Liu and Gorovsky 1993). Moreover, the mating pheromone *Er*-1 in the ciliate *Euplotes raikovi* has been shown to have the unusual polyadenylation signal AACAAA (Miceli *et al.* 1992). Obviously, these consensus motifs have little sequence identity in common with each other, or with the "universal" polyadenylation signal thought to be characteristic of animals.

Here we describe a bioinformatical analysis of the 3' untranslated regions (UTR) of a number of cDNA sequences obtained by random sequencing of a cDNA library from the anaerobic ciliate *Nyctotherus ovalis* var. *Blaberus* sp. Amsterdam (Armophorea, Clevelandellida). This is an organism, which in keeping with other ciliate species, has two nuclei - a micronucleus (involved in sexual reproduction) and a macronucleus (involved in asexual reproduction). Within the macronucleus chromosomes have been shown to exist as highly amplified gene-sized mini-chromosomes (Akhmanova *et al.* 1998). Thus, every gene is located on a short chromosome with telomeres at both ends, and these genes function as a single transcription unit. Here we demonstrate that many, if not most, of these genes lack the "universal" polyadenylation signals.

MATERIALS AND METHODS

Obtaining cDNA clones. *Nyctotherus ovalis* from strain *Blaberus* spec. Amsterdam thrives in the hindgut of the giant cockroach (Van Hoek *et al.* 1998), where it has been maintained in laboratory culture for more than 12 years. Ciliates were harvested by electro-migration making use of their unique anodic galvanotactic swimming behaviour (Van Hoek *et al.* 1999). Immediately after isolation, the ciliates were lysed in 8 M guanidinium chloride. RNA was extracted with the aid of the Rneasy Plant mini-kit (Qiagen) following the recommendatiosn of the manufacturer. Total RNA was reverse transcribed, amplified, and the cDNA molecules cloned into pDNR-LIB (Clontech), and grown in *E. coli* strain DH5α by Genterprise, Mainz, Germany. Briefly, this was carried out as follows. The cDNA library was constructed using the "Creator SMART cDNA Library Construction" Kits from BD Biosciences/Clontech. cDNA was amplified using the primers CDS III and SMART IV (CDS III: 5´- ATT CTA GAG GCC GAG GCG GCC GAC ATG d(T)30N_1N 3´; SMART IV 5´- AAG CAG TGG TAT CAA CGC AGA GTG GCC ATT ACG GCC GGG - 3´). After amplification, the cDNAs were size fractionated on Sepahryl S500 columns, and cloned into pDNR-LIB.

DNA sequencing. 96 clones were picked at random and sequenced using the ABI Prism™ BigDye terminator sequencing ready reaction kit (Perkin Elmer Corporation, Norwalk, CT, USA) on an ABI Prism™ 377XL DNA sequencer (Perkin Elmer Corporation).

Only sequences where a stop codon could be identified unequivocally (based on a combination of Blast analysis and translation in three different reading frames), were included into the study. Se-

quences analysed further in this study have been deposited in the EBI sequence database with accession numbers AJ965632-AJ965670.

RESULTS AND DISCUSSION

In the current dataset 39 cDNA sequences were recovered, which allowed the unequivocal identification of a stop codon. Of these the 3' UTR region of 25 cDNAs were analysed initially, with 14 clones which encode cathepsin (cysteine protease) analysed separately in more detail (see below). Firstly, all of these clones used TAA as a stop codon, as observed earlier (Akhmanova *et al.* 1998, Voncken *et al.* 2002, Van Hoek *et al.* unpublished). This supports the hypothesis that *N. ovalis* uses a TAA or TAG to encode a stop codon (Knight *et al.* 2001, Lozupone *et al.* 2001), in contrast to other ciliates, which use TAA or TAG to encode glutamine (Hoffman *et al.* 1995, Lozupone *et al.* 2001). The absence of codons for TGA, which is a stop codon but in *Euplotes octocarinatus* is the only codon for cysteine (Grimm *et al.* 1998) and has previously been discussed as having an unknown function in *N. ovalis* (Knight *et al.* 2001, Lozupone *et al.* 2001), may argue for *N. ovalis* using the universal genetic code.

However, the sequences which have been studied previously for stop codon usage represent macronuclear genomic sequences. Hence it was unknown where the polyadenylation site would lie within the messages transcribed from these genes. What was clear from these sequences is that the "universal" polyadenylation signals could not be identified. Consequently, it remained unclear how much of these sequences is transcribed beyond the stop codon.

The sequences studied here were recovered from total RNA, and all are polyadenylated. Since, in addition, they are likely to be derived from a macronuclear minichromosome suggesting that they are likely to encode a functional gene. Fig. 1 shows, that the sequences between the stop codon and the poly-A tail are rather short for all of the cDNA sequences studied here. These sequences generally lack the motifs which have previously been described as polyadenylation signals in other organisms. Furthermore, there is no obvious alternative motif common to the 3' UTR of all of these sequences. This conclusion is based on visual inspection, attempts to

Fig 1. The sequence of the 3' UTR of 25 randomly selected cDNA clones from the ciliate *Nyctotherus ovalis*.

Sequence Nr	Gene Encoded	Stop codon	3'UTR Sequence
255	Hypothetical	TAA	TCTCTTAACACACAACGTTGAGTAAT
257	Lactoylglutathione lyase	TAA	GTAATTCCTCACTCTCATTTCCATTCCATG
259	Hypothetical	TAA	CCGCTTCTAACCCTTAACCCACTTATTCAC
260	Hypothetical	TAA	CCATAATTCACAGTTCC
261	Glutamate dehydrogenase	TAA	GCATACTAACCCATTCACTTATTGAC
262	Beta/alpha-amylase	TAA	ATGATTTATTACCGTCTACTGAATTC
277	Hypothetical	TAA	TCTCTTAACACACAACGTTGAGTAAT
279	Hypothetical	TAA	CCCATCTAATCTATCACCACACCCTGCTTTACAAG
284	Hypothetical	TAA	TTCACCTGCGCCGCACCAGTATGTCTTCAC
285	Ribosomal protein L32	TAA	TCCCTGCCATCTCACGTACATATCACACCACATGC
294	Hypothetical	TAA	CGATTAACAATATCTTTGAC
299	Hypothetical	TAA	TCTCTTAACACACAACGTTGAGTAACCT
303	Hypothetical	TAA	CTGCCTAACCCTGACTAACTCACGTGCTCCG
309	Cathepsin H	TAA	GCGACTAACGCTAACCTAACTTCTC
312	Ribosomal protein L21	TAA	GCTATTAACCTGCATACACCCAAGCATCCC
321	Hypothetical	TAA	AACCTTAATGGCTTAACTCACTTATTGATTTC
324	Beta tubulin	TAA	GACTTTAACATTCACAAAACCTTTACG
325	Hypothetical	TAA	GCCCTTAACCCTCATTAATTAATCC
335	Beta tubulin	TAA	GACTTTAACATTCACAAAACCTAG
496	Hypothetical	TAA	GCCCTTAACCCTGATTAATTAATGC
503	Hypothetical	TAA	ATTTCATTAACCCTCCGCTCACTCTTTCGATCC
508	Hypothetical	TAA	AACCTTAATGGCTTAACTCACTTATTGATTC
556	Hypothetical	TAA	GCTCTAACCCTCTCCTAATTAATTCAC
557	Hypothetical	TAA	AACCTTAATGGCTTAACTCACTTATTGATTCC
586	Hypothetical	TAA	CCGCTTCTAACCCTTAACCCACTTATTCGTG

Fig 2. Alignment of the DNA for 14 cDNA sequences from *Nyctotherus ovalis*. The stop codons are shown in bold and are underlined. Within the translated region of the gene only 3 nucleotides are different across all of these sequences. Two of these gives synonymous amino acid substitutions, the other (blocked in grey) gives rise to an amino acid change. Positions of identity to the top sequence are indicated '.'. To maintain alignment of the first 'A' of the poly(A) tail and the last nucleotide which is not 'A', the areas with no nucleotide are shown '-'.

```
311  ATGAACTACAAGAGCGGAGTTTTCAAGTGCCACAACACTAACTACATCGGAGGCCACGCCGTTCTCGCTATGGGATACCATGAGGAAGATGAGAAGGGAAAGAAGGATCCTAACTACGAAGTAAAGAAC
263  ....................................................................................................................................
330  ....................................................................................................................................
267  ....................................................................................................................................
290  ....................................................................................................................................
271  ....................................................................................................................................
329  ....................................................................................................................................
286  ....................................................................................................................................
337  ....................................................................................................................................
287  ....................................................................................................................................
316  ....................................................................................................................................
323  ....................................................G...............................................................................
328  ....................................................................................................................................
326  ....................................................................................................................................
     ************************************************************************************ **********************************

311  TCCTGGGGAGCCCACTGGGGACTTGCTGGATACTTCAGAATTGCACCAGGAACCTGCAATATGCAAGGAGGCGTTGTTTGCACAGAATTTTAAGACACTTAAGCAACTAATGCTAATCCAACCTG--
263  ..................................................................................CTAA..............................----
330  ..................................................................................CTAA..............................C---
267  ........G.........................................................................TAA..............................TAG
290  ..................................................................................CTAA..............................C.T-
271  ..................................................................................TAA..............................AC--
329  ..................................................................................TAA..............................AG---
286  ..................................................................................TAA..............................CTG-
337  ..................................................................................CTAA..............................C---
287  ..................................................................................TAA..........T.....................G---
316  ..................................................................................TAA..............................TGT
323  ..................................................................................TAA..............................G.--
328  ..................................................................................TAA..............................AC--
326  ..................................................................................TAA..............................AC----
     ******** ************************************************************************** ************* *****************
```

align sequences and searches carried out using the UTResource database (http://bighost.area.ba.cnr.it/BIG/UTRHome).

Notably, within the clones which were selected at random for sequencing were 14 which encoded a cysteine protease - cathepsin (Fig. 2). This number of copies of this cDNA may at first appear rather high. However, due to the variability seen immediately prior to the polyadenylation site (discussed in more detail below) it appears unlikely that this is a reflection solely due to cDNA bank amplification. Furthermore, cysteine proteases are known to have a major role to play in ciliates (e.g. Parama *et al.* 2004), suggesting that they may be represented as abundant messages.

In the cathepsin cDNAs the sequence immediately prior to the stop codon was analysed to evaluate levels of variability within this region. This allowed analysis back 219 nucleotides (encoding 73 residues) prior to the stop codon for each clone. In total, only 6 nucleotide substitutions were detected - 4 of which were identical (i.e. 6 from 3066 nucleotides) and with one exception these encoded synonymous substitutions - with the four identical substitutions occurring in the codon immediately prior to the stop codon. This level of sequence conservation is also observed in the first 28 nucleotides following the stop codon, with only one cDNA having a single nucleotide deviation from the others. However, in the subsequent nucleotides, which precede the polyA tail - ranging in length from 2 to 6 nucleotides - there are 12 unique sequences within the 14 clones (clones 330 and 337 are identical to each other, as are clones 271 and 328). This is a high level of variability, both in terms of sequence length and sequence content, and is unprecedented in the sequence prior to the stop codon.

The reason for this variability immediately prior to the polyadenylation site is unknown. A number of different mechanisms may be proposed as the answer to this dilemma, but there are probably three most likely causes: (1) it may be due to non-specific addition of nucleotides to the nascent message prior to polyadenylation; (2) the polymorphisms may have arisen in the DNA as a consequence of re-arrangements during the formation of macronuclear mini-chromosomes; or (3) a number of different copies of the gene exist within the micronucleus - effectively different paralogues which still share the same function due to conservation within the coding region. It is unclear which of these mechanisms is taking place, and they should not be considered as being mutually exclusive, with more than one of these factors being possible.

However, it is interesting to note that in a study which included analysis of different cDNAs from messages for actin genes (Ghosh *et al.* 1994) a similar observation was made whereby the actin messages were polyadenylated at one of two different sites. The authors point out that it is unclear if the two forms of messages co-exist in a cell, or if they are used in a developmental-specific manner. The range in number of different messages identified here, although not precluding developmental-specific versions of the message, would appear to argue against there only being a single form of the message present in different developmental stages.

Thus, it has to be concluded from the genes analysed here that: (i) *Nyctotherus ovalis* does not make use of any of the "universal" polyadenylation signals, or of putative polyadenylation signals which have been described previously; (ii) that there is no evidence for any obvious candidate sequence to signal the onset of polyadenylation; and (iii) that, at least in the case of the cathepsin cDNA clones, the precise initiation site for polyadenylation is also not clearly determined, since this region exhibits a hyper-variability in the region 29-34 nucleotides following the stop codon - both in terms of sequence length and composition.

Acknowledgements. This work was performed as part of the EU Framework V Quality of Life and Management of Living Resources Research Programme grant CIMES (QLK3-2002-02151). The Rowett Research Institute receives funding from SEERAD.

REFERENCES

Akhmanova A., Voncken F., Van Alen T., Van Hoek A., Boxma B., Vogels G., Veenhuis M., Hackstein J. H. P. (1998) A hydrogenosome with a genome. *Nature* **396:** 527-528

Corliss J. O. (2004) Why the world needs protists! *J. Euk. Microbiol.* **51:** 8-22

Ghosh S., Jaraczewski J. W., Klobutcher L. A., Jahn C. L. (1994) Characterization of transcription initiation, translation initiation, and poly(A) addition sites in the gene-sized macronuclear DNA molecules of *Euplotes*. *Nucleic Acids Res.* **22:** 214-221

Graber J. H. (2003) Variations in yeast 3'-processing cis-elements correlate with transcript stability. *Trends Genet.* **19:** 473-476

Graber J. H., Cantor C. R., Mohr S. C., Smith T. F. (1999) *In silico* detection of control signals: mRNA 3'-end-processing sequences in diverse species. *Proc. Natl. Acad. Sci. USA* **96:** 14055-14060

Grimm M., Brunen-Nieweler C., Junker V., Heckmann K., Beier H. (1998) The hypotrichous ciliate *Euplotes octocarinatus* has only one type of $tRNA^{Cys}$ with GCA anticodon encoded on a single macronuclear DNA molecule. *Nucleic Acids Res.* **26:** 4557-4565

Hoffman D. C., Anderson R. C., DuBois M. L., Prescott D. M. (1995) Macronuclear gene-sized molecules of hypotrichs. *Nucleic Acids Res.* **23:** 1279-1283

Hyman L. E., Seiler S. H., Whoriskey J., Moore C. L. (1991) Point mutations upstream of the yeast ADH2 poly(A) site significantly reduce the efficiency of the 3'-end formation. *Mol. Cellular Biol.* **11:** 2004-2012

Knight R. D, Freeland S. J., Landweber L. F. (2001) Rewiring the keyboard: evolvability of the genetic code. *Nat. Rev. Genet*. **2:** 49-58

Li Q., Hunt A. G. (1997) The polyadenylation of RNA in plants. *Plant Physiol*. **115:** 321-325

Lozupone C. A., Knight R. D., Landweber L.F. (2001) The molecular basis of nuclear genetic code change in ciliates. *Curr. Biol*. **11:** 65-74

Liu X., Gorovsky M. A. (1993) Mapping the 5' and 3' ends of *Tetrahymena thermophila* mRNAs using RNA ligase mediated amplification of cDNA ends (RLM-RACE). *Nucleic Acids Res.* **21:** 4954-4960

MacDonald C.C., Redondo J.L. (2001) Reexamining the polyadenylation signal: were we wrong about AAUAAA? *Mol. Cell Endocrinol*. **90:** 1-8

McEwan N. R., Eschenlauer S. C. P., Calza R .E., Wallace R. J., Newbold C. J. (2000) The 3' untranslated region of messages in the rumen protozoan *Entodinium caudatum*. *Protist* **151:** 139-146

Miceli C., La Terza A., Bradshaw R. A., Luporini P. (1992) Identification and structural characterization of a cDNA clone encoding a membrane-bound form of the polypeptide pheromone Er-1 in the ciliate protozoan *Euplotes raikovi*. *Proc. Natl. Acad. Sci USA.* **89:** 1988-1992

Parama A., Iglesias R., Alvarez M. F., Leiro J., Ubeira F. M., Sanmartin M. L. (2004) Cysteine proteinase activities in the fish pathogen *Philasterides dicentrarchi* (Ciliophora: Scuticociliatida). *Parasitology* **128:** 541-548

Proudfoot N. (2004) New perspectives on connecting messenger RNA 3' end formation to transcription. *Curr. Opin. Cell. Biol*. **16:** 272-278

Proudfoot N., O'Sullivan J. (2002) Polyadenylation: a tail of two complexes. *Curr. Biol*. **12:** R855-R857

Rothnie H. M. (1996) Plant mRNA 3'-end formation. *Plant Mol. Biol.* **32:** 43-61

Sheets M. D, Ogg S. C., Wickens M. P. (1990) Point mutations in AAUAAA and the poly(A) addition site: effects on the accuracy and efficiency of cleavage and polyadenylation *in vitro*. *Nucleic Acids Res.* **18:** 5799-5805

Sparks K. A., Dieckmann C. L. (1998) Regulation of poly(A) site chice of several yeast mRNAs. *Nucleic Acids Res.* **20:** 4676-4687

Van Hoek A. H., van Alen T. A., Sprakel V. S., Hackstein J. H. P., Vogels G. D. (1998) Evolution of anaerobic ciliates from the gastrointestinal tract: phylogenetic analysis of the ribosomal repeat from *Nyctotherus ovalis* and its relatives. *Mol. Biol. Evol*. **15:** 1195-1206

Van Hoek A. H., Sprakel V. S., Van Alen T. A., Theuvenet A. P., Vogels G. D., Hackstein J. H. P. (1999) Voltage-dependent reversal of anodic galvanotaxis in *Nyctotherus ovalis*. *J. Euk. Microbiol*. **46:** 427-433

Voncken F., Boxma B., Tjaden J., Akhmanova A., Huynen M., Verbeek F., Tielens A.G., Haferkamp I., Neuhaus H. E., Vogels G., Veenhuis M., Hackstein J. H. P. (2002) Multiple origins of hydrogenosomes: functional and phylogenetic evidence from the ADP/ATP carrier of the anaerobic chytrid *Neocallimastix* sp. *Mol. Microbiol.* **44:** 1441-1454

Williams K.R., Herrick G. (1991) Expression of the gene encoded by a family of macronuclear chromosomes generated by alternative DNA processing in *Oxytricha fallax*. *Nucleic Acids Res.* **19:** 4717-4724

Zhao J., Hyman L., Moore C. (1999) Formation of mRNA 3' ends in eukaryotes: mechanism, regulation, and interrelationships with other steps in mRNA synthesis. *Microbiol. Mol. Biol. Rev*. **63:** 405-45

Received on 21st February, 2005; revised version on 6th May, 2005; accepted on 12th May, 2005

Acta Protozool. (2005) 44: 237 - 243

ACTA
PROTOZOOLOGICA

Phylogenetic Relationships among Trichodinidae (Ciliophora: Peritricha) Derived from the Characteristic Values of Denticles

Yingchun GONG[1, 2], Yuhe YU[1], Weisong FENG[1] and Yunfen SHEN[1]

[1]Laboratory of Taxonomy and Ecology of Protozoa, Institute of Hydrobiology, The Chinese Academy of Sciences; [2]Graduate School of the Chinese Academy of Sciences, Wuhan, P. R. China

Summary. The phylogenetic relationships among trichodinids remain obscure. As an important diagnostic marker, the morphology of the denticles in the adhesive disc as well as the adoral spiral has been widely used in generic discrimination and species identification of trichodinids. We studied the characters of denticles of the ten genera of Trichodinidae and the sole genus *Urceolaria* of Urceolariidae by using a quantitative method. The characteristic values were used to generate Manhattan distance, on which the dendrogram was based to construct with the Unweighted Paired Group Method using the Arithmetic mean (UPGMA). The investigations show that all the genera of the family Trichodinidae were clearly separate from the outgroup *Urceolaria*, and within the Trichodinidae: (i) *Dipartiella* grouped with *Trichodinella* and *Tripartiella* and lay in the closest position to the outgroup with a low dissimilarity, suggesting *Dipartiella* might be the most primitive genus in the family; (ii) *Hemitrichodina* clustered in a single clad and lay in the farthest position to the outgroup with the highest dissimilarity, indicating that it might be the most advanced genus; and (iii) the other 6 genera, *Trichodina*, *Paratrichodina*, *Semitrichodina*, *Vauchomia*, *Pallitrichodina* and *Trichodoxa* clustered in a big clad with very low dissimilarity, showing that they are closely related to each other. We discuss the evolutionary trend of the denticle and conclude that the denticles of the adhesive disc should be an apomorphic feature of the trichodinids and their changes could reflect the evolutionary tendencies of these ciliates.

Key words: denticle, phylogenetic relationships, quantitative method, Trichodinidae.

INTRODUCTION

Trichodinids (Ciliophora: Peritrichida) are one of the most common parasitic ciliates that are well characterized by two main features: the morphology of the denticles in the adhesive disc and the development of the adoral ciliary spiral (Lom 1958, Small and Lynn 1985, Basson and Van As 1989). Since the original description by Ehrenberg (1838) of *Trichodina pediculus*, many protozoologists paid a lot of attention to the taxonomy (Lom 1958, 1959, 1962, 1963; Lom and Haldar 1976, 1977; Van As and Basson 1989, 1992, 1993; Xu *et al.* 1999a, b, 2002) and systematics (Raabe 1963, Corliss 1979, Small and Lynn 1985). So far, more than 260 species representing ten genera have been described from the skins, gills and urinary bladder of fishes and amphibians and also from the integument of invertebrates (Kazubski 1958, Sirgel 1983, Basson and Van As 1989, Van As and Basson 1993, Gong *et al.* 2004). At the present time, studies on trichodinids still concern mainly with their taxonomy especially with re-investigating or

Address for correspondence: Yuhe Yu, Laboratory of Taxonomy and Ecology of Protozoa, Institute of Hydrobiology, The Chinese Academy of Sciences, 430072 Wuhan, P. R. China; Fax: (8627)-68780773; E-mail: yhyu@ihb.ac.cn

re-describing the old species using modern techniques (Őzer 2003, Mitra and Haldar 2004).

However, very little attention has been given to the phylogenetic relationships of these ciliates, consequently these studies were fragmentary. Raabe (1963) was the first worker to discuss the phylogeny of the genera of Trichodinidae according to the length of the adoral ciliary spiral and the shape of the denticles (Fig. 1). Xu (1999) carried on the cluster analysis of 11 genera in Mobilina including ten genera of Trichodinidae based on eight main morphological characters (Fig. 2). However, there is as yet no firm conclusion on the phylogenetic relationships among trichodinids because of the confusion of the phylogenetic markers with high systematic values.

The morphology of the denticles in the adhesive disc has been widely used in generic discrimination and species identification of trichodinids (Van As and Basson 1989, 1990). It was supposed that the evolution of these complex ciliates would be made clear by studies on the ontogeny of the denticles of all the genera in the family Trichodinidae (Kruger *et al.* 1995). However, the phylogenetic relationships among trichodinids remain unresolved because data on the ontogeny of the denticles are available only from the genus *Trichodina* (Kazubski 1967, Feng 1985, Kruger *et al.* 1995), and the application of the ontogeny studies to the other genera were postponed since it is difficult to collect the materials for narrow host-specificity and special geographical distribution of some genera, such as *Hemitrichodina*, *Trichodoxa*, and *Dipartiella*. Since the ontogeny of the denticles of each genus of Trichodinidae is presumably similar, and their differences mainly lie in the extent of the development of the mature denticle, we attempted to study their phylogenetic relationships based on the characteristic values of the mature denticles which can indicate the developmental extent of the blade, central part, and thorn using the quantitative method described by Gong *et al.* (2004). The method can be applied to material already published, provided clear micrographs or drawings are available and based on silver impregnated specimens. Because we have access to literature with micrographs that include all the genera of Trichodinidae and one genus of Urceolariidae, it was feasible to study the phylogeny of trichodinids with this numerical method.

The object of the paper is to attempt to provide a new way to study the phylogenetic relationships for trichodinids by taking advantage of the existing material and technology.

MATERIALS AND METHODS

Materials. Thirty-five species representing ten genera of Trichodinidae and one genus of Urceolariidae were investigated in this study. These include 2 out of 16 species of *Urceolaria* described; 1 *Hemitrichodina* species; 20 out of over 200 species of *Trichodina*; 2 out of 11 species of *Paratrichodina*; 1 out of 2 species of *Semitrichodina*; 1 out of 2 species of *Vauchomia*; 2 *Pallitrichodina* species; 1 out of 2 species of *Trichodoxa*; 2 out of 15 species of *Tripartiella*; 2 out of 8 species of *Trichodinella*; and 1 *Dipartiella* species. The drawings of all ciliates studied in the paper were made from those of various researchers (Table 1). Among 11 genera studied, *Trichodina* is one of the largest and most widely distributed ciliate genera (Xu *et al.* 2000b), so we tried to select many species representing different types. In contrast, few were selected from the other genera because the data available in the literature are very scant.

Quantification of denticles. The quantitative method has been put forward in our early paper (Gong *et al.* 2004) and the description was based on the denticulate ring of *Trichodina nobilis* Chen, 1963, but can also be applied to other genera of Trichodinidae. In the case of representatives of the Urceolariidae, we regarded the denticles as made up of only the central part, having no blade and thorn. The method required photomicrography to enlarge denticles and the software Axionvision of Zeiss to calculate the area of denticles.

Quantitative descriptions for the denticle were achieved by measuring the percentages of the areas of the blade, central part and thorn respectively to that of a single denticle and the percentage of the total area of all the denticles in the adhesive disc to that of the loop of the denticulate ring (Figs 3, 4). The formulae were as follows: Pbd (Percentage of the area of blade to that of denticle) = Sb/Sd ; Pcd (Percentage of the area of central part to that of denticle) = Sc/Sd ; Ptd (Percentage of the area of thorn to that of denticle) = St/Sd ; Pdr (Percentage of the area of all the denticles to that of the loop of the denticulate ring) = n*Sd/Sr.

In the formulae, “n” represents the number of the denticles in the adhesive disc; “Sd”, “Sb”, “Sc”, “St’“ and “Sr” represent the area of denticle, blade, central part, thorn and the loop of the denticulate ring, respectively. Though the blade, central part and thorn are irregular, “Sb”, “Sc” and “St” can be computed by the software Axionvision of Zeiss or similar software; “Sd” is calculated according to the formula: Sd = Sb + Sc + St; “Sr” can be calculated using the areas of the excircle and the central circle of denticulate ring which can be computed using the diameters of the excircle and the central circle of denticulate ring (Fig. 3).

When calculating the areas of the blade, central part, and thorn in a drawing of a trichodinid, a denticle is selected as a reference marker, and each three or four denticles are then used for the calculations.

Data analysis. The mean characteristic values of the denticles of all the representative species of each genus were regarded as the characteristic values of the corresponding genus and analyzed by the program NTSYSpc (Numerical Taxonomy System, Version 2.0). A range standardized Manhattan distance was used to generate a dissimilarity matrix between the individual operational taxonomic units based on the characteristic values. The resulting distance matrix was analyzed using UPGMA (Unweighted Paired Group Method using the Arithmetic mean) to construct the dendrogram. We took *Urceolaria* as outgroup, since representatives of the Trichodinidae are considered to be more advanced than representatives of the Urceolariidae in Mobilina (Kruger *et al.* 1995).

RESULTS

Comparison of the characteristic values of denticles among genera of Mobilina

Nearly all the genera have their own fluctuation range of the characteristic values, for example, Pbd (Percentage of the area of blade to that of denticle) and Ptd (Percentage of the area of thorn to that of denticle) of the genus *Trichodina* range from 47 to 66% and 16 to 30%, respectively, but those of *Trichodinella* range from 79 to 80% and 0 to 4%, respectively (Table 1). Overlapping occurs in the values of some genera, as shown in Table 1. For example, the Ptd of *Pallitrichodina rogenae* and those of *Trichodina compacta* and *Trichodina raabei* share 51% which, however, can be differentiated with the other three values.

Comparing to the four characteristic values, Pbd and Ptd vary significantly among genera (Table 2), such as Pbd decreasing from 84% in *Dipartiella* to 20% in *Hemitrichodina* and Ptd increasing from 0% in *Dipartiella* to 47% in *Hemitrichodina*; Pcd (Percentage of the area of central part to that of denticle) and Pdr (Percentage of the area of all the denticles to that of the loop of the denticulate ring) change a little, only from 14 to 33% and 43 to 81% respectively. From the Table 2, we also found the characteristic values of the denticles of *Dipartiella*, *Trichodinella*, *Tripartiella*, and *Hemitrichodina* can be clearly differentiated from others, however that of *Trichodina*, *Paratrichodina*, *Semitrichodina*, *Vauchomia*, *Pallitrichodina*, and *Trichodoxa* were similar with little difference.

Phylogenetic analysis

From the UPGMA dendrogram (Fig. 5), the ten genera of Trichodinidae are clearly separate from the outgroup *Urceolaria* and are grouped into three clusters: *Dipartiella*, *Trichodinella* and *Tripartiella* clustered in a small clad; *Dipartiella* lay in the nearest position to *Urceolaria* with a low dissimilarity of 0.219 (Table 3) and *Trichodinella* and *Tripartiella* grouped together showing high similarity; *Hemitrichodina* clustered in a single clad and lay in the farthest position to the outgroup with the highest dissimilarity of 0.486 (Table 3); the other six genera including *Trichodoxa*, *Pallitrichodina*, *Vauchomia*, *Semitrichodina*, *Paratrichodina*, and *Trichodina* clustered in a big clad with very low dissimilarity (Table 3), and *Semitrichodina* and *Paratrichodina* constituted a sister group showing their close relation to each other.

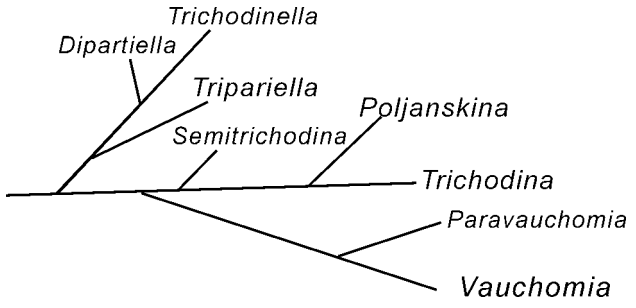

Fig. 1. Phylogenetic diagram of Trichodinidae (redrawn from Raabe 1963). *Paravauchomia* for *Trichodina urinaria* Dogiel, 1940; *Poljanskina* for *Trichodina oviducti* Poljansky, 1955.

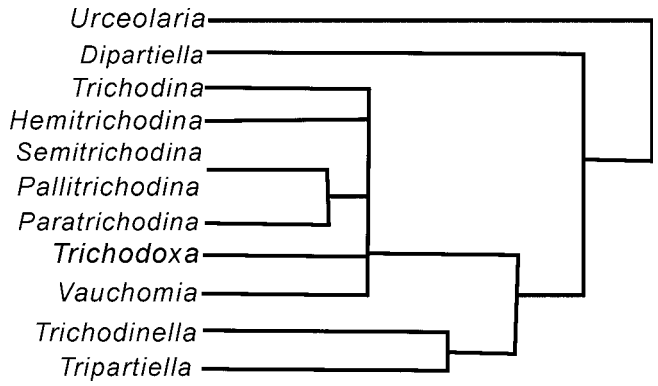

Fig. 2. Cluster analysis of the morphological similarities of 11 genera of Mobilina (redrawn from Xu 1999).

DISCUSSION

Phylogeny within the family Trichodinidae

Which is the most primitive genus in the family Trichodinidae? According to the dendrogram (Fig. 5) based on the characteristic values of the denticles, *Dipartiella* was confirmed to be the most primitive genus in the existing genera of Trichodinidae for it lay nearest to the outgroup. However, our results showed contrary to the theory put forwarded by Raabe (1963) who considered *Trichodina* with the adoral ciliary spiral of an arc over 360º (400º) was initial and fundamental form in Trichodinidae mainly based on the evolutive trend of the adoral ciliary spiral. Though both the adoral ciliary spiral and the denticle of the adhesive disc are

Table 1. Comparison of characteristic values of denticles of 33 species of trichodinids and 2 species of *Urceolaria*. (1) Xu and Song 1998; (2) Laird 1961; (3) Xu *et al.* 1999a; (4) Lom 1963; (5) Lom and Haldar 1977; (6) Sirgel 1983; (7) Van As and Basson 1993; (8)Lom and Haldar 1976; (9) Kazubski 1971; (10) Kazubski and Migala 1968; (11) Van As and Basson 1989; (12) Basson *et al.* 1983; (13) Van As and Basson 1992; (14) Lom and Laird 1969; (15) Lom 1962; (16) Lom 1970a; (17) Loubser *et al.* 1995; (18) Basson and Van As 1991; (19) Lom 1970b (20) Asmat and Haldar 1998; (21) Basson and Van As 1993; (22) Lom 1959; (23) Xu *et al.* 1999b; (24) Lom 1960; (25) Basson and Van As 1989. N- the number of the drawings used for calculations. Pbd - percentage of the area of blade to that of denticle, Pcd - percentage of the area of central part to that of denticle, Ptd - percentage of the area of thorn to that of denticle, Pdr - percentage of the area of all the denticles to that of the loop of the denticulate ring.

Species	Pbd	Pcd	Ptd	Pdr	N	References
Urceolaria cheni Xu *et* Song, 1998	0%	100%	0%	100%	1	(1)
U. karyodactyla Laird, 1961	0%	100%	0%	100%	1	(2)
Dipartiella simplex Stein, 1961	84%	16%	0%	43%	1	(3)
Trichodinella epizootica Raabe, 1950	82%	17%	1%	67%	2	(4) (5)
T. lomi Xu, Song *et* Warren, 1999	79%	18%	3%	49%	3	(3)
Tripatiella copiosa Lom, 1959	72%	18%	10%	64%	1	(5)
T. obtusa Ergens *et* Lom, 1970	75%	16%	9%	56%	1	(4)
Trichodoxa genitalis Sirgel, 1983	65%	25%	10%	81%	1	(6)
Pallitrichodina rogenae Van As *et* Basson, 1993	51%	33%	16%	60%	5	(7)
P. stephani Van As *et* Basson, 1993	47%	31%	21%	59%	3	(7)
Vauchomia renicola Mueller, 1938	61%	14%	25%	53%	1	(8)
Semitrichodina sphaeronuclea Kazubski, 1958	63%	17%	20%	68%	1	(9)
Paratrichodina degiustii Lom *et* Haldar, 1976	64%	15%	21%	54%	1	(8)
P. phoxini Lom, 1963	60%	18%	22%	78%	2	(10)
Trichodina acuta Lom, 1961	53%	25%	22%	70%	3	(11) (12)
T. compacta Van As *et* Basson, 1989	51%	27%	23%	63%	4	(11) (13)
T. cottidarum Dogiel, 1940	58%	16%	26%	53%	3	(14)
T. domerguei Wallengren, 1897	61%	20%	19%	66%	3	(15) (10)
T. heterodentata Ducan, 1977	47%	23%	30%	62%	4	(11) (12)
T. jadranica Lom *et* Laird, 1969	61%	23%	16%	65%	3	(16) (17)
T. maritinkae Basson *et* Van As, 1991	49%	24%	27%	68%	5	(18) (13)
T. modesta Lom, 1970	61%	22%	17%	71%	3	(19)
T. murmanica Poljansky, 1955	53%	24%	23%	60%	4	(3)
T. mutabilis Kazubski *et* Migala, 1968	58%	21%	21%	61%	4	(12) (19)
T. mystusi Asmat *et* Halder, 1998	55%	22%	23%	57%	5	(20)
T. nigra Lom, 1960	54%	24%	22%	65%	4	(19)
T. oviducti Poljansky, 1955	57%	19%	24%	54%	1	(8)
T. polycirra Lom, 1960	52%	20%	58%	59%	1	(8)
T. puytoraci Lom, 1962	60%	18%	22%	53%	4	(15) (20)
T. raabei Lom, 1962	51%	19%	30%	65%	3	(15)
T. rectuncinata Raabe, 1958	66%	17%	17%	56%	3	(15) (4)
T. reticulata Hirschman *et* Partsch, 1955	55%	20%	25%	58%	3	(21) (22)
T. sinonovaculae Xu, Song *et* Warren, 1999	60%	20%	20%	63%	3	(23)
T. urinaria Dogiel, 1940	58%	13%	29%	55%	1	(24)
Hemitrichodina robusta Basson *et* Van As, 1989	20%	33%	47%	68%	3	(25)

evolutive, the latter is a peculiarity of the Mobilina peritrichs not occurring in Sessilina, while the former exist in both Mobilina and Sessilina. Since the Mobilina is derived from the Sessilina (Lom 1964), the adoral ciliary spiral should be a plesiomorphic feature for trichodinids, and the denticle of the adhesive should be an apomorphic feature. However, only the apomorphic feature could be used for constructing phylogenetic research (Bardele 1989), therefore the denticle characters were more suitable to be the phylogenetic marker of trichodinids than the adoral ciliary spiral. Consequently we argue that the denticles have a very high systematic value and therefore its changes ought to reflect the evolutionary tendencies of trichodinids.

From the topological position of *Hemitrichodina* in the dendrogram (Fig. 5), it was difficult to establish its status within the Trichodinidae. However, the dissimilarity distance between *Hemitrichodina* and the outgroup *Urceolaria* was higher than that between any other genus and the outgroup (Table 3), therefore

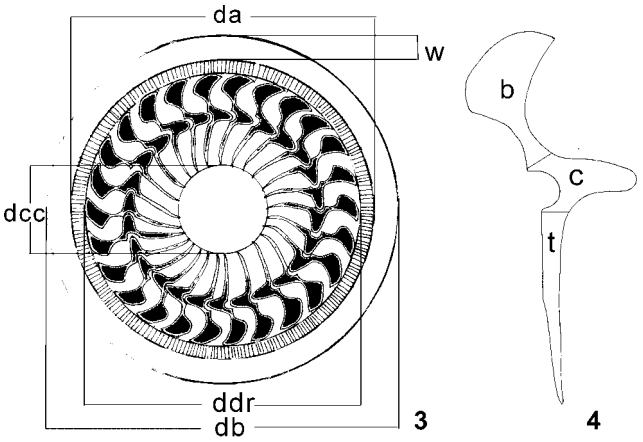

Figs 3, 4. The diagram to illustrate the adhesive disc and the denticles from the adoral view (redrawn from Gong *et al.* 2004). b - blade, c - central part, da - adhesive diameter, db - body diameter, dcc - central circle diameter, ddr - excircle of denticle ring diameter, t - thorn, w - border membrane width.

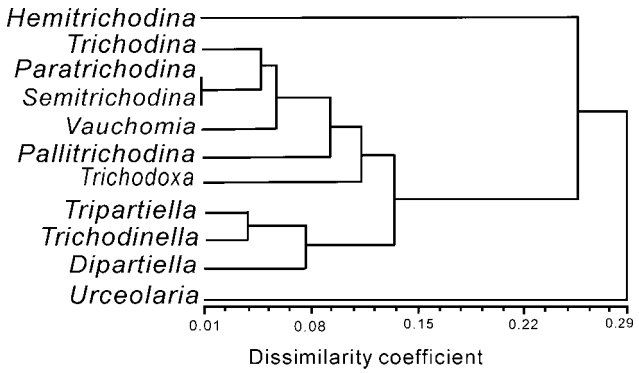

Fig. 5. Dendrogram of the family Trichodinidae based on characteristic values of denticles using UPGMA.

Table 2. Character values of denticles of ten genera of Trichodinidae and the outgroup *Urceolaria*. Abbreviations as in Table 1.

Genera	Pbd	Pcd	Ptd	Pdr
Urceolaria Stein, 1867	0%	100%	0%	100%
Dipartiella Stein G., 1961	84%	16%	0%	43%
Trichodinella Raabe, 1950	80%	18%	2%	58%
Tripartiella Lom, 1959	74%	17%	9%	60%
Trichodoxa Sirgel, 1983	65%	25%	10%	81%
Pallitrichodina Van As *et* Basson, 1993	49%	32%	19%	59%
Vauchomia Mueller, 1938	61%	14%	25%	53%
Semitrichodina Kazubski, 1958	63%	17%	20%	68%
Paratrichodina Lom, 1963	62%	17%	21%	66%
Trichodina Ehrenberg, 1838	56%	21%	23%	61%
Hemitrichodina Basson *et* Van As, 1989	20%	33%	47%	68%

Table 3. Manhattan distance matrix of the characteristic values of denticles among 11 genera of Mobilina. 1 - *Hemitrichodina*, 2 - *Trichodina*, 3 - *Paratrichodina*, 4 - *Semitrichodina*, 5 - *Vauchomia*, 6 - *Pallitrichodina*, 7 - *Trichodoxa*, 8 - *Tripartiella*, 9 - *Trichodinella*, 10 - *Dipartiella*, 11 - *Urceolaria*.

Genera	1	2	3	4	5	6	7	8	9	10	11
1	0.000	0.196	0.214	0.216	0.243	0.166	0.255	0.288	0.322	0.383	0.478
2	0.196	0.000	0.042	0.054	0.057	0.062	0.115	0.092	0.125	0.187	0.317
3	0.214	0.042	0.000	0.012	0.053	0.095	0.093	0.075	0.116	0.169	0.275
4	0.216	0.054	0.012	0.000	0.064	0.101	0.083	0.075	0.116	0.167	0.264
5	0.243	0.057	0.053	0.064	0.000	0.110	0.146	0.097	0.131	0.150	0.313
6	0.166	0.062	0.095	0.101	0.110	0.000	0.134	0.124	0.155	0.217	0.357
7	0.255	0.115	0.093	0.083	0.146	0.134	0.000	0.094	0.128	0.190	0.223
8	0.288	0.092	0.075	0.075	0.097	0.124	0.094	0.000	0.041	0.095	0.232
9	0.322	0.125	0.116	0.116	0.131	0.155	0.128	0.041	0.000	0.061	0.207
10	0.383	0.187	0.169	0.167	0.150	0.217	0.190	0.095	0.061	0.000	0.219
11	0.478	0.317	0.275	0.264	0.313	0.357	0.223	0.232	0.207	0.219	0.000

Hemitrichodina should be the most advanced in Trichodinidae. The results support the view that *Hemitrichodina* might be *Trichodina* in an advanced form (Xu *et al.* 2000a).

Phylogenetic relationships of the six genera of *Trichodina, Paratrichodina, Semitrichodina, Vauchomia, Pallitrichodina* and *Trichodoxa* need further research for their low dissimilarity distances (Table 3), which was caused by their similar type of denticles.

The evolutive trend of denticles within Trichodinidae

The obliquely positioned simple plate of Urceolariidae should be the plesiomorphic feature of the denticle of Mobilina ciliates (Raabe 1963). In Trichodinidae, the denticle of *Dipartiella* which has simple blade and undeveloped central part should be considered as the initial form. With the evolution of the denticle, the thorn appeared gradually, like in the denticle of *Trichodinella* which has weakly developed short thorn curved along the delicate central part; then like in that of *Tripartiella* which bears developed straight ray besides the delicate central part. *Trichodinella* and *Tripartiella* are closely related to each other for their denticles are wedged together by a double system of central conical parts and anterior projection of the blades (Lom and Haldar 1977). The denticle continued to evolve to make the blade, central part and thorn all well developed to form the denticle of the type similar to *Trichodina*. Finally the denticle degenerated, like that of *Hemitrichodina* with triangular blade and robust central part and robust thorn. In a word, it can be concluded from Table 2 and Fig. 5 that with the evolution of trichodinids, the blades degenerated gradually and the thorn developed gradually, but the central part did not change much.

We tried to explain the evolutive trend of the denticles from the view of the function of their components. The thorn is relatively inflexible and doubtless this enhanced the action of maintaining constancy of shape of the central part. On the other hand the blade is very flexible (Sandon 1965), which allows enough flexibility for adhesive disc. Therefore the adhesive disc maintains its basic shape whilst allowing enough flexibility to attach to an uneven surface by the blade and thorn (Van As and Basson 1990). Perhaps with the evolution of the denticle, that the blade degrades gradually and thorn develops gradually is to adapt to special niche, in which, the adhesive disc needed stronger stability and less flexibility. Further study of the behavior of each genus of Trichodinidae and the special environment they exist in will contribute to access this explanation. The central parts which revealed a remarkable analogy with the spinal column of the vertebrates (Van As and Basson 1990), are indispensable for the denticles in that they play an important role not merely in connecting both the blade and thorn, but also in integrating all the denticles. This might be the reason for the central parts not changing such a lot during the evolution of the denticles.

Conclusions

In this paper, we investigated the phylogeny of the trichodinids based only on the morphology of the denticles by making full use of the existing material and knowledge of trichodinids. However, purely morphological characters are inadequate for phylogenetic studies, and molecular technology provides a much-needed alternative method to resolve problematic phylogeny. Therefore, we will continue the study of the systematic evolution of the family Trichodinidae inferred from molecular information such as the small subunit rRNA (SSrRNA), large subunit rRNA (LSrRNA) and Hsp70, etc. Up till now, we have successfully sequenced the SSrRNA of *Trichodina heterodentata* (AY788099) and *Trichodina reticulata* (AY741748). More molecular information of other genera will hopefully shed light on the evolution of these complex ciliates and aid in assessing the validity of our quantitative method.

Acknowledgements. The authors are much grateful to Prof. W. Song of Ocean University of China for offering literature on trichodinids, and to Dr K. Xu of Universität Salzburg for helpful suggestions and revising the text, and to Dr C. Fu of Institute of Hydrobiology, The Chinese Academy of Sciences, for helping with analysis program. We would like also to express our deep appreciation for the helpful comments of two anonymous reviewers. The work was supported by NSFC (the National Natural Science Foundation of China) grant No. 30270164 to Yuhe Yu.

REFERENCES

Asmat G. S. M., Haldar D. P. (1998) *Trichodina mystusi*, a new species of trichodinid ciliophoran from Indian estuarine fish, *Mystus gulio* (Hamilton). *Acta Protozool.* **37:** 173-177

Bardele C. F. (1989) From ciliate ontogeny to ciliate phylogeny: a program. *Boll. Zool.* **56:** 235-243

Basson L., Van As J. G. (1989) Differential diagnosis of the genera in the family Trichodinidae (Ciliophora; Peritricha) with the description of a new genus ectoparasitic on freshwater fish from southern Africa. *Syst. Parasitol.* **15:** 153-160

Basson L., Van As J. G. (1991) Trichodinids (Ciliophora: Peritrichia) from a calanoid copepod and catfish from South Africa with notes on host specificity. *Syst. Parasitol.* **18:** 147-158

Basson L., Van As J. G. (1993) First record of the European Trichodinids (Ciliophora: Peritrichida), *Trichodina acuta* Lom, 1961 and *T. reticulata* Hirschamann et Partsch, 1955 in South Africa. *Acta Protozool.* **32:** 101-105

Basson L., Van As J. G., Paperna I. (1983) Trichodinid ectoparasites of cichlid and cyprinid fishes in South Africa and Israel. *Syst. Parasitol.* **5:** 245-257

Corliss J. O. (1979) The Ciliated Protozoa: Characterization, Classification and Guide to the Literature. 2nd ed., Pergamon Press, New York

Ehrenberg C. G. (1838) Die Infusionstierchen als volkommene Organismes. Leipzig

Feng S. (1985) A biological investigation of asexual production of *Trichodina nobillis* Chen. *Acta Hydrobiol. Sin.* **9:** 331-342

Gong Y., Yu Y., Shen Y. (2004) Quantitative analysis of *Trichodina* denticulating characters and phylogenetic relationship studies on interspecies and intraspecies. *Acta Hydrobiol. Sin.* **28:** 225-233

Kazubski S. L. (1958) *Semitrichodina* gen. nov. *sphaeronuclea* (Lom, 1956) (*Peritricha-Urceolariidae*) in *Schistophallus orientalis* Cless. (*Plumonata-Zonitidae*) in Poland. *Bull. Acad. Polon. Sci.* **6:** 109-112

Kazubski S. L. (1967) Study on the growth of skeletal elements in *Trichodina pediculus* Ehrbg. *Acta Protozool.* **5:** 37-48

Kazubski S. L. (1971) Morphological variability of *Semitrichodina sphaeronuclea* (Lom, 1956). *Acta Protozool.* **8:** 251-259

Kazubski S. L., Migala K. (1968) *Urceolariidae* from breeding carp-*Cyprinus carpio* L. in Zabieniec and remarks on the seasonal variability of trichodinids. *Acta Protozool.* **6:** 137-170

Kruger J., Van As J. G., Basson L. (1995) Observations on the adhesive disc of *Trichodina xenopodos* Fantham, 1924 and *T. heterodentata* Duncan, 1977 (Ciliophora: Peritricha) during binary fission. *Acta Protozool.* **34:** 203-209

Laird M. (1961) *Urceolaria karyodactyla* n. sp. (Ciliata: Peritricha) from *Ischnochiton rubber* (L.) at Saint Andrews, New Brunswick. *Can. J. Zool.* **39:** 827-832

Lom J. (1958) A contribution to the systematics and morphology of endoparasitic trichodinids from amphibians with a proposal of uniform specific characteristics. *J. Protozool.* **5:** 251-263

Lom J. (1959) *Trichodina reticulata* Hirschmann and Partsch 1955 from Crucian Carp, and *T. domerguei* f. *latispina* Dogel 1940 from *Diaptomus*. *Vest. Èsl. Spol. Zool.* **24:** 246-257

Lom J. (1960) On two endozoic trichodinids, *Trichodina urinaria* Dogiel, 1940 and *Trichodina polycirra* sp. n. (Contribution to the knowledge of Trichodinids, III) *Acta Parasit. Pol.* **8:** 169-180

Lom J. (1962) Trichodinid ciliates from fishes of the Rumanian Black Sea coast. *Parasitology* **52:** 49-61

Lom J. (1963) The ciliates of the family Urceolariidae inhabiting gills of fishes (The *Trichodinella*-group). *Vest. Èsl. Spol. Zool.* **27:** 7-19

Lom J. (1964) The morphology and morphogenesis of the buccal ciliary organelles in some peritrichous ciliates. *Arch. Protistenk.* **107:** 131-162

Lom J. (1970a) Trichodinid ciliates (Peritrichida: Urceolariidae) from some marine fishes. *Folia Parasit.* **14:** 113-125

Lom J. (1970b) Observations on trichodinid ciliates from freshwater fishes. *Arch. Protistenk.* **112:** 153-177

Lom J., Haldar D. P. (1976) Observations on trichodinids endocommensal in fishes. *Trans. Am. Micros. Soc.* **95:** 527-541

Lom J., Haldar D. P. (1977) Ciliates of the genera *Trichodinella*, *Tripartiella* and *Paratrichodina* (Peritricha, Mobilina) invading fish gills. *Folia Parasit.* **24:** 193-210

Lom J., Laird M. (1969) Parasitic protozoa from marine and euryhaline fish of Newfoundland and New Brunswick. I. Peritrichous ciliates. *Can. J. Zool.* **47:** 1367-1380

Loubser G. J. J., Van As J. G., Basson L. (1995) Trichodinid ectoparasites (Ciliophora: Peritrichida) of some fishes from the Bay of Dakar, Senegal (West Africa). *Acta Protozool.* **34:** 211-216

Mitra A. K., Haldar D. P. (2004) First record of *Trichodinella epizootica* (Raabe, 1950) Šramek-Hušek, 1953, with description of *Trichodina notopteridae* sp. n. (Ciliophora: Peritrichida) from freshwater fishes of India. *Acta Protozool.* **43:** 269-274

Őzer A. (2003) The occurrence of *Trichodina domerguei* Wallengren, 1987 and *Trichodina tenuidens* Fauré-Fremiet, 1944 (Peritrichia) on three-spined stickleback, *Gasterosteus aculeatus* L., 1758 found in a brackish and freshwater environment. *Acta Protozool.* **42:** 41-46

Raabe Z. (1963) Systematics of the family *Urceolariidae* Dujardin 1841. *Acta Protozool.* **1:** 121-138

Sandon H. (1965) Some species of *Trichodina* from South Africa. *Acta Protozool.* **15:** 39-56

Sirgel W. F. (1983) A new ciliate genus *Trichodoxa* n. g. (Ciliate, Peritricha, Mobilina, Trichodinidae) with two new species from the genital system of terrestrial pulmonates. *J. Protozool.* **30:** 118-125

Small E. B., Lynn D. H. (1985) Phylum Ciliophora Doflein, 1901. In: An Illustrated Guide to the Protozoa (Eds. J. J. Lee, S. H. Hutner, E. C. Bovee). Allen Press, Kansas, 393-575

Van As J. G., Basson L. (1989) A further contribution to the taxonomy of the Trichodinidae (Ciliophora: Peritricha) and a review of the taxonomic status of some fish ectoparasitic trichodinids. *Syst. Parasitol.* **14:** 157-179

Van As J. G., Basson L. (1990) An articulated internal skeleton resembling a spinal column in a ciliated Protozoan. *Naturwissenschaften* **77:** 229-231

Van As J. G., Basson L. (1992) Trichodinid ectoparasites (Ciliophora: Peritrichida) of freshwater fishes of the Zambesi River System, with a reappraisal of host specificity. *Syst. Parasitol.* **22:** 81-109

Van As J. G., Basson L. (1993) On the biology of *Pallitrichodina rogenae* gen. n., sp. n. and *P. stephani* sp. n. (Ciliophora: Peritrichida), mantle cavity symbionts of the giant African snail *Achatina* in Mauritius and Taiwan. *Acta Protozool.* **32:** 47-62

Xu K. (1999) Parasitic and commensal ciliated Protozoa from marine molluscs and fishes off the coast of the Yellow Sea and the Bohai Bay, with the review of Mobiline peritrichous ciliates (Protozoa, Ciliophora). Doctoral dissertation, Ocean University of Qingdao, Qingdao, China

Xu K., Song W. (1998) A morphological study on a new species of gill parasitic ciliate, *Urceolaria cheni* nov. spec. from the clam *Scapharca subcrenata*. *J. Fish. Sc. China* **5:** 13-17

Xu K., Song W., Warren A. (1999a) Trichodinid ectoparasites (Ciliophora: Peritrichida) from the gills of cultured marine fishes in China, with the description of *Trichodinella lomi* n. sp. *Syst. Parasitol.* **42:** 219-227

Xu K., Song W., Warren A. (1999b) Trichodinid ectoparasites (Ciliophora: Peritrichida) from the gills of mariculture molluscs in China, with the descriptions of four new species of *Trichodina* Ehrenberg, 1838. *Syst. Parasitol.* **42:** 229-237

Xu K., Song W., Lei Y., Choi J. K., Warren, A. (2000a) Diagnoses and probable phylogenetic relationships of the genera in the family Trichodinidae (Ciliophora, Peritrichia). *The Yellow Sea* **6:** 42-49

Xu K., Song W., Warren A. (2000b) Observations on trichodinid ectoparasites (Ciliophora: Peritricha) from the gills of maricultured molluscs in China, with descriptions of three new species of *Trichodina* Ehrenberg, 1838. *Syst. Parasitol.* **45:** 17-24

Xu K., Song W., Warren A. (2002) Taxonomy of trichodinids from the gills of marine fishes in coastal regions of the Yellow Sea, with descriptions of two new species of *Trichodina* Ehrenberg, 1830 (Protozoa: Ciliophora: Peritrichia). *Syst. Parasitol.* **51:** 107-120

Received on 10th December, 2004; revised version on 23rd March, 2005; accepted on 14th April, 2005

Acta Protozool. (2005) 44: 245 - 251

ACTA
PROTOZOOLOGICA

Studies on the Effectiveness of *Tanacetum parthenium* Against *Leishmania amazonensis*

Tatiana Shioji TIUMAN[1], Tânia UEDA-NAKAMURA[3], Benedito Prado DIAS FILHO[3], Diógenes Aparício Garcia CORTEZ[2], and Celso Vataru NAKAMURA[3]

[1]Programa de Pós-graduação em Ciências Farmacêuticas; [2]Departamento de Farmácia e Farmacologia; [3]Departamento de Análises Clínicas, Laboratório de Microbiologia Aplicada aos Produtos Naturais e Sintéticos, Universidade Estadual de Maringá, Maringá, Paraná, Brasil

Summary. We assessed the biological activity of a plant powder, crude extracts, and several fractions obtained from *Tanacetum parthenium* on *Leishmania amazonensis.* The medicinal plant *T. parthenium* is indicated for prevention of migraine headache crises, and several investigations have already demonstrated its anti-inflammatory activity. This study included the extraction process and bioassay-guided fractionation by the adsorption chromatography method. A progressive increase in the antileishmanial effect was observed in the course of the purification process. The plant powder (PTP) had a 50% inhibitory concentration (IC_{50}) at 490 µg/ml, whereas the dichloromethane fraction (DF) showed an IC_{50} of 3.6 µg/ml against the growth of promastigote forms after 48 h of culturing. In axenic amastigote forms, the IC_{50} of the PTP and DF were 74.8 µg/ml and 2.7 µg/ml, respectively. Cytotoxicity analysis indicated that the toxic concentrations of the PTP, ethyl-acetate crude extract (ECE), and DF were much higher for J774G8 macrophages than for the protozoans. Haemolytic experiments were performed, and the ECE and DF did not cause lysis at concentrations higher than the IC_{50} for promastigotes.

Key words: antileishmanial activity, cytotoxicity, *Leishmania amazonensis*, medicinal plants, *Tanacetum parthenium.*

INTRODUCTION

Leishmaniasis is a major global public-health problem, with 1.5-2 million humans affected by the disease annually. Approximately 350 million people in 88 countries are estimated to be threatened by the disease (World Health Organization 2001). This parasitosis is caused by organisms of the genus *Leishmania,* and has three clinical forms: visceral, cutaneous, and mucocutaneous. *Leishmania amazonensis* is one of the principal agents of diffuse cutaneous leishmaniasis, but visceralisation of strains has often been observed in patients with *Leishmania*-human immunodeficiency virus coinfection (Alvar *et al.* 1997). Despite the tremendous progress made in the understanding of the biochemistry and molecular biology of the parasite, the first-choice treatment for the several forms of leishmaniasis still relies on pentavalent antimonials developed more than 50 years ago (Croft and Coombs 2003). These drugs are potentially toxic and often ineffective (Berman 1996, 1997; Grevelink and Lerner 1996), and second-

Adress for correspondence: Celso Vataru Nakamura, Universidade Estadual de Maringá, Departamento de Análises Clínicas, Laboratório de Microbiologia Aplicada aos Produtos Naturais e Sintéticos, Bloco I-90 Sala 123 CCS, Avenida Colombo, 5790; BR-87020-900, Maringá, PR, Brazil; Fax: +55 44 261-4860; E-mail: cvnakamura@uem.br

choice drugs such as amphotericin B and pentamidine may be even more toxic (Grevelink and Lerner 1996, Croft and Coombs 2003). The spread of drug resistance, combined with other shortcomings of the available antileishmanial drugs, emphasises the importance of developing new, effective, and safe drugs against leishmaniasis.

Plants provide unparalleled chemical diversity and bioactivity, which has led to the development of hundreds of pharmaceutical drugs (Shu 1998). The species *Tanacetum parthenium* (Asteraceae), popularly known as feverfew, is a traditional remedy used in the prophylactic treatment of migraine. Its effects have been attributed to the plant´s content of sesquiterpene lactones, notably parthenolide (Martindale 1999). Several studies have also shown that feverfew is effective as an anti-inflammatory and antinociceptive agent (Heptinstall *et al.* 1985, Murphy *et al.* 1988, Sumner *et al.* 1992, Jain and Kulkarni 1999, Williams *et al.* 1999, Piela-Smith and Liu 2001).

The study reported here was undertaken to examine the antileishmanial activity of *T. parthenium*, which has not been tested previously against trypanosomatids. The cytotoxic activity against J774G8 macrophages and sheep blood cells was also determined.

MATERIALS AND METHODS

Plant material. Powder of aerial parts of *T. parthenium* (Lot 166871) (PTP) was kindly furnished by the Herbarium Laboratório Botânico Ltda (Colombo, Paraná, Brazil).

Extraction and fractionation. The plant material was sequentially extracted by exhaustive maceration at room temperature in the dark in ethanol:water (90:10). The supernatants were filtered, evaporated under vacuum and lyophilised. The powder resulting from lyophilisation was termed the aqueous crude extract, and the residue was dissolved in ethyl acetate or hexane and was named according to the solvent used. The aqueous (ACE), ethyl-acetate (ECE), and hexane (HCE) crude extracts were directly assayed against *L. amazonensis*. Subsequently, the ethyl-acetate extract was chromatographed on a silica-gel column using hexane, dichloromethane, ethyl acetate, methanol, and methanol:water (90:10). Each fraction (hexane, HF; dichloromethane, DF; ethyl acetate, EF; methanol, MF; methanol:water, MWF) was tested for antiprotozoal activity.

Parasite culture. Promastigote forms of *Leishmania amazonensis* (WHOM/BR/75/Josefa) were cultured at 28°C in Warren´s medium (brain-heart infusion plus haemin and folic acid) supplemented with 10% heat-inactivated fetal bovine serum in a tissue flask. Axenic amastigote cultures, obtained by *in vitro* transformation of infective promastigotes (Ueda-Nakamura *et al.* 2001), were maintained in Schneider's insect medium (Sigma Chemical Co., St. Louis, Missouri, USA), pH 4.5, with 20% fetal bovine serum at 32°C.

Cells. Murine macrophage J774G8 cells were maintained in tissue flasks in medium composed of RPMI 1640 medium (Gibco Invitrogen Corporation, New York, USA), sodium bicarbonate, L-glutamine, and heat-inactivated fetal bovine serum (10%). The cultures were maintained at 37°C in 5% CO_2-air mixture.

Preparation of stock solutions. The PTP and the crude extracts and fractions were solubilised in DMSO prior to adding them to the appropriate culture medium. The final concentration of DMSO in the test medium never exceeded 0.5%, a concentration which has no effect on the growth of parasites. The stock solution of Amphotericin B (AMPB) (Cristália Produtos Químicos Farmacêuticos Ltda, Itapira, São Paulo, Brazil) was prepared in phosphate-buffered saline.

Antileishmanial assays. The effects of the PTP as well as the crude extracts and fractions were evaluated in 24-well microtitre plates. Cultures of promastigotes and amastigotes in the logarithmic phase (10^6 cells/ml) were incubated in appropriate medium and heat-inactivated fetal bovine serum in the presence of different concentrations of the extracts. In all tests, 0.5% DMSO and medium alone were used as controls. AMPB was used as the reference drug. Parasites were counted daily for 5 days in a haemocytometer with a light microscope, and the results were compared with those from the controls. Each assay was performed in duplicate and repeated in separate experiments.

Cytotoxicity assay against J774G8 cells. The cytotoxic effect of the plant, expressed as cell viability, was assessed on macrophage strain J774G8. The test was carried out in 24-well microtitre plates. A suspension of 5×10^5 macrophages was added to each well. The cells were grown as monolayers in culture medium at 37°C and 5% CO_2-air mixture. Confluent cultures were treated with medium containing different concentrations of PTP, ECE, DF, and AMPB for 48 h. Next the supernatant cells were homogenised with adhered cells, equal volumes of cell suspension and 0.4% erythrosin B (vital dye) were mixed, and at least 200 cells were counted and evaluated by light microscopy.

Red blood cell lysis assay. This experiment also evaluated the cytotoxicity of *T. parthenium*. A 4% suspension of freshly defibrinised sheep blood was prepared by adding blood to sterile 5% glucose solution. One ml of red-blood-cell suspension was added to each test tube, and different concentrations of ECE, DF, and AMPB (a reference drug, which may cause anaemia) (Bennett 1996) were added, gently mixed, and incubated at 37°C for 120 minutes. Samples were centrifuged at 1,000 g for 10 min. Absorbance of the supernatant was determined at 540 nm. The inhibition of haemolysis was calculated according to the equation: Inhibition (%) = (Ap-As)/(Ap-Ac) × 100; where Ap, As, and Ac are the absorbance of the positive control, test sample, and negative control, respectively. The negative control was the red-blood-cell suspension alone or with 0.5% DMSO, and the positive control was Triton X-114. These tests were performed in duplicate on separate occasions.

RESULTS

Antileishmanial assays. PTP inhibited the growth of promastigote and axenic amastigote forms of *L. amazonensis in vitro* after 48 h of incubation. At 1000 µg/ml it inhibited 93.6% of the promastigotes,

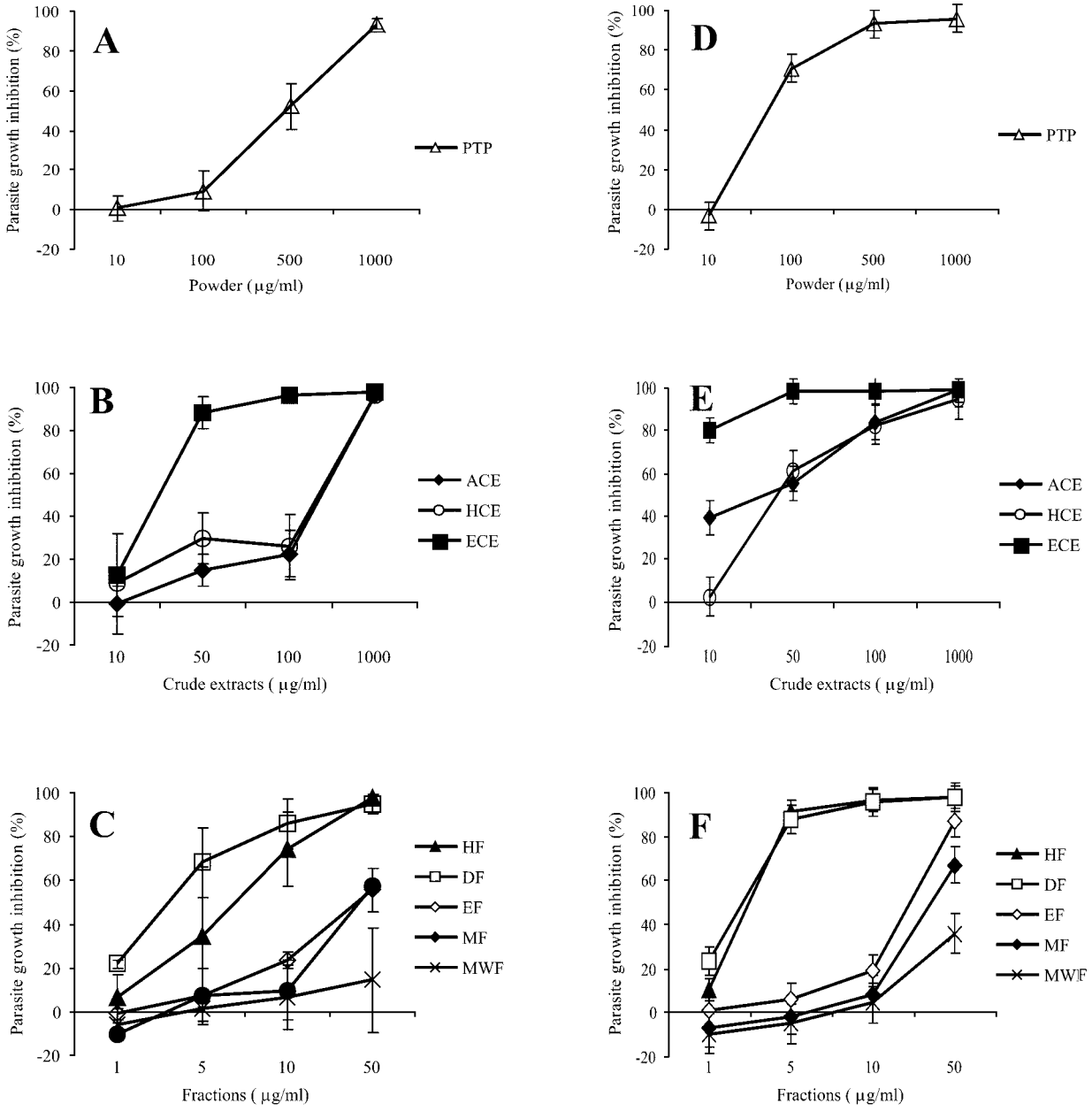

Figs 1A-F. Effects of *Tanacetum parthenium* against promastigote (**A-C**) and axenic amastigote (**D-F**) forms of *Leishmania amazonensis* cultured for 48 h in the presence of the indicated concentrations. **(A, D)** powder (PTP), **(B, E)** crude extracts (ACE, ECE, and HCE), and **(C, F)** fractions (HF, DF, EF, MF, and MWF). The results are from two experiments in duplicate and are shown as percentages ± standard deviations of growth inhibition in relation to untreated control protozoans.

growth and 95.9% of the amastigotes, and had a 50% inhibitory concentration (IC_{50}) of 490 µg/ml (Fig. 1A) and 74.8 µg/ml (Fig. 1D) respectively. ACE at 1000 µg/ml inhibited 96.6% of the promastigote forms and 98.9% of the amastigote forms, and had an IC_{50} of 434 µg/ml and 36.7 µg/ml respectively. HCE gave a similar result, with 96.6% growth inhibition of promastigotes and 95% of amastigotes, and an IC_{50} of 409 µg/ml and 42.4 µg/ml respectively. ECE was more effective, with an inhibition of 96.2% at 100 µg/ml for promastigote forms and 98.8% at 50 µg/ml for amastigote forms; it had an IC_{50} of 29 µg/ml and <10 µg/ml respectively

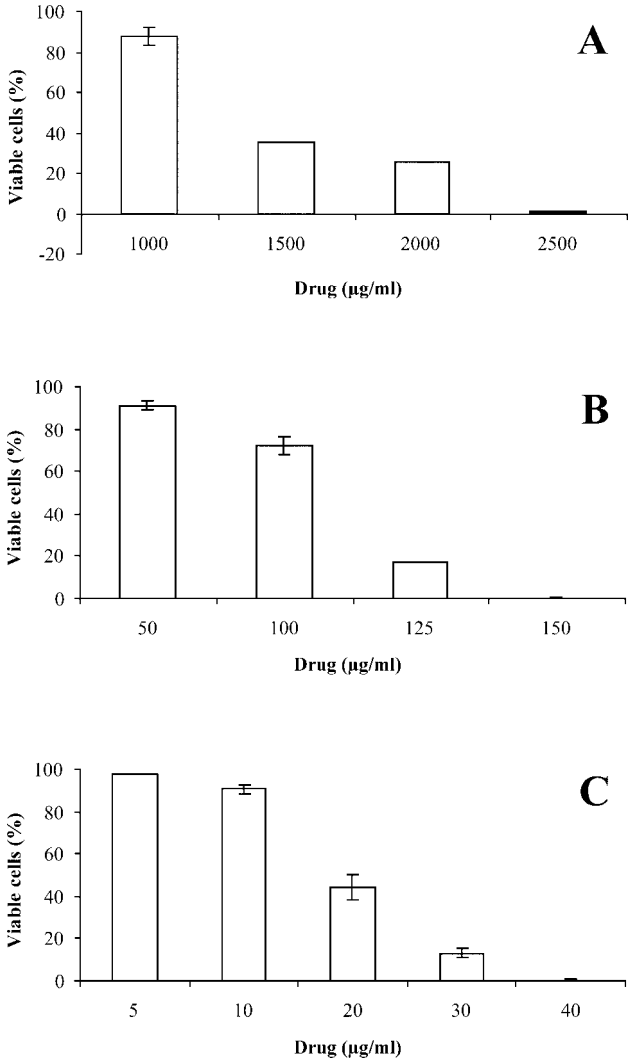

Figs 2A-C. Effects of *Tanacetum parthenium* powder (PTP) **A** - the ethyl-acetate crude extract (ECE) **B** - and the dichloromethane fraction (DF) **C** - on the survival of J774G8 macrophages with different concentrations of the drugs after 48 h of incubation. The results are from two experiments in duplicate and are shown as percentages ± standard deviations of viable cells in relation to the untreated control.

(Figs 1B, F). This last extract showed the highest antileishmanial activity, and was submitted to chromatography on a silica-gel column. Five fractions were obtained: HF, DF, EF, MF, and MWF. The HF and DF at a concentration of 50 µg/ml inhibited promastigote growth by 96% and amastigote growth by 98% after culturing for 48 h. Under the same conditions, the EF and MF inhibited promastigote growth by 56%. For amastigotes, EF showed 87%, and MF 67% growth inhibition. The MWF showed the lowest activity of all, with 14.4% and 36% inhibition for promastigote and

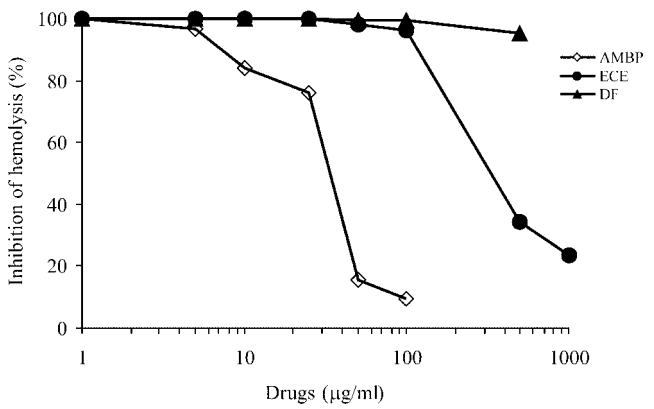

Fig. 3 Haemolytic properties of ethyl-acetate crude extract (ECE) and the dichloromethane fraction (DF) obtained from aerial parts of *Tanacetum parthenium*. Amphotericin B (AMPB) was included in the assay as a reference drug.

Table 1. Comparison of values of CC_{50} for J774G8 macrophages and IC_{50} for promastigote forms of *Leishmania amazonensis*, and their respective selectivity indexes (SI).

	J774G8 CC_{50}	Promastigote IC_{50}	SI
	µg/ml		
PTP	1400	490	2.9
ECE	110	29	3.8
DF	19	3.6	5.3

SI = CC_{50} J774G8 / IC_{50} promastigotes

amastigote forms respectively (Figs 1C, F). The IC_{50} values for promastigotes observed for the HF, DF, EF, MF, and MWF were 7.0, 3.6, 43.1, 43.8, and >50.0 µg/ml, and for amastigotes were 2.9, 2.7, 28.3, 48.4 and >50 µg/ml respectively. A concentration of 0.058 µg/ml of the reference drug AMPB inhibited 65.8% and 2.9% of promastigote and amastigote growth respectively (data not shown).

Cytotoxicity assay against J774G8 cells. J774G8 macrophages treated with 1000, 1500 and 2000 µg/ml of the PTP, showed 88.5, 35.2 and 25.6% viable cells, respectively (Fig. 2A). The toxicity to J774G8 cells and the antiprotozoal activity were compared using the selective index (SI) ratio: CC_{50} J774G8 cells/IC_{50} protozoans, where CC_{50} is 50% of the cytotoxic concentration. A value greater than 1 is considered to be more selective

against protozoans, and a value lower than 1 is considered to be more selective to the cells. In this case, the SI was 2.9, demonstrating that the PTP is less toxic to the cells than to the protozoans (Table 1). For macrophages treated with the ECE at 50 µg/ml, 91.1% of the cells remained viable. However, a concentration of 125 µg/ml of ECE showed only 17% viable cells, after 48 h of incubation (Fig. 2B). The SI for the ECE was 3.8 (Table 1). J774G8 macrophages treated with 5 µg/ml of the DF showed 97.6% viability. At concentrations of 20 and 30 µg/ml, 44.5% and 12.9% of the cells remained viable, respectively (Fig. 2C). In this case, the fraction was 5.3 times more selective against the parasites than the macrophages (Table 1). The CC_{50} for AMPB was 13.9 µg/ml (data not shown).

Red blood cell lysis assay. The red-blood-cell control did not show haemolysis, nor did the 0.5% DMSO control. On the other hand, the positive control TritonX-114 showed 100% haemolysis. Fig. 3 shows that red blood cells treated with 100 µg/ml of ECE caused only 4.0% lysis after 120 min of incubation. EC_{50} (50% effective concentration) of haemolysis was 397 µg/ml, a value 13.7-fold higher than the IC_{50} for promastigote forms. The DF added to a suspension of red blood cells caused 4.6% haemolysis at 500 µg/ml (the highest concentration tested), which is 138.9-fold higher than the IC_{50} for promastigote forms. At 100 µg/ml, this fraction showed only 0.5% haemolysis. Cells treated with AMPB at 6.25 µg/ml showed 3.9% lysis, while at 100 µg/ml they showed 90.5% lysis. The haemolysis EC_{50} was 36 µg/ml.

DISCUSSION AND CONCLUSION

There is a general lack of effective and inexpensive chemotherapeutic agents for the treatment of leishmaniasis. Pentavalent antimonial drugs are the first-line treatment for this disease, with amphotericin B and pentamidine being used as alternative drugs. All of these have serious side effects, and resistance has become a severe problem; therefore, new drugs are urgently required. Natural products have potential in the search for new and selective agents for the treatment of important tropical diseases caused by protozoans. Alkaloids, terpenes, quinones, and miscellaneous compounds well illustrate the diversity of antiprotozoal compounds found in higher plants. Some of these have been shown to act on systems present in parasites but which are absent or different from those in the host, and these merit further study in order to improve their activity and lessen toxic effects (Wright and Phillipson 1990).

Plants belonging to the genus *Tanacetum* are reputed to have excellent medicinal value, and a large number of sesquiterpenoids and sesquiterpene lactones, which are typical constituents of these drugs, have been isolated from *Tanacetum* species. These compounds might be responsible for the effects exhibited by the plants (Abad *et al.* 1995). The species *Tanacetum parthenium* has been used in folk medicine for treatment of migraine, tinnitus, giddiness, arthritis, fever, menstrual disorders, difficulty in labor, stomachache, toothache, and insect bites (Newall *et al.* 2002).

We demonstrated that crude extracts and fractions prepared from *T. parthenium* showed excellent antileishmanial activity. A progressive increase in the antileishmanial effect was observed in the course of the purification process. Bioassay-guided fractionation led us to a dichloromethane fraction which was 136-fold and 28-fold more active against promastigote and amastigote forms respectively, than the crude plant powder from aerial parts. Several studies have shown that crude extracts from different species of plants show antileishmanial activity. Screening of extracts from Bolivian plants against *L. braziliensis*, *L. amazonensis* and *L. donovani* demonstrated that five plants used in folk medicine to treat cutaneous leishmaniasis (*Bocconia integrifolia, Bocconia pearcei, Ampelocera edentula, Galipea longiflora*, and *Pera benensis*) showed antileishmanial activity (Fournet *et al.* 1994). Another study with extracts from Colombian plants found that four species used traditionally for treatment of leishmaniasis (*Conobea scoparioides, Hygrophila guianensis, Otoba novogranatensis* and *Otoba parviflora*) showed activity against promastigote forms of *Leishmania* spp. at 100 µg/ml (Weniger *et al.* 2001). Salvador *et al.* (2002) demonstrated that aqueous and ethanol crude extracts of roots from *Blutaparon portulacoides* showed antileishmanial activity against axenic amastigote forms of *L. amazonensis*. Additionally, crude extracts from *Alstonia macrophylla, Rhazya stricta, Swietenia macrophylla, Stephania dinklagei, Triclisia patens,* and *Cephaelis camponutans*, selected either from ethnobotanical or chemotaxonomic data, showed strong activity against promastigote forms of *L. donovani,* with IC_{50} values below 10 µg/ml. These extracts had stronger cytotoxic effects on the parasite than on mammalian cells (Camacho *et al.* 2003). The linalol-rich essential oil from the leaves of *Croton cajucara* showed excellent inhibition of the growth of promastigote and amastigote

forms of *L. amazonensis* (Rosa *et al.* 2003). Recently, Mendonça-Filho *et al.* (2004) demonstrated that the polyphenolic-rich extract from *Cocos nucifera* at 10 µg/ml inhibited the growth of promastigote forms of *L. amazonensis* and reduced by approximately 44% the association index between peritoneal mouse macrophages and this protozoan. Experiments with axenically cultured amastigotes should be of interest for developmental investigations of the disease-maintaining stage of this parasite (Pan *et al.* 1993).

A progressive decrease in the cytotoxic effect was observed in the course of the purification process. *In vitro* tests with J774G8 cells showed that the IC_{50}s of the PTP, ECE, and DF were more toxic to the protozoans. This is demonstrated by their SI ratio values of >1 (Table 1). Also, cytotoxicity studies with *T. parthenium* demonstrated that toxic concentrations for red blood cells are higher than for promastigote forms. Toxicity tests for medicinal plants are essential because of the growing interest in alternative therapies and the therapeutic use of natural products. This interest in drugs of plant origin is due to several reasons, e.g., conventional medicine can be inefficient, synthetic drugs may have side effects, or folk medicine suggests that natural products are harmless (Rates 2001). However, traditional use is no guarantee of safety (Edzard 1998), and relatively few drugs have been evaluated scientifically to prove their safety, potential benefits, or effectiveness (Calixto 2000).

Natural products can be lead compounds, allowing the design and rational planning of new drugs, biomimetic synthesis development, and the discovery of new therapeutic properties not yet attributed to known compounds (Hamburguer and Hostettmann 1991). Considering that the Brazilian flora is very rich, reliable scientific knowledge is required for the transformation of medicinal plants into industrialised medicines (Rates 2001). Natural products have made, and are continuing to make, an important contribution to this area of therapeutics; perhaps their future potential will be even greater.

In this study we report the biological effect of crude extracts and fractions obtained from *T. parthenium* on promastigote and amastigote forms of *L. amazonensis*. This activity represents an exciting advance in the search for novel antileishmanial agents from natural sources, since a significant and important effect against the intracellular stage of the protozoan was demonstrated. This plant showed significant activity against *Leishmania* pathogens, but further synthesis and *in vitro* studies are indicated to validate these results. Therefore, the most promising fraction was given priority for further phytochemical analysis of the isolation and identification of the particular compounds which have antiprotozoal activity.

Acknowledgements. This study was supported through grants from Conselho Nacional de Desenvolvimento Científico e Tecnológico - CNPq, Capacitação de Aperfeiçoamento de Pessoal de Nível Superior CAPES, Financiadora de Estudos e Projetos - FINEP, and Programa de Pós-graduação em Ciências Farmacêuticas da Universidade Estadual de Maringá. One of the authors (TST) thanks CAPES for scholarship.

REFERENCES

Abad M. J., Bermejo P., Villar A. (1995) An approach to the genus *Tanacetum* L. (Compositae): phytochemical and pharmacological review. *Phytother. Res.* **9:** 79-92

Alvar J., Cañavate C., Gutiérrez-Solar B., Jiménez M., Laguna F., López-Vélez R., Molina R., Moreno J. (1997) *Leishmania* and human immunodeficiency virus coinfection: the first 10 years. *Clin. Microbiol. Rev*. **10:** 298-319

Bennett J. E. (1996) Fármacos antimicrobianos (continuação): fármacos antifúngicos. In: As Bases Farmacológicas da Terapêutica, (Eds. L.S. Goodman, A. Gilman). McGraw-Hill, México, 9ed., 864-875

Berman J. D. (1996) Treatment of New World cutaneous and mucosal leishmaniasis. *Clin. Dermatol*. **14:** 519-522

Berman J. D. (1997) Human leishmaniasis: clinical, diagnostic, and chemotherapeutic developments in the last 10 years. *Clin. Infect. Dis.* **24:** 684-703

Calixto J. B. (2000) Efficacy, safety, quality control, marketing and regulatory guidelines for herbal medicines (phytotherapeutic agents). *Braz. J. Med. Biol. Res.* **33:** 179-189

Camacho D. D. R., Phillipson J. D., Croft S. L., Solis P. N., Marshall S. J., Ghazanfar S. A. (2003) Screening of plant extracts for antiprotozoal and cytotoxic ativities. *J. Ethnopharmacol*. **89:** 185-191

Croft S. L., Coombs G. H. (2003) *Leishmaniasis* - current chemotherapy and recent advances in the seach for novel drugs. *Trends Parasitol*. **19:** 502-508

Edzard E. (1998) Harmless herbs? A review of the recent literature. *Am. J. Med.* **104:** 170-178

Fournet A., Barrios A. A., Muñoz V. (1994) Leishmanicidal and trypanocidal activities of Bolivian medicinal plants. *J. Ethnopharmacol*. **41:** 19-37

Grevelink S. A., Lerner E.A. (1996) Leishmaniasis. *J. Am. Acad. Dermatol.* **34:** 257-272

Hamburger M., Hostettmann K. (1991) Bioactivity in plants: the link between phytochemistry and medicine. *Phytochemistry* **30:** 3864-3874

Heptinstall S., Williamson L., White A., Mitchell J. R.A. (1985) Extracts of feverfew inhibit granule secretion in blood platelets and polymorphonuclear leucocytes. *Lancet North Am. Ed.* **325:** 1071-1074

Jain N. K., Kulkarni S. K. (1999) Antinociceptive and anti-inflammatory effects of *Tanacetum parthenium* L. extract in mice and rats. *J. Ethnopharmacol*. **68:** 251-259

Martindale (1999) Feverfew. In: Martindale: the Complete Drug Reference, (Ed. K. Parfitt). The Pharmaceutical Press, London, 32ed., 447

Mendonça-Filho R. R., Rodrigues I. A., Alviano D. S., Santos A. L. S., Soares R. M. A., Alviano C. S., Lopes A. H. C. S., Rosa M. S. S. (2004) Leishmanicidal activity of polyphnolic-rich extract from husk fiber of *Cocos nucifera* Linn. (Palmae). *Res. Microbiol.* **155:** 136-146

Murphy J. J., Heptinstall S., Mittchel J. R. A. (1988) Randomised double-bind placego-controlled trial of feverfew in migraine prevention. *Lancet North Am. Ed.* **332:** 189-192

Newall C. A., Anderson L. A., Phillipson J. D. (2002) Matricária. In: Plantas Medicinais: Guia Para Profissional de Saúde, (Eds. C. A. Newall, L. A. Anderson, J. D. Phillipson). Editorial Premier, São Paulo, 191-193

Pan A. A., Duboise M., Eperon S., Rivas L., Hodgkinson V., Traub-Cseko Y., McMahon-Prati D. (1993) Developmental life cycle of Leishmania - cultivation and characterization of cultured extracellular amastigotes. *J. Euk. Microbiol.* **40:** 213-223

Piela-Smith T. H., Liu X. (2001) Feverfew and the sesquiterpene lactone parthenolide inhibit intercellular adhesion molecule-1 expression in human synovial fibroblasts. *Cell. Immunol*. **209:** 89-96

Rates S. M. K. (2001) Plants as source of drugs. *Toxicon* **39:** 603-613

Rosa M. S. S., Mendonça-Filho R. R., Bizzo H. R., Rodrigues I. A., Soares R. M. A., Souto-Padrón T., Alviano C. S., Lopes A. H. C. S. (2003) Antileishmanial activity of a linalool-rich essential oil from *Croton cajucara*. *Antimicrob. Agents Chemother.* **47:** 1895-1901

Salvador M. J., Ferreira E. O., Pral E. M. F., Alfieri S. C., Albuquerque S., Ito I. Y., Dias D. A. (2002) Bioactivity of crude extracts and some constituents of *Blutaparon protulacoides* (Amarantheceae). *Phytomedicine* **9:** 566-571

Shu Y. (1998) Recent natural products based drug development: a pharmaceutical industry perspective. *J. Nat. Prod*. **61:** 1053-1071

Sumner H., Salan U., Knight D. W., Hoult J. R. S. (1992) Inhibition of 5-lipoxigenase and cyclo-oxigenase in leukocytes by feverfew. Involvement of sesquiterpene lactones and other components. *Biochem. Pharmacol*. **43:** 2313-2320

Ueda-Nakamura T., Attias M., De Souza W. (2001) Megasome biogenesis in *Leishmania amazonensis*: a morphometric and cytochemical study. *Parasitol. Res.* **87:** 89-97

Weniger B., Robledo S., Arango G. J., Deharo E., Aragón R., Muñoz V., Callapa J., Lobstein A., Anton R. (2001) Antiprotozoal activities of Colombian plants. *J. Ethnopharmacol*. **78:** 193-200

Williams C. A., Harborne J. B., Geiger H., Hoult J. R. S. (1999) The flavonoids of *Tanacetum parthenium* and *T. vulgare* and their anti-inflamatory properties. *Phytochemistry* **51:** 417-423

World Health Organization (2001) Leishmaniasis: the disease and its impact. [Online] http://www.who.int/emc/diseases/leish/leisdis1.html, acessed in 14 April 2003

Wright C. W., Phillipson J. D. (1990) Natural products and the development of selective antiprotozoal drugs. *Phytother. Res.* **4:** 127-139

Received on 26th November, 2004; revised version on 3rd February, 2005; accepted on 18th February, 2005

Acta Protozool. (2005) 44: 253 - 263

ACTA
PROTOZOOLOGICA

Habitat Selection of Aquatic Testate Amoebae Communities on Qeqertarsuaq (Disko Island), West Greenland

Roel MATTHEEUSSEN[1], Pieter LEDEGANCK[1], Sofie VINCKE[1], Bart VAN DE VIJVER[1], Ivan NIJS[2] and Louis BEYENS[1]

[1]Department of Biology, Polar Ecology, Limnology and Palaeobiology Unit, Universiteit Antwerpen, Antwerp; [2]Department of Biology, Plant Ecology Unit, Universiteit Antwerpen, Antwerp (Wilrijk), Belgium

Summary. The testate amoebae communities living in different substrate types of 31 aquatic sites on Qeqertarsuaq (West-Greenland) were studied. A total of 74 taxa, belonging to 21 genera was observed. While most taxa belonged to the genera *Difflugia*, *Euglypha* and *Centropyxis*, most counted tests were identified as *Trinema lineare*. The substrate type showed the largest influence on testate amoebae communities, regardless of the habitat type. *Centropyxis aerophila*, *C. aerophila* var. *sphagnicola*, *Difflugia pristis* and *D. tenuis* showed a clear preference for sediments (sapropelium and rock scraping), both in standing and running water bodies. The differences in site characteristics induced also differences among the epiphytic communities. *Assulina muscorum*, *A. seminulum*, *Difflugia glans*, *D. tenuis*, *Difflugiella crenulata* var. *globosa* and *Euglypha strigosa* were typical taxa living on macrophytes in standing water bodies. No typical epiphytic taxa were found in running water bodies. Homothermic systems, which are ice-free year-round, accommodate more developed testate amoebae communities. This reflects in a higher ratio of K-strategic lobose testate amoebae as compared to r-strategic *Filosa* (LF-index).

Key words: Arctic, Disko Island, ecology, filosa, Greenland, homothermic system, LF-index, lobosa, multivariate community analysis, Qeqertarsuaq, testate amoebae.

INTRODUCTION

To understand the effects of Global Change on Arctic ecosystems, knowledge of the current biogeography and ecological preferences of the composing organisms is required. A very sensitive group of organisms is formed by the testate amoebae (Protozoa, Sarcodina, Rhizopoda). Studies on rhizopods in Greenland started with some data from the east coast (Dixon 1939). Later-on, more substantial work was published dealing with rhizopods from the western (Decloître 1954), the eastern (Stout 1970) and the north-eastern Greenlandic coast (Beyens and Chardez 1986; Beyens *et al.* 1986a, b; Trappeniers *et al*. 1999, 2002; Van Kerckvoorde *et al*. 2000). Data from the transition zone between Low and High Arctic however are scarce and the ecological preferences of many species remain unknown. Unfortunately, this transition zone might be one of the first areas affected by Global Change effects.

Address for correspondence: Pieter Ledeganck, Department of Biology, Polar Ecology, Limnology and Palaeobiology Unit, Universiteit Antwerpen, Groenenborgerlaan 171 B-2020 Antwerp, Belgium; Fax: +32 3 265 32 95; E-mail: pieter.ledeganck@ua.ac.be

Testate amoebae are present in a variety of habitats, ranging from lakes, pools and rivers to wet soils, moss vegetation and peatlands. Their short generation times make them useful indicators of environmental changes. The most important factor in controlling their distribution, activity and population fluctuations is supposed to be the moisture content of their habitat (Smith 1992, Mitchell and Buttler 1999 and references therein). A broad range of other factors are shown to be correlated with the testacean community structure such as pH (Costan and Planas 1986, Beyens and Chardez 1995, Ellison 1995), eutrophication (Schönborn 1962), temperature regime (Medioli and Scott 1988), light, oxygen and food availability (Charman *et al*. 2000).

The aim of this study is to enhance our knowledge of the distribution and ecology of testate amoebae, in particular in the transition zone between Low and High Arctic. Special attention will be given to the ecological differences between homo- and heterothermic systems, an exceptional feature on Qeqertarsuaq. This paper is the first in a series of three describing the testate amoebae communities in different habitats on Qeqertarsuaq.

MATERIALS AND METHODS

Study site

Field sampling was carried out between 11 and 31 July 2002 at Qeqertarsuaq (Disko Island), situated on the western coast of Greenland (69°15'N, 53°34W, Fig. 1). The island is 8578 km^2 large, has a typical arctic maritime climate and is located on the transition zone between Low Arctic and High Arctic (Alexandrova 1980). Mean annual precipitation never reaches 242 mm water equivalent whereas the mean annual air temperature is -4.3°C. Minimum and maximum monthly mean temperatures of -16.2°C and 7.1°C are registered in February and July respectively (Arctic Station meteorological data 1996-2002). The prevailing wind directions are east during winter (cold katabatic air from the Greenlandic ice sheet) and west during summer (warm maritime air from the ocean). Geological and periglacial phenomena, such as glacial valleys and braided rivers, create a broad range of aquatic habitats (Svendsson 1978). The terrestrial vegetation is mainly dominated by dwarf-shrub heaths, with a prominent role for sedges and mosses on wetter areas. Several homothermic systems (Fig. 2) can be found on Qeqertarsuaq having a constant temperature regardless of the season, due to a passage through geothermal or radioactive layers (Heegaard *et al*. 1994). A large number of plants [e.g. *Angelica archangelica* L., *Alchemilla glomerulans* Buser, *Platanthera hyperborea* (L.) Lindley and *Leucorchis albida* (L.) E. Mey] usually limited much farther south, are capable of surviving near these systems, contributing in that way to the botanical diversity of Qeqertarsuaq (more than 50% of all flowering plants of Greenland are present on the island).

Sampling

Seventy-six water samples were collected from 31 different water bodies ranging from small pools to lakes and rivers (Appendix 1). Sampling sites were randomly chosen in the vicinity of the Arctic Station on the south coast of Qeqertarsuaq (Fig. 1), maximising the differences in site characteristics (e.g. water body type, vegetation, distance to the sea, height, microclimate). Water temperature, pH, oxygen content (% and mg/l) and specific conductance were measured *in situ* using a WTW Multiline P4. Homothermic influence was determined based on the observed vegetation and translated in three classes: 1 - homothermic, 2 - heterothermic with significant homothermic influence and 3 - heterothermic. Samples were taken from three types of substratum: sapropelium, epilithon (rock scraping) and macrophytes (aquatic plants and mosses) and stored in 50 ml polyethylene bottles. Formaldehyde (3%) was added for fixation. Moss vegetation humidity was based on the classification of Jung (1936) with F-value I for completely submerged mosses and F-value II for surfacing/floating mosses. Moss samples were taken by squeezing out water of a considerable part of the sampled moss vegetation. Fresh moss was added to the sample to include also strongly adhered testate amoebae specimens. Sapropelium and rock samples were obtained by scraping the substrate with a bottle.

Laboratory methods

Water chemistry analysis for SO^{2-}_4, Cl^-, NH^+_4, NO^-_3, NO^-_2, PO^{3-}_4, colour and hardness of the site samples was performed using a Palintest interface spectrophotometer. Details of the analytical methods are fully described by MacQuaker (1976).

Samples were passed over a sieve with a mesh diameter of 300 µm and concentrated by centrifugation (5 min at 1250 rpm). To distinguish dead from living tests rose bengal was added. Since the thanatocoenose was a good estimator for the living population ($F_{1;1053}$= 1139.4 with $p<0.001$), all further calculations were based on the total of death and living individuals on the moment of sampling.

In each sample a total of 150 tests (including both coloured and uncoloured specimens) were counted using an Olympus BX50 microscope at 400x magnification. Previous research (Warner 1988, Woodland *et al*. 1998) suggested that this number represents the principal taxa in the sample. Identifications were based mainly on Decloître (1962, 1978, 1979, 1981), Deflandre (1928, 1929, 1936), Grospietsch (1964), Hoogenraad and de Groot (1940), Ogden (1983) and Ogden and Hedley (1980). Sixteen samples (on a total of 76) where withdrawn from further analysis since they contained little (less then 5 individuals in 1 slide) or no testate amoebae. Withdrawn samples were taken from glacial melt water streams or contained fine grained clay sediment, preventing any clear microscopical analysis.

Data analysis

The Shannon-Wiener (Shannon and Weaver 1949) and Gini-evenness (Nijssen *et al*. 1998) indices were calculated respectively for diversity and evenness.

To estimate the developmental stage of a testate amoebae community, the LF-index (Bonnet 1976) was used. Based on the assumption that filose testate amoebae (Filosa) are r-strategic, while Lobosa follow a more K-based strategy, this index is calculated as the ratio between the number of testate amoebae with lobose and filose pseudopodia [LF = (Lobosa - Filosa)/(Lobosa + Filosa)] and varies

theoretically from -1 (only Filosa, undeveloped communities) to +1 (only Lobosa, developed, stabilised communities).

All means are given ± 1 SD.

A hierarchic-agglomerative Cluster Analysis, based on a minimum variance strategy with the Squared Euclidian Distance as a dissimilarity index, was carried out to group the sites (MVSP, Kovach Computing Services 1993). We used Principal Components Analysis (PCA) to determine the main patterns of variation in the chemical variables of the sites. This PCA was based on a standardized correlation matrix of the ln-transformed physical and chemical data, except for pH that is already a logarithmic variable, due to their skewed distributions.

If a taxon didn't show a relative abundance of minimum 2% in at least one sample, it was removed from further community analysis. Since not all the environmental variables influence the distribution of testate amoebae independently, a Canonical Correspondence Analysis (CCA) was used with forward selection and unrestricted Monte Carlo permutation tests (999 permutations, $p \leq 0.05$). The statistical techniques used in this study are described in full detail in Jongman *et al.* (1987). Ordination analyses were performed using the computer program CANOCO 4.0 (ter Braak 1987).

To test whether the distribution pattern of the testacean fauna was determined by either the sampled substrate, the habitat type or a combination of both parameters, a logistic model was used (data did not follow a normal distribution) (SAS version 8). The dependent variable was the abundance of a testate amoeba taxon in a certain sample (with a specific substrate in a certain habitat). The abundance data can be seen as discrete variables since there was always a fixed number of individuals (150) counted per sample. The independent variables were: testate amoebae species, substratum type and habitat type. Two types of substratum were chosen: macrophytes (including submerged plants and mosses) and sediment (combining both scrapings and sapropelium samples), while all 4 categories for habitat were maintained (pool, lake, brook with weak or strong current). Because of the overall dominance of *Trinema lineare* in all samples showing no preference at all, this species was excluded from the analysis. The analysis was performed on the 15 most frequently occurring testate amoebae taxa (PSEFUL, CENAER, TRIENC, DIFGL3, DIFGL2, EUGTUB, DIFOBL, EUGROT, CENPLAT, DIFPRI, PSEGRA, DIFTEN, CENASY, CENASP, DILOVF; abbreviations see Appendix 2). The estimates of the Least Squares Means were used to calculate the proportion of a certain testate amoebae taxon per substrate type and per habitat type.

Fig. 1. Sketch maps of Greenland, Qeqertarqsuaq (Disko Island) and the sampling area with site numbers.

RESULTS

Species Composition

Seventy-four taxa (including species, varieties and forms) belonging to 21 genera were recorded (Appendix 2, Table 1). This number does not include 12 unidentified taxa, of which only a few individuals were found. On average 18 ± 5 taxa per sample were found, with a maximum of 32 taxa in DW042 (submerged moss) and a minimum of 6 taxa in DW043 (rock scraping). The highest proportion of all counted tests was constituted by *Trinema lineare* (30.7%) present in all samples except DW004. Most taxa belonged to the genera *Difflugia* (19 taxa), *Euglypha* (11 taxa) and *Centropyxis* (10 taxa). Other important taxa were *Pseudodifflugia fulva* (6.6%; 74% occurrence), *Centropyxis aerophila* (6.5%; 90% occurrence), *Trinema enchelys* (6.3%; 87% occurrence), *Difflugia globulus* (6.2%; 75% occurrence) and *D. globulosa* (5.5%; 87% occurrence). Sixty-eight taxa showed mean relative frequencies below 1%.

Based on the currently available literature, only 7 taxa were likely to be recorded for the first time in the Arctic Region (the Arctic being defined as these regions spread-

Fig. 2. Examples of heterothermic (top) and homothermic (below) systems, with the typical vegetation of the latter.

Fig. 3. Cluster dendrogram showing all sampled sites. The different clusters based on the physico-chemical LN transformed data, are shown on the right.

ing northwards from the tree limit (Alexandrova 1980), mostly correlated with the 10°C July isotherm).

The mean Shannon-Wiener diversity was 0.93 ± 0.16. The diversity was significantly higher in sediment samples (1.01 ± 0.16), compared to samples taken from macrophytes (0.88 ± 0.16) ($t_{2.58}$ = -2.75; p = 0.008). The Gini evenness index did not vary between different groups and reached an overall mean of 0.43 ± 0.09. The ratio of death to living testate amoebae amounts to 2.35.

Site characteristics

To summarize the major patterns of variation within the chemistry data, PCA and cluster analysis were used. The results are shown as a cluster dendrogram (Fig. 3) and a PCA-correlation biplot (Fig. 4). The first two PCA-axes accounted for 79.4% of the total cumulative variance (λ_1 = 0.852, λ_2 = 0.212). Long arrows represent environmental parameters that explain most of the variation and are therefore more important within the data. Two major groups of variables can be recognized. Total Hardness, oxygen content, pH and water temperature are highly linked to each other while the second group contained all variables related to salinity (specific conductance, SO_4^{2-} and chloride).

Cluster analysis divides the sampled sites into two groups, with DS020 set apart as a third separate cluster. Cluster A contained all standing waters, whereas cluster B comprised all running waters. The first cluster was further subdivided into subcluster A1.1 (lakes) and A1.2 (shallow pools); while in cluster B an additional subdivision was made between homothermic (cluster B1) and heterothermic sites (cluster B2). Although total hardness values were very low for all sites, it still seems to be the determining factor separating clusters A1.2 (28.0 ± 8.9 mg/l) and B (2.2 ± 2.6 mg/l), with the cluster A1.1 showing intermediate hardness values (16.7 ± 9.0 mg/l). The separation of DS020 (cluster A2) was based on the elevated salinity variables of this site

Table 1. The main observed testate amoebae genera with their relative abundance (%) and the number of present taxa.

	Relative abundance (%)	Number of taxa
Trinema	37.65	3
Difflugia	18.92	19
Centropyxis	14.44	10
Euglypha	11.93	11
Pseudodifflugia	8.76	3
Other	8.30	40
	100	86

Table 2. The effect of habitat type, substrate and their interaction on the occurrence of the most important testate amoebae taxa.

	Habitat	Substratum	Habitat × Substratum
Centropyxis aerophila		**	
Centropyxis aerophila var. *sphagnicola*		*	
Difflugia globulosa	**	*	
Difflugia globulus	*	*	***
Difflugia pristis		*	
Difflugia tenuis		**	
Euglypha rotunda			*
Trinema enchelys	*		

* significant at 0.05 level; ** significant at 0.01 level; *** significant at 0.001 level

(spec. cond. = 477 µS/cm^2), compared to an average 76.1 ± 31.02 µS/cm^2 for all other sites.

Community analysis

The original set of 22 environmental variables was reduced to 6 based on the selection procedures described in the methods section, leaving oxygen content (%), total hardness, pH, habitat type 'lake' and substratum type's 'scrapings' and 'mosses' as determining variables. When constrained to these 6 environmental variables, the CCA explained only a small proportion of the variance in the species data (Fig. 5). The first two axes account for only 7.3 % of the variance in the testate amoebae data (λ_1 = 0.139, λ_2 = 0.104). This low percentage is typical for noisy datasets containing many zero values (Stevenson *et al.* 1991). In contrast, a rather large proportion of the variance was explained by the testate amoebae-environment relationship (75.2 % for the first two axes).

In the CCA diagram axis 1 is strongly related to pH (inter-set correlation 0.55) separating samples with rela-

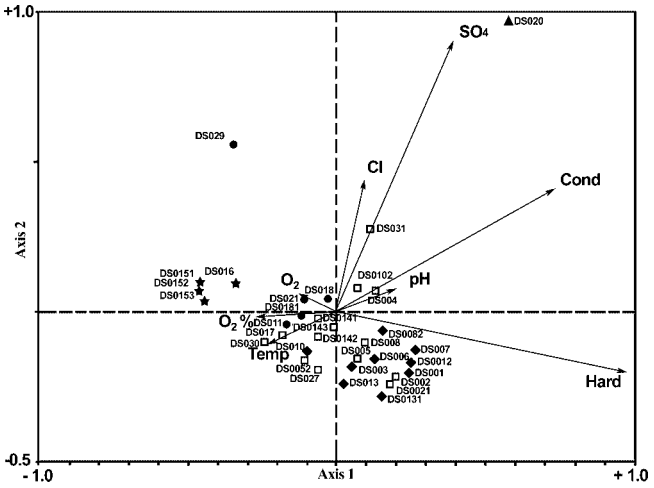

Fig. 4. Diagram of the Principal Components Analysis (PCA) showing the different site clusters based on LN transformed dataset (symbols referring to clusters: open square - A 1.1, filled rhomb - A 1.2, filled triangle - A 2, filled circle -B 1, asterisk - B 2).

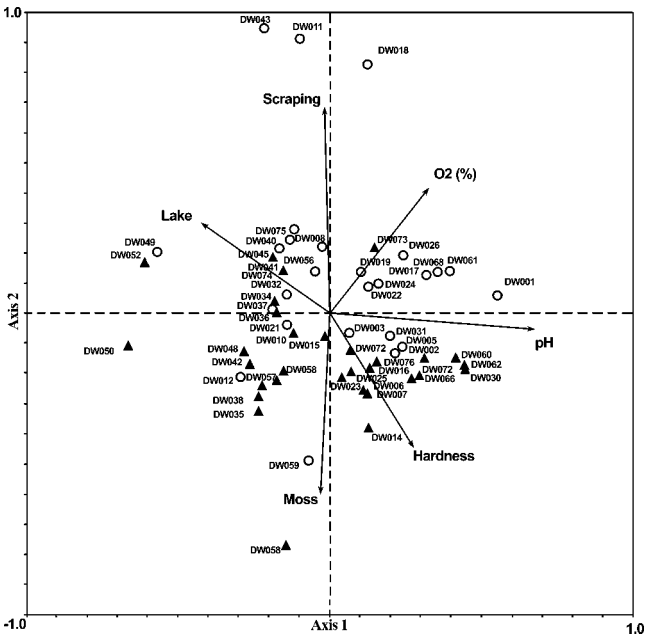

Fig. 5. Canonical Correspondence Analysis (CCA) ordination diagram showing the relation between samples (open circle sediment and filled triangle vegetation samples) and environmental variables. *Arrows* indicate environmental variables as detected by forward selection.

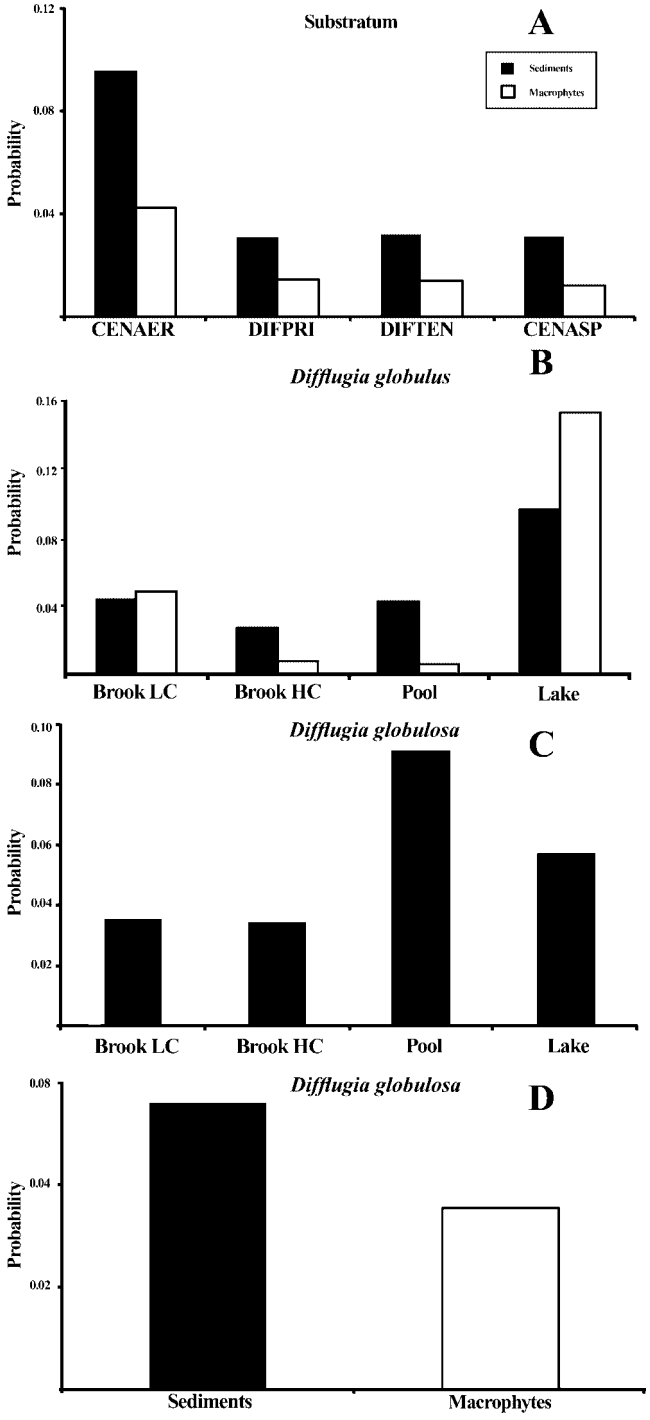

Figs 6 A-D. The significant probabilities of occurrence for (**A**) *Centropyxis aerophila, Difflugia pristis, Difflugia tenuis* and *Centropyxis aerophila* v. *sphagnicola* in different substrates and habitat types, (**B**) *Difflugia globulus* and (**C, D**) *Difflugia globulosa* in both substrate types and all habitat types. Habitat types Brook HC and Brook LC refer to brooks with high current and low current respectively.

tively high pH on the right side from more acid lakes on the left side. *Difflugia globularis, Cyphoderia ampulla* and *Tracheleuglypha dentata* seem to prefer the more alkaline conditions. *Lesquereusia epistomium* and *Assulina muscorum* on the other hand showed their highest abundances in the acid samples. Axis 2 is related to the sampled substratum (moss and scrape samples; inter-set correlations -0.58 and 0.64). Samples taken from submerged moss vegetations are grouped together and the same applies for the samples from scrapings. *Difflugiella sacculus* and *D. crenulata* seem to be more abundant in scrape samples whereas *Tracheleuglypha acolla, Tracheleuglypha dentata* and *Difflugia globularis* tend to prefer bryophyte substrates.

Since habitat type was the determining factor in clustering the samples on the physico-chemical base, while substratum type seemed to classify samples based on the testate amoebae composition, a logarithmic regression was performed to detect effects of habitat, substratum type and their interaction on the distribution of testate amoebae species.

The results showed that for 8 species habitat type, substratum type and the interaction habitat × substratum were significant (χ^2) at different levels (Table 2). In general, substratum type seemed to be the most important parameter within all sampled habitats. *Centropyxis aerophila, C. aerophila* var. *sphagnicola, Difflugia pristis* and *D. tenuis* showed a preference for sediments in all habitat types (Fig. 6A). *Difflugia globulus*, on the other hand, only preferred sediments in small pools and brooks with a strong current. In lakes, *D. globulus* tended to live epiphytic (Fig. 6B). *D. globulosa* seemed to prefer calm aquatic conditions with no or a low streaming velocity (Fig. 6C), and showed a general tendency to prefer sediments (Fig. 6D).

Homothermic versus heterothermic systems

The mean LF-index of samples taken in entirely homothermic systems (LF= 0.279 ± 0.242) is significantly higher than these of completely heterothermic systems (LF= 0.066 ± 0.276) ($t_{2.41}$ = 2.577; p = 0.014). Samples from the homothermic sites never showed negative LF-values. No differences in species richness between both systems were observed ($t_{2.41}$ = -0.893; p = 0.377) but the species composition seemed to vary. Taxa with a clear preference for homothermic systems were *Difflugia globulosa, D. pyriformis, Nebela penardiana* and *Difflugiella minuta*. All cited species belong to the lobose or reticulolobose (*D. minuta*) type. Taxa with a clear preference for the heterothermic

systems comprise among others: *Trinema complanatum*, *Euglypha strigosa*, *Nebela collaris*, *N. dentistoma* and *Corythium dubium*, covering both *Filosa* and *Lobosa*.

DISCUSSION

Species composition

The high number of testate amoebae taxa (i.e. 74) found in this study confirms the diversity potential of Qeqertarsuaq. Previous studies on aquatic testate amoebae from Greenland reported only 41 (Beyens *et al.* 1992) and 67 testate amoebae taxa (Trappeniers *et al.* 1999). This high species richness is not surprising since also the phanerogamic diversity of the studied area is remarkably high. Smith (1992) and Ledeganck *et al.* (2002) already demonstrated the close correlation between vegetation and testate amoebae diversity.

Trinema lineare dominated all communities, confirming its typical ubiquistic distribution. The species has been reported from all over the arctic region (overview in Beyens and Chardez 1995). Beyens *et al.* (1986b) suggested that, as the number of species diminishes towards the north, *T. lineare*, if present, tends to become the dominant species, a trend also recognised in various alpine studies (Lousier 1976, Todorov 1998). *Difflugia* comprises the major part of the observed taxa. Taxa of this genus were present in all samples with *D. globulus* and *D. globulosa* as the dominant species. However, the relatively small dimensions of the latter two species protect them against the cold, minimizing the risk of frost fractures (Beyens *et al.* 2000). Therefore, inclusion of a considerable number of empty (=dead) tests might produce this overabundance and this could be an artefact. The process of frost fracture is driven by the expansion of frozen water and diminishes the death/living ratio from 10 in temperate areas to 1 to 3 in arctic conditions (Balik 1994). The highly diverse presence of *Difflugia* is commonly observed in arctic (Beyens *et al.* 1986b, 1992; Beyens and Chardez 1994; Trappeniers *et al.* 1999) as well as antarctic aquatic habitats (Vincke *et al.* in press).

Community analysis

Habitat specificity

The grouping of the sites into 4 clusters based on total hardness and salinity is explained by the nature of the sites. Most sampled pools were situated directly on basaltic rocks, where Ca^{2+} could easily dissolve into the system. This accumulation of Ca^{2+} was slower in larger lakes, while no Ca^{2+}-accumulation appeared in running waters. This could explain why the clusters of running waters (B), lakes (A1.1) and shallow pools (A1.2) were ordinated along the hardness gradient. Compared to non-arctic standards, the $CaCO_3$ amount and hardness values in all sites were very low, raising the question whether the impact of the amount of $CaCO_3$ on the testate amoebae community could be due to Ca^{2+}-limitation, rather than hardness levels.

The high salinity values in site DS020 are caused by sea spray since the sampling site was located only a few meters from the shore.

Habitat and substratum specificity

Habitat type clearly influences the testate amoebae communities. *D. globulus* is more likely to be found in lakes then in the other habitat types, while *D. globulosa* seems to prefer the more stagnant habitat types (pools and lakes) (Figs 6C, D).

Our results indicate that the composition of the testate amoebae communities is highly influenced by the substratum type. This observation should be carefully taken into account when comparing different studies. Although no species were typical for either the macrophyte samples or the sediment samples, *Centropyxis aerophila*, *C. aerophila* var. *sphagnicola*, *Difflugia pristis*, *D. tenuis* and *D. globulosa* all preferred the sediment niche within all habitat types (Figs 6A, D). These 4 species are all so-called xenosomic testate amoebae that need exogenous particles for the construction of their test. Idiosomic testate amoebae on the other hand, such as the genus *Trinema*, construct their own building units and are thus not depending on the substrate to provide construction material. This could explain why substratum type did not affect the distribution of these species. *D. globulus*, another xenosomic testate amoeba, preferred both substrates equally, or had a slight preference for sediments. It is unclear why this taxon prefers a more epiphytic substrate in lakes (Fig. 6B). Although no influence on the presence/absence status of the genus *Euglypha* (idiosomic) was found, it was clear that their relative abundance was higher on macrophytes.

Thermal properties

Besides habitat type, the testacean communities are also influenced by the thermal properties of their habitat. Homothermic systems are characterized by an annual

positive water temperature, even during the cold arctic winter, keeping them ice-free during periods of lower soil and air temperature (although sometimes free-flowing through a tunnel of snow and ice). During this winter period organisms are still capable of surviving in the homothermic systems, without going into the cyst stadium. Homothermic systems therefore can accommodate more developed, stabilized testate amoebae assemblages, characterized by lobose testate amoebae species.

This is in marked contrast to the heterothermic systems. These systems are completely frozen during wintertime, and the stable communities are usually not preserved, resulting in the formation of pioneer communities with a high proportion of r-strategic filose species. Balik (1994) already reported the correlation between a high LF-index in successively developed habitats, such as peat sediments and wet mosses versus lower LF values in instable habitats such as undeveloped soils. However, the results of our study did not demonstrate higher species richness in the homothermic systems but classified them rather as a totally different habitat, favouring a testate amoebae community characterised by lobose taxa such as *Difflugia globulosa*, *D. pyriformis*, *Nebela penardiana* and *Difflugiella minuta*. A possible explanation can be given considering the much lower mean summer temperature. In heterothermic systems, this temperature values over 15°C during sunny days, while it will never exceed 5°C in most homothermic systems.

Conclusions

Substratum type clearly influences the composition of aquatic testate amoebae communities. In some cases, the distribution of several species is affected by some hydrological characteristics of the habitat type (running *vs*. standing waters), independently from their choice for a specific substratum type. These two parameters can easily mask the effects of all other physico-chemical variables.

The thermal properties within a specific habitat can have a major influence on the testate amoebae communities that inhabit them. Homothermic systems, year-round ice-free, accommodate more developed communities, dominated by K-strategic lobose testate amoebae. On the other hand, heterothermic systems are dominated by r-strategic filose testate amoebae.

Acknowledgements. The authors wish to thank Dr. B. Jessen Graae for her support with the fieldwork and Drs. V. Sluydts for his help with some of the statistics. Fieldwork on Qeqertarsuaq has been made possible by the Arktisk Station of det naturvidenskabelige Fakultet, Københavns Universitet, and has been carried out under project G.0357.02 of the FWO (Fund for Scientific Research - Flanders). Dr. Bart Van de Vijver is a post-doctoral researcher at the FWO, Flanders.

REFERENCES

Alexandrova V. (1980) The Arctic and Antarctic: Their Divisions Into Geobotanical Areas. Cambridge University Press, Cambridge

Balik V. (1994) On the soil testate amoebae fauna (protozoa: Rhizopoda) of the Spitsbergen Islands (Svalbard). *Arch. Protistenk.* **144:** 365-372

Beyens L., Chardez D. (1986) Some new and rare testate amoebae from the arctic. *Acta Protozool.* **24:** 81-91

Beyens L., Chardez D. (1994) On the habitat specificity of the testate amoebae assemblages from Devon Island (NWT, Canadian Arctic), with the description of a new species: *Difflugia ovalisina*. *Arch. Protistenk.* **144:** 137-142

Beyens L., Chardez D. (1995) An annotated list of testate amoebae observed in the Arctic between the longitudes 27°E and 168°W. *Arch. Protistenk.* **146:** 219-233

Beyens L., Chardez D., de Landtsheer R. (1986a) Testate amoebae from moss and lichen habitats in the Arctic. *Polar Biology* **5:** 165-173

Beyens L., Chardez D., de Landtsheer R., de Baere D. (1986b) Testate amoebae communities from aquatic habitats in the Arctic. *Polar Biology* **6:** 197-205

Beyens L., Chardez D., de Baere D., de Bock P. (1992) The testate amoebae from the Søndre Strømfjord region (West-Greenland): Their biogeographic implications. *Arch. Protistenk.* **142:** 5-13

Beyens L., Chardez D., Van de Vijver B. (2000) A contribution to the protist-diversity in the polar regions: testate amoebae data from the Russian Arctic. In: Topics in Ecology: Structure and Function in Plants and Ecosystems, (Eds. R. Ceulemans, J. Bogaert, G, Deckmyn, I. Nijs). University of Antwerp, Wilrijk, 101-110

Bonnet L. (1976) Le peuplement thécamoebien édaphique de la Cote-d'Ivoire. Sols de la region de Lamto. *Protistologica* **4:** 539-554

Braak C. ter (1987) Canoco - a Fortran program for canonical community ordination by (partial) (detrended) (canonical) correspondence analysis, principal components analysis and redundancy analysis. ITI-TNO, Wageningen

Charman D., Hendon D., Woodland W. (2000) The identification of testate amoebae (Protozoa: Rhizopoda) in peats. *Quat. Res. Technical Guide* **9:** 1-147

Costan G., Planas D. (1986) Effects of a short-term experimental acidification on a microinvertebrate community (Rhizopoda, Testacea). *Can. J. Zool.* **64:** 1224-1230

Decloître L. (1954) Les thécamoebiens de l'Eqe (Groenland). Paris

Decloître L. (1962) Le genre *Euglypha* Dujardin. *Arch. Protistenk.* **106:** 51-100

Decloître L. (1978) Le genre *Centropyxis* I. Compléments à jour au 31 décembre 1974 de la Monographie du genre parue en 1929. *Arch. Protistenk.* **120:** 63-85

Decloître L (1979) Le genre *Centropyxis* II. Compléments à jour au 31 décembre 1974 de la Monographie du genre parue en 1929. *Arch. Protistenk.* **121:** 162-192

Decloître L (1981) Le genre *Trinema* Dujardin 1841. Révision à jour au 31 décembre 1979. *Arch. Protistenk.* **124:** 193-218

Deflandre G. (1928) Le genre *Arcella*. *Arch. Protistenk.* **64:** 152-287

Deflandre G. (1929) Le genre *Centropyxis* Stein. *Arch. Protistenk.* **67:** 322-375

Deflandre G. (1936) Etude monographique sur le genre *Nebela* Leidy (Rhizopoda- Testacea). *Annls Protist.* **5:** 201-322, pls. 10-27

Dixon A. (1939) The protozoa of some east Greenland soils. *J. Anim. Ecol.* **8:** 162-167

Ellison R. (1995) Paleolimnological analysis of Ullswater using testate amoebae. *J. Paleolimnol.* **13:** 51-63

Grospietsch T. (1964) Die Gattungen *Cryptodifflugia* und *Difflugiella* (Rhizopoda Testacea). *Zoolog. Anz.* **172:** 243-257

Heegaard M., Heldbjerg H., Jespen B. (1994) Homotherme kilder og deres påvirkning af fugletætheden. In: Arktisk Biologisk Feltkursus Qeqertarsuaq / Godhavn, (Ed. Charlotte Ehrhardt). 23-52

Hoogenraad H., de Groot A. (1940) Zoetwaterrhizopoden en -heliozoën. In: Fauna van Nederland (Ed. H. Boschma). IX Leiden, 303

Jongman R., Braak C. ter, Tongeren O. (1987) Data Analysis in Community and Landscape Ecology. Pudoc, Wageningen

Jung W. (1936) Thecamöben ursprünglicher lebender deutscher Hochmoore. *Abh. Landesmus. Naturk. Münster* **7:** 1-87

Kovach Computing Services (1993) Multivariate statistical package version 2.1, users manual. Kovach Computing Services, Pentraeth, Wales

Ledeganck P., Nijs I., Beyens L. (2002) Plant Functional Group Diversity Promotes Soil Protist Diversity. *Protist* **154:** 239-249

Lousier J. (1976) Testate amoebae (Rhizopoda, Testacea) in some Canadian Rocky Mountain Soils. *Arch. Protistenk.* **118:** 191-201

MacQuaker, N.R. (1976) A Laboratory Manual for the Chemical Analysis of Waters, Waste Waters, Sediments and Biological Tissues, 2ed. Department of Environment, Water Resources Service, Province of British Columbia

Medioli F., Scott D. (1988) Lacustrine thecamoebians (mainly Arcellaceans) as potential tools for paleolimnological interpretations. *Paleogeog. Paleoclim. Paleoecol.* **62:** 361-386

Mitchell E., Buttler A. (1999) Ecology of testate amoebae (Protozoa: Rhizopoda) in *Sphagnum* peatlands in the Jura mountains, Switserland and France. *Ecoscience* **6:** 565-576

Nijssen D., Rousseau R., Van Hecke P. (1998) The lorentz curve: a graphical presentation of evenness. *Coenoses* **13:** 33-38

Ogden C. (1983) Observations on the systematics of the genus Difflugia in Britain (Rhizopoda, Protozoa). *Bull. Br. Mus. (Nat. Hist.)* **44:** 1-73

Ogden C. G., Hedley R. H. (1980) An Atlas of Freshwater Testate Amoebae. British Museum (Natural History) and Oxford University Press (London and Oxford)

Schönborn W. (1962) Die Ökologie der Testaceen im oligotrophen See, dargesellt am Beispiel des Grossen Stechlinsees. *Limnologica* **1:** 111-182

Shannon C., Weaver W. (1949) The Mathematical Theory of Communication. University of Illinois Press, Urbana IL

Smith H. (1992) Distribution and ecology of the testate rhizopod fauna of the continental Antarctic zone. *Polar Biol.* **12:** 629-634

Stevenson A., Juggings S., Birks H., Anderson D., Anderson N., Battarbee R., Berge F., Davis R., Flower R., Haworth E., Jones V., Kingston J., Kreiser A., Line J., Munro M., Renberg I (1991) The Surface Waters Acidification Project Paleolimnology Programme: modrn diatom/lake water chemistry data-set. Ensis Publ., London

Stout J. (1970) The bacteria and protozoa of some soil samples from Scoresby land, East Greenland. *Medd. Groen.* **184:** 1-22

Svendsson H. (1978) Artisk Geomorfologi. In: Godhavns Geomorfologi (Eds. B. Andersen *et al.*). Geografforlaget, Brenderup, 215- 254

Todorov M. (1998) Observation on the soil and moss testate amoebae (Protozoa: Rhizopoda) from Pirin Mountain (Bulgaria). *Acta Zool. Bulg.* **50:** 19-29

Trappeniers K., Van Kerckvoorde A., Chardez D., Nijs I., Beyens L. (1999) Ecology of testate amoebae communities from aquatic habitats in the Zackenberg area, (northeast Greenland). *Polar Biol.* **22:** 271-287

Trappeniers K., Van Kerckvoorde A., Chardez D., Nijs I., Beyens L. (2002) Testate amoebae assemblages from soils in the Zackenberg area, northeast Greenland. *Arct. Antarct. Alp. Res.* **34:** 94-101

Van Kerckvoorde A., Trappeniers K., Chardez D., Nijs I., Beyens L. (2000) Testate amoebae communities from terrestrial moss habitats in the Zackenberg Area (North-East Greenland). *Acta Protozool.* **39:** 27-33

Vincke S., Van de Vijver B., Mattheeussen R., Beyens L. (0000) Freshwater testate amoebae communities from Île de la Possession, Crozet Archipelago, Subantarctica. *Arct. Antarct. Alp. Res.* (in press)

Warner B. (1988) Methods in quaternary ecology. Testate amoebae (Protozoa). *Geosc. Can.* **15:** 251-260

Woodland W., Charman D., Sims P. (1998) Quantitative estimates of water tables and soil moisture in Holocene peatlands from testate amoebae. *The Holocene* **8:** 261-273

Received on 15th June, 2004; revised version on 7th February, 2005; accepted on 14th March, 2005

Appendix 1. Physico-chemical site and sample characteristics (S.C.: Specific Conductance)

Site	Sample	pH	T (°C)	S.C. (µS/cm)	O_2 (%)	Cl (mg/l)	NO_2 (mg/l)	NO_3 (mg/l)	PO_4 (mg/l)	NH_4 (mg/l)	$CaCO_3$ (mg/l)	Habitat	Substratum	Thermal class
DS001	DW001	7.14	2.8	97	95.1	39	0.003	0.09	0.37	0.01	40	running	sediment	1
DS0012	DW002	6.78	3.4	97	69.5	39	0.003	0.09	0.37	0.01	40	standing	sediment	1
DS002	DW003	7.16	11.6	90	68.6	45	0	0	0.2	0.03	35	standing	sediment	2
DS0021	DW004	8.08	14.4	68	105.6	45	0	0	0.2	0.03	35	running	sediment	2
DS003	DW005	7.18	11.2	82	63.5	43	0	0.013	0.07	0.05	30	standing	sediment	2
DS004	DW006	7.24	9.4	77	83.8	72	0	0.017	0.06	0.03	20	running	macrophytes	2
DS004	DW007	7.24	9.4	77	83.8	72	0	0.017	0.06	0.03	20	running	macrophytes	2
DS005	DW008	7.98	13.8	62	98.1	56	0.001	0.05	0.04	0	15	standing	sediment	3
DS0052	DW010	7.97	14.3	63	102	56	0.001	0.05	0.04	0	15	standing	macrophytes	3
DS005	DW011	7.98	13.8	62	98.1	56	0.001	0.05	0.04	0	15	standing	sediment	3
DS006	DW012	6.71	6.3	71	42.8	80	0.004	0.02	0	0	20	standing	sediment	3
DS003	DW014	7.18	14.6	82	64.9	43	0	0.013	0.07	0.05	30	running	macrophytes	2
DS007	DW015	7.54	9	197	79.9	78	0	0.14	0.1	0.25	35	standing	sediment	3
DS008	DW016	7.57	8.9	90	92.4	64	0	0.05	0.33	0.04	20	running	macrophytes	2
DS008	DW017	7.57	8.9	90	92.4	64	0	0.05	0.33	0.04	20	running	sediment	2
DS008	DW018	7.57	8.9	90	93.7	64	0	0.05	0.33	0.04	20	running	sediment	2
DS0082	DW019	7.36	3.3	136	98.9	64	0	0.05	0.33	0.04	20	standing	sediment	2
DS009	DW021	6.79	8.4	85	68	62	0.001	0.17	0.29	0.05	20	standing	sediment	2
DS010	DW022	7.22	5.5	76	84.5	52	0	0.01	0.25	0.05	15	standing	sediment	1
DS010	DW023	7.22	5.5	76	84.5	52	0	0.01	0.25	0.05	15	standing	macrophytes	1
DS0102	DW024	7.37	8.2	73	85.3	54	0	0.11	0.26	0.05	15	running	sediment	1
DS0102	DW025	7.37	8.2	73	85.3	54	0	0.11	0.26	0.05	15	running	macrophytes	1
DS011	DW026	8.61	5	72	94.2	40	0	0.04	0.11	0.08	5	running	sediment	1
DS013	DW030	7.19	1.4	60	96.5	22	0.01	0.06	0.2	0.2	30	standing	macrophytes	3
DS0131	DW031	6.95	7.8	57	65.1	22	0.01	0.06	0.2	0.2	30	standing	sediment	3
DS0141	DW032	7.29	13.2	112	76.2	66	0.01	0.02	0.25	0	10	running	sediment	3
DS0142	DW034	7.44	13.8	100	69.1	66	0.01	0.02	0.25	0	10	running	macrophytes	3
DS0142	DW035	7.44	13.8	100	69.1	66	0.01	0.02	0.25	0	10	running	macrophytes	3
DS0143	DW036	7.19	11.8	101	67.8	66	0.01	0.02	0.25	0	10	running	macrophytes	3
DS0143	DW037	7.19	11.8	101	67.8	66	0.01	0.02	0.25	0	10	running	sediment	3
DS0141	DW038	7.29	13.2	112	76.2	66	0.01	0.02	0.25	0	10	running	macrophytes	3
DS0151	DW040	6.53	16.2	41	88.8	45	0.001	0.08	0.03	0.03	0	running	sediment	3
DS0152	DW041	6.7	12.4	40	95.2	45	0.001	0.08	0.03	0.03	0	running	macrophytes	3
DS0153	DW042	6.28	13.7	41	82.7	45	0.001	0.08	0.03	0.03	0	running	macrophytes	3
DS0153	DW043	6.28	13.7	41	96.5	45	0.001	0.08	0.03	0.03	0	running	sediment	3
DS016	DW045	6.67	13.6	44	87	45	0.001	0.06	0.03	0.1	0	running	macrophytes	3
DS016	DW047	6.67	13.6	44	87	45	0.001	0.06	0.03	0.1	0	running	macrophytes	3
DS016	DW048	6.67	13.6	44	87	45	0.001	0.06	0.03	0.1	0	running	macrophytes	3
DS017	DW049	5.98	15.1	41	85.2	80	0	0.02	0.03	0.09	5	standing	macrophytes	3
DS017	DW050	5.98	15.1	41	85.2	80	0	0.02	0.03	0.09	5	standing	macrophytes	3
DS017	DW052	5.98	15.1	41	85.2	80	0	0.02	0.03	0.09	5	standing	macrophytes	3
DS018	DW053	7	4.5	77	84.1	80	0	0.02	0.03	0.09	5	running	macrophytes	1
DS018	DW055	7	4.5	77	84.1	80	0	0.02	0.03	0.09	5	running	macrophytes	1
DS018	DW056	7	4.5	77	84.1	80	0	0.02	0.03	0.09	5	running	sediment	1
DS0181	DW057	7.12	3.2	80	81.8	80	0	0.02	0.03	0.09	5	running	macrophytes	1
DS020	DW058	7.19	8.8	477	68.6	105	0	0	0.04	0.05	95	running	macrophytes	1
DS020	DW059	7.19	8.8	477	68.6	105	0	0	0.04	0.05	95	running	sediment	1
DS021	DW060	9.78	3.5	63	86.4	54	0.001	0.04	0.07	0.06	5	running	macrophytes	1
DS021	DW061	9.78	3.5	63	86.4	54	0.001	0.04	0.07	0.06	5	running	sediment	1
DS021	DW062	9.78	3.5	63	86.4	54	0.001	0.04	0.07	0.06	5	running	macrophytes	1
DS026	DW066	7.78	11.3	63	93.3	46	0.001	0.04	0.06	0.05	20	running	macrophytes	2
DS026	DW067	7.78	11.3	63	93.3	46	0.001	0.04	0.06	0.05	20	running	macrophytes	2
DS026	DW068	7.78	11.3	63	93.3	46	0.001	0.04	0.06	0.05	20	running	sediment	2
DS026	DW069	7.78	11.3	63	93.3	46	0.001	0.04	0.06	0.05	20	running	macrophytes	2
DS027	DW070	7.36	10.9	64	93.5	46	0.001	0.04	0.06	0.05	20	running	macrophytes	2
DS029	DW072	8.18	2.6	70	94.9	56	0	0.01	0.08	0.03	0	running	macrophytes	1
DS029	DW073	8.18	2.6	70	94.9	56	0	0.01	0.08	0.03	0	running	macrophytes	1
DS030	DW074	7.96	19.3	33	94.6	65	0	0	0.03	0.05	5	standing	macrophytes	3
DS030	DW075	7.96	19.3	33	94.6	65	0	0	0.03	0.05	5	standing	sediment	3
DS031	DW076	7.89	3.7	64	95.4	55	0.001	0.01	0.1	0.14	15	running	macrophytes	2

Appendix 2. Taxonomical list of all observed taxa with their corresponding letter codes. New taxa for the Arctic (according to Alexandrova 1980) are marked (*)

ARCDIS	*Arcella discoides* Ehrenberg	**DILOVI**	*Difflugiella oviformis* (Penard) Bonnet et Thomas
ASSMUS	*Assulina muscorum* Greeff	**DILOVF**	* *Difflugiella oviformis* var. *fusca* (Penard) Bonnet et Thomas
ASSSEM	*Assulina seminulum* Penard	**DILSAC**	* *Difflugiella sacculus* Penard
CAMSP	*Campascus* sp1	**EUGACA**	*Euglypha acanthophora* Perty
CENAER	*Centropyxis aerophila* Deflandre	**EUGCIL**	*Euglypha ciliata* Ehrenberg
CENASP	*Centropyxis aerophila* var. *sphagnicola* Deflandre	**EUGCOM**	*Euglypha compressa* Carter
CENASY	*Centropyxis aerophila* var. *sylvatica* Deflandre	**EUGCRI**	*Euglypha cristata* Leidy
CENCAS	*Centropyxis cassis* Wallich	**EUGFIL**	*Euglypha filifera* Penard
CENCON	*Centropyxis constricta* Deflandre	**EUGLAE**	*Euglypha laevis* (Ehrenberg) Perty
CENORB	*Centropyxis orbicularis* Deflandre	**EUGROT**	*Euglypha rotunda* Wailes
CENPLAT	*Centropyxis platystoma* Penard	**EUGSTR**	*Euglypha strigosa* (Ehrenberg) Leidy
CENPLARM	*Centropyxis platystoma* var. *armata* Deflandre	**EUGSTG**	*Euglypha strigosa* f. *glabra* Wailes
CENSP1	*Centropyxis* sp1	**EUGTUB**	*Euglypha tuberculata* Dujardin
CENSP2	*Centropyxis* sp2	**EUGTUM**	*Euglypha tuberculata* var. *minor* Taranek
CORDUB	*Corythion dubium* Taranek	**HELSP1**	*Heleopera* sp1
CRYCOM	*Cryptodifflugia compressa* Penard	**HELSYL**	*Heleopera sylvatica* Penard
CYCEUR	*Cyclopyxis eurystoma* Deflandre	**HYAMIN**	*Hyalosphenia minuta* Cash
CYCGIG	*Cyclopyxis gigantea* Bartos	**HYAPAP**	*Hyalosphenia papilio* Leidy
CYCSP1	*Cyclopyxis* sp1	**HYASUB**	*Hyalosphenia subflava* Cash
CYPAMP	*Cyphoderia ampulla* (Ehrenberg) Leidy	**LESEPI**	*Lesquereusia epistomium* Penard
CYPPER	*Cyphoderia perlucidus* Beyens, Chardez et De Bock	**LESSPI**	*Lesquereusia spiralis* Bütschli
DIFAMPH	* *Difflugia amphoralis* (Leidy) Hopkinson	**NEBPEN**	*Nebela penardiana* Deflandre
DIFAMPU	* *Difflugia ampullula* Playfair	**NEBCOL**	*Nebela collaris* (Ehrenberg) Leidy
DIFBAC	*Difflugia bacillifera* Penard	**NEBDEN**	*Nebela dentistoma* Penard
DIFELE	*Difflugia elegans* Penard	**NEBLAG**	*Nebela lageniformis* Penard
DIFGL1	*Difflugia globularis* Wallich	**NEBMIL**	*Nebela militaris* Penard
DIFGL2	*Difflugia globulosa* Dujardin	**NEBTUB**	*Nebela tubulata* Brown
DIFGL3	*Difflugia globulus* (Ehrenberg) Hopkinson	**NEBWAL**	*Nebela wailesi* Deflandre
DIFGLA	*Difflugia glans* Penard	**PARIRR**	*Paraquadrula irregularis* (Archer) Deflandre
DIFMIC	*Difflugia mica* Frenzel	**PARMUL**	*Parmulina* sp1
DIFOBL	*Difflugia oblonga* Ehrenberg	**PHRNID**	*Phryganella nidulus* Penard
DIFPEN	*Difflugia penardi* Hopkinson	**PHRPAR**	*Phryganella paradoxa* Penard
DIFPRI	*Difflugia pristis* Penard	**PLACAL**	*Plagiopyxis callida* Penard
DIFPUL	*Difflugia pulex* Penard	**PSEFUL**	*Pseudodifflugia fulva* (Archer) Penard
DIFPYR	*Difflugia pyriformis* Perty	**PSEGRA**	*Pseudodifflugia gracilis* Schlumberger
DIFTEN	* *Difflugia tenuis* (Penard) Chardez	**PSESP1**	*Pseudodifflugia* sp1
DIFSP1	*Difflugia* sp1	**TRACPU**	*Trachelocorythion pulchellum* (Penard) Bonnet
DIFSP2	*Difflugia* sp2	**TRACSP1**	*Trachelocorythion* sp1
DIFSP3	*Difflugia* sp3	**TRAEAC**	*Tracheleuglypha acolla* Bonnet et Thomas
DIFSP4	*Difflugia* sp4	**TRAEDE**	*Tracheleuglypha dentata* Deflandre
DILCRE	*Difflugiella crenulata* (Playfair) Grospietsch	**TRICOM**	*Trinema complanatum* Penard
DILCRG	* *Difflugiella crenulata* var. *globosa (*Playfair) Grospietsch	**TRIENC**	*Trinema enchelys* (Ehrenberg) Leidy
DILMIN	* *Difflugiella minuta* Playfair	**TRILIN**	*Trinema lineare* Penard

Acta Protozool. (2005) 44: 265 - 270

ACTA
PROTOZOOLOGICA

Paraluffisphaera tuba gen. n., sp. n. - a Newly-discovered Eukaryote

Genoveva F. ESTEBAN[1], Ken J. CLARKE[2] and Bland J. FINLAY[1]

[1]Centre for Ecology and Hydrology, Winfrith Technology Centre, Winfrith Newburgh, Dorchester; [2]Freshwater Biological Association, The Ferry House, Far Sawrey, Ambleside, Cumbria, UK

Summary. *Paraluffisphaera tuba* gen. n., sp. n. is a very small (~ 3 µm), enigmatic organism, that was isolated from montane grassland in Scotland, and from inland saline water in Spain. The cell surface of this new protist is covered with scales of two types: base scales and tubular scales. No flagella or pseudopodia were observed. The gross morphology resembles scale-bearing protists of the genus *Luffisphaera*, but the new organism is distinctly different. Like *Luffisphaera*, *Paraluffisphaera* should be considered an *incertae sedis* protist.

Key words: *Luffisphaera*, nanoplankton, picoeukaryotes, picoplankton, scaly protists, soil protozoa.

INTRODUCTION

We present a new genus of eukaryotes. The micro-organisms within the genus are unicellular, probably free-living protists that live in aquatic environments, including re-wetted soils. They are very small, and almost indistinguishable from other particles when using light microscopy alone. Isolation of individual specimens for establishment of cultures has so far proved impossible. As in other cases where micro-organisms were found to be too small to resolve and study optically, we relied on the electron microscope examination of direct preparations of aquatic samples to initially detect and then examine the new genus (e.g. Vørs 1993, Tong 1997). The small size of the new organism and the difficulties associated with detecting and handling it presented a severe challenge in probing its natural history.

Ironically, the most interesting thing we can report is how little we have been able to discover about this organism. Thus far, it has been detected only in two distinctly different habitat types separated by about 1500 km. As the abundance of protist species populations is inversely proportional to cell size (Finlay 2002), we might predict that this minute enigmatic organism is probably represented worldwide by vast numbers of individuals (although this is not usually obvious because they are so small as to be almost undetectable) and filling an ecological niche about which we still know very little.

MATERIALS AND METHODS

Field sites. Samples were taken from two contrasting habitats: montane grassland in Scotland, and inland saline groundwater in Spain. Grassland samples were obtained from the experimental site at

Address for correspondence: Genoveva F. Esteban, Centre for Ecology and Hydrology, Winfrith Technology Centre, Winfrith Newburgh, Dorchester DT2 8ZD, UK; E-mail: gent@ceh.ac.uk

the Macaulay Land Use Research Institute's Sourhope Research Station, situated 15 miles south of Kelso. The land rises to 605 m and the annual rainfall is 1015 mm (10 year mean). The experimental site (Grid reference NT854 196) is representative of mid-altitude (304-313 m) temperate upland grasslands on base-poor, damp, mineral soils (see Finlay *et al.* 2000). The source of the new protist was a sample taken in November 1998. It included turf and soil down to grass-root depth, plus a centimetre of soil below this. In the lab, the soil was dampened with 0.2 µm-pore size membrane-filtered Volvic mineral water, covered and placed on a shaded bench at room temperature. At this stage of the investigation, we were recording all the protist species we could find in the sample.

The sampling site in NE Spain is located at Los Monegros (Zaragoza), a semi-arid plateau at 340 m above sea level placed on a Tertiary basin rich in marl and gypsum with limestone in the upper part (Alcorlo *et al.* 2001). The local climate is semi-arid Mediterranean with low annual rainfall (average 300 mm) and high evaporation (Pueyo and Inglés 1987). Winds are strong and persistent, and mainly from the north-west. We sampled the saline spring water of a permanent concrete-built well (41° 25'229''N and 0° 1'669'' W) next to Laguna de la Playa, where the salinity was 13ppt. Samples were collected on 22nd and 23rd December 2003 using screw-capped sterile centrifuge tubes, which were kept cold (*ca* 4 °C) until they reached the laboratory. *Artemia salina* and a variety of protists typical of saline environments were observed in the well samples (Esteban and Finlay 2004).

Electron microscopy. Transmission Electron Microscopy (TEM) was carried out on whole cells. 4 µl of a "weak dilution" from the superficial sediment of Sourhope's re-wetted soil material was placed on specimen grids pre-coated with a Formvar support film. The "weak solution" was prepared as a sub-sample from the re-wetted soil that was diluted subjectively to the point where it would give sufficient separation of dried material on the grid to enable clear examination of individual cells and the scales. Each sub-sample for TEM examination was fixed for 30 seconds with osmium tetroxide vapour, dried, and shadowed with chromium metal.

For TEM investigations of the Spanish saline well samples, subsamples were fixed with osmium tetroxide or glutaraldehyde fixatives; replicates of these fixed samples were washed twice in distilled water to remove salt and fixative, using centrifugation and Eppendorf tubes. Each sample was then resuspended before a 3-4 µl-sized drop was placed on Formvar-coated specimen grids. The dried samples were shadowed with chromium. Cell dimensions were measured from EM negatives.

Deposited material. Following established practise in descriptions of new species of scale-bearing protists (see, e.g. Vørs 1993, Tong 1997, Backe-Hansen and Throndsen 2002, Schroeckh *et al.* 2003), we use uninterpreted illustrations as type material.

RESULTS

Paraluffisphaera gen. n.

Diagnosis: Probably free-living protists, oval in shape and with the cell surface entirely covered with two types of scales: (1) base scales that are elliptical, flat, and with a "closed" slit in the centre, and (2) structures resembling the base scale whose slit is open to house a tubular structure. With the present stage of knowledge, it is not clear whether the tubular structure is attached at its proximal end to the open base scale, or if it emerges from the slit opening. No flagella or similar swimming structures were observed. This diagnosis may change if further species of the genus are found.

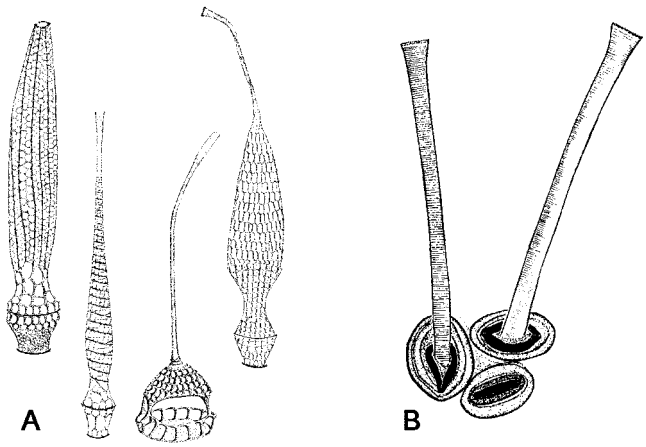

Figs 1A, B. Line drawings of the scales that cover the cell surface of the protists *Luffisphaera* and *Paraluffisphaera*, respectively, based on electron microscope micrographs. **A** - examples of the elongate scales of *Luffisphaera*, illustrating their reticulated architecture (after Belcher and Swale 1975); **B** - *Paraluffisphaera tuba* gen. n., sp. n.: schematic representation of the base scales and the tubular scales.

Type species: *Paraluffisphaera tuba* sp. n.

Etymology: *para* from Greek, "alongside, near", meaning "resembling *Luffisphaera*", and *Sphaera* from Greek *Sphairã*, a sphere.

The original description of the genus *Luffisphaera* Belcher *et* Swale, 1975 does not provide the etymology of the generic name. However, the type species *Luffisphaera cucumiformis*, and the shape of some of its scales, suggest "*cucumiformis*" must refer to the cucumber-shaped cylindrical scales that project from the cell surface (Fig. 1A). The cucumber-shaped fruit of the tropical plant *Luffa* are similar in form to *L. cucumiformis* scales - hence we credit the generic name *Luffisphaera* to a sphere bearing *Luffa*-fruit-shaped scales.

Differential diagnosis: There is no other described eukaryote such as *Paraluffisphaera* - and this alone justifies its erection as a new genus. The presence of two types of scales wrapping the cell surface resembles organisms of the genus *Luffisphaera* - hence the generic name *Paraluffisphaera*. However, the organisational level of *Paraluffisphaera* is far simpler

than that of *Luffisphaera*. The base and the tubular scales of *Paraluffisphaera* lack the lattice network configuration of *Luffisphaera*. In the latter, the lattice structure is present in the basal and tubular scales. The structure of this lattice network is one of the characters used for the discrimination of species. As this character does not appear in *Paraluffisphaera*, the segregation of species is based on the shape of the base and/or tubular scales, e.g. base scale flat and elliptical, or cup-shaped, etc. Furthermore, in *Paraluffisphaera* the tubular scales do not sit on prominent basal scales, as in *Luffisphaera*. Finally, both basal and tubular scales of *Paraluffisphaera* lack the conspicuous rigidness of *Luffisphaera* scales (for assessment see Figs 1A, B; 3A, B).

***Paraluffisphaera tuba* sp. n.**

Diagnosis: Scale-bearing protists with the characteristics of the genus. Cells are oval, with a size range of 3 to 3.8 µm in length and 2.4 µm to 3 µm in width. The base scales are 0.4×0.3 µm; the elongate scales have a base scale and a trumpet-shaped tubular structure that is 1.5 µm long and projects upright from a basal elliptical scale. The cell surface is associated with one or several bacteria but the nature of this association is unknown.

Etymology: *tuba* (feminine) from Latin "the straight war-trumpet of the Romans", in reference to the shape of the tubular scales.

Type location: Montane grassland soil from Sourhope Research Station, Macaulay Land Use Research Institute, Natural Environment Research Council, near Kelso, Southern Scotland (UK).

Type specimen: The uninterpreted illustration of the specimen in Fig. 2A.

Holotype: The uninterpreted illustration of the specimen in Fig. 2D.

Description: This description of *Paraluffisphaera tuba* gen. n., sp n. is based on observations of shadow-cast cells using transmission electron microscopy. Cells are ovoid (Figs 2A, D) and, in the specimens we recorded, range in size from 3×2.4 µm to 3.8×3 µm. We could not observe flagella, pseudopodia or any other structures that might be noticeably involved in locomotion or feeding. However, the specimens appeared associated with bacteria of various sizes and with detrital particles (see below and Figs 2A, D).

The cell surface of *P. tuba* is entirely covered with scales of two types (Figs 2B, C): (1) base scales, these are flat and elliptical, 0.4×0.3 µm in size, they interweave in all directions, and have a slit across the scale surface, with a thickened rim that gives the appearance of two lips in the centre of the scale (Figs 1B; 2B, C); (2) elongate scales, which seem to arise from the "open" slit of some of the base scales described above. The elongate scales are composed of two parts: (a) a trumpet-shaped structure consisting of a tube (maximum 1.5 µm long and 0.06 µm wide in our specimens) of cylindrical bore ending in a flared bell, with thickened rim. The tubular structures do not show any pattern or network on their surface apart from an inconspicuous transversal striation (Fig. 2C). The tubes seem to emerge through (b) the labiated 'open' slit of base scales, and in most specimens they look as though they are in contact with or embedded in detritus particles and bacteria (Figs 2C-E), but this might be a preparation-generated artefact. Most scales are of the base-type described above (Fig. 2A). The cell surface of *P. tuba* also appears associated with one or several bacteria whose size relative to the protist becomes immediately obvious (see, e.g. Fig. 2A). The nature of this association is unknown.

DISCUSSION

The EM micrographs of *Paraluffisphaera tuba* gen. n., sp. n. show no flagella, pseudopodia or any other structure that might enable the organism to glide or swim. We may speculate that if *P. tuba* is a planktonic organism, the tubular scales might endow some buoyancy.

The EM preparations of *P. tuba* show that the tubular scales seem to be in contact with bacteria and detrital particles (Figs 2A-E). This could be the result of the flattening of cells that occurs when they are dried onto EM grids. Alternatively, the tubular scales may actually be ingesting food. Their function may bear some resemblance to the tentacles of suctorian ciliated protozoa (which 'suck out' the internal content of the prey). However, suctorian tentacles are contractile, which is probably not the case in the tubular scales of *Paraluffisphaera*. We cannot begin to answer the question until thin sections are cut, and electron micrographs are obtained.

Species of *Luffisphaera*, the protistan genus that morphologically most resembles *Paraluffisphaera*, also appear to have attached bacteria to the cell surface (Belcher and Swale 1975, Vørs 1993, Backe-Hansen and Throndsen 2002), although none of these authors comment on them in the context of a potential food source. We have also considered the possibility of

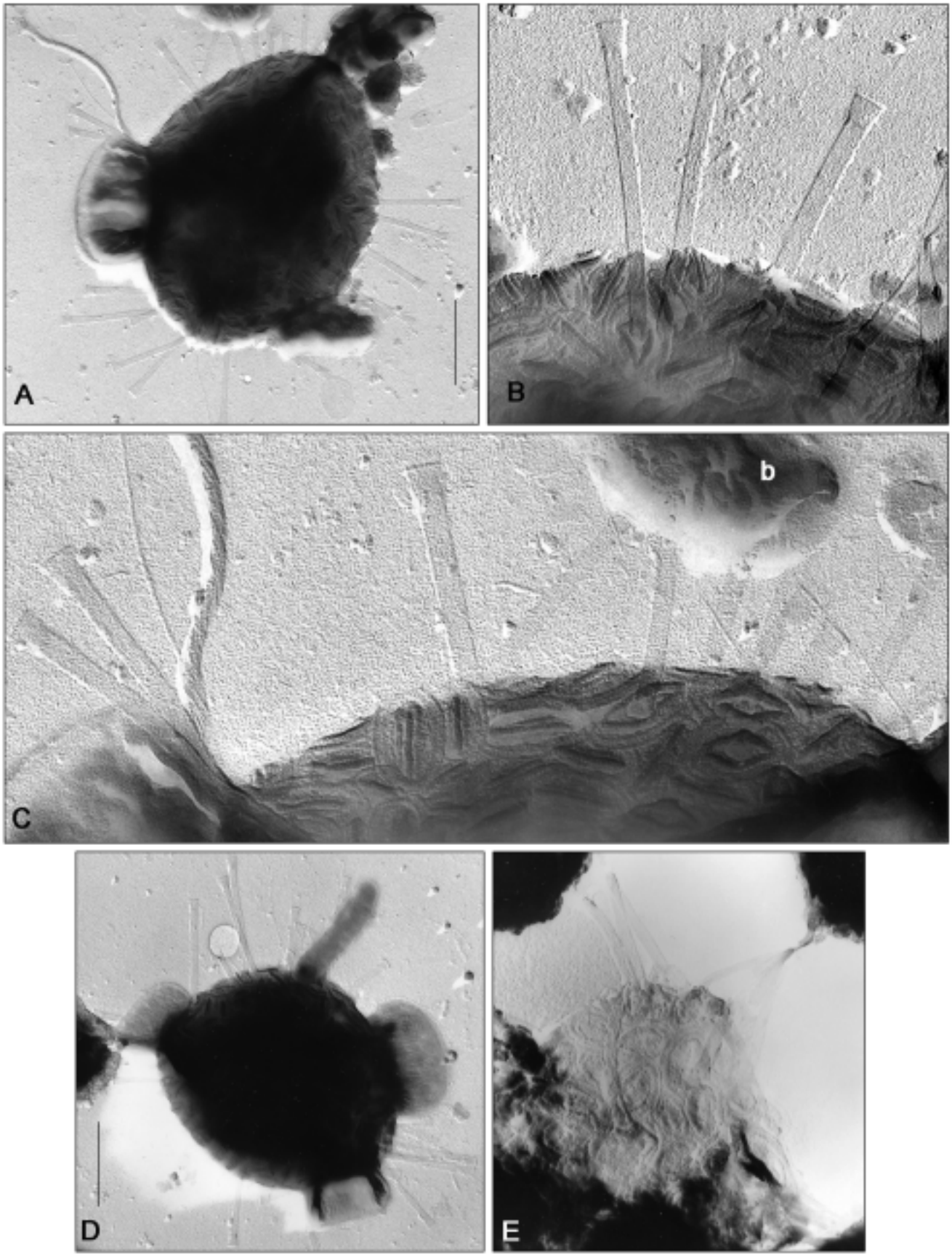
A
B
b
C
D
E

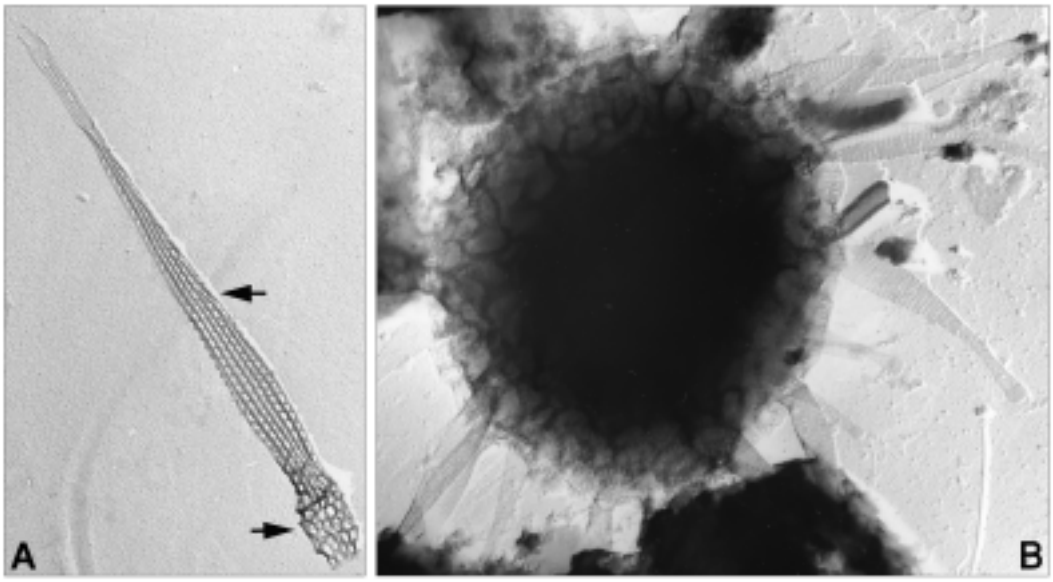

Figs 3A, B. Specimen of *Luffisphaera lanceolata* from a productive freshwater pond ('Priest Pot') in the UK. Original TEM direct preparations. **A** - elongate scale showing the reticulated scale base (arrow, bottom of the image) and the narrowly lanceolate, reticulated scale (arrow, centre of the image). The split end of this scale is atypical for this species. **B** - specimen (less than 3 µm in diameter) showing the cell scales.

P. tuba being a dormant resting form or spore of some kind rather than an active protist. However, although spores and other dormant forms can be quite ornamented, they also have conspicuous protective layers that can be resolved by electron microscopy; and these are scale-free and reticulated. In contrast, all scale-bearing protists, whether photo- or heterotrophic, have their cell surfaces covered by scales and other kinds of extraordinary structures - as also in *Paraluffisphaera*. We can safely say that *P. tuba* is not a spore, resting cyst or dormant form.

Similar species

Apart from size and shape, *Paraluffisphaera* shares with *Luffisphaera* the characteristics of being without flagella and having a long-form and an elliptical-form of scale. But the ultrastructural morphology of the scales is entirely different (see "Differential diagnosis" above), e.g. the tubular scales of *Paraluffisphaera* lack the elaborated networked pattern typical of *Luffisphaera* scales (Figs 1A, B; 3A, B).

Luffisphaera was first reported from a ditch in Cambridge UK, (Belcher and Swale 1975), and all species described since have been found in marine environments (Thomsen 1982; Vørs 1992a, b, 1993; Tong 1997; Backe-Hansen and Throndsen 2002). However, a recent intensive investigation of "scaly" protists in a productive freshwater pond ("Priest Pot") in England recorded 220 scale-bearing protist species. These included a small number of ciliates and a larger number of amoebae and flagellates, sixteen of which were *Luffisphaera* (e.g. Fig. 3) - the five originally described from the ditch in Cambridge, and ten that have not been reported before and that are probably new to science (Clarke - unpublished results), but none of the marine ones. *Paraluffisphaera tuba* was not found. Similar intensive investigations took place at the grassland site of Sourhope, but *P. tuba* was reported only once throughout the three-year project. In contrast, the finding of *P. tuba* in the Spanish brackish water occurred on a single isolated sampling occasion. It may be that *P. tuba* is more common in saline or marine environments.

Figs 2A-E. Transmission electron microscopy of *Paraluffisphaera tuba.* Direct preparations. **A** - specimen from re-wetted soil (Scotland, UK) with the scales easily visible. Note the flagellated bacterium (left of the image) in relation to the small size of *P. tuba*. **B** - close-up of the scale-like structures of *P. tuba*: base scales and tubular scales; **C** - attachment (but see text) of tubular scales to bacteria (b); **D** - specimen from re-wetted grassland soil in Scotland (UK) is also attached to bacteria of different shapes, and to detrital particles. **E** - specimen from a saline-water spring in NE Spain, partially hidden by detritus. Scale bars 1 µm;

Another scale-bearing protist observed in the well was *Paraphysomonas imperforata*, a common freshwater and marine flagellate, and in the adjoining Laguna de la Playa, the marine choanoflagellates *Platypleura* sp. and *Cosmoeca* sp. were also found.

Paraluffisphaera should be considered an *incertae sedis* Taxon (International Code of Zoological Nomenclature), i.e. a protist of uncertain taxonomic position, possibly heterotrophic, and possibly related to *Luffisphaera*, an *incertae sedis* genus of protists itself.

Acknowledgements. Dr A. Baltanás (Universidad Autónoma de Madrid, Spain) for sampling logistics in Los Monegros, and the Natural Environment Research Council (UK, grants NER/T/2000/01351 and GST 2130) for financial support.

REFERENCES

Alcorlo P., Baltanás A., Montes C. (2001) Food-web structure in two shallow salt lakes in Los Monegros (NE Spain): energetic vs dynamic constraints. *Hydrobiologia* **466:** 307-316

Backe-Hansen P., Throndsen J. (2002) Pico- and nanoplankton from the inner Oslofjord, eastern Norway, including description of two new species of *Luffisphaera* (incerta sedis). *Sarsia* **87:** 55-64

Belcher J. H., Swale E. M. F. (1975) *Luffisphaera* gen. nov., an enigmatic scaly micro-organism. *Proc. R. Soc. Lond. B.* **188:** 495-499

Esteban G. F., Finlay B. J. (2004) Marine ciliates (Protozoa) in central Spain. *Ophelia* **58:** 1-10

Finlay B. J. (2002) Global dispersal of free-living microbial eukaryote species. *Science* **296:** 1061-1063

Finlay B. J., Black H. I. J., Brown S., Clarke K., Esteban G. F., Hindle R. M., Olmo J. L., Rollett A., Vickerman K. (2000) Estimating the growth potential of the soil protozoan community. *Protist* **151:** 69-80

Pueyo J. J., Inglés M. (1987) Magnesite formation in recent playa lakes, Los Monegros, Spain. In: Diagenesis of Sedimentary Sequences (Ed. J. D. Marshall). Geological Society Special Publication, 119-122

Schroeckh S., Lee W. J., Patterson D. J. (2003) Free-living heterotrophic euglenids from freshwater sites in mainland Australia. *Hydrobiologia* **493:** 131-166

Thomsen H. A. (1982) Planktonic choanoflagellates from Disko Bugt, West Greenland, with a survey of the marine nanoplankton of the area. *Meddr. Grønland, Biosc.* **8:** 1-35

Tong S. M. (1997) Heterotrophic flagellates and other protists from Southampton Water, U.K. *Ophelia* **47:** 71-131

Vørs N. (1992a) Heterotrofe protister (ekskl. dinoflagellater, loricabærende choanoflagellater og ciliater). In: Plankton i de indre danske farvande, (Ed. H. A. Thomsen). Havforskning fra Miljøstyrelsen, Copenhaguen, **11:** 195-250

Vørs N. (1992b) Heterotrophic amoebae, flagellates and heliozoan from the Tvärminne area, Gulf of Finland, in 1988-1990. *Ophelia* **36:** 1-109

Vørs N. (1993) Marine heterotrophic amoebae, flagellates and heliozoa from Belize (Central America) and Tenerife (Canary Islands), with descriptions of new species, *Luffisphaera bulbochaete*, n. sp., *L. longihastis*, n. sp., *L. turriformis* n. sp. and *Paulinella intermedia* n. sp. *J. Euk. Microbiol.* **40:** 272-287

Received on 11th February, 2005; revised version on 11th April, 2005; accepted on 14th April, 2005

Acta Protozool. (2005) 44: 271 - 278

ACTA
PROTOZOOLOGICA

Psammonobiotus dziwnowi and *Corythionella georgiana*, Two New Freshwater Sand-dwelling Testate Amoebae (Rhizopoda: Filosea)

Kenneth H. NICHOLLS

Sunderland, Ontario, Canada

Summary. Two new species of the predominantly marine sand-dwelling testate rhizopod genera *Psammonobiotus* and *Corythionella* were discovered in sand beaches of the Canadian Laurentian Great Lakes. The most important differences between *P. dziwnowi* sp. n. its closest relative *P. communis* are (i) much smaller size of *P. dziwnowi*, (ii) greater length-to-width ratio in *P. dziwnowi*, (iii) greater angle of the plane of the oral aperture relative to the long axis of the test of *P. dziwnowi*. The only other known freshwater species of *Corythionella*, *C. golemanskyi* Nicholls, occurred together with *C. georgiana* sp. n. in samples from Wasaga Beach, Georgian Bay (Lake Huron) and enabled a direct comparison of test morphology of both populations occurring under the same environmental conditions. As well as a significantly smaller test size in *C. georgiana*, other differences with *C. golemanskyi* include smaller more elongate scales arranged in a more open non-overlapping pattern on the test surface of *C. georgiana*. Notwithstanding some uncertainties about the taxonomy of *C. acolla*, which is the only one of six marine species of *Corythionella* lacking a flared pseudostomal collar, the differences between it and *C. georgiana*, which has a minimally flared collar, include a generally shorter length, a much broader post-pseudostomal region and greater ratio of test width-to-pseudostome diameter in *C. georgiana*. These differences (ignoring, for the present, possible additional differences in the structure of the scale layer on the tests of *C. georgiana* and *C. acolla*), substantiate the designation of *C. georgiana* as an independent species.

Key words: *Corythionella georgiana* sp. n., Cyphoderiidae, freshwater testate amoebae, Psammonobiotidae, *Psammonobiotus dziwnowi* sp. n., Testaceafilosia.

INTRODUCTION

Although beach sand-dwelling testate rhizopod communities represented by many genera and species have long been recognized in the supra-littoral zones of the world's oceans (e.g. Chardez 1977, Golemansky 1998 and references therein), only recently has this community been investigated in freshwater lakes (Nicholls and MacIsaac 2004). Nicholls and MacIsaac (2004) encountered relatively abundant populations of a small unknown species of *Psammonobiotus* at several locations in the Great Lakes, which they referred to as "sp. # 2". Also, after publication of the of the Great Lakes survey, a previously undescribed species of *Corythionella* was discovered in beach sand samples from Wasaga Beach (Georgian Bay, Lake Huron), one of the original Great Lakes sampling locations included in Nicholls and MacIsaac (2004). This new species is similar in some respects to the only other known freshwater species, *C. golemanskyi* Nicholls (2003), but differs from it and its closest marine relative, *C. acolla* Gol. (Golemansky 1970a) in several ways relating to the shape and struc-

Address for correspondence: Kenneth H. Nicholls, S-15 Concession 1, RR # 1 Sunderland, Ontario, Canada L0C 1H0; E-mail: khnicholls@interhop.net

ture of its test. Test morphology is the primary criterion in distinguishing among several species of both *Psammonobiotus* and *Corythionella* (Meisterfeld 2002). The purpose of this paper is to describe *Psammonobiotus dziwnowi* and *Corythionella georgiana* as two new members of the Testaceafilosia inhabiting freshwater beach sands.

MATERIALS AND METHODS

All field and laboratory methods were as previously described in Nicholls and MacIsaac (2004). Test dimensions and terminology were as portrayed in Figs 1 and 15. Statistical data describing test morphology (mean, standard deviation, median, minimum, maximum, coefficient of variation) and Mann-Whitney *U*-tests of significant difference between populations were done in *CoStat* (CoHort Software 1995) with reference to Neave (1981) for levels of significance.

In a Wasaga Beach (Georgian Bay of Lake Huron) sample containing both *Corythionella golemanskyi* and a smaller unidentified *Corythionella* (described herein as a new species), an objective measurement routine was set up to characterize each morphologic entity as follows: (i) a subsample was prepared from a few drops of the original sample mixed together with several drops of glycerine on a 22 × 50 mm No. 1 cover glass positioned on the stage of an inverted microscope; (ii) the subsample was allowed to evaporate over night to concentrate the specimens in 100% glycerine. This viscous medium enabled a more stable orientation of the specimens for height measurements and observation of optical cross-sections of tests after manipulation into position with a single hair brush; (iii) the subsample was searched systematically in a grid pattern using a 10× objective and dark ground illumination; (iv) all specimens of the two morphotypes were measured as they were encountered during the search regardless of which size group they were in; (v) after plotting test lengths *vs* widths of 37 measured specimens, it was apparent that there existed two distinct size categories, and the measurements were then grouped into the two groups, A (larger) and B (smaller); (vi) measurements were made on three additional randomly selected group B specimens to achieve a total of 20 measured specimens in each size group for more detailed statistical analysis.

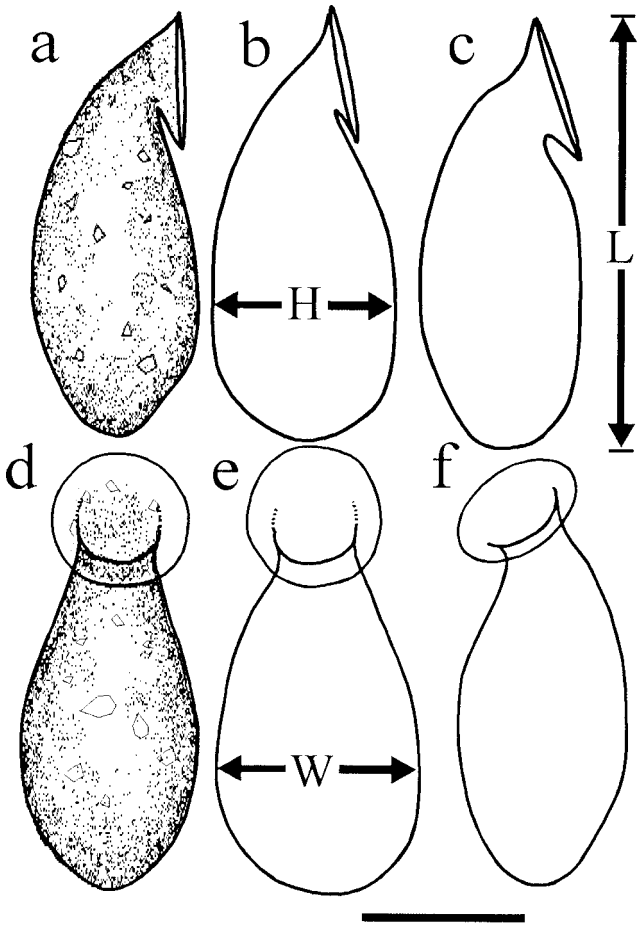

Fig. 1. Drawings of tests of *Psammonobiotus dziwnowi* sp. n. [from Nicholls and MacIsaac (2004; their "sp #2") with permission from *J. Great Lakes Res.*]. **a-c** - morphological variation of three tests in lateral views. **d-f** - morphological variation of three tests in ventral views. L, H, and W - test length, height, and width, respectively. Scale bar 10 μm.

RESULTS

Psammonobiotus dziwnowi sp. n.; Figs 1-13

Phylum: Rhizopoda, Class: Filosea, Subclass: Testaceafilosia, Family: Psammonobiotidae.

Diagnosis: Protoplast was similar to that known for *Psammonobiotus communis* and emerged from the pseudostome as a single (less frequently, two, branched) long, filose pseudopod. Test shape was elongated-elliptical in outline in ventral and dorsal views and asymmetrically oblong-ovate in lateral view with a rounded dorsal edge and slightly flattened ventral edge. Median test length, width and height were 23, 11 and 10 μm, respectively (N=63). The oral aperture (pseudostome) was at the end of a bent neck-like anterior extension of the test and was surrounded by a flared collar. In ventral and dorsal views, the test body was always wider than the pseudostome collar. The test was covered with small, mainly angular, polymorphic and flat particles more easily seen in dried specimens impregnated with Canada Balsam or Styrax®. In lateral view, the angle of the plane of the pseudostome collar ranged from near zero degrees to about 45°.

Etymology: The specific epithet (*dziwnowi*) is derived from the name of the Polish town of Dziwnów on

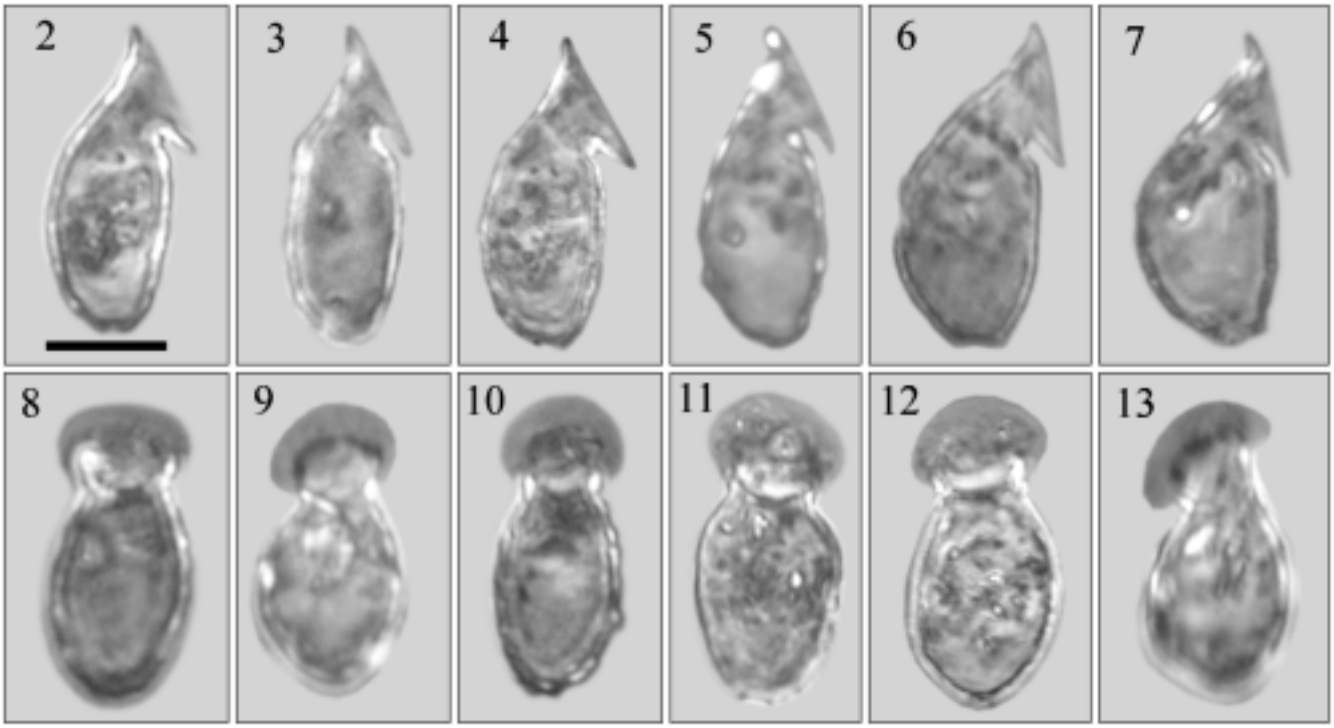

Figs 2-13. Digital images of tests of *Psammonobiotus dziwnowi* sp. n. [from Nicholls and MacIsaac (2004; their "sp. #2") with permission from *J. Great Lakes Res.*]. **2-7** - lateral views showing range in form; **8-12** - ventral views showing range in form; **13** - a specimen in oblique-ventral view. Scale bar 10 µm applies to all figures.

the southern Baltic Sea, in the vicinity of which the first specimens of this species were apparently collected by Dr. V. Golemansky (see below). An approximate phonetic English pronunciation of the specific epithet is "dvee-nov-ee", with the accent on the second syllable.

Type specimen: The type specimen, mounted in Canada Balsam on a glass slide, was deposited with the Canadian Museum of Nature (Ottawa, Ontario, Canada) under catalogue No. CMNI-2005-0001.

Material from type locality: Retained by the author in sample No. V-1706, collected 4 September, 2002.

Type locality: Beach sand in the wave zone (supralittoral) at Providence Bay, south shore of Manitoulin Island, Lake Huron (45° 40' 0" N; 82° 16' 11" W).

Test measurements (Table 1) on 63 specimens [Nicholls and MacIsaac's (2004) original 47 + 16 additional specimens] did not change the median length, width and height of tests reported by Nicholls and MacIsaac (2004) for *P. dziwnowi* (their "sp. #2"). Using the size data summarized in Nicholls and MacIsaac's (2004) Table 2, the differences between *P. dziwnowi* and *P. communis* in their Rondeau Bay, Lake Erie sample, where both species were relatively abundant, were highly significant for all test dimensions (Mann-Whitney *U*-tests; $P<0.001$). Measurements of tests from the other Great Lakes locations were not made systematically; however, at none of the seven other locations where both *P. communis* and *P. dziwnowi* were found together was there any overlap in test size or shape.

There was some variation in the test shape of this species (Figs 1-13). Most notable was the angle of the plane of the pseudostomal aperture (compare, for example Figs 4 and 6). The main body of the test also showed some differences in shape, ranging from nearly cylindrical (Fig. 3) to those with very rounded dorsal surfaces (Figs 6, 7) and intermediate forms (Figs 2, 4, 5). The most typical ventral profiles found were like those in Figs 1d, 8, 10 and 11. Unusually wide tests (Fig. 9) or those with somewhat pointed aboral ends (Fig. 12) were less frequently encountered.

The most important differences between *P. dziwnowi* and *P. communis* can be summarized as (i) much smaller

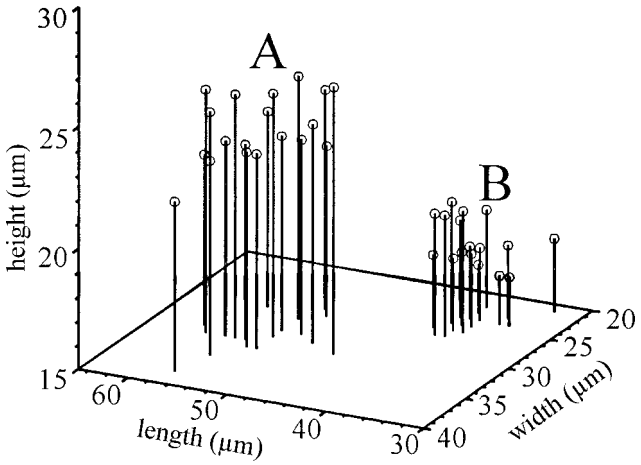

Fig. 14. Test dimensions in 20 specimens of *Corythionella golemanskyi* Nicholls (A) and *C. georgiana* sp. n. (B) co-existing in the same sample of Georgian Bay beach sand. Some specimens had measurements identical to those determined for other specimens, so they were not revealed in this plot (because of overlap).

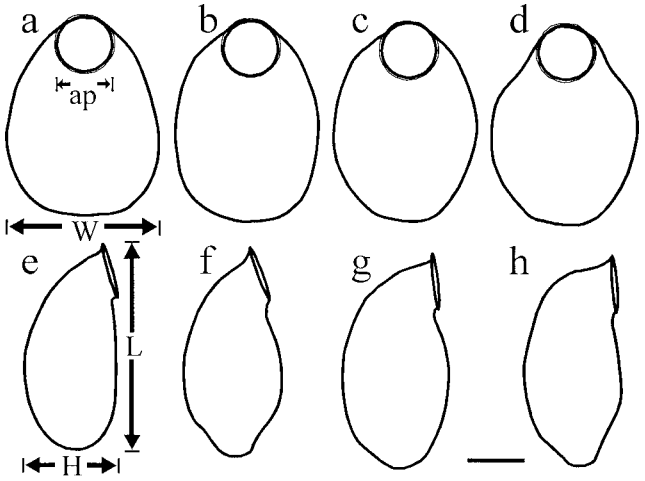

Fig. 15. Form variation in tests of *Corythionella georgiana* sp. n. **a-d** - ventral views of four tests; **e-h** - lateral views of four tests. L, W, H, and ap - test length, width, height and pseudostomal aperture diameter, respectively. Scale bar 10 µm.

size of *P. dziwnowi*, (ii) greater length-to-width ratio in *P. dziwnowi*, (iii) *P. dziwnowi* shows much more variability in the angle of the plane of the oral collar relative to the long axis of the test, ranging from zero to about 45° (in contrast to zero to about 5° in *P. communis*). No *P. dziwnowi* tests with nearly circular outlines in ventral or dorsal views post-pseudostomal region were found; such shapes, although not common, were found occasionally in *P. communis* (see Nicholls and MacIsaac's

Table 1. Test size in *Psammonobiotus dziwnowi* sp. n. (N = 63), *Corythionella georgiana* sp. n. and *Corythionella golemanskyi* (N = 20 each). The diameter of the pseudostomal aperture in *P. dziwnowi* could not be clearly determined in many specimens, so this variable was not included in the descriptive statistics for this species. Definitions of L, W, H and ap are as depicted in Figs 1 and 15. Test measurements (in µm) for 47 of the 63 specimens of *P. dziwnowi* were included in Nicholls and MacIsaac (2004; their "sp. #2").

	length (L)	width (W)	height (H)	ap	L/W
P. dziwnowi					
median	23	11	10		2.2
minimum	21	9	9		1.7
maximum	27	14	12		2.6
mean	23.4	11	10.2		2.1
st.dev.	1.4	1	0.8		0.2
coef.var.(%)	5.9	8.8	8.1		7.5
C. georgiana					
median	39	24.5	18	10	1.56
minimum	33	21	17	9	5.7
maximum	41	27	20	11	1.8
mean	38.4	24.6	18.5	9.7	1.6
st.dev.	2	1.6	1.1	0.6	0.1
coef.var.(%)	5.2	6.7	5.8	6	5.7
C. golemanskyi					
median	54.5	32	23	12	1.7
minimum	46	26	22	11	1.4
maximum	60	38	26	13	2.1
mean	54.2	31.4	23.6	12	1.7
st.dev.	3.4	2.9	1.2	0.7	0.2
coef.var.(%)	6.3	9.4	5.1	6.1	9.9

Table 2. Mann-Whitney *U*-test values in tests of statistical difference between the median morphometric descriptors of Group A specimens (*Corythionella golemanskyi*) and Group B specimens (*Corythionella georgiana* sp. n.) in Fig. 14. The null hypothesis, that the medians of the two groups are not different (i.e. are drawn from the same "population"), was rejected for all *U* values < 127 (2-tailed $\alpha = 0.05$; Neave 1981).

Median	Group A	Group B	*U*-value
L	54.5	39	0
W	32	24.5	7.5
H	23	18	0
ap	12	10	2.5
L/W	1.7	1.6	67
L/H	2.3	2.1	199
W/H	1.3	1.4	165

Fig. 3e). Although it could not be measured reliably on all specimens for which the other morphologic contrast data

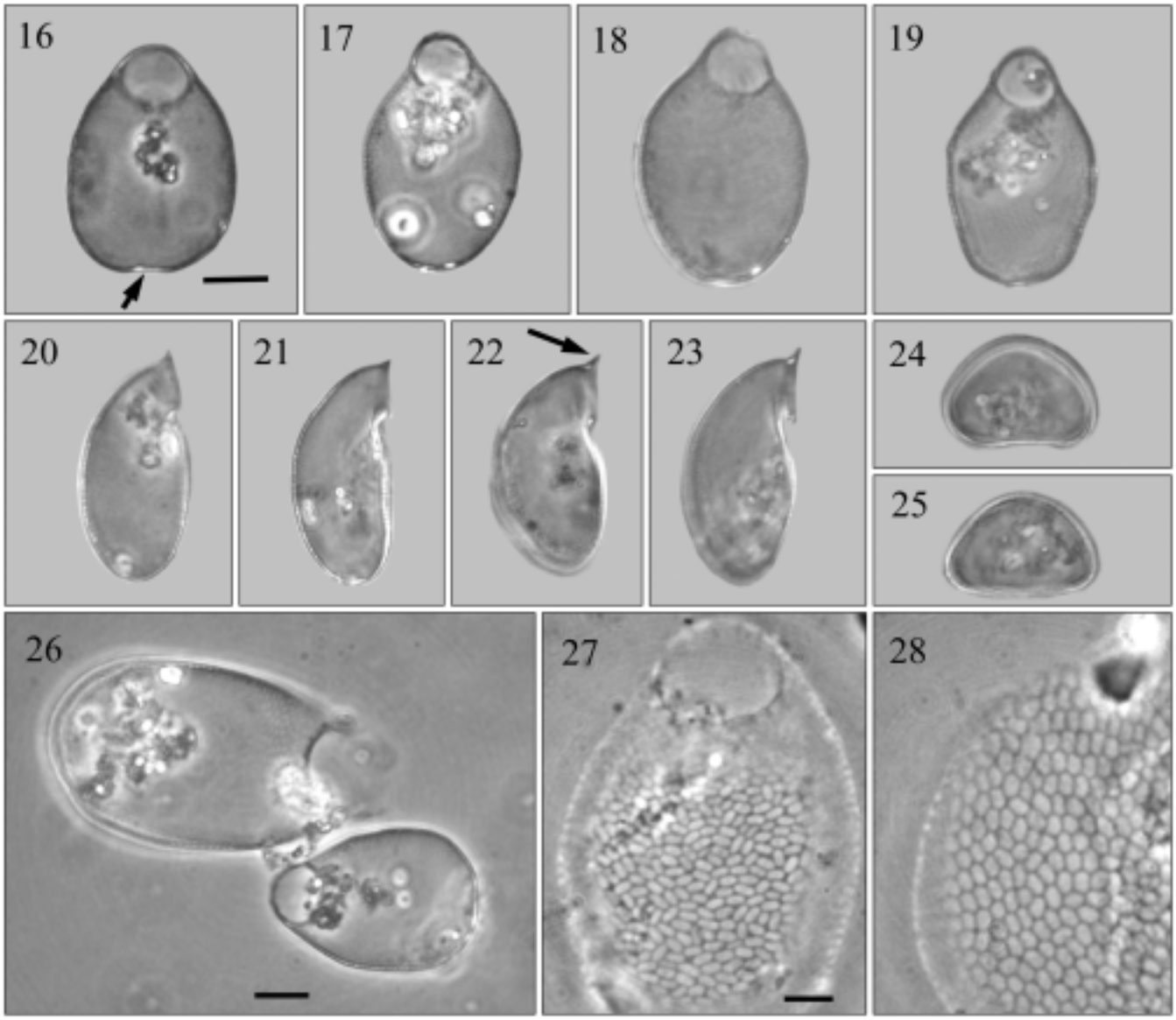

Figs 16-28. Digital images of tests of *Corythionella georgiana* sp. n. **16-19** - images of four different specimens in ventral views (the arrow in Fig. 16 shows the aboral thickened depression in the test wall); **20-23** - images of four different specimens in lateral views (the arrow in Fig. 22 shows the small anterior flare of the pseudostomal collar; **24-25** - optical cross-sectional images of two different specimens; **26** - test of *Corythionella golemanskyi* (larger of the two) beside a test of *C. georgiana* illustrating size difference (scale bar 10 µm); **27** - scales on the test surface of *C. georgiana*; **28** - scales on the test surface of *C. golemanskyi*. Scale bars 10 µm (16 applies to 16-25, 26); 5 µm (27 applies to 28).

were obtained, the diameter of *P. dziwnowi*'s oral collar was usually in the range of about 8-10 µm, in contrast to that of *P. communis* which generally ranged between 15 and 20 µm.

Corythionella georgiana sp. n.

Phylum: Rhizopoda, Class: Filosea, Subclass: Testaceafilosia, Family: Cyphoderiidae

The measurements of *Corythionella* tests in the Wasaga Beach sample clearly revealed the existence of two well defined groups (Fig. 14), one of which was *C. golemanskyi* since it conformed in size and shape to the original description of this species (Nicholls 2003). The other was clearly a distinct morphological entity that differed in other significant aspects of test form as well as length, width and height. It was for those reasons that a formal description of this taxon was needed.

Diagnosis: Tests were translucent, and colourless to pale yellow in colour, elongate-elliptical to nearly circular in outline (ventral and dorsal views). Test length, width

and height were 33-41 µm, 21-27 µm and 17-20 µm, respectively. Tests had a rounded-triangular outline in optical cross-section. The pseudostomal aperture (9-11 µm) was separated from the main body of the test by a short bent neck having a slightly flared anterior rim (not readily observed in some specimens). Tests were covered with small (0.7-0.9 × 1-2.3 µm) elongated silica scales. Scales were randomly arranged with no overlapping of their margins. Protoplast with long, sometimes branching filose pseudopodia.

Etymology: The specific epithet is derived from the sample collection location (Georgian Bay of Lake Huron) where this species was relatively abundant.

Type specimen: The type specimen mounted in Canada Balsam on a glass slide, was deposited with the Invertebrate Zoology Division, Canadian Museum of Nature (Ottawa, Ontario, Canada), Catalogue No. CMNI-2005-0002.

Material from type locality: Retained by the author in sample No. V-1854, collected 2 September, 2002 as a composite of four samples of supra-littoral Wasaga Beach sand.

Type locality: Beach sand in the wave zone (supra-littoral) at Beach Number 2, Wasaga Beach, Georgian Bay, Lake Huron. Ontario, Canada (44° 29' 18" N; 80° 04' 17" W).

Variability in *C. georgiana* test dimensions was low; coefficients of variation for all size variables were all <7% (Table 1). Variability in test shape was also low with all specimens examined exhibiting a broadly rounded elliptical outline in ventral views (Figs 15a-d, 16, 17). Some tests also showed some minor constriction of the anterior region of the test immediately posterior to the pseudostome (Figs 15d, 18, 19). Others revealed a small depression and thickening in the test wall at the aboral end of the test (Fig. 16, arrow). In lateral views (Figs 15e-h, 20-23), there were also several different variations in form identified. The most commonly observed shape was a smooth rounded form (Figs 15e, 20), but variations included those with a flattening on both the dorsal and ventral surfaces near the posterior of the test. This resulted in a "pinched" appearance in lateral views (Figs 15f, g). Others showed a slightly more "humpbacked" appearance in the anterior-dorsal region (Fig. 15h) or in the mid-dorsal region of the test (Fig. 22). The angle of the plane of the pseudostomal aperture with the long axis of the test was also variable among specimens, ranging from a minimum of about -5° (Fig. 23) to a maximum of about +20° (Figs 15e, 20). Some specimens (Fig. 22, arrow; Fig. 23) revealed more flare in the pseudostomal collar, especially along the anterior margin, than others (e.g. Fig. 21). Little variability was seen in the optical cross-sectional views of the test of this species; all tests were wider than high and were in the form of rounded triangles (Figs 24, 25).

The size difference between *C. georgiana* and *C. golemanskyi* was highly significant for all test dimensions except the length-to-height and width-to-height ratios (Table 2). When specimens of each species were together in the same microscopic field of view (Fig. 26), such differences were immediately apparent. These species also differed significantly in the structure and arrangement of scales covering their tests. The scales of *C. georgiana* (0.7-0.9 × 1-2.3 µm; Fig. 27) were smaller and more elongate than those of *C. golemanskyi* (1-1.3 × 1.5-2.7 µm; Fig. 28). In addition to the size and shape differences, the scales of *C. georgiana* were also more loosely arranged and only occasionally overlapped at their margins, whereas those of *C. golemanskyi* were always densely arranged with scale edges overlapping those of adjacent scales.

DISCUSSION

Specimens fitting our description of *P. dziwnowi* were reported by Golemansky (1973) from samples of beach sand collected in 1969 near the SW Baltic Sea town of Dziwnów in Poland. Golemansky found only a few empty tests of this species, which, because of the absence of *P. communis* in the same sample, he believed might be a small atypical form of *P. communis*. There have been no other reports of this taxon in the intervening three decades (V. Golemansky, Zoological Institute, Sofia, Bulgaria, personal communication, December 14, 2002). With the discovery of *P. dziwnowi* in abundance at several Great Lakes beaches, including some where *P. communis* was also abundant (Nicholls and MacIsaac 2004), there can no longer be a question of its possible identity as *P. communis*. The major reasons for this include the significant differences between the dimensions and shapes of the tests of these two species coexisting under the same environmental conditions. Differences of the magnitude reported here in test shape and size observed in widely separated populations of these two species are therefore unlikely to be related to possible environmental effects on growth and development of the tests of these species.Among the test shape variables most discriminating between these two species was the very low angle of inclination of the plane of the

pseudostomal aperature in *P. communis* and the contrasting greater angle *P. dziwnowi*.

Because *Corythionella acolla* Golemansky has a test length about equal to that of *C. georgiana*, and because of the nearly imperceptible flare on the rim of the pseudostomal aperture in *Corythionella georgiana*, its morphology must be discussed with reference to *C. acolla*, the only one of six marine species of this genus that lacks a flared rim. All but one of the published illustrations of *C. acolla* (Golemansky 1970b, 1973; Chardez 1971, 1977; Golemansky and Todorov 1999) are in mutual agreement with regard to general shape of the *C. acolla* test, although Golemansky (1973) illustrated a lateral view of a specimen with a slight flare along the posterior edge of the pseudostomal rim. Only Chardez (1977) included an illustration that is not in agreement with the others; his portrayal of this taxon shows a test with a curiously wide rim surrounding the pseudostome and relatively large scales on the surface of the test that were oriented more or less at right angles to the long axis of the test. Chardez (1977) also listed the test length of this *C. acolla* as 23-28 µm, well below the 33-68 µm given by Golemansky (1971). The other illustration provided by Chardez (Chardez 1971) illustrates densely arranged, very elongate scales oriented mainly along the long axis of the test. The other published depictions of this species illustrate smaller, more tightly arranged scales, but here too there are inconsistencies; compare, for example, the very small densely arranged scales in Golemansky (1970b) with the larger much more loosely arranged scales in Golemansky and Todorov (1999). None of the published illustrations of test scales in *C. acolla* is similar to that found for *C. georgiana*, although some of the previously published illustrations may be somewhat schematic and lacking in detail (no photographic images have been yet published for *C. acolla*).

With the exception of Chardez's (1977) illustration, the other published shapes of the test of *C. acolla* are in good agreement. In ventral view, all show a large pseudostomal aperture equal to about 1/2 the test width (in *C. georgiana* test width equals about 2.5 × aperture diameter) and a gradual widening of the test below the pseudostome towards the posterior one-half of the test. This shape is in marked contrast to that seen in *C. georgiana* which has a much wider test immediately posterior to the pseudostome.

In summary, there may be more than one taxon represented in the published literature under the *C. acolla* binomen. New reports of this species need to define more rigorously the range of form variation and provide photographic detail of the scale covering on the test. In particular, some further research on the taxonomy of *C. acolla* in view of its lack of a flared apertural collar is needed. Because all other species of the genus have a flared collar (but is reduced in the freshwater species *C. golemanskyi* and much more reduced in *C. georgiana*), all or part of what has been considered to be *C. acolla* in the past may have to be transferred to another genus defined, in part, by a non-flared apertural collar.

Notwithstanding the uncertainties surrounding the taxonomy of the marine *C. acolla*, the differences between it and *C. georgiana* in test size and shape (ignoring, for the present, possible additional differences in the structure of the scale layer on the test), are entirely adequate in my view to validate *C. georgiana* as an independent species. As well, the case for its independence from the only other known freshwater species, *C. golemanskyi*, has been clearly established on the basis of test morphology, and the microstructure of the test scale layer.

Acknowledgements. I thank Prof. Dr. Vassil Golemansky (Zoological Institute, Sofia, Bulgaria) for his correspondence and copies of reprints not otherwise available to me.

REFERENCES

Chardez D. (1971) Étude sur les thécamoebiens des biotopes interstitiels, psammons littoraux et zones marginales souterraines des eaux douces. *Bull. Rech. Agr. Gembloux* **6:** 257-268

Chardez D. (1977) Thécamoebiens du mésopsammon des plages de la Mer du Nord. *Revue verviét. Hist. Nat.* **34:** 1-19

CoHort Software (1995) *CoStat*. Minneapolis, Minnesota, 55419, U.S.A

Golemansky V. (1970a) Rhizopodes nouveaux du psammon littoral de la mer Noire. *Protistologica* **6:** 365-371

Golemansky V. (1970b) Contribution à la connaissance des thécamoebiens (Rhizopoda, Testacea) des eaux souterraines littorales du Golf de Gdansk (Pologne). *Bull. Inst. Zool. & Mus. (Bulgaria)* **32:** 77-87

Golemansky V. (1971) Taxonomische und zoogeographische Notizen über die thekamöbe Fauna (Rhizopoda, Testacea) der Küstengrundgewässer der sowjetischen Fernostküste (Japanisches Meer) und der Westküste Kanadas (Stiller Ozean). *Arch. Protistenk.* **113:** 235-249

Golemansky V. (1973) Deuxième contribution à la connaissance des thécamoebiens (Rhizopoda, Testacea), du psammal littoral de la Mer Baltique. *Bull. Inst. Zool. & Mus. (Bulgaria)* **38:** 49-60

Golemansky V. (1998) Interstitial testate amoebae (Rhizopoda: Arcellinida and Gromida) from the Finnish coast of the Baltic Sea and summary check list of the interstitial amoebae in the Baltic Sea. *Acta Protozool*. **37:** 133-137

Golemansky V., Todorov M. T. (1999) First report of the interstitial testate amoebae (Protozoa: Testacea) in the marine supralittoral of the Livingston Island (the Antarctic). *Bulg. Antarctic Res. (Life Sci.)* **2:** 43-47

Meisterfeld R. (2002) Testate amoebae with filopodia. In: An Illustrated Guide to the Protozoa. 2nd ed. (Eds. J. J. Lee, G. F. Leedale, P. Bradbury). Society of Protozoologists, Lawrence, Kansas, **2:** 1054-1084

Neave H. R. (1981) Elementary Statistics Tables For All Users of Statistical Techniques. George Allen & Unwin Ltd., London

Nicholls K. H. (2003) *Corythionella golemanskyi* sp. n.: a new, freshwater, filose, testate rhizopod. *Acta Protozool*. **42:**75-80

Nicholls K. H., MacIsaac H. J. (2004) Euryhaline, sand-dwelling, testate rhizopods in the Great Lakes. *J. Great Lakes Res.* **30:** 123-132

Received on 8th November, 2004; revised version on 9th February, 2005; accepted on 5th March, 2005

Acta Protozool. (2005) 44: 279 - 284

ACTA
PROTOZOOLOGICA

Short Communication

Light-induced Interaction of Putative Phosducin with Gβγ-subunits of G-protein in the Ciliate *Blepharisma japonicum*

Katarzyna SOBIERAJSKA and Stanisław FABCZAK

Department of Cell Biology, Nencki Institute of Experimental Biology, Polish Academy of Sciences, Warsaw, Poland

Summary. Immunoblot of whole-cell lysate from *Blepharisma japonicum* with a polyclonal antibody raised against the rat phosducin display one major protein band of molecular weight of 28 kDa. Immunoprecipitation of detected phosducin immunoanalogue from lysate of dark- and light-adapted ciliates with the anti-phosducin antibody and subsequent analysis of the precipitated protein with a monoclonal antibody raised against phosphoserine residues revealed also the presence of a 28 kDa protein phosphorylated on a serine residues. This phosphoprotein exists in a highly phosphorylated form in ciliates adapted to darkness and its dephosphorylation occurs in illuminated cells. An immunoblot assay of the precipitated phosducin-related protein with a rabbit polyclonal antibody directed against β-subunit of G-protein showed one major protein band of molecular weight of about 34 kDa in lysate obtained from ciliates exposed to light. In addition, based on partial cloning of the putative ciliate phosducin nucleotide sequence homology to the phosducin belonging to the subgroup I of phosducin protein family was deduced. The results obtained in this study confirm the previously reported hypothesis that in the ciliated protist *Blepharisma japonicum* phosducin does exist and resembles that observed in a wide variety of higher eukaryotes and also in some microorganisms.

Key words: *Blepharisma japonicum*, ciliate, G-protein, phosducin, protein phosphorylation, photophobic response, photosensory transduction.

INTRODUCTION

The family of large G-proteins plays an essential role in transducing extracellular signals from the cell-surface receptors to the intracellular effectors (Hamm 1998). G-protein-coupled signaling is regulated at the G-protein level by two different mechanisms. The slow intrinsic GTP-ase activity of α-subunit (Gα) of G-protein can be accelerated by a large family of G-proteins, the regulators of G- protein signaling (RGS) (Berman *et al*. 1996, Hepler 1999). The second mechanism prevents βγ-subunit (Gβγ) of G-protein from modulating its downstream effectors and reassociating with Gα-GDP to undergo another cycle of receptor-mediated activation. The regulatory protein carrying out this task is a cytosolic phosphoprotein, phosducin. It was first discovered in vertebrate retinas and developmentally related pineal glands (Lee *et al.* 1984, Reig *et al.* 1990). Nowadays, there is increasing evidence that phosducin and many phosducin-related proteins are widely expressed also in other tissues (Bauer *et al.* 1992, Danner and Lohse 1996). Existence of proteins of the phosducin

Address for correspondence: Stanisław Fabczak, Department of Cell Biology, Nencki Institute of Experimental Biology, ul. Pasteura 3, Pl- 02-093 Warszawa, Poland; Fax: (+48 22) 822 5342; E-mail: s.fabczak@nencki.gov.pl

family has recently been reported in some lower eukaryotic organisms as well. In the yeast *Saccharomyces cerevisiae*, two phosducin-like proteins, PLp1 and PLp2 were detected, that *in vivo* can bind and regulate Gβγ activity (Flanary *et al*. 2000). In the case of the fungus *Cryphonecteria parasitica*, one gene bdm-1 was identified and shown to encode phosducin-like protein involved in regulation of Gβγ function and accumulation of Gα (Kasahara *et al*. 2000). Moreover, three genes, designated as *phlp*-1, *phlp*-2 and *phlp*-3, encoding distinct phosducin-like proteins, phosducin-1, phosducin-2 and phosducin-3, were discovered in *Dictyostelium discoideum* and it was firmly established that at least one of them, phosducin-1, also plays a role in G-protein-coupled signaling control (Blaauw *et al*. 2003). As reported lately, a cytosolic protein of 28 kDa showing properties similar to those described for phosducin has also been detected in the lower eukaryote, the photosensitive ciliate *Blepharisma japonicum* (Fabczak *et al*. 2001, 2004; Sobierajska *et al*. 2005). This phosphoprotein was shown to be highly phosphorylated in dark-adapted cells and dephosphorylated in ciliates exposed to light. The light-dependent dephosphorylation of phosducin immunoanalogue matches the light-dependent motile behaviour of the cell (photophobic responses). The observed modification of the cell photobehavior results from activation of a specific cellular photoreceptor system (Giese 1973, Tao *et al*. 1994, Maeda *et al*. 1997, Matsuoka *et al*. 2000, Fabczak 2000a). The light harvesting system is coupled to the cell locomotory system *via* G-protein-mediated signaling and membrane potential changes (Fabczak *et al*. 1993; 1998; 1999; 2000a, b) as in the case of photoreceptor cells of higher organisms (Rayer *et al*. 1990).

The present study was initiated to identify the 28 kDa protein detected in the ciliate *Blepharisma japonicum* and to characterize its light-dependent changes in phosphorylation levels with immunoblotting, immunoprecipitation and PCR assays. Furthermore, examinations were attempted to show possible interaction of phosducin immunoanalogue with β-subunit of G-protein in ciliates exposed to light.

MATERIALS AND METHODS

Cell culture

Ciliates *Blepharisma japonicum* were grown as described elsewhere (Fabczak 2000b). Before each experiment, cells were collected by a low-speed centrifugation and then washed in an excess of fresh culture medium lacking nutritional components. Finally, the cell samples were used for biochemical assays following cell incubation in darkness or light in the fresh culture medium. Cell illumination was provided by a 150 W fiberoptic white light source (MLW, Germany), which was equipped with an electromagnetic programmable shutter (mod. l22-841, Ealing Electro-Optics, England).

Immunoblotting

Cell samples were mixed with sample buffer supplemented with protease and phosphatase inhibitors (50 mM NaF, 2 mM PMSF, 10 μM okadaic acid, 10 μg/ml aprotinin, 100 μg/ml leupeptin) to terminate reactions (Laemmli 1970), and then boiled for 5 min. Proteins from solubilized cells were separated by 10% SDS-PAGE with a Hoefer System (Amersham, USA) and transferred to nitrocellulose membranes (Bio-Rad, USA) for 60 min at 100 V in a transfer buffer solution (Towbin *et al*. 1979). Membranes were exposed to TBS-BSA-Tween blocking solution (150 mM NaCl, 10 mM Tris, pH 7.5, 2% bovine serum albumin (BSA), 0.2% Tween-20) for 2 h at room temperature followed by incubation with a polyclonal antibody raised against rat phosducin (kindly provided by Professor Craig Thulin from Brigham Young College in Provo, USA; Thulin *et al*. 1999) at 1:5000 dilution or a rabbit polyclonal antibody directed against β-subunit of G-protein (Santa Cruz Biotechnol. Inc., USA) at 1:1000 dilution in TBS-BSA-Tween solution overnight at 4°C. After several washes in TBS with 0.1% Tween-20, blots were incubated for 60 min at room temperature with secondary antibody, anti-rabbit IgG-horseradish peroxidase conjugate (Calbiochem, Germany) at a 1:10000 dilution in TBS-BSA-Tween solution. Finally, membranes were washed in TBS-Tween buffer and developed with an ECL detection system (Amersham, Sweden). Protein molecular weights were determined based on their relative electrophoretic mobilities with prestained molecular weight markers (Bio-Rad). In control set of experiments the incubations with primary antibody were omitted. A protein concentration in an individual cell sample was estimated with a method reported by Bradford (1976) using BSA as a standard.

Immunoprecipitation

Samples of dark- or light-adapted cells were solubilized in Triton buffer (150 mM NaCl, 1% Triton X-100, 1 mM EDTA, 20 mM Tris, pH 7.4) and then centrifuged for 15 min at 13200*g* at 4°C. The supernatants with protease and phosphatase inhibitors (10 μg/ml leupeptin, 5 μg/ml aprotinin, 1 mM PMSF, 1 μM okadaic acid, 5 mM NaF) were used for immunoprecipitation assays. The cell samples were subjected to preclearance for 1 h with 30% (v/v) protein A-Sepharose CL-4B (Amersham, Sweden) at 4°C. After this, the mixture was centrifuged for 1 min at 13200g at the same temperature. The supernatant fraction was incubated for 1.5 h at 4°C with serum containing anti-phosducin and then incubated again for 1.5 h with a new portion of protein-A-Sepharose. The resin was washed three times in washing buffer (150 mM NaCl, 20 mM Tris, pH 7.4) transferred to new tubes for the third wash then resuspended in sample buffer, boiled for 5 min and analyzed with SDS-PAGE according to the method of Laemmli (1970). Western blot analysis with the anti-phosphoserine residues (clone PSER-4A9 from Alexis, Switzerland) or anti-α-subunit of G-protein antibodies (Santa Cruz Biotechnol. Inc., USA) were carried out as described in previous immunoblotting section.

PCR analysis and cloning

Messenger RNA was isolated from *Blepharisma japonicum* cells using PolyATract System 1000 (Promega) and used as the template for cDNA synthesis by a Universal RiboClone cDNA Synthesis System (Promega). PCR reaction was performed in Minicycler TM (MJ Research) with synthesized primers homologous to a highly conserved Gβ-protein-binding motif of phosducin in N-terminal domain , Phd - F (5'ACGGG(C/T)CCAAA(A/G)GGGGTGAT- 3') and CRX domain, Phd - R (5'-GATAC(C/T)AA (A/T) AGGTTAGTA-3') characteristic for I subgroup of phosducin The amplification reaction was run for 30 cycles of the following sequence: 94°C (30 s), 36°C (45 s) and 72°C (60 s) and final extension step at 72°C for 10 min. The PCR products were analyzed by 1.5 % agarose gel electrophoresis. DNA was extracted from the gel by a NucleoSpin (Macherey-Nagel) and then ligated into pUC19 plasmid (Promega). *Escherichia coli* JM109 competent cells were transformed with this construct according to standard protocols (Sambrook and Russel 2001). Finally, plasmids were isolated from *Escherichia coli* cells by alkaline minilyses and the obtained constructs were cut by restriction enzymes. The reaction products were visualized in agarose gel stained with ethidium bromide. The obtained clone was sequenced and used to search the GeneBank with the BLAST algorithm.

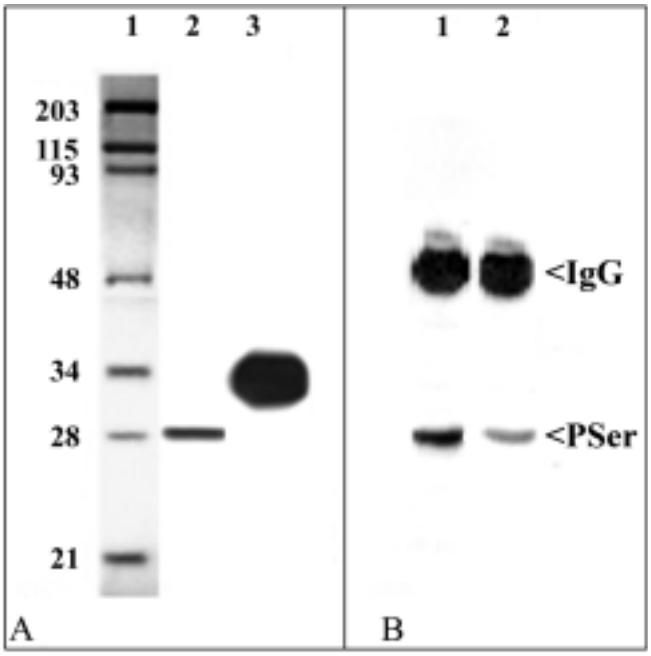

Fig. 1. Identification and light-induced changes in phosphorylation level of phosducin immunoanalogue in *Blepharisma japonicum*. **A** -Immunoblotting for identification of phosducin immunoanalogue in whole-cell lysate from ciliates and phosducin in homogenate from bovine rod outer segment used as a specificity control of the antibody applied. A polyclonal antibody raised against phosducin recognized protein band of 28 kDa in lysate from ciliates (lane 2) and 33 kDa protein band in homogenate from bovine rod outer segment (lane 3). Positions of molecular marker stained by Comassie Brilliant Blue are shown on the left (lane 1). **B** - Immunoprecipitation assay of putative phosducin in ciliates with anti-phosducin antibody. The precipitated proteins in lysates from dark-adapted (lane 1) and illuminated (lane 2) ciliates were analyzed by the anti-phosphoserine antibody.

RESULTS AND DISCUSSION

Immunoblotting of a whole-cell lysate from *Blepharisma japonicum* (Fig. 1A, lane 2) with a polyclonal antibody raised against rat retinal phosducin showed immunoreactivity with one protein of 28 kDa only. A clear immunoreactivity was also displayed with protein band of 33 kDa in bovine rod outer segment homogenate used for specificity control of applied antibody (Fig. 1A, lane 3). The results of this examinations indicated that labeled ciliate protein has molecular weight of 28 kDa similar to that of protein exhibiting light-dependent phosphorylation previously described (Fabczak *et al.* 2004).

To examine *in vivo* whether changes in phosphorylation levels of the identified ciliate phosducin immunoanalog can be induced by light, the whole-cell lysate prepared from dark-adapted and from light-exposed cells were immunoprecipitated with the anti-phosducin antibody. Subsequently, the precipitated proteins were analyzed by means of monoclonal antibody raised against phosphoserine residues. Under both experimental conditions, the anti-phosducin antibody precipitated exclusively one 28 kDa protein phosphorylated on phosphoserine residues (Fig. 1B). These experiments also corroborated previous observations that the illumination significantly decreased phosphorylation levels of the phosphoprotein in the cells (Fig. 1B, lane 2), while the phosphorylation level of this protein was much higher in untreated cells (Fig. 1B, lane 1) (Fabczak *et al.* 2004). These results showed that the tested organisms possess indeed the 28 kDa protein, highly analogous to phosducin from higher organisms, which shows enhanced phosphorylation in dark-kept organisms and becomes markedly dephosphorylated in cells exposed to light (Shulz 2001).

In successive experiments the immunoprecipitated proteins were probed by immunoblotting with rabbit polyclonal antibody raised against β-subunit (Gβ) of G-protein. As shown in Fig. 2A, in lysate from ciliates adapted to light a robust coimmunoprecipitation of the Gβ at protein band of 34 kDa was observed (lane 3), while in lysate prepared from dark-adapted cells this protein band was missing (lane 2). These data

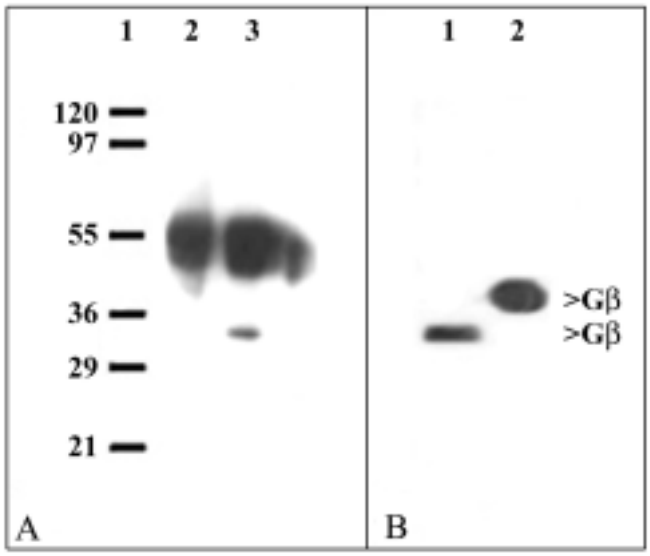

Fig. 2. Interaction between Gβ and phosducin immunoanalogue in ciliate *Blepharisma japonicum*. **A** - Co-immunoprecipitation of phosducin immunoanalogue in ciliates. Lysates from cells adapted to darkness and cells exposed to light, were immunoprecipitated with anti-phosducin antibody and immunoblotted with anti-Gβ-antibody. Bands at 55 kDa correspond to high chains of IgG. **B** - Immunodetection of Gβ immunoanalogue in whole-cell lysate from ciliates with anti-Gβ-antibody. Other details as in Fig. 1.

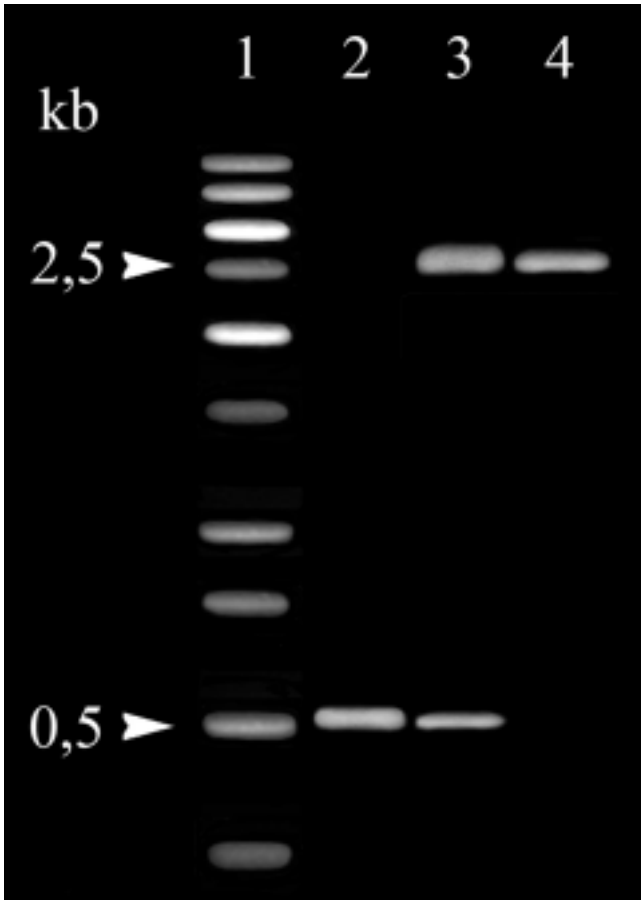

Fig. 3. PCR amplification and cloning of the putative phosducin in ciliate *Blepharisma japonicum*. Lane 1, molecular weight marker; lane 2, PCR product of 500 bp (bottom arrowhead) with synthesized primers homologous to highly conserved Gβ-protein-binding motif of the phosducin in N-terminal domain and CRX domain characteristic for I subgroup of phosducin protein family; lane 3, visualization of construct after alkaline minilysis isolation and restriction enzyme cutting; lane 4, pUC19 plasmid alone.

are consistent with the effect of the light on phosphorylation level of protein identified as the phosducin immunoanalogue in immunoprecipitation assay (Fig 1B). Additionally, immunoblotting of whole-cell lysate with anti-Gβ-antibody also revealed a major protein band of molecular weight of about 34 kDa (Fig. 2B, lane 1) as well as a protein band of 36 kDa in bovine rod outer segment homogenate (Fig. 2B, lane 2), confirming that the antibody possess sufficient selectivity for the Gβ. The ciliate protein had molecular weight of 40 kDa, similar to that showed in coimmunoprecipitation assay with the anti-phosducin antibody shown in Fig. 2A. The results of these experiments provide evidence that the ciliate phosducin immunoanalogue in its dephosphorylated form may translocate towards cell membrane and interact with a protein analogous to β-subunit of G-proteins.

Since the results of Western blot analysis suggested the presence of phosducin immunoanalogue in *Blepharisma japonicum* further characterization of this phosphoprotein was undertaken by a cloning procedure. When primers homologous to a highly conserved Gα-protein-binding motif of the phosducin in the N-terminal and CRX domain, characteristic for subgroup I of the phosducin protein family (Blaauw *et al.* 2003), were employed in PCR analysis, a single band of approximately 500 pb was generated (Fig. 3, lane 2). This is the appropriate molecular value for cDNA of the expected fragment of known phosducin. The deduced amino acid sequence displayed a significant degree of homology (~ 41%) to phosducin, which belongs to the subgroup I of phosducin protein family (Blaauw *et al.* 2003) (Fig. 4).

The results obtained in this study support the hypothesis that in the ciliate *Blepharisma japonicum* phosducin exists and highly resembles those found in a wide variety of higher eukaryotes (Shulz 2001) and also in some lower eukaryotic cells (Blaauw *et al.* 2003, Flanary *et al.* 2000, Kasahara *et al*. 2000). In these organisms

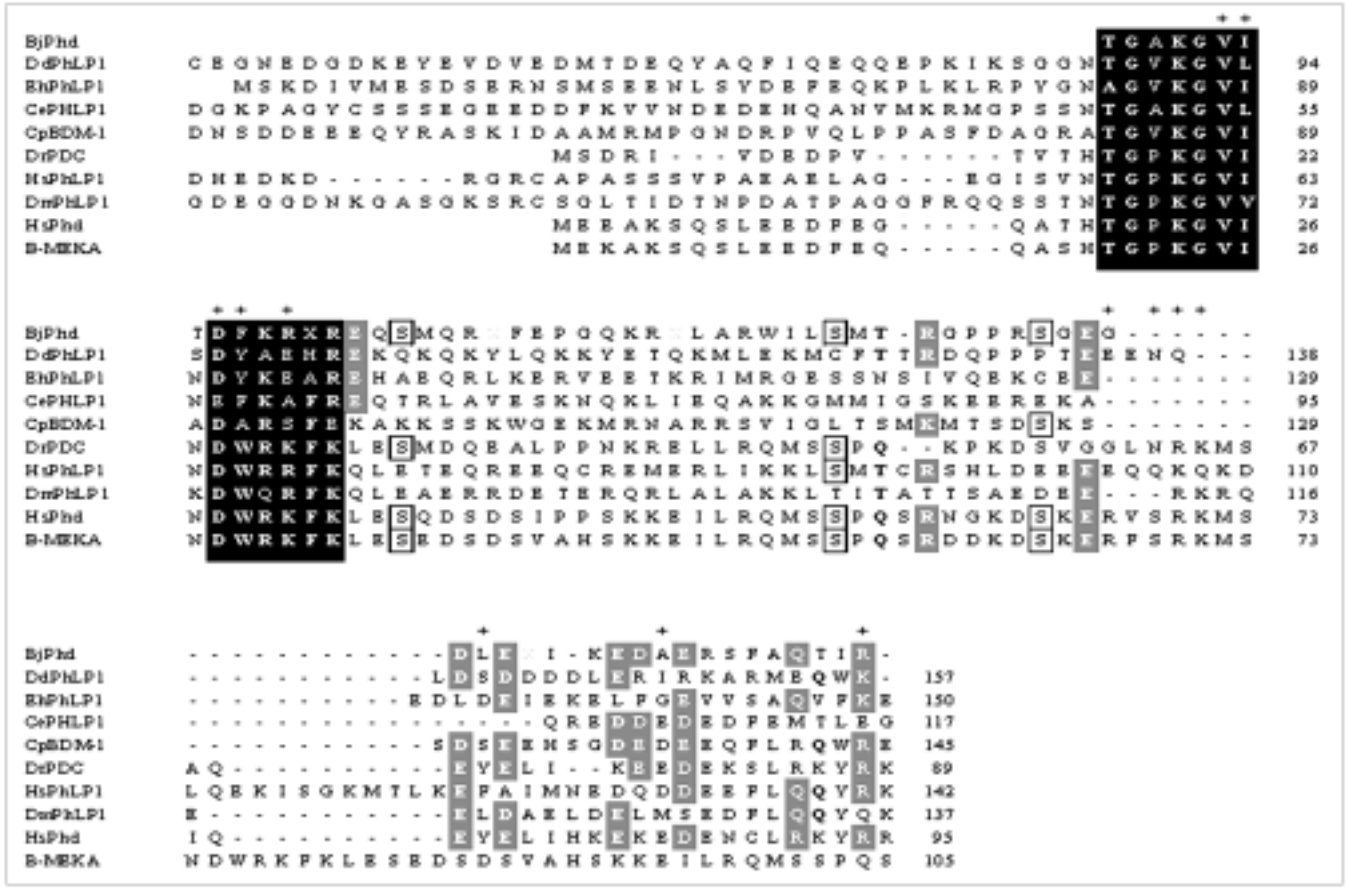

Fig. 4. Alignment of the derived amino acid sequences of *Blepharisma japonicum* phosducin and members of the subgroup I of phosducin protein family. Residues shaded in black are conserved in 70 - 100% of all sequences; residues shaded in grey are conserved in 60-70% of all sequences; residues bold characters are conserved in 75 -100% of all sequences of this subgroup; serine residues localized in the same place in *Blepharisma japonicum* and other organisms are in frames. The Gβ-containing residues of human phosducin (HsPh) are denoted by + above the aligned sequences. The abbreviations used are: Phd - phosducin; PhLP - phosducin like protein; BjPhd - putative fragment of Phd from *Blepharisma japonicum*; DdPhLP1 - PhLP from *Dictyostelium discoideum*, gi 333331889; EhPhLP1 - PhLP from *Entamoeba histolytica*, gi 56467495; CePhLP1- PhLP from *Ceanorhabditis elegans*, gi 17543862; CpBDM-1 - PhLP from *Cryphonectria parasitica*, gi 6714950; DrPDC - PhLP from *Danio rerio*, gi 56207464; HsPhLP1 - PhLP from *Homo sapiens*, gi 13642199; DmPhLP1 - PhLP from *Drosophila melanogaster*, gi 23093421; HsPhd - Phd from *Homo sapiens*, gi 187517; B-MEKA - Phd from *Bos taurus*, gi130133

phosducin was found to be ubiquitous cytosolic G-protein regulator, since in its dephosphorylated form can bind several different G-proteins, such as Gs, Go, or Gi and prevents reassociation of α-subunit of G-proteins with Gβγ, resulting in lower signal amplification at the G-protein level (Bauer *et al.* 1992). It appears that phosducin immunoanalogue found in the photosensitive *Blepharisma japonicum* might also play distinct physiological roles in the ciliate photobehavior. The obtained data may also have important evolutionary significance, since they suggest that the sensory transduction cascade in this ciliate is under the control of phosducin phosphorylation changes processes similar to those operating in evolutionarily distant photoreceptor like the cells of vertebrate retina (Thulin *et al.* 1999, Lee *et al*. 2004).

Acknowledgements. The presented study was supported by grant no. 2 P04C 014 27 from the Committee for Scientific Research and by statutory funding for the Nencki Institute of Experimental Biology in Warsaw, Poland.

REFERENCES

Bauer P. H., Muller S., Puzicha M., Pippig S., Obermaier B., Helmreich E. J., Lohse M. J. (1992) Phosducin is a protein kinase A-regulated G-protein regulator. *Nature* **358:** 73-76

Berman D. M., Kozasa T., Gilman A. G. (1996) The GTPase-activating protein RGS4 stabilizes the transition state for nucleotide hydrolysis. *J. Biol. Chem*. **271:** 27209-27212

Blaauw M., Knol J. C., Kortholt A., Roelofs J., Ruchira, Postma M., Visser A. J., van Haastert P. J. (2003) Phosducin-like proteins in *Dictyostelium discoideum*: implications for the phosducin family of proteins. *EMBO J*. **22:** 5047-5057

Bradford M. M. (1976) A rapid and sensitive method for the quantitation of microgram quantities of protein utilizing the principle of protein-dye binding. *Anal. Biochem*. **72:** 248-254

Danner S., Lohse M. J. (1996) Phosducin is a ubiquitous G-protein regulator. *Proc. Nat. Acad. Sci. USA* **93:** 10145-10150

Fabczak H. (2000a) Protozoa as model system for studies of sensory light transduction: photophobic response in the ciliate *Stentor* and *Blepharisma*. *Acta Protozool*. **39:** 171-181

Fabczak H. (2000b) Contribution of the phosphoinositide-dependent signal pathway to photomotility in *Blepharisma*. *J. Photochem. Photobiol*. B. **55:** 120-127

Fabczak H., Tao N., Fabczak S., Song P.-S. (1993) Photosensory transduction in ciliates. IV. Modulation of the photomovement response of *Blepharisma japonicum* by cGMP. *Photochem. Photobiol*. **57:** 889-892

Fabczak H., Walerczyk M., Fabczak S. (1998) Identification of protein homologous to inositol trisphosphate receptor in ciliate *Blepharisma*. *Acta Protozool.* **37:** 209-213

Fabczak H., Groszyńska B., Fabczak S. (2001) Light regulation of protein phosphorylation in *Blepharisma japonicum. Acta Protozool.* **40:** 311-315

Fabczak H., Sobierajska K, Fabczak S. (2004) Identification of possible phosducins in the ciliate *Blepharisma japonicum*. *Protist* **155:** 181-192

Fabczak H., Walerczyk M., Groszyńska B., Fabczak S. (1999) Light induces inositol trisphosphate elevation in *Blepharisma japonicum. Photochem. Photobiol*. **69:** 254-258

Flanary P. L., DiBello P. R., Estrada P., Dohlman H. G. (2000) Functional analysis of Plp1 and Plp2, two homologues of phosducin in yeast. *J. Biol. Chem*. **275:** 18462-18469

Giese A. C. (1973) *Blepharisma*. The Biology of a Light-sensitive Protozoan. Stanford Univ. Press, Stanford, USA

Hamm H. E. (1998) The many faces of G-protein signaling. *J. Biol. Chem.* **273:** 669-672

Hepler J. R. (1999) Emerging roles for RGS proteins in cell signaling. *Trends Pharmacol. Sci.* **20:** 376-382

Kasahara S., Wang P., Nuss D. L. (2000) Identification of bdm-1, a gene involved in G-protein beta-subunit function and alpha-subunit accumulation. *Proc. Nat. Acad. Sci. USA* **97:** 412-417

Laemmli U. K. (1970) Cleavage of structural proteins during the assembly of the head of bacteriophage T4. *Nature* **277:** 680-685

Lee R. H., Brown B. M., Lolley R. N. (1984) Light-induced dephosphorylation of a 33K protein in rod outer segments of rat retina. *Biochem.* **23:** 1972-1977

Lee B. Y., Thulin C. D., Willardson B. M., (2004) Site-specific phosphorylation of phosducin in intact retina. Dynamics of phosphorylation and effects on G-protein beta-gamma dimer binding. *J. Biol. Chem.* **279:** 54008-54017

Matsuoka T., Tokumori D., Kotsuki H., Ishida M., Matsushita M., Kimura S., Itoh T., Checcucci G. (2000) Analyses of structure of photoreceptor organelle and blepharismin-associated protein in unicellular eukaryote *Blepharisma*. *Photochem. Photobiol.* **72:** 709-713

Rayer B., Naynert M., Stieve H. (1990) Phototransduction; Different mechanisms in vertebrates and invertebrates. *J. Photochem. Photobiol. B.* **7:** 107-148

Reig J. A., Yu L., Klein D. C. (1990) Pineal transduction. Adrenergic-cyclic AMP-dependent phosphorylation of cytoplasmic 33 kDa protein (MEKA), which binds beta-gamma-complex of transducin. *J. Biol. Chem.* **265:** 5816-5824

Sambrook J., Russel D. W. (2001) Molecular cloning. In: A Laboratory Manual. 3rd Ed. Cold Spring Harbor Lab. Press, New York

Schulz R. (2001) The pharmacology of phosducin. *Pharmacol. Res*. **43:** 1-10

Sobierajska K., Fabczak H., Fabczak S. (2005) Alterations of ciliate phosducin phosphorylation in *Blepharisma japonicum* cells. *J. Photochem. Photobiol. B.* **79:** 135-143

Tao N., Diforce L., Romanowski M., Meza-Keuthen S., Song P.-S., Furuya M. (1994) *Stentor* and *Blepharisma* photoreceptors: structure and function. *Acta Protozool.* **39:** 171-181

Thulin C. D., Howes K., Driscoll C. D., Savage J. R., Rand T. A., Baehr W., Willardson B. M. (1999) The immunolocalization and divergent roles of phosducin and phosducin-like protein in the retina. *Mol. Vision* **5:** 40-49

Towbin H., Staehelin T., Gordon J. (1979) Electrophoretic transfer of proteins from polyacrylamide gels to nitrocellulose sheet: Procedure and some applications. *Proc. Nat. Acad. Sci. USA* **76:** 4350-4354

Received on 19th May, 2005; accepted on 22nd July, 2005

Acta Protozool. (2005) 44: 285 - 288

ACTA
PROTOZOOLOGICA

Short Communication

Amoeboid Stage of *Gigantomonas herculea* (Parabasalia) Attached to the Hindgut o the Termite Host *Hodotermes mossambicus*

Guy BRUGEROLLE

Biologie des Protistes, UMR 6023, CNRS and Université Blaise Pascal de Clermont-Ferrand, Aubière Cedex, France

Summary. A light microscopy examination of the luminal surface of the hindgut of *Hodotermes mossambicus* revealed large amoeboid cells attached to the cuticle. Sections observed by transmission electron microscopy showed cells with large finger-like pseudopodia adhering to the cuticle and containing conspicuous bundles of microfilaments. The cuticle surface was covered by these large pseudopodial processes, and the usual bacterial covering was removed. The spiralled rows of the axostyle and the cresta structure in these large amoeboid cells indicated that they belong to *Gigantomonas herculea* which, to date, was only known to live free in the hindgut fluid.

Key words: *Gigantomonas herculea*, hindgut attachment, *Hodotermes mossambicus*, microfilaments, ultrastructure.

INTRODUCTION

Hodotermes mossambicus is a subterranean grass-eating "lower termite" living in East Africa. It harbours a varied fauna of symbiotic protozoa in the hindgut (Dogiel 1916, 1922; Yamin 1979) that I have reinvestigated using immunofluorescence and transmission electron microscopy techniques (Brugerolle and Bordereau 2003, Brugerolle 2005). One of these protozoa, *Gigantomonas herculea*, is a large amoeboid flagellate that presents a flagellate, an amoeboid and a plasmodial stage of development (Dogiel 1916, Kirby 1946). A recent study has dealt with the most numerous amoeboid forms in the hindgut fluid (Brugerolle 2005). These cells have an internalized flagellar apparatus typical of devescovinid parabasalids with a large cresta structure associated with the enlarged recurrent flagellum. More remarkably, these amoeboid cells present a thick cytoplasmic margin with a microfibrillar network and internal bundles of microfilaments similar to those of lobose amoebae. A further examination of the termite hindgut's luminal surface has revealed the presence of large adhering amoeboid cells attached to the cuticle, and the ultrastructural study has allowed me to identify them as *Gigantomonas herculea.*

Address for correspondence: Guy Brugerolle, Biologie des Protistes, UMR 6023, CNRS and Université Blaise Pascal de Clermont-Ferrand, 63177 Aubière Cedex, France; Fax: +33 (04) 73 40 76 70; E-mail: Guy.Brugerolle@univ-bpclermont.fr

MATERIALS AND METHODS

Hodotermes mossambicus termites were collected in Kenya several years ago and maintained in a laboratory terrarium at the Université de Bourgogne in Dijon, France (Brugerolle 2005). The hindgut of a termite was opened with a pair of tweezers into a drop of Ringer's solution. The first hindgut paunch, or P3 segment according to Noirot

(1995) numbering, was fixed in a solution of 1% glutaraldehyde (Polysciences) in 0.1 M phosphate buffer solution, pH 7, for 1 h at room temperature. After two washes in the buffer, the gut was postfixed in 1% osmium tetroxide in the buffer for 1 h. After a water rinse, it was pre-embedded in 1% agar (Difco), stained "en bloc" with saturated uranyl acetate in 70% ethanol for 1 h, completely dehydrated in an alcohol series, and embedded in Epon 812 resin (Merck). Sections were cut with a diamond knife (Drukker) on a Reichert Ultracut S microtome (Leica). Semi-thin sections 1 mm thick were stained for 1 min with a 0.2% blue Azur II solution at pH 8.5, followed by destaining with a 0.1 N NaOH solution and were observed under a Leica DMR light microscope equipped with a G-Fish Light Station. Ultra-thin sections were stained with lead citrate for 15 min and examined under a JEOL 1200 EX electron microscope at 80 kV.

RESULTS

Globular cells attached along the lumen surface of the hindgut were first observed under a stereomicroscope. Semi-thin sections of fixed and stained hindgut showed aligned amoeboid cells adhering to the cuticle, and most of the hindgut surface was covered with these cell processes (Fig. 1). The electron microscopy study revealed that the amoeboid cells adhered to the cuticle via fingerlike pseudopodial processes containing numerous microfilaments (Figs 2, 3). Bundles of microfilaments of variable thickness, often associated with tubular vesicles, joined the pseudopod surfaces to the cell body (Figs 3, 4). Bacteria were present between the pseudopodia, and also inside the food vacuoles of the protozoan. Within the zone of adhesion of these amoeboid cells, the bacteria adhering to the cuticle and usually forming a thick and dense coverage were removed (Fig. 3). The cytoplasm of the cell body of these amoeboid cells contained spread Golgi bodies, hydrogenosomes, and food vacuoles filled with wood particles and with the various bacteria present in the hindgut fluid, including easy-identifiable spirochetes. Through the sections, the cells contain one or two nuclei that are accompanied by the spiralled microtubular rows of the axostyle, parabasal filaments supporting Golgi bodies and the cresta structure (Fig. 5). Sections of flagella, basal bodies and their appendages, atractophores and a paradesmosis were also observed close to the nuclei (not shown).

DISCUSSION

The amoeboid cells attached to the hindgut and having a microtubular spiralled row as an axostyle, a cresta structure, a parabasal apparatus, free Golgi bodies and hydrogenosomes, resemble those described in the fluid content, and have been identified as *Gigantomonas herculea* (Brugerolle 2005). The attached forms of *G. herculea* were not mentioned in the previous studies of Dogiel (1916) and Kirby (1946), who only observed this amoeboid flagellate in the hindgut fluid as the other symbiotic flagellates of this termite. However, Cleveland (1966) using Kirbys' preparations mentioned that "*Gigantomonas* is attached to the chitinous intima of its host" and he drawn an attached cell with a holdfast and a rostellum but did not further comment these observations. A major highlight is the remarkable development of the cell processes and pseudopodia and their microfilament bundles in the attached forms that confirm previous observations in the amoeboid cells collected in fluid content (Brugerolle 2005). Similar conspicuous microfilament bundles in the pseudopodia have not been reported in any other parabasalid flagellates. Parabasalid flagellates living in the hindgut of "lower termites" or in the wood-feeding roach *Cryptocercus* have not been reported as being attached to the gut, as they usually swim in the hindgut fluid. This contrasts with oxymonad flagellates living in the hindgut of the same hosts, which are attached to the cuticle by a finger-like holdfast apparatus containing microfilaments such as *Pyrsonympha* (Hollande and Carruette-Valentin 1970) and a rostellum containing microtubules such as *Oxymonas* (Brugerolle and König 1997). In these oxymonads, the holdfast apparatus is situated at the anterior tip of the cell and is connected to the flagellar apparatus. In the large amoeboid forms of *G. herculea*, the whole cell surface is surrounded by a microfilament margin that transforms into finger-like pseudopodia able to adhere to the gut surface, but there is no microtubular rostellum in *Gigantomonas.* Amoeboid trichomonads, such as *Histomonas meleagridis* (Wenrich 1943) which is parasitic of birds or *Trichomonas vaginalis* which is parasitic of humans, are known to adhere to the host cells in infested organs (Brugerolle et al. 1974, Gonzales-Robles et al. 1995) but they nether contain microfilament bundles as large as those of *Gigantomonas herculea*.

In the largest amoeboid forms of *Gigantomonas*, Dogiel (1916) and (Kirby 1936) generally observed two nuclei linked by a paradesmosis and an internalized flagellar apparatus at variable stages of development. Only Kirby (1946) mentioned a very large amoeboid or plasmodial form containing 36 nuclei without crestas, axostyles or paradesmoses around the nuclei, from the

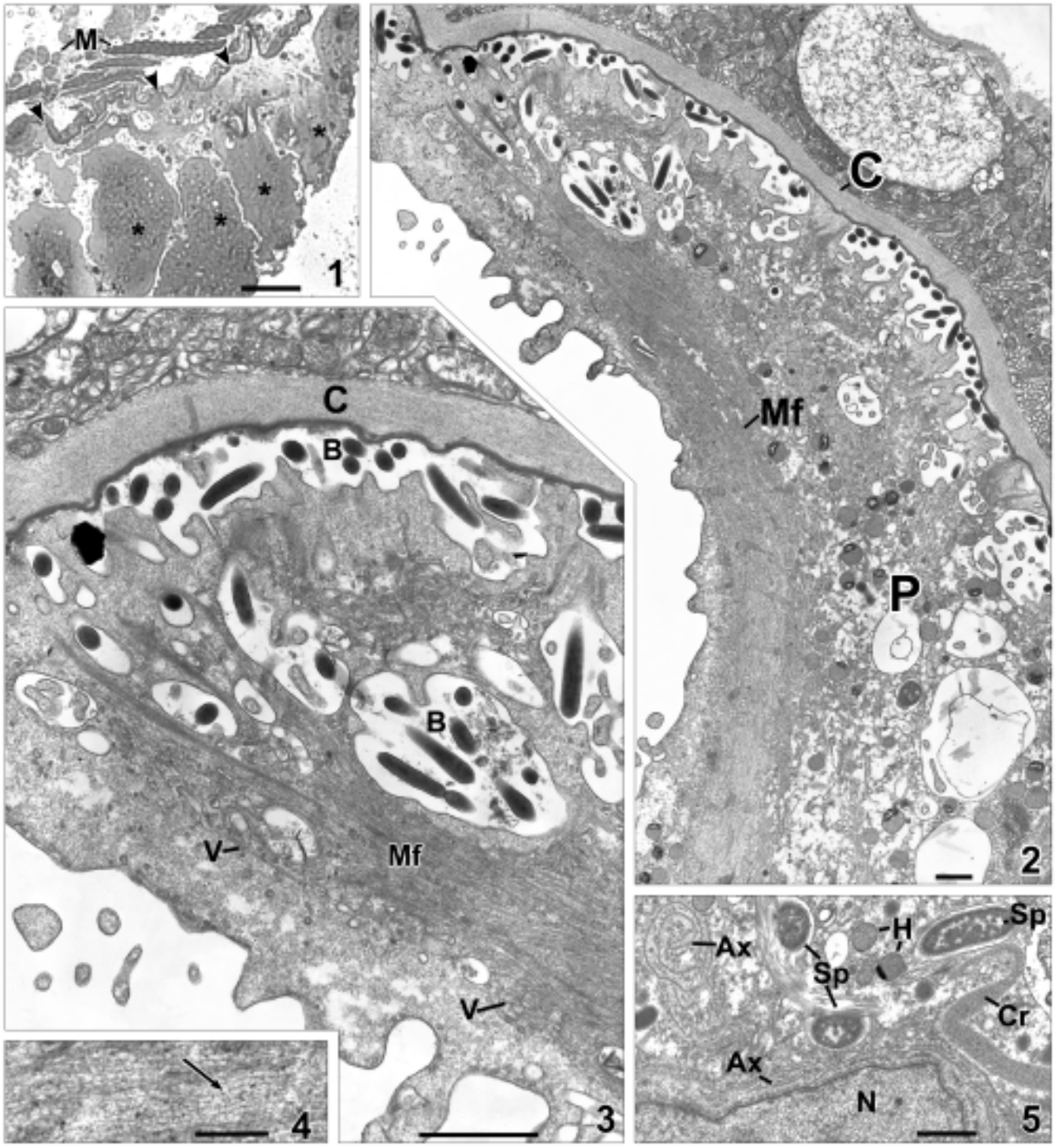

Fig. 1. Light microscopy micrograph of a semi-thin section of the hindgut of *Hodotermes mossambicus* where amoeboid cells of *Gigantomonas herculea* (*) are attached to the cuticle (arrowheads); muscle layer (M). Scale bar 50 µm.
Figs 2-4. Transmission electron micrographs. **2 -** finger-like pseudopod (P) of an amoeboid *Gigantomonas* adherent to the hindgut cuticle (C). **3 -** bundle of microfilaments (Mf) associated with vesicles (V), stretched between the pseudopod surface and the cell body, and numerous bacteria (B) close to the pseudopod surface and inside food vacuoles. **4 -** microfilaments (arrow) at high magnification. Scale bars 1 µm (2, 3); 0.25 µm (4).
Fig. 5. Section of the nucleus (N), showing the microtubular rows of the axostyle (Ax), cresta structure (Cr), hydrogenosome (H) and spirochetes (Sp) of an attached cell. Scale bar 1 µm.

hindgut of *Microhodotermes viator*, a termite which has the same protozoan fauna as *Hodotermes mossambicus*. That was corroborated by Cleveland (1966) who described multinucleate forms that divide by plasmotomy. Two parabasalid flagellates *Kirbinia pulchra* and *Rhizonympha jahieri* do have a plasmodial stage attached to the hindgut of the termite *Anacanthotermes ochraceus* (Grassé and Hollande 1951; Grassé 1952a, b), but unfortunately these flagellates have not been re-examined using modern techniques.

Acknowledgments. I would like to thank Dr C. Bordereau and A. Robert from the University of Dijon for culturing the termites, and J.-L. Vincenot for printing the photographs.

REFERENCES

Brugerolle G. (2005) The amoeboid flagellate *Gigantomonas herculea* of the African termite *Hodotermes mossambicus* reinvestigated using immunological and ultrastructural techniques. *Acta Protozool.* **44:** 189-199

Brugerolle G., Bordereau C. (2003) Ultrastructure of *Joenoides intermedia* (Grassé 1952), a symbiotic parabasalid flagellate of *Hodotermes mossambicus*, and its comparison to other joeniid genera. *Europ. J. Protistol.* **39:** 1-10

Brugerolle G., König H. (1997) Ultrastructure and organization of the cytoskeleton in *Oxymonas*, an intestinal flagellate of termites. *J. Eukaryot. Microbiol.* **44:** 305-313

Brugerolle G., Gobert G., Savel J. (1974) Etude ultrastructurale des lésions viscérales provoquées par l'injection intra-péritonéale de *Trichomonas vaginalis* chez la souris. *Ann. Parasitol. hum. comp. (Paris)*, **49:** 301-318

Cleveland L. R. (1966) Reproduction by binary fission and multiple fission in *Gigantomonas*. *J. Protozool*. **13:** 573-585

Dogiel V. A. (1916) Researches on the parasitic protozoa from the intestine of termites. I. Tetramitidae. *Zool. Zh.* **1:** 1-35 (Russian), 36-54 (English)

Dogiel V. A. (1922) Untersuchungen an parasitischen Protozoen aus dem Darmkanal der termiten. III. Trichonymphidae. *Russk. Arkh. Protist.* **1:** 172-234

Gonzales-Robles A., Lazaro-Haller A., Espinosa-Cantellano M., Anaya-Velazquez F., Martinez-Palomo A. (1995) *Trichomonas vaginalis*: ultrastructure bases of the cytopathic effect. *J. Eukaryot. Microbiol.* **42:** 641-651

Grassé P.-P. (1952a) Ordre des Trichomonadines. In: Traité de Zoologie, Flagellés, (Ed. P.-P. Grassé). Masson et Cie, Paris, **1:** 705-779

Grassé P.-P. (1952b) Famille des Rhizomastigidae Grassé et Hollande, 1951. In: Traité de Zoologie, Flagellés, (Ed. P.-P. Grassé). Masson et Cie, Paris, **1:** 848-850

Grassé P.-P., Hollande A. (1951) Recherches sur les symbiotes des termites Hodotermitidae nord-africains. I. Le cycle évolutif du genre *Kirbinya*. II. Les Rhizonymphidae fam. nov. III. *Polymastigoides*, nouveau genre de Trichomonadidae. *Ann. Sci. Nat., Zool. Paris*, **13:** 1-32

Hollande A., Carruette-Valentin J. (1970) La lignée des Pyrsonymphines et les caractères infrastructuraux communs aux autres genres *Opisthomitus, Saccinobaculus, Pyrsonympha* et *Streblomastix*. *C. R. Acad. Sci. Paris* **270:** 1587-1590

Kirby H. (1946) *Gigantomonas herculea* Dogiel, a polymastigote flagellate with flagellated and amoeboid phases of development. *Univ. Calif. Publ. Zool.* **53:** 163-226

Noirot Ch. (1995) The gut of termites (Isoptera). Comparative anatomy, systematics, phylogeny. I. Lower termites. *Ann. Soc. Entomol. Fr.* (N. S.) **31:** 197-226

Wenrich D. H. (1943) Observations on the morphology of *Histomonas* (Protozoa, Mastigophora) from pheasants and chickens. *J. Morphol.* **72:** 279-303

Yamin M. A. (1979) Flagellates of the Orders Trichomonadida Kirby, Oxymonadida Grassé, and Hypermastigida Grassi & Foà reported from lower termites (Isoptera families Mastotermitidae, Kalotermitidae, Hodotermitidae, Termopsidae, Rhinotermitidae, and Serritermitidae) and from the wood-feeding roach *Cryptocercus* (Dictyoptera: Cryptocercidae). *Sociobiology* **4:** 1-120

Received on 24th June; accepted on July 1st, 2005

INSTRUCTIONS FOR AUTHORS

Acta Protozoologica is a quarterly journal that publishes current and comprehensive, experimental, and theoretical contributions across the breadth of protistology, and cell biology of lower Eukaryote including: behaviour, biochemistry and molecular biology, development, ecology, genetics, parasitology, physiology, photobiology, systematics and phylogeny, and ultrastructure. It publishes original research reports, critical reviews of current research written by invited experts in the field, short communications, book reviews, and letters to the Editor. Faunistic notices of local character, minor descriptions, or descriptions of taxa not based on new, (original) data, and purely clinical reports, fall outside the remit of *Acta Protozoologica.*

Contributions should be written in grammatically correct English. Either British or American spelling is permitted, but one must be used consistently within a manuscript. Authors are advised to follow styles outlined in The CBE Manual for Authors, Editors, and Publishers (6th Ed., Cambridge University Press). Poorly written manuscripts will be returned to authors without further consideration.

Research, performed by "authors whose papers have been accepted to be published in *Acta Protozoologica* using mammals, shall have been conducted in accordance with accepted ethical practice, and shall have been approved by the pertinent institutional and/or governmental oversight group(s)"; this is Journal policy, authors must certify in writing that their research conforms to this policy.

Nomenclature of genera and species names must agree with the International Code of Zoological Nomenclature (ICZN), International Trust for Zoological Nomenclature, London, 1999; or the International Code of Botanical Nomenclature, adopted by XIV International Botanical Congress, Berlin, 1987. Biochemical nomenclature should agree with "Biochemical Nomenclature and Related Documents" (A Compendium, 2nd edition, 1992), International Union of Biochemistry and Molecular Biology, published by Portland Press, London and Chapel Hill, UK.

Except for cases where tradition dictates, SI units are to be used. New nucleic acid or amino acid sequences will be published only if they are also deposited with an appropriate data bank (e.g. EMBL, GeneBank, DDBJ).

All manuscripts that conform to the Instructions for Authors will be fully peer-reviewed by members of Editorial Board and expert reviewers. The Author will be requested to return a revised version of the reviewed manuscript within four (4) months of receiving the reviews. If a revised manuscript is received later, it will be considered to be a new submission. There are no page charges, but Authors must cover the reproduction cost of colour illustrations.

The Author(s) of a manuscript, accepted for publication, must transfer copyrights to the publisher. Copyrights include mechanical, electronic, and visual reproduction and distribution. Use of previously published figures, tables, or brief quotations requires the appropriate copyright holder's permission, at the time of manuscript submission; acknowledgement of the contribution must also be included in the manuscript. Submission of a manuscript to *Acta Protozoologica* implies that the contents are original, have not been published previously, and are not under consideration or accepted for publication elsewhere.

SUBMISSION

Authors should submit manuscript to: Dr Jerzy Sikora, Nencki Institute of Experimental Biology, ul. Pasteura 3, 02-093 Warszawa, Poland, Fax: (4822) 8225342; E-mail: jurek@nencki.gov.pl or j.sikora@nencki.gov.pl.

At the time of submission, authors are encouraged to provide names, E-mails, and postal addresses of four persons who might act as reviewers. Extensive information on *Acta Protozoologica* is available at the website: **http://www.nencki.gov.pl/ap.htm**; however, please do not hesitate to contact the Editor.

Hard copy submission: Please submit three (3) high quality sets of text and illustrations (figures, line drawing, and photograph). When photographs are submitted, arranged these in the form of plate. A copy of the text on a disk or CD should also be enclosed, in PC formats, preferably Word for Windows version 6.0 or higher (IBM, IBM compatible, or MacIntosh). If they do not adhere to the standards of the journal the manuscript will be returned to the corresponding author without further consideration.

E-mail submission: Electronic submission of manuscripts by e-mail is acceptable in PDF format only. Illustrations must be prepared according to journal requirement and saved in PDF format. The accepted manuscript should be submitted as a hard copy with illustrations (two copies, one with lettering + one copy without lettering) in accordance with the standards of the journal.

ORGANIZATION OF MANUSCRIPTS

Text: Manuscripts must be typewritten, double-spaced, with numbered pages (12 pt, Times Roman). The manuscript should be organized into the following sections: Title, Summary, Key words, Abbreviations, Introduction, Materials and Methods, Results, Discussion, Acknowledgements, References, Tables, and Figure legends. Figure legends must contain explanations of all symbols and abbreviations used. The Title Page should include the title of the manuscript, first name(s) in full and surname(s) of author(s), the institutional address(es) where the work was carried out, and page heading of up to 40 characters (including spaces). The postal address for correspondence, Fax and E-mail should also be given. Footnotes should be avoided.

Citations in the text should be ordered by name and date but not by number, e.g. (Foissner and Korganova 2000). In the case of more than two authors, the name of the first author and *et al.* should be used, e.g. (Botes *et al.* 2001). Different articles by the same author(s) published in the same year must be marked by the letters a, b, c, etc. (Kpatcha *et al.* 1996a, b). Multiple citations presented in the text must be arranged by date, e.g. (Small 1967, Didier and Detcheva 1974, Jones 1974). If one author is cited more than once, semicolons should separate the other citations, e.g. (Lousier and Parkinson 1984; Foissner 1987, 1991, 1994; Darbyshire *et al.* 1989).

Please observe the following instructions when preparing the electronic copy: (1) label the disk with your name; (2) ensure that the written text is identical to the electronic copy; (3) arrange the text as a single file; do not split it into smaller files; (4) arrange illustrations as separate files; do not use Word files; *.TIF, *.PSD, or *.CDR graphic formats are accepted; (5) when necessary, use only italic, bold, subscript, and superscript formats; do not use other electronic formatting facilities such as multiple font styles, ruler changes, or graphics inserted into the text; (6) do not right-justify the text or use of the hyphen function at the end of lines; (7) avoid the use of footnotes; (8) distinguish the numbers 0 and 1 from the letters O and l; (9) avoid repetition of illustrations and data in the text and tables.

References: References must be listed alphabetically. Examples for bibliographic arrangement:

Journals: Flint J. A., Dobson P. J., Robinson B. S. (2003) Genetic analysis of forty isolates of *Acanthamoeba* group III by multilocus isoenzyme electrophoresis. *Acta Protozool.* **42:** 317-324

Books: Swofford D. L. (1998) PAUP* Phylogenetic Analysis Using Parsimony (*and Other Methods). Ver. 4.0b3. Sinauer Associates, Sunderland, MA

Articles from books: Neto E. D., Steindel M., Passos L. K. F. (1993) The use of RAPD's for the study of the genetic diversity of *Schistosoma mansoni* and *Trypanosoma cruzi*. In: DNA Fingerprinting: State of Science, (Eds. S. D. J. Pena, R. Chakraborty, J. T. Epplen, A. J. Jeffreys). Birkhäuser-Verlag, Basel, 339-345

Illustrations and tables: After acceptance of the paper, drawings and photographs (two copies one with lettering + one copy without) must be submitted. Each table and figure must be on a separate page. Figure legends must be placed, in order, at the end of the manuscript, before the figures. Figure legends must contain explanations of all symbols and abbreviations used. All line drawings and photographs must be labelled, with the first Author's name written on the back. The figures should be numbered in the text using Arabic numerals (e.g. Fig. 1).

Illustrations must fit within either a single column width (86 mm) or the full-page width (177 mm); the maximum length of figures is 231 mm, including the legend. Figures grouped as plates must be mounted on a firm board, trimmed at right angles, accurately mounted, and have edges touching. The engraver will then cut a fine line of separation between figures.

Line drawings should be suitable for reproduction, with well-defined lines and a white background. Avoid fine stippling or shading. Prints are accepted only in *.TIF, *.PSD, and *.CDR graphic formats (Grayscale and Colour - 600 dpi, Art line - 1200 dpi) on CD. Do not use Microsoft Word for figure formatting.

Photographs should be sharp, glossy finish, bromide prints. Magnification should be indicated by a scale bar where appropriate. Pictures of gels should have a lane width of no more than 5 mm, and should preferably fit into a single column.

PROOF SHEETS AND OFFPRINTS

After a manuscript has been accepted, Authors will receive proofs for correction and will be asked to return these to the Editor within 48-hours. Authors will be expected to check the proofs and are fully responsible for any undetected errors. Only spelling errors and small mistakes will be corrected. Twenty-five reprints (25) will be furnished free of charge. Additional reprints can be requested when returning the proofs, but there will be a charge for these; orders after this point will not be accepted.

Indexed in: Current Contents, Biosis, Elsevier Biobase, Chemical Abstracts Service, Protozoological Abstracts, Science Citation Index, Librex-Agen, Polish Scientific Journals Contents - Agric. & Biol. Sci. Data Base at: **http://psjc.icm.edu.pl**, Microbes.info "Spotlight" at **http://www.microbes.info**, and electronic version at Nencki Institute of Experimental Biology website in *.PDF format at http://www.nencki.gov.pl/ap.htm now free of charge.

ACTA
PROTOZOOLOGICA

ORIGINAL ARTICLES

SHORT COMMUNICATION

2005 AUGUST
VOLUME 44 NUMBER 3